

UC San Diego

UC San Diego Electronic Theses and Dissertations

Title

Loop effects in de Sitter spacetime

Permalink

<https://escholarship.org/uc/item/4b3522fn>

Author

Premkumar, Akhil

Publication Date

2022

Peer reviewed|Thesis/dissertation

UNIVERSITY OF CALIFORNIA SAN DIEGO

Loop effects in de Sitter spacetime

A dissertation submitted in partial satisfaction of the
requirements for the degree Doctor of Philosophy

in

Physics

by

Akhil Premkumar

Committee in charge:

Professor Daniel Green, Chair
Professor Daniel Arovas
Professor Aneesh Manohar
Professor John McGreevy
Professor Justin Roberts

2022

Copyright

Akhil Premkumar, 2022

All rights reserved.

The Dissertation of Akhil Premkumar is approved, and it is acceptable in quality and form for publication on microfilm and electronically.

University of California San Diego

2022

DEDICATION

To my parents, whose love and sacrifice, inspire me to be the best version of myself.

EPIGRAPH

It does not matter how slowly you go as long as you do not stop.

Confucius

TABLE OF CONTENTS

Dissertation Approval Page	iii
Dedication	iv
Epigraph	v
Table of Contents	vi
List of Figures	ix
List of Tables	xii
Acknowledgements	xiii
Vita	xvi
Abstract of the Dissertation	xvii
Chapter 1 Introduction	1
Chapter 2 Dynamical RG and Critical Phenomena in de Sitter Space	5
2.1 Introduction	5
2.2 Conformal Perturbation Theory	7
2.2.1 Definition	7
2.2.2 Perturbative Flow between Fixed Points	9
2.2.3 Dynamical RG	13
2.2.4 Summary	15
2.3 Scalar Field Theory	16
2.3.1 The $\langle \phi^2 \phi^2 \rangle$ correlator	16
2.3.2 Implications for $\lambda \phi^4$ in Four-Dimensions	20
2.4 Yukawa Interaction	20
2.5 Conclusions	23
2.A Analytic Continuation of the In-In Formalism	24
2.B Details of Loop Integration	25
2.B.1 Dimensional Regularization	26
2.B.2 de Sitter Conformal Perturbation Theory	27
2.B.3 Integrals in the $\lambda \phi^4$ theory	28
2.B.4 Integrals for the Yukawa calculation	30
Chapter 3 Regulating Loops in dS	33
3.1 Introduction	33
3.2 dS loops in Mellin space	35
3.2.1 General structure	36
3.2.2 Divergences in MB integrals	38

3.2.3	N -dimensional MB integrals	41
3.2.4	Analytic continuation	42
3.3	The tree level 4-point function	46
3.4	The anomalous dimension of ϕ^2	48
3.4.1	The conformal mass case	51
3.4.2	γ_{ϕ^2} for other masses	58
3.5	Mixing of ϕ^3 and ϕ	60
3.5.1	The massless case	61
3.6	Conclusions	72
Chapter 4	Stochastic Inflation at NNLO	75
4.1	Introduction	75
4.2	Stochastic Inflation	78
4.2.1	Leading Order	79
4.2.2	Beyond Leading Order	80
4.3	Soft de Sitter Effective Theory	86
4.3.1	In-In Correlators	86
4.3.2	Taking the Long Wavelength Limit	89
4.3.3	(Dynamical) Renormalization	92
4.3.4	Matching and Initial Conditions	94
4.3.5	Stochastic Inflation from SdSET	98
4.4	Matching $\lambda\phi^4$ Onto SdSET at One-Loop	101
4.4.1	Tree-level Matching and Field Redefinitions	101
4.4.2	One-loop Matching	108
4.4.3	Initial Conditions for Composite Operators	115
4.5	Composite Operator Mixing	118
4.5.1	One-loop Corrections	120
4.5.2	Two-loop Corrections	122
4.5.3	Stochastic Inflation at NNLO	125
4.6	Implications	128
4.6.1	Equilibrium Probability Distribution	128
4.6.2	Relaxation Eigenvalues	131
4.7	Conclusions	135
4.A	Matching the Six-point Function	137
4.B	Hard Cutoff Calculations	141
4.B.1	Matching	141
4.B.2	Composite Operator Mixing	145
Chapter 5	A Tail of Eternal Inflation	151
5.1	Introduction	151
5.2	Non-Gaussian Corrections to Stochastic Inflation	157
5.2.1	Stochastic Inflation for Single Field Inflation	159
5.3	Eternal Inflation and Non-Gaussian Tails	163
5.4	The de Sitter Entropy and Microstate Counting	169

5.5	On the Breakdown of Stochastic Inflation	172
5.5.1	Breakdown in DBI	174
5.6	Conclusions	176
5.A	Calculations for Single Field Inflation.....	177
5.A.1	EFT of Inflation: Power Spectrum and Bispectrum	178
5.A.2	Dynamical Dimensional Regularization	179
5.A.3	Perturbative Unitarity from Scattering	182
5.B	Solving the Fokker-Planck with Steepest Descents	185
	References	186
	Bibliography	187

LIST OF FIGURES

Figure 1.1.	A cartoon of de Sitter spacetime. Three dimensional space is visualized as a plane that expands over time. Also shown is a path covered with balls of fixed size H^{-1} , the characteristic length scale of a fixed dS manifold.	2
Figure 1.2.	A line in dS that reveals more structure as it expands, a consequence of which is a change in its dimensions.	3
Figure 2.1.	The Feynman diagrams involved in the calculation of $\langle \phi^2 \phi^2 \rangle$	17
Figure 3.1.	Regulating divergences in MB integrals. The overlap of the zeroth left and right poles in (a) makes (3.9) undefined because no contour can separate all the left poles from right ones. In (b) we have shifted the left poles to the left by ε , allowing us to drive a contour between the two kinds of poles. In the limit $\varepsilon \rightarrow 0$ we approach the situation in (a), known as <i>contour pinching</i> , which results in a divergence $\Gamma(\varepsilon)$. This is simply the residue at $s_* = 0$, as we close the contour on the RHP. The residues at the other poles are finite in the same limit.	39
Figure 3.2.	A contour that does not separate left/right poles.	40
Figure 3.3.	Pole structure of an MB integral $\int_{\mathcal{C}} \frac{ds}{2\pi i} \Gamma(a+s)\Gamma(b-s)x^{-s}$. The contour satisfies $a < s^{\mathcal{C}} < b$, which is equivalent to the condition that the arguments of the Γ functions in the integrand are positive when evaluated on the contour (cf. (3.15)).	42
Figure 3.4.	An MB integral is defined by shifting its poles around till the left/right poles are separated by a straight line contour. Analytic continuation involves reverting these shifts and allowing the poles to cross back to their original position. As a pole crosses the contour, we isolate the contribution at that pole (cf. (3.11)). Some of the left/right poles (encircled) nearly overlap, resulting in divergences. For an N -fold MB integral all this happens across N complex s_ℓ -planes simultaneously. Note: The poles in these figures have been staggered vertically for clarity; they are all real valued in our examples. See sec. 3.2.4 for further explanation.	44
Figure 3.5.	The 4-pt correlation function at tree level.	46
Figure 3.6.	$\langle \phi^2 \phi^2 \rangle$ at tree level.	48
Figure 3.7.	The first order correction to $\langle \phi^2 \phi^2 \rangle$	49

Figure 3.8.	Anomalous dimension of ϕ^2 for different masses. Larger values of $ v $ correspond to smaller masses (see (3.3)). The encircled points are given in table 3.1.	59
Figure 3.9.	The leading contribution to $\langle \phi^3 \phi \rangle$	61
Figure 3.10.	The poles of the integrand are represented by straight lines on a $\Re(s_1) - \Re(s_2)$ plane. Residues are computed at the intersections of these lines. Poles that cross over to the other side are represented by dashed lines in (b). The residues at \bullet contain a $\Gamma(\alpha)^2$ divergence whereas those at \bullet give a $\Gamma(\alpha)$. The latter encode subhorizon physics, as explained in sec. 3.5.1. . .	67
Figure 4.1.	Visualization of the Kramers-Moyal expansion. The top panel shows the probability of “hopping” from ϕ to ϕ' , $W(\phi' \phi)$ or from ϕ' to ϕ , $W(\phi \phi')$, or equivalently any other point such as ϕ'' . On the bottom, we see the process in terms of the probability $\tilde{W}(\Delta\phi \phi)$ to hop from a specific starting point ϕ by a distance $\Delta\phi$	81
Figure 4.2.	Diagrams for the one-loop matching, as computed in the UV theory. The horizontal line indicates a surface on constant conformal time τ_0 on which our in-in correlators are evaluated. <i>Left</i> : One-loop power spectrum. <i>Right</i> : One-loop trispectrum.	109
Figure 4.3.	Tree level pentaspectrum	118
Figure 4.4.	One loop correction to φ_+^2 that looks like an anomalous dimension ($\varphi_+^2 \rightarrow \varphi_+^2$). We start from the tree level trispectrum and integrate over two of the fields to form the composite operator φ_+^2 . <i>Left</i> : The Witten diagram with a boundary at future infinity. <i>Right</i> : The Feynman diagram with the same momentum flow.	120
Figure 4.5.	Diagram of contribution one loop contribution to $\Gamma_{2,4}$ ($\varphi_+^2 \rightarrow \varphi_+^4$). We start from the tree level pentaspectrum (6 points function) and integrate over two of the fields to form the composite operator φ_+^2 . <i>Left</i> : The Witten diagram with a boundary at future infinity. <i>Right</i> : The Feynman diagram with the same momentum flow.	123
Figure 4.6.	Diagram of contribution two loop contribution to the mixing $\varphi_+^3 \rightarrow \varphi_+$. We start from the tree level trispectrum and integrate over <i>three</i> of the fields to form the composite operator φ_+^3 . We first drew this as a Witten diagram with a boundary at future infinity. At the bottom we have shown the Feynman diagram with the same momentum flow.	124
Figure 4.7.	The tree level in-in six-point function.	138

Figure 5.1. The relevant energy scales for single field inflation and the regimes of validity of the EFT of Inflation [orange] and Soft de Sitter Effective Theory (SdSET) [blue]. The background time evolution leads to a scale f_π , below which the time translation symmetry is spontaneously broken (SSB). Primordial non-Gaussianity arises from interactions that are suppressed by the EFT cutoff scale Λ , which is related to the amplitude for equilateral non-Gaussianity $f_{\text{NL}}^{\text{eq}}$ by $\Lambda^2 \simeq f_\pi^2 / f_{\text{NL}}^{\text{eq}}$. Requiring the EFT of Inflation is weakly coupled at horizon crossing allows both $\Lambda > f_\pi$ [left] and $\Lambda < f_\pi$ [right]. Deviations from a de Sitter background arise at $|\dot{H}| \ll H^2$ 153

Figure 5.2. The solid blue region shows where primordial non-Gaussianity naively implies eternal inflation, suggesting a breakdown of Stochastic Inflation and/or the EFT of Inflation. The region allowed by perturbative unitarity at horizon crossing, derived in [1], corresponds to the region enclosed by the dashed purple line. The current 1-,2- and 3- σ limits from Planck [2] are shown as solid red lines. We see there is a significant region where the calculation of the transition to external inflation is breaking down, that is nonetheless consistent with the theory being weakly coupled at horizon crossing (as determined by unitarity) and current observations. The parameters $\bar{\alpha}$ and c_s are related to the two allowed cubic couplings in the EFT of Inflation, as defined in Sec. 5.3. Perturbative unitarity as defined in [1] is particularly conservative and may explain why regions of parameter space allowed by Planck are excluded. We simply wish to emphasize that there are regions of parameter space in blue that are perturbative even by that definition. 155

Figure 5.3. Illustration of the correlation function $\langle \zeta^3(\vec{x} = 0) \rangle$ represented as an integral over the bispectrum $B(k_1, k_2, k_3)$ computed at tree-level. The momentum integration is analogous to a two-loop integral. 162

LIST OF TABLES

Table 3.1. Anomalous dimension of ϕ^2 for different masses..... 60

ACKNOWLEDGEMENTS

This document is an important milestone in a journey I started seven years ago, when I quit my job as a software engineer to learn something about the universe. This transition was spurred by some friends at work, most notably Tuo Wu, who urged me to further my education, and Madhu Babu, who alerted me to the dangers of living life on auto-pilot. The final push came from my friend and brother, James Acevedo, who took the leap of faith with me to go back to school.

I was on a safe, stable career trajectory, and my departure from it was no doubt worrisome to my parents. But they trusted my instincts and supported my decision, even if they did not fully understand it. To this day, they remain curious about my career prospects with a physics degree (as do I), but they deferred to my happiness and satisfaction when it mattered most. For this, and almost everything else, I am grateful to my Amma and Achan.

After 3 years of working as a programmer, my math skills were rusty as I entered the Masters program at IIT Bombay. However, I was extremely fortunate to study Mathematical Physics under the tutelage of Prof. Dibyendu Das, who single-handedly built my confidence to work on difficult calculations. He was also the first to teach me about Renormalization Group theory, which would become an integral part of my research later. Prof. Das is proof that one great teacher can undo the damage of several bad ones.

I am indebted to my other great teachers at UCSD — John McGreevy, Aneesh Manohar, Michael Fogler, and Daniel Arovas — for teaching me most of the advanced physics I know. Equally important were all the students I had the opportunity to teach over the years. There is no greater test of one's understanding than having to explain it to someone else, and I hope that my students learned as much from me as I did from them.

The first year of grad school somehow simultaneously feels so long ago, and not that long ago. I suspect the pandemic has something to with it. Grad school can be a long and arduous process without having to live through a cataclysmic event. The period stretching from early 2020 to mid 2021 was trying in many ways, and for the bulk of this time the only real human

interaction I had was with my friend and colleague Megan. Her kindness, humor, and the ability to simply be present helped me stay afloat during this time. I will also miss the conversations with Brian, Evgueni, Ethan, and Meng which vacillated between the inane and the profound, with everything in between. The last five years have challenged and transformed us in different ways, but I would like to think that it has left us in a better place than when we started.

Finally, and most importantly, I want to thank my advisor, Daniel Green, for the incalculable kindness, patience, and support he showed me over the years. Dan taught me that research was about more than just problem solving. In one of our first meetings, Dan went to his blackboard and plotted a graph of progress made on a problem vs. the time spent working on it. He told me that if the graph was a straight line the problem I picked was not hard enough. Instead, good research is characterized by long plateaus interrupted by small jumps. What we do on the plateaus defines who we are as scientists.

Dan gave me the space to develop my own interests and approach to research. Over the years I have often asked him the same questions over and over again, and each time he answered patiently, nudging me toward the problems that I continue to investigate to this day. He taught me that it was okay to not understand something perfectly the first time I was exposed to it. At times Dan would tell me about some subtle detail of basic QFT that tripped him up much later in his career. To hear that from someone as smart as Dan gave me hope that I was not entirely out of my depth as I grappled with fundamental ideas.

Dan also introduced me to Tim Cohen, who in many ways served as a second advisor to me. Many of our joint meetings were an excuse for me to witness Dan and Tim spin ideas in real time. Vast chunks of this document were seeded in their imagination, I simply dotted the *i*'s and crossed the *t*'s.

Chapter 2, in full, is a reprint of the material as it appears in Daniel Green, Akhil Premkumar, *Journal of High Energy Physics* **04** (2020) 064. The dissertation author was one of the primary investigators and authors of this paper.

Chapter 3, in full, is a reprint of the material as it appears in Akhil Premkumar, arXiv:

2110.12504. The dissertation author was the primary investigator and author of this paper.

Chapter 4, in full, is a reprint of the material as it appears in Timothy Cohen, Daniel Green, Akhil Premkumar, Alexander Ridgway, *Journal of High Energy Physics* **09** (2021) 159.

The dissertation author was one of the primary investigators and authors of this paper.

Chapter 5, in full, has been submitted for publication of the material as it may appear in Timothy Cohen, Daniel Green, Akhil Premkumar, *Journal of High Energy Physics* (2022). The dissertation author was one of the primary investigators and authors of this paper.

VITA

- 2011 B.Tech in Electronics and Instrumentation, College of Engineering, Trivandrum
2017 M.Sc in Physics, Indian Institute of Technology, Bombay
2022 Ph.D in Physics, University of California San Diego

PUBLICATIONS

Daniel Green, Akhil Premkumar, *Dynamical RG and Critical Phenomena in de Sitter Space*, JHEP 04 (2020) 064, arXiv: 2001.05974 [hep-th]

Timothy Cohen, Daniel Green, Akhil Premkumar, Alexander Ridgway, *Stochastic Inflation at NNLO*, JHEP 09 (2021) 159, arXiv: 2106.09728 [hep-th]

Akhil Premkumar, *Regulating Loops in dS* , arXiv: 2110.12504 [hep-th]

Timothy Cohen, Daniel Green, Akhil Premkumar, *A Tail of Eternal Inflation*, arXiv: 2111.09332 [hep-th]

ABSTRACT OF THE DISSERTATION

Loop effects in de Sitter spacetime

by

Akhil Premkumar

Doctor of Philosophy in Physics

University of California San Diego, 2022

Professor Daniel Green, Chair

de Sitter spacetime plays a central role in modern (quantum) cosmology. Yet, there are various aspects of quantum field theory in de Sitter that we do not understand at the same level as we do Minkowski spacetime. In particular, perturbative calculations in de Sitter give rise to a variety of contributions that grow with time (secular divergences). We study how such terms can be interpreted using a renormalization group approach, which eventually culminates in an effective theory description of the long wavelength physics. We also introduce techniques to compute loop integrals in de Sitter, a problem for which the standard flat space QFT methods are inadequate. These methods complement and validate the EFT description, and allow us to calculate higher order corrections to the Stochastic Inflation framework for massless scalars.

Chapter 1

Introduction

The theory of Inflation tells us that the very early universe underwent a period of rapid expansion, driven by an inflaton field. During this era the universe could most simply be described by an approximately de Sitter (dS) metric, characterized by a single energy scale H , the Hubble parameter. As points in coordinate space become separated by distances larger than H^{-1} , they fall out of causal contact, and can no longer influence one another. Eventually inflation ends, and these *superhorizon* fluctuations re-enter the horizon, seeding the structures we see in the night sky. The quantum dynamics of the inflaton are thus embedded in our cosmological observations.

We can get some intuition for how quantum fluctuations manifest in QFT calculations by a simple analogy. Consider the de Sitter (dS) metric

$$ds^2 = -dt^2 + a(t)^2 d\vec{x}^2, \quad a(t) = e^{Ht}, \quad (1.1)$$

where H is the Hubble parameter, which is assumed to be a constant in this work. This metric defines an expanding spacetime, which we may visualize as shown in Fig. 1.1. Imagine now, some path of arbitrary shape in space, which will also expand with the scale factor $a(t)$. We can define the *dimension* of this object by counting the minimum number of H^{-1} sized balls required

to cover the path. We will assume that this number, N , is related to H^{-1} as

$$N \propto H^\Delta \tag{1.2}$$

where Δ is the *dimension* of the path. For instance, if the path were a straight line of length $a(t)|\vec{x}|$, we could cover it with $N_{\text{line}} = \left(\frac{a(t)|\vec{x}|}{H^{-1}}\right)^1$ balls. Therefore, the dimension of a line is $\Delta_{\text{line}} = 1$, which makes sense. For simplicity, let us take the path in Fig. 1.1 to be a line also. Furthermore, let us imbue this line with the property that, as it expands it reveals more structure. This is depicted in Fig. 1.2. How does this behavior affect the dimension of the line?

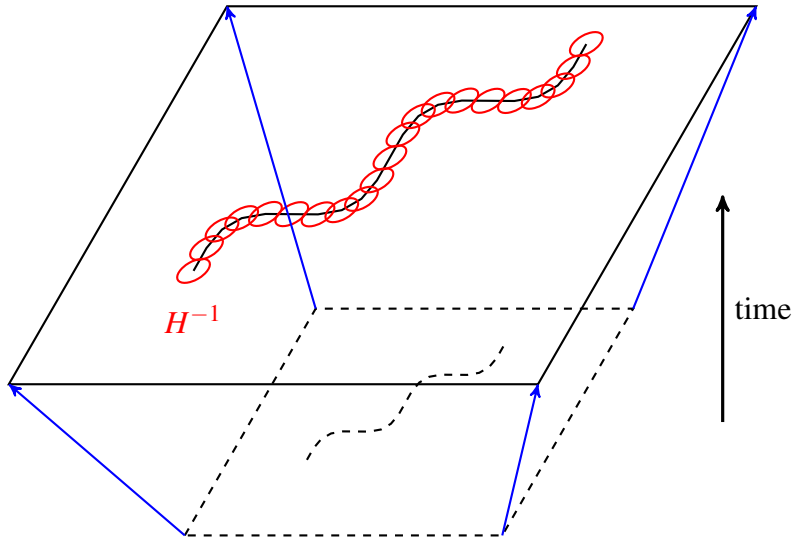


Figure 1.1. A cartoon of de Sitter spacetime. Three dimensional space is visualized as a plane that expands over time. Also shown is a path covered with balls of fixed size H^{-1} , the characteristic length scale of a fixed dS manifold.

Once again we cover the line with balls of size H^{-1} and add up their number. Due to its newly revealed structure we will require more balls to cover the line than if it were a perfectly straight line. If we still assume that N scales with H as in (1.2), we can get the new number of balls required by modifying the value of $\Delta_{\text{line}} \rightarrow 1 + \gamma$,

$$N_{\text{line}} = \left(\frac{a(t)|\vec{x}|}{H^{-1}}\right)^{1+\gamma} . \tag{1.3}$$

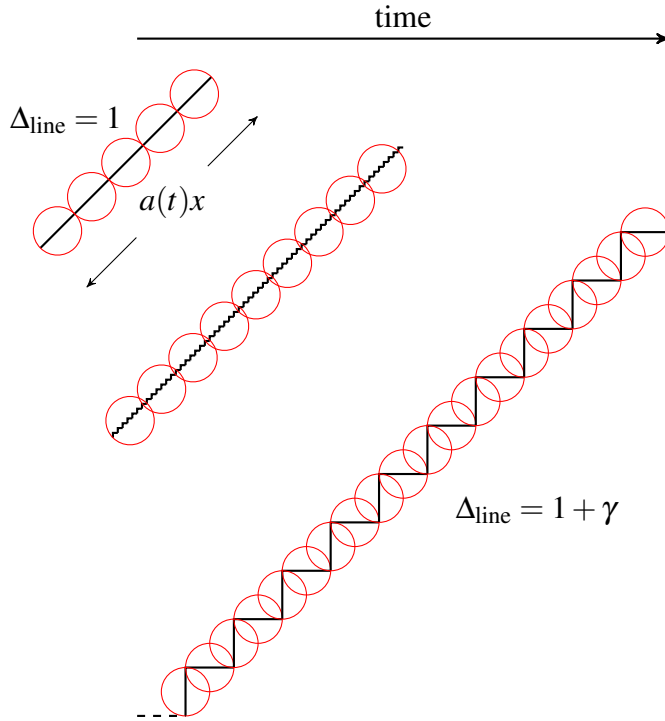


Figure 1.2. A line in dS that reveals more structure as it expands, a consequence of which is a change in its dimensions.

The number γ is called the *anomalous dimension* of the expanded line, and it is smaller than 1. This captures the intuition that the jagged line is not a one-dimensional object anymore, but it is not quite a two-dimensional object either. Similar considerations apply for paths of arbitrary shapes as well.

But why would these paths reveal more structure as space expands? You see, all this time ‘paths’ in dS were just a stand in for quantum fields, and the structure that gets added over time are generated by quantum fluctuations which get stretched out by the expansion of dS. In other words, anomalous dimensions encode the ‘quantumness’ in cosmic structure.

Before we leave this example, we may use the fact that $\gamma < 1$ to expand (1.3) to

$$N_{\text{line}} = \left(\frac{a(t)|\vec{x}|}{H^{-1}} \right)^1 (1 + \gamma \log(aH|\vec{x}|) + \dots). \quad (1.4)$$

That is, if we were doing perturbative calculations in some parameter of size $O(\gamma)$, we should

watch out for $\log(aH|\vec{x}|)$ to identify anomalous scaling. If we were working in Fourier space we would have $\log(|\vec{k}|/aH)$ instead. Such logs often arise from loop calculations in dS. This is a reasonable¹ but non-trivial claim, owing to the appearance of special functions in the actual integrals we need to compute. The first two chapters that follow develop some techniques to extract and interpret such logs from ‘full’ theory calculations.

Notice that (1.3) involves a ratio of length scales $a(t)|\vec{x}|$ and H^{-1} . The first one grows exponentially with time whereas the latter remains fixed. A physics problem with such a large separation of scales must admit an effective description. In the present case this is would be an EFT of the long wavelength (soft) modes. The second half of this work explores physics in dS with this EFT, and culminates in a rigorous derivation of the Stochastic Inflation framework, and corrections to it.

¹This is consistent with our understanding of logs that show up in flat space loop integrals — loops in standard QFT can be organized as an expansion in \hbar . If we set $\hbar \rightarrow 0$ all the loop effects vanish and we would be left with a purely classical theory.

Chapter 2

Dynamical RG and Critical Phenomena in de Sitter Space

2.1 Introduction

The physics of de Sitter space has posed both conceptual and technical challenges to our understanding of the universe. Ultimately, the lack of a fixed boundary in the presence of dynamical gravity is an unavoidable challenge in defining physics in de Sitter space [3, 4, 5, 6, 7, 8]. Yet, there have long been more mundane challenges associated with divergences in perturbation theory [9, 10, 11, 12, 13, 14, 15, 16, 17, 18], with and without dynamical gravity. Resolving the origin of these divergences is a more tangible problem than quantum gravity in de Sitter itself and is surely a necessary step towards a complete theory of (quantum) cosmology.

Significant progress has been made in our understanding of perturbation theory in cosmological spacetimes. In the particular case of cosmological correlators in single-field inflation, it has been shown to all-loop order that time-dependent contributions from individual diagrams must vanish when all the diagrams are summed together [19, 20]. In essence, in the case of single-field inflation, the secular divergences are not physical. The absence of such divergences is unique to the metric fluctuations due to the nonlinear symmetries of these modes [21, 22], which are also responsible for the separate universe description of cosmology [23] and the single-field consistency conditions [7, 24].

In contrast to the metric fluctuations, the divergences associated with conventional

quantum fields in cosmological backgrounds are physical [16, 25, 26, 27, 28, 29, 30, 31, 32]. In some cases, these divergences can be re-summed using known techniques from quantum field theory (QFT) [11, 33, 34, 35, 36, 37]. The dynamical renormalization group (DRG) [38, 39, 40] is one such approach that is well-suited for secular divergences in cosmology [41, 42, 43, 44]. These divergences are at most logarithmic in the scale factor [15, 16] and thus the leading logs can be resummed using the DRG. Unfortunately, the meaning of this resummation lacks the clear physical interpretation that we associate to the renormalization group in flat space.

In recent work, a number of non-trivial features of tree-level perturbation theory in de Sitter space have been connected to conventional physics in flat space. For instance, the analytic structure of correlations functions has been seen to encode the flat space S-matrix [45, 46, 47, 48]. In addition, these cosmological correlators display the analogues of simple poles and factorization associated with the exchange of new particles [49, 50]. These types of observations have helped demystify otherwise peculiar properties of these calculations.

In this work, we will explore the origin of secular divergences in de Sitter space and their relation to physics in flat space. To make the origin of these divergences manifest, we will study theories that flow to perturbative IR fixed points in flat space. At the fixed point, the theories are conformal and their de Sitter correlators are determined by a Weyl transformation [51] from flat space to de Sitter,

$$\langle \mathcal{O}_1(\vec{x}_1, \tau_1) \cdots \mathcal{O}_n(\vec{x}_n, \tau_n) \rangle_{\text{dS}} = \left(\prod_{i=1}^n a(\tau_i)^{-\tilde{\Delta}_i} \right) \langle \mathcal{O}_1(\vec{x}_1, \tau_1) \cdots \mathcal{O}_n(\vec{x}_n, \tau_n) \rangle_{\text{flat}}, \quad (2.1)$$

where $\tilde{\Delta}_i$ are the dimensions of the operators at the IR fixed point, τ is the conformal time, $a(\tau) = (-H\tau)^{-1}$ is the scale factor and \vec{x} are the spatial coordinates. In perturbation theory, $\tilde{\Delta}_i = \Delta_i + \gamma_i$ where Δ_i is the dimension at the UV fixed point and γ_i is the anomalous dimension calculated in perturbation theory. Expanding the dS correlator in γ_i , one sees that perturbation theory in de Sitter must contain $(\gamma_i \log a(\tau_i))^N$ divergences that are not present in the flat space calculation. Given only the lowest order divergence, $\gamma_i \log a(\tau_i)$, one can use the DRG to recover

the full power-law in Equation (2.1) as required by conformal invariance.

When the coupling is not tuned to be at the IR fixed point, the theory is not conformal and the de Sitter correlators are not necessarily related to flat space correlators by a Weyl transformation. Yet, the perturbative calculation does not depend on the precise value of the coupling and the form of the secular divergences remains unchanged. We will show that these logarithmic divergences can still be resummed and the resulting power law is determined by the (scale-dependent) flat space anomalous dimension, $\gamma(\mu)$, calculated at the scale of horizon crossing, $\mu = H$.

We will first analyze a general version of this problem using conformal perturbation theory in de Sitter space. When conformal perturbation theory is applicable in flat space, the same expansion can be used in de Sitter space using the map described in Equation (2.1). We show explicitly in conformal perturbation theory that anomalous dimensions in flat space become secular divergences in de Sitter. We then show how they can be resummed using the DRG equations. These insights will apply to a wide variety of theories, including perturbative QFTs involving gauge fields, fermions and/or conformally coupled scalars. We will show this explicitly in several examples.

The organization of this paper is as follows: in Section 2.2, we demonstrate our main results using conformal perturbation theory. In Sections 2.3 and 2.4, we show how these general results arise in the specific examples of a conformally coupled scalar with a $\lambda\phi^4$ interaction in $d = 4 - \varepsilon$ dimensions and Yukawa interactions in four dimensions. We conclude in Section 2.5. Details of the calculations are presented in the Appendices.

2.2 Conformal Perturbation Theory

2.2.1 Definition

Conformal perturbation theory in flat space is a powerful tool for understanding a deformation around any fixed point, whether weakly or strongly coupled. We imagine that the

fixed point is described in terms of some action, S_{CFT} , that is deformed by one of the operators in the CFT,

$$S = S_{\text{CFT}} + \lambda \mu^{d-\Delta} \int d^d x \mathcal{O}(\mathbf{x}) , \quad (2.2)$$

where \mathbf{x} is a d -vector, μ is the renormalization scale, λ is the dimensionless coupling, and Δ is the dimension of the operator. From the Euclidean path integral description, it is easy to see that a correlation function in the perturbed theory can be related to a correlation function in the CFT via

$$\langle \mathcal{O}_i(\mathbf{y}) \dots \rangle = \langle \mathcal{O}_i(\mathbf{y}) \dots e^{-\lambda \mu^{d-\Delta_j} \int d^d x \mathcal{O}_j(\mathbf{x})} \rangle_{\text{CFT}} , \quad (2.3)$$

where $\langle \dots \rangle_{\text{CFT}}$ means we are calculating a correlation function in the (unperturbed) CFT. Taylor expanding the exponential then gives the result in terms of correlation functions CFT,

$$\langle \mathcal{O}_i(\mathbf{y}) \dots \rangle = \sum_n \frac{(-\lambda \mu^{d-\Delta_j})^n}{n!} \left(\prod_{k=1}^n \int d^d x_k \right) \langle \mathcal{O}_i(\mathbf{y}) \dots \prod_{k=1}^n \mathcal{O}_j(\mathbf{x}_k) \rangle_{\text{CFT}} . \quad (2.4)$$

This procedure is very general and is even applicable to theories where S_{CFT} is unknown (or doesn't exist). Of course, as a practical tool for calculations, it is limited to cases where the correlation functions are known and can be integrated.

Given a theory in flat space described by conformal perturbation theory, we can apply the same procedure to define perturbation theory in de Sitter space, now writing $S = S_{\text{CFT}} + \lambda \mu^{d-\Delta_j} \int d\tau d^{d-1} x \sqrt{-g} \mathcal{O}_j(\mathbf{x})$. Using $ds^2 = a(\tau)^2 (-d\tau^2 + d\vec{x}^2)$ and $\sqrt{-g} = a^d(\tau)$ in conformal time, we can write

$$\langle \mathcal{O}_i(\mathbf{y}) \dots \rangle_{\text{dS}} = a^{-\Delta_i}(\tau_y) \sum_n \frac{(-\lambda \mu^{d-\Delta_j})^n}{n!} \left(\prod_{k=1}^n \int d^d x_k a^{d-\Delta_j}(\tau_k) \right) \langle \mathcal{O}_i(\mathbf{y}) \dots \prod_{k=1}^n \mathcal{O}_j(\mathbf{x}_k) \rangle_{\text{CFT}} \quad (2.5)$$

where $\langle \dots \rangle_{\text{CFT}}$ is the correlation function at the UV fixed point in flat space.

2.2.2 Perturbative Flow between Fixed Points

We will consider a CFT in $d = 4$ dimensions that contains an operator of dimension $\Delta = 4 - \varepsilon$. We will first consider the RG flow in flat space and then address the behavior in de Sitter. In flat space, we deform the theory by $S = S_{\text{CFT}} + \lambda \mu^\varepsilon \int d^4x \mathcal{O}(\mathbf{x})$.

The first thing we must determine is what happens under RG flow. At leading order, the β -function is given¹ in terms of the dimension of the operator, $\beta_\lambda = \mu \frac{d\lambda}{d\mu} = -(4 - \Delta)\lambda = -\varepsilon\lambda$. We calculate the correction to the β function, noticing that a generic correlator of quadratic order in λ takes the form

$$\langle \dots \lambda^2 \mu^{2\varepsilon} \int d^4x_1 d^4x_2 \mathcal{O}(\mathbf{x}_1) \mathcal{O}(\mathbf{x}_2) \rangle. \quad (2.6)$$

We will assume the operator product expansion (OPE) of \mathcal{O} contains the term

$$\mathcal{O}(\mathbf{x}_1) \mathcal{O}(\mathbf{x}_2) \supset \frac{C}{|\mathbf{x}_{12}|^\Delta} \mathcal{O}(\mathbf{x}_2), \quad (2.7)$$

where $\mathbf{x}_{ij} = \mathbf{x}_i - \mathbf{x}_j$, and $C \neq 0$ is the OPE coefficient. Using the OPE, our generic correlator contains the term

$$\begin{aligned} \langle \dots \frac{1}{2!} \lambda^2 \mu^{2\varepsilon} \int d^4x_1 d^4x_2 \mathcal{O}(\mathbf{x}_1) \mathcal{O}(\mathbf{x}_2) \rangle &\supset \langle \dots \frac{1}{2!} \lambda^2 \mu^{2\varepsilon} C \int d^4x_{12} |\mathbf{x}_{12}|^{-4+\varepsilon} \int d^4x_2 \mathcal{O}(\mathbf{x}_2) \rangle \\ &\supset \langle \dots \frac{1}{2!} \lambda^2 \mu^{2\varepsilon} C 2\pi^2 \int_0^{\frac{1}{\mu}} \frac{dx_{12}}{|\mathbf{x}_{12}|^{1-\varepsilon}} \int d^4x_2 \mathcal{O}(\mathbf{x}_2) \rangle \\ &\supset \langle \dots \frac{\lambda^2 \mu^\varepsilon \pi^2 C}{\varepsilon} \int d^4x_2 \mathcal{O}(\mathbf{x}_2) \rangle, \end{aligned} \quad (2.8)$$

where μ is the normalization scale in units of energy. We have regulated the divergent integral with a cutoff in position space for clarity, but we will otherwise use dimensional regularization throughout. This divergence can be absorbed into a counterterm $\delta_\lambda = +\frac{\pi^2 C \lambda}{\varepsilon}$ by changing the action to $S + (\lambda \mu^\varepsilon)(1 + \delta_\lambda) \int d^4x \mathcal{O}(x)$. Differentiating this modified coupling constant with

¹ μ is an energy scale which decreases to zero as we flow from the UV fixed point to the IR fixed point.

respect to μ , we find

$$\beta_\lambda = -\varepsilon\lambda + \pi^2 C \lambda^2 + O(\lambda^3). \quad (2.9)$$

This beta function drives the theory from the UV fixed point at $\lambda = 0$ to the IR fixed point at $\lambda_{\text{IR}} = \frac{\varepsilon}{\pi^2 C}$. Since $\varepsilon \ll 1$, the behavior at the IR (UV) fixed point can be understood purely from perturbation theory around the UV (IR) fixed point.

Two-point function in flat space: Let us now derive the perturbative correction to the equal time two point function in flat space, in anticipation of the cosmological calculation. Expanding to first order in conformal perturbation theory, we have

$$\langle \mathcal{O}(\vec{x}_1, \tau_0) \mathcal{O}(\vec{x}_2, \tau_0) \rangle = \langle \mathcal{O}(\vec{x}_1, \tau_0) \mathcal{O}(\vec{x}_2, \tau_0) \rangle_* - \lambda \mu^\varepsilon \langle \mathcal{O}(\vec{x}_1, \tau_0) \mathcal{O}(\vec{x}_2, \tau_0) \int d^4 x_3 \mathcal{O}(\vec{x}_3) \rangle_*,$$

where $\langle \dots \rangle_*$ is a correlation function calculated at the UV fixed point. Inserting the correlation function (2.46) with $a = 1$ and using (2.48) to perform the integral, we find

$$\begin{aligned} \langle \mathcal{O}(\vec{x}_1, \tau_0) \mathcal{O}(\vec{x}_2, \tau_0) \int d\tau_3 d^3 x_3 \mathcal{O}(\vec{x}_3, \tau_3) \rangle_* &= \frac{C}{x_{12}^\Delta} \int \frac{d\tau_3 d^3 x_3}{|x_{13}^2 + \tau_E^2|^{\Delta/2} |x_{32}^2 + \tau_E^2|^{\Delta/2}} \\ &\stackrel{\varepsilon \rightarrow 0}{\approx} \frac{4\pi^2 C}{x_{12}^{2\Delta}} \left(\frac{1}{\varepsilon} + \log(\mu x_{12}) + \dots \right), \end{aligned}$$

where $x_{ij} = |\vec{x}_{ij}|$. Reintroducing the coupling, λ , the bare two point correlation function is then

$$\langle \mathcal{O}(\vec{x}_1, \tau_0) \mathcal{O}(\vec{x}_2, \tau_0) \rangle \approx \frac{1}{x_{12}^{2\Delta}} \left(1 - \frac{4\pi^2 C \lambda}{\varepsilon} (\mu x_{12})^\varepsilon \right)$$

The $\frac{1}{\varepsilon}$ divergence can be removed by introducing a counterterm $\delta_Z = -\frac{2\pi^2 C \lambda}{\varepsilon}$ so that the two-

point function of the renormalized operator, $\mathcal{O} = Z\mathcal{O}_R$, takes the form

$$\begin{aligned} \langle \mathcal{O}_R(\vec{x}_1, \tau_0) \mathcal{O}_R(\vec{x}_2, \tau_0) \rangle &= (1 - 2\delta_Z) \langle \mathcal{O}(\vec{x}_1, \tau_0) \mathcal{O}(\vec{x}_2, \tau_0) \rangle \\ &= \frac{1}{x_{12}^{2\Delta}} (1 - 4\pi^2 C \lambda \log(\mu x_{12}) + \dots) . \end{aligned} \quad (2.10)$$

As a result, \mathcal{O}_R acquires the anomalous dimension

$$\gamma_{\mathcal{O}} = \mu \frac{d}{d\mu} (\delta_Z) = 2\pi^2 C \lambda . \quad (2.11)$$

Notice that at the IR fixed point the dimension of operator \mathcal{O} becomes

$$\Delta_{\text{IR}} = \Delta + \gamma_{\mathcal{O}} = 4 - \varepsilon + 2\pi^2 C \lambda_{\text{IR}} = 4 + \varepsilon , \quad (2.12)$$

which is consistent with the IR fixed point being attractive. In fact, from the perspective of the IR fixed point, the RG flow from the deformation of $\lambda = \lambda_{\text{IR}} + \delta\lambda$ should be controlled by the dimension of the operator at the IR fixed point,

$$\beta_{\delta\lambda} = -(4 - \Delta_{\text{IR}}) \delta\lambda + \mathcal{O}(\delta\lambda^2) . \quad (2.13)$$

Taylor expanding Equation (2.9) around the fixed point, one finds $\beta_{\delta\lambda} = \varepsilon \delta\lambda$ as required from Equation (2.12).

Two-point function in de Sitter space: Now let us consider what happens to this theory when we compute late-time correlation functions in dS. At the UV fixed point, the power spectrum in dS follows from the conformal map from flat space to de Sitter, Equation (2.1),

$$\langle \mathcal{O}(\vec{x}_1, \tau_0) \mathcal{O}(\vec{x}_2, \tau_0) \rangle_{*,\text{dS}} = \frac{a(\tau_0)^{-2\Delta}}{x_{12}^{2\Delta}} .$$

We will use conformal perturbation theory in de Sitter, Equation (2.5), to determine the leading correction to this two point function. From the outset, we know the theory in flat space flows to a CFT in the IR where \mathcal{O} acquires a non-trivial anomalous dimension. Therefore, as explained in the introduction, there must be a $\log a(\tau_0)$ divergence associated with this two-point function in de Sitter space. Our goal is to find this divergence explicitly and understand the behavior away from the fixed point.

Equal-time *in-in* correlators are most easily computed using the analytic continuation to Euclidean time, as explained in Appendix 2.A. Applying this formalism at linear order in λ requires that we calculate the quantity

$$\begin{aligned}
I &= -\lambda \mu^\varepsilon \int d^3 x_3 \int_{-\infty}^{\infty} d\tau_E a(i\tau_E + \tau_0)^4 \langle \mathcal{O}(\vec{x}_1, \tau_0) \mathcal{O}(\vec{x}_2, \tau_0) \mathcal{O}(\vec{x}_3, i\tau_E + \tau_0) \rangle_* \\
&= -\lambda \mu^\varepsilon C \frac{a(\tau_0)^{-2\Delta}}{x_{12}^\Delta} \int_{-\infty}^{\infty} d\tau_E \int d^3 x_3 \frac{a(i\tau_E + \tau_0)^\varepsilon}{|x_{23}^2 + \tau_E^2|^{\Delta/2} |x_{31}^2 + \tau_E^2|^{\Delta/2}}. \tag{2.14}
\end{aligned}$$

A priori, it might seem surprising that the above integral contains a divergence as $\tau_0 \rightarrow 0$. At fixed $x_3 \neq x_1, x_2$, the integral in τ_E is manifestly convergent. Similarly, at fixed τ_E the integral over \vec{x}_3 converges. However, we are integrating over both τ_E and \vec{x}_3 and there are divergences associated with taking $\vec{x}_3 \rightarrow \vec{x}_1, \vec{x}_2$ and $\tau_E \rightarrow 0$ simultaneously. We can estimate the degree of this divergence by noting that the integral of \vec{x}_3 around either \vec{x}_1 or \vec{x}_2 is regulated by τ_E so that $\int d^3 x_3 \approx \tau_E^3$. If we then perform the τ_E integral, it scales as $\tau_E^{d-\Delta} = \tau_E^\varepsilon$ which becomes a logarithmic divergence as $\varepsilon \rightarrow 0$.

The integral in Equation (2.14) is performed explicitly in Appendix 2.B.2 using Fourier transforms. The resulting log-divergence arises precisely as expected from the above scaling argument, and leads to

$$I \stackrel{(2.50)}{\approx} -\lambda C \frac{a(\tau_0)^{-2\Delta}}{x_{12}^{2\Delta}} 4\pi^2 \left(\frac{1}{\varepsilon} + \log \left(-\frac{\mu x_{12}}{H \tau_0} \right) - \gamma_E + \dots \right). \tag{2.15}$$

Putting it all together, the two point function of \mathcal{O} is given by

$$\boxed{\langle \mathcal{O}(\vec{x}_1, \tau_0) \mathcal{O}(\vec{x}_2, \tau_0) \rangle_{\text{dS}} = \frac{a(\tau_0)^{-2\Delta}}{x_{12}^{2\Delta}} \left(1 - 4\pi^2 C \lambda \left(\frac{1}{\varepsilon} + \log \left(-\frac{\mu x_{12}}{H \tau_0} \right) + \dots \right) \right)} \quad (2.16)$$

We see that the coefficient of the log is the anomalous dimension in flat space, $4\pi^2 C \lambda = 2\gamma_{\mathcal{O}}$.

2.2.3 Dynamical RG

The two-point function in de Sitter space contains a number of divergent terms. The first thing we should do is remove the $\frac{1}{\varepsilon}$ divergence. Introducing a counterterm $\delta_Z = -\frac{4\pi^2 C \lambda}{\varepsilon}$, we get the renormalized two point function:

$$\begin{aligned} \langle \mathcal{O}_R(\vec{x}_1, \tau_0) \mathcal{O}_R(\vec{x}_2, \tau_0) \rangle &= \frac{a(\tau_0)^{-2\Delta}}{x_{12}^{2\Delta}} \left(1 - 4\pi^2 C \lambda \left(\frac{1}{\varepsilon} + \log \left(-\frac{\mu x_{12}}{H \tau_0} \right) + \dots - \delta_Z \right) \right) \\ &= \frac{a(\tau_0)^{-2\Delta}}{x_{12}^{2\Delta}} \left(1 - 4\pi^2 C \lambda \log \left(-\frac{\mu x_{12}}{H \tau_0} \right) + \dots \right). \end{aligned}$$

The interpretation of the remaining log is more transparent if we separate the two dimensionless ratios as follows,

$$\log \left(-\frac{\mu x_{12}}{H \tau_0} \right) = \log \left(\frac{\mu}{H} \right) + \log \left(\frac{x_{12}}{|\tau_0|} \right). \quad (2.17)$$

The distance must appear in the ratio $x_{12}/|\tau_0|$ in order to remain invariant under the rescaling $x \rightarrow \rho x$ and $a(\tau) \rightarrow \rho^{-1} a(\tau)$ which leaves the metric fixed. Furthermore, additional interactions are known to give rise to pure $\log \mu/H$ [17] and $\log x/\tau$ divergences and therefore must be treated separately.

We can easily eliminate $\log \mu/H$ divergences by choosing $\mu = H$. Physically, this means that we should use standard RG to run the effective couplings of the theory to the energy scale H (or simply define them at the scale H). Since H is fixed in de Sitter, this choice ensures that there will be no large logs associated with μ . We will define $\lambda_H = \lambda(\mu = H)$ as a reminder that we fixed the renormalization scale. This is also a physically sensible result as H is usually the

physical scale where non-trivial (cosmological) correlations are generated.

Renormalization in the conventional sense does not address the logarithmic growth in conformal time. In fact, the mode is only super horizon when, $x_{12}/|\tau_0| \gg 1$, and our log is necessarily large. We can formally resum the large logs in analogy with the renormalization group via the DRG. Following the procedure in [42, 44], we introduce a reference time and distance, τ_* and x_* . We then add a counter-term to the operator, $\delta_Z \rightarrow \delta_Z(1 + 2\pi^2 C \lambda_H \log x_*/|\tau_*|)$, to get

$$\langle \mathcal{O}_R(\vec{x}_1, \tau_0) \mathcal{O}_R(\vec{x}_2, \tau_0) \rangle = \frac{a(\tau_0)^{-2\Delta}}{x_{12}^{2\Delta}} \left[1 - 4\pi^2 C \lambda_H \log \left(\frac{x_{12} \tau_*}{x_* \tau_0} \right) \right].$$

Of course the operators of the theory are independent of x_* and τ_* so that we have a differential equation for the two point function

$$\frac{\partial}{\partial \log(x_*/|\tau_*|)} \langle \mathcal{O}_R(\vec{x}_1, \tau_0) \mathcal{O}_R(\vec{x}_2, \tau_0) \rangle = 2\gamma(H) \langle \mathcal{O}_R(\vec{x}_1, \tau_0) \mathcal{O}_R(\vec{x}_2, \tau_0) \rangle \quad (2.18)$$

where we have defined

$$\gamma(H) = \frac{\partial}{\partial \log(x_*/|\tau_*|)} \delta_Z|_{\mu=H} = 2\pi^2 C \lambda_H + \mathcal{O}(\lambda_H^2). \quad (2.19)$$

Here we make a crucial assumption that all the secular terms can be absorbed with counter-terms such they vanish when $\tau_* = \tau_0$ and $x_* = x_{12}$. We will return to discuss the justification for this assumption.

By construction, x_*/τ_* only appears in the ratio $x_{12} \tau_*/(x_* \tau_0)$ so we can rewrite this equation as

$$\frac{\partial}{\partial \log(x_{12}/|\tau_0|)} \langle \mathcal{O}_R(\vec{x}_1, \tau_0) \mathcal{O}_R(\vec{x}_2, \tau_0) \rangle = -(2\Delta + 2\gamma(H)) \langle \mathcal{O}_R(\vec{x}_1, \tau_0) \mathcal{O}_R(\vec{x}_2, \tau_0) \rangle, \quad (2.20)$$

where we introduced the additional factor of 2Δ to account for the tree-level power spectrum.

We can solve this equation to find

$$\langle \mathcal{O}_R(\vec{x}_1, \tau_0) \mathcal{O}_R(\vec{x}_2, \tau_0) \rangle = \frac{1}{|a(\tau_0)_{x_{12}}|^{2\Delta+2\gamma(H)}} (1 + \mathcal{O}(\lambda_H)) . \quad (2.21)$$

where the $\mathcal{O}(\lambda_H)$ corrections are not logarithmically enhanced. We have used our freedom to choose the overall normalization of the operator to write the result in terms of $a(\tau_0) = -1/(H\tau_0)$.

An important open question we will not address in this work is the range of applicability of the DRG for cosmological correlators. Instead, we will use the proximity to a conformal fixed point ensures that the DRG is accurately resumming our secular terms in the cases of interest. At the conformal fixed point, the DRG will resum all the secular logs as required by symmetry. Away from the fixed point, the structure of perturbation theory ensures the DRG will resum the leading logs as desired. However, for a generic theory in de Sitter space, the applicability of the DRG is less certain. It would be desirable to have a general result, like in flat space [52], that characterizes the validity and limitations of the DRG.

2.2.4 Summary

Using conformal perturbation theory, we have seen that for a theory that flows between two fixed points, the (leading-log) two-point function in de Sitter space is given by

$$\boxed{\langle \mathcal{O}_R(\vec{x}_1, \tau_0) \mathcal{O}_R(\vec{x}_2, \tau_0) \rangle = \frac{1}{|a(\tau_0)_{x_{12}}|^{2\Delta+2\gamma(H)}}} , \quad (2.22)$$

where $\gamma(H) = \gamma(\lambda(\mu = H))$ is the anomalous dimension calculated in flat space at the renormalization scale $\mu = H$. Since the correlators in de Sitter are invariant under the group of de Sitter isometries, the higher point correlators must be de Sitter invariant with an effective scaling dimension of $\bar{\Delta} = \Delta + \gamma(H)$.

The derivation of this result implicitly assumed that we were studying a deformation by a slightly relevant operator. However, we must also find the same result from the perspective of

the IR fixed point, in which case the deformation would have been slightly irrelevant.

These results will apply to a wide range of interacting theories, including massless particles with spin and conformally coupled scalars. When these theories are perturbative, they are close to the Gaussian fixed point and therefore can be understood as being close to a CFT. Light scalar fields in de Sitter are not captured by this description because Equation (2.1) does not apply when $m^2/H^2 \neq d(d-2)/4$.

2.3 Scalar Field Theory

We would like to see how the general behavior described in Section 2.2 arises in explicit examples. In this section, we will calculate the power spectrum of the ϕ^2 operator in the $\lambda\phi^4$ theory in dS. These types of self-interactions are particularly common for inflationary models and are of broad interest. From flat space, we know an anomalous dimension arises at one-loop and thus the same should be true in de Sitter. Furthermore, by choosing $d = 4 - \epsilon$, the theory flows to the Wilson-Fisher fixed point and, as a consequence, the dynamics in de Sitter must approach the behavior of the CFT by construction.

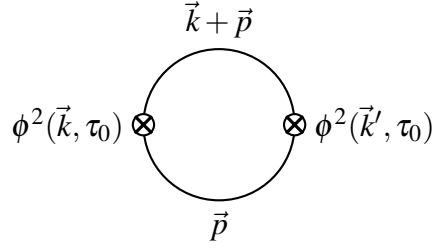
2.3.1 The $\langle\phi^2\phi^2\rangle$ correlator

Given a free real scalar field ϕ of mass m in de Sitter space, one expands the fields in modes according to

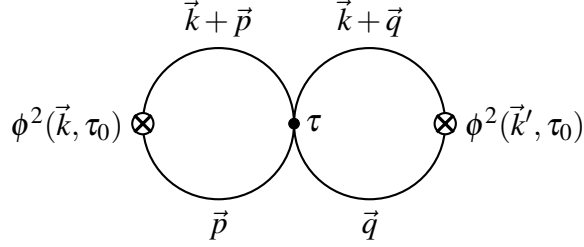
$$\phi(\vec{x}, \tau) = \int \frac{d^{d-1}k}{(2\pi)^{d-1}} e^{i\vec{k}\cdot\vec{x}} \{v_{\vec{k}}(\tau)a_{\vec{k}} + v_{\vec{k}}^*(\tau)a_{\vec{k}}^\dagger\}.$$

In the Bunch-Davies vacuum, the modes are given by

$$v_{\vec{k}}(\tau) = -ie^{i(v+\frac{1}{2})\frac{\pi}{2}} \frac{\sqrt{\pi}}{2} H^{\frac{d-2}{2}}(-\tau)^{\frac{d-1}{2}} H_\nu(-k\tau),$$



(a) The tree level diagram



(b) The order λ correction

Figure 2.1. The Feynman diagrams involved in the calculation of $\langle \phi^2 \phi^2 \rangle$.

where $k = |\vec{k}|$ and H_ν is the Hankel function of the first kind with $\nu = \sqrt{\frac{(d-1)^2}{4} - \frac{m^2}{H^2}}$. The free field theory in flat space maps to the conformal theory with mass $m^2 = d(d-2)H^2/4$ in dS, which means $\nu = \frac{1}{2}$. Therefore the mode functions are

$$v_{\vec{k}}(\tau) = \frac{-i}{a(\tau)^{\frac{d-2}{2}}} \frac{e^{-ik\tau}}{\sqrt{2k}}.$$

These are just the modes for a free massless theory in flat space, scaled by factors of $a^{-\Delta_\phi}$ as it should be in a conformal field theory.

As explained in Appendix 2.A, we can compute equal-time (*in-in*) correlation functions as an anti-time-ordered Euclidean correlation function. The anti-time-ordered propagator for our perturbative calculations is therefore

$$\langle \bar{T} \left(\phi(\vec{k}, i\tau_E + \tau_0) \phi(-\vec{k}, \tau_0) \right) \rangle = \frac{1}{a(i\tau_E + \tau_0)^{\Delta_\phi} a(\tau_0)^{\Delta_\phi}} \frac{e^{-k|\tau_E|}}{2k}. \quad (2.23)$$

Note that $\tau_0 < 0$ will be fixed throughout the calculation and $\tau_E \in (-\infty, \infty)$.

We begin by computing the equal-time *in-in* correlator $\langle \phi^2 \phi^2 \rangle$ in $d = 4 - \varepsilon$ dimensions using the expression [53]

$$\langle \phi^2(\vec{k}, \tau_0) \phi^2(-\vec{k}, \tau_0) \rangle = \langle \bar{T} \left(\phi^2(\vec{k}, \tau_0) \phi^2(-\vec{k}, \tau_0) \exp \left[- \int_{-\infty}^{\infty} d\tau_E H_{\text{int}}(i\tau_E + \tau_0) a(i\tau_E + \tau_0) \right] \right) \rangle, \quad (2.24)$$

where $H_{\text{int}}(\tau) = +\frac{\lambda\mu^\varepsilon}{4!} \int d^{d-1}x \sqrt{-g} \phi^4(\tau, x)$. The lowest order term in this expansion corresponds to Fig. 2.1a and it evaluates to

$$\langle \phi^2(\vec{k}, \tau_0) \phi^2(-\vec{k}, \tau_0) \rangle_* = \frac{1}{2a^{4\Delta_\phi}(\tau_0)} \int \frac{d^D p}{(2\pi)^D} \frac{1}{|\vec{k} + \vec{p}|^p} = \frac{c}{2a(\tau_0)^{2\Delta_\phi^2}} k^{1-\varepsilon}, \quad (2.25)$$

where $D = 3 - \varepsilon$, $d = D + 1$ and $c \approx -1/(4\pi^2)$ is a constant (see (2.53)). Note that, $\Delta_\phi = \frac{d-2}{2}$ and $\Delta_{\phi^2} = d - 2$. The computation of the momentum integral is detailed in Appendix 2.B.3.

Now we can calculate the first order correction to $\langle \phi^2 \phi^2 \rangle$ from the diagram in Figure 3.7. Expanding Equation (2.24) to first order gives

$$\begin{aligned} & -\frac{\lambda\mu^\varepsilon}{4!} \langle \bar{T} \left(\phi^2(\vec{k}, \tau_0) \phi^2(-\vec{k}, \tau_0) \int_{-\infty}^{\infty} d\tau_E a(\tau_3)^{D+1} \phi^4(\tau_3) \right) \rangle \\ & = -\lambda\mu^\varepsilon \int_{-\infty}^{\infty} d\tau_E a^d(\tau_3) \left(\int \frac{d^D p}{(2\pi)^D} \frac{1}{a(\tau_3)^{2\Delta_\phi} a(\tau_0)^{2\Delta_\phi}} \frac{e^{-|\vec{k}+\vec{p}||\tau_E|} e^{-p|\tau_E|}}{2|\vec{k}+\vec{p}|} \frac{1}{2p} \right)^2. \end{aligned} \quad (2.26)$$

We have used the shorthand $\tau_3 \equiv i\tau_E + \tau_0$ in the interest of space. The loop integral in the parentheses is computed in (2.56). Substituting this into (2.26) the first order correction simplifies to

$$-\lambda\mu^\varepsilon \frac{k^{1-\varepsilon}}{a(\tau_0)^{4\Delta_\phi}} M^2 \int_{-\infty}^{\infty} d\tau_E \frac{a(i\tau_E + \tau_0)^\varepsilon}{|\tau_E|^{1-\varepsilon}} K_{\frac{\varepsilon-1}{2}}^2(k|\tau_E|). \quad (2.27)$$

Comparing this with (2.25) we see that tree level behavior of the correlation function has already factorized out.

Finally, we are left with only the time integral to compute. This integral is the source of

the secular divergence. In the limit $|\vec{k}\tau_0| \ll 1$ and $\varepsilon \rightarrow 0$, (2.27) is approximately

$$+\frac{\lambda}{64\pi^4} \frac{k^{1-\varepsilon}}{a(\tau_0)^{4\Delta_\phi}} \left(\frac{1}{\varepsilon} + \log\left(\frac{\mu}{H}\right) - \log(-k\tau_0) + \dots \right), \quad (2.28)$$

where \dots are terms that vanish in the limit $|\vec{k}\tau_0| \ll 1$. The $\langle \phi^2 \phi^2 \rangle$ correlation function at order λ is then

$$\langle \phi^2(\vec{k}, \tau_0) \phi^2(-\vec{k}, \tau_0) \rangle = \frac{c}{2a(\tau_0)^{2\Delta_{\phi^2}}} k^{1-\varepsilon} \left[1 + \frac{\lambda}{32\pi^4 c} \left(\frac{1}{\varepsilon} + \log\left(\frac{\mu}{H}\right) - \log(-k\tau_0) + \dots \right) \right]. \quad (2.29)$$

Removing the divergence in (2.29) and performing a dynamic RG resummation:

$$\begin{aligned} \langle \phi^2(\vec{k}, \tau_0) \phi^2(-\vec{k}, \tau_0) \rangle &\stackrel{\mu=H}{=} \frac{c}{2a(\tau_0)^{2\Delta_{\phi^2}}} k^{1-\varepsilon} \exp\left(-\frac{\lambda_H}{32\pi^4 c} \log(-k\tau_0) + \dots\right) (1 + \dots) \\ &= \frac{c}{2a(\tau_0)^{2\Delta_{\phi^2}}} k^{1-\varepsilon} (-k\tau_0)^{2\gamma_{\phi^2}(H)} (1 + O(\lambda_H^2)) \\ &= \frac{cH^{-2\gamma_{\phi^2}(H)}}{2a(\tau_0)^{2\Delta_{\phi^2}+2\gamma_{\phi^2}(H)}} k^{1-\varepsilon+2\gamma_{\phi^2}(H)} (1 + O(\lambda_H^2)) \end{aligned}$$

where

$$\gamma_{\phi^2}(H) = -\frac{\lambda_H}{64\pi^4 c} = +\frac{\lambda_H}{16\pi^2}. \quad (2.30)$$

Comparing with (2.25) we see that the effective dimension of the ϕ^2 operator is corrected to:

$$\Delta_{\phi^2} \rightarrow \Delta_{\phi^2} + \gamma_{\phi^2}(H) = 2 - \varepsilon + \frac{\lambda_H}{16\pi^2}$$

which is precisely $\Delta_{\phi^2} + \gamma_{\phi^2}(\mu = H)$ at one-loop, where $\gamma_{\phi^2}(\mu = H)$ is the anomalous dimension in flat space at the scale $\mu = H$.

2.3.2 Implications for $\lambda\phi^4$ in Four-Dimensions

As we discussed in Section 2.2.4, our results don't crucially require that there is an interacting IR fixed point. As such, we can also view the above calculation as the dimensional regularization of $\lambda\phi^4$ in four-dimensions by taking the $\varepsilon \rightarrow 0$ limit. In that case,

$$\Delta_{\phi^2} = 2 + \frac{\lambda_H}{16\pi^2} \quad (2.31)$$

where $\lambda_H = \lambda(\mu = H)$ as before. Unlike the $\varepsilon > 0$ case, in four-dimensions the theory flows to the trivial fixed point in the IR, $\lambda(\mu \rightarrow 0) = 0$. Nevertheless, since the anomalous dimension is fixed at $\mu = H$ we still have a finite λ_H . As a result, the power spectrum of ϕ^2 in de Sitter space will acquire a fixed anomalous scaling with time and space in the super-horizon limit.

We can similarly conclude that conformally coupled scalars in de Sitter will acquire anomalous scaling in four-dimensions. The anomalous dimension for ϕ in $\lambda\phi^4$ is generated at two-loops and a direct calculation is beyond the scope of this work. Nevertheless, we can conclude that such a two-loop de Sitter calculation should find that Equation (2.22) holds with

$$\gamma_\phi(H) = \frac{\lambda_H^2}{12(4\pi)^4}, \quad (2.32)$$

in accordance with the anomalous dimension in flat space.

2.4 Yukawa Interaction

As a final example, we will study the RG flow of a scalar field theory in $d = 4$ dimensions that is perturbed by a Yukawa coupling $\mathcal{L}_{\text{int}} = \lambda\phi\bar{\psi}\psi$, where ψ is a massless Dirac fermion. In flat space, ϕ acquires an anomalous dimension at one loop and therefore will exhibit a 1-loop secular divergence in dS. In this sense, the Yukawa coupling is the simplest example where the power spectrum of a fundamental scalar (as opposed to a composite operator) exhibits secular divergences of the type discussed in this paper.

The calculation of this effect does not require us to discuss the mode functions of the fermions directly. For the purpose of our calculation, $\bar{\psi}\psi = \mathcal{O}$ is just an operator of dimension $\Delta = 3 - \varepsilon$ in a free CFT, where we have introduced ε as our regulator. We can therefore use the action

$$S[\phi] + \lambda \mu^\varepsilon \int d^4x \sqrt{|g|} \phi \mathcal{O} \quad (2.33)$$

and evaluate the correlation functions of \mathcal{O} using the same conformal perturbation theory approach described in Equation (2.5).

The two point correlation function for ϕ receives a 1-loop ($O(\lambda^2)$) correction from the Yukawa interaction,

$$I \equiv \langle \phi(\vec{k}, \tau_0) \phi(-\vec{k}, \tau_0) \rangle_{1\text{-loop}} = \frac{(\lambda \mu^\varepsilon)^2}{2!} \int_{-\infty}^{\infty} d\tau_E a^4(\tau) \int_{-\infty}^{\infty} d\tau'_E a^4(\tau') \quad (2.34)$$

$$\langle \bar{T} \left(\phi(\vec{k}, \tau_0) \phi(-\vec{k}, \tau_0) \phi(-\vec{k}, \tau) \mathcal{O}(\vec{k}, \tau) \phi(\vec{k}, \tau') \mathcal{O}(-\vec{k}, \tau') \right) \rangle ,$$

where $\tau \equiv i\tau_E + \tau_0$ and $\tau' \equiv i\tau'_E + \tau_0$. We evaluate this correlator by Fourier transforming the real-space correlation function of \mathcal{O} given in Equation (2.1). Using (2.61) and (2.23) in (2.58), we find

$$I = \frac{(\lambda \mu^\varepsilon)^2}{a(\tau_0)^2} N \int_{-\infty}^{\infty} d\tau_E a^\varepsilon(\tau) \int_{-\infty}^{\infty} d\tau'_E a^\varepsilon(\tau') \int_{-\infty}^{\infty} \frac{d\omega}{2\pi} \frac{e^{-k(|\tau_E| + |\tau'_E|) + i\omega(\tau_E - \tau'_E)}}{(2k)^2} (k^2 + \omega^2)^{1-\varepsilon}$$

$$= \frac{(\lambda \mu^\varepsilon)^2}{a(\tau_0)^2} N \int_{-\infty}^{\infty} \frac{d\omega}{2\pi} \mathcal{J}(\omega, k) \mathcal{J}(-\omega, k) (k^2 + \omega^2)^{1-\varepsilon} , \quad (2.35)$$

where we have factorized the two time integrals by defining:

$$\mathcal{J}(\omega, k) = \int_{-\infty}^{\infty} d\tau_E a^\varepsilon(i\tau_E + \tau_0) \frac{e^{-k|\tau_E| + i\omega\tau_E}}{2k} . \quad (2.36)$$

We could compute this integral explicitly and substitute it back into (2.35) to proceed. However, the calculations become complicated if we take that route. We will therefore pursue a simpler

strategy: first, we will evaluate (2.36) in flat space-time i.e. we set $a(\tau) = 1$. Next, we will compute (2.36) setting $\tau_0 = 0$. In each case we substitute the result back into (2.35) and extract the $\varepsilon \rightarrow 0$ behavior. The final answer for the general $\tau_0 \neq 0$ case is then obtained by requiring that it match with these calculations in the respective limits. The details are given in Appendix 2.B.4; the final results are (see (2.62) and (2.64))

$$I \stackrel{a=1}{=} -\frac{\lambda^2}{16\pi^2 k} \left(\frac{1}{\varepsilon} + 2\log\left(\frac{\mu}{k}\right) - \gamma_E + \dots \right) \quad (2.37)$$

$$I \stackrel{\tau_0 \rightarrow 0}{=} -\frac{\lambda^2}{16\pi^2 a(\tau_0)^2 k} \left(\frac{1}{\varepsilon} + 2\log\left(\frac{\mu}{H}\right) + \mathcal{A} + \dots \right), \quad (2.38)$$

where \mathcal{A} is a divergent piece defined in (2.65). Requiring that the general answer must reduce to these expressions, we find the first order correction (2.35) is

$$I \stackrel{\varepsilon, \tau_0 \rightarrow 0}{\approx} -\frac{\lambda^2}{16\pi^2 a(\tau_0)^2 k} \left(\frac{1}{\varepsilon} + 2\log\left(-\frac{\mu}{kH\tau_0}\right) + \dots \right). \quad (2.39)$$

Note that setting $\tau_0 = 0$ in the log will cause it to blow up. This is the origin of the term \mathcal{A} in (2.38). Putting it all together, $\langle \phi \phi \rangle$ is

$$\langle \phi(\vec{k}, \tau_0) \phi(-\vec{k}, \tau_0) \rangle = \frac{1}{2a(\tau_0)^2 k} \left(1 - \frac{\lambda^2}{8\pi^2} \left(\frac{1}{\varepsilon} + 2\log\left(-\frac{\mu}{kH\tau_0}\right) + \dots \right) \right). \quad (2.40)$$

We remove the divergence in (2.40) using a counterterm $\delta_Z = -\frac{\pi^2 \lambda^2}{8\varepsilon}$ and perform a dynamical RG resummation to find

$$\langle \phi(\vec{k}, \tau_0) \phi(-\vec{k}, \tau_0) \rangle \stackrel{\mu=H}{=} \frac{H^{-2\gamma_\phi(H)}}{2a(\tau_0)^{2+2\gamma_\phi(H)} k^{1-2\gamma_\phi(H)}},$$

where

$$\gamma_\phi(H) = +\frac{\lambda_H^2}{8\pi^2}. \quad (2.41)$$

Comparing with (2.23) we see that the dimension of the ϕ^2 operator is corrected to:

$$\Delta_\phi \rightarrow \Delta_\phi + \gamma_\phi(H) = 1 + \frac{\lambda_H^2}{8\pi^2}.$$

As expected, $\gamma_\phi(H)$ is precisely the anomalous dimension found in four-dimensional flat space from a Yukawa coupling of a scalar to a Dirac fermion.

2.5 Conclusions

Secular divergences present a significant challenge to perturbative calculations of cosmological correlators. In this paper, we have shown that a certain class of such divergences have their origins as anomalous dimensions in flat space. Like anomalous dimensions, they can be resummed to give corrections to the power law behavior at late times. This interpretation of the divergences is unambiguous as this resummation is required to match the predictions at the conformal fixed point.

Our results apply to a wide range of quantum field theories in de Sitter space. Massless particles with spin are generically conformally coupled and admit a description in terms of conformal perturbation theory. In contrast, scalar fields with generic masses are not conformal in de Sitter and thus our treatment is limited to the case $m^2 \approx d(d-2)H^2/4$. Scalar fields of generic masses are far from conformal and display a wider range of IR phenomena not addressed here. Ultimately, one hopes to have a complete understanding of secular divergences both of quantum fields in de Sitter and in the presence of dynamical gravity.

The main conclusion from this paper is that there is a broad class of secular divergences that is expected in QFT in de Sitter space and has an unambiguous and simple interpretation. The meaning of IR divergences in de Sitter (particularly in the presence of gravity) has been the subject of significant ongoing interest and we believe these simple calculable examples can serve as a useful test-bed for future investigations.

The broader problem of characterizing all possible IR divergences of cosmological

correlators remains an outstanding problem. Significant progress has been made recently on the divergences associated with massless scalars in de Sitter [30, 31, 32] and ultimately confirm the validity of the stochastic inflation framework [11] for understanding the non-trivial long distance behavior. While light scalar fields have certainly presented a unique challenge to perturbative calculations, we have seen here that there are still secular terms associated with massive fields that arise as an interplay between the short-distance and late-time behavior. A complete understanding of all such divergences at the same level as QFT in flat space would be a desirable outcome of a renewed focus on IR effects in de Sitter.

Acknowledgements

We are grateful to Daniel Baumann, Matthew Baumgart, Tim Cohen, Victor Gorbenko, Enrico Pajer and Ben Wallisch for helpful conversations. D. G. is supported by the US Department of Energy under grant no. DE-SC0019035.

This chapter, in full, is a reprint of the material as it appears in Daniel Green, Akhil Premkumumar, *Journal of High Energy Physics* **04** (2020) 064. The dissertation author was one of the primary investigators and authors of this paper.

2.A Analytic Continuation of the In-In Formalism

Throughout the paper, we have integrated in Euclidean time to simplify time integration. In this appendix, we will review this procedure following [53].

We will use the in-in formalism to define equal-time correlations functions in the Bunch-Davies vacuum. These are most easily calculated using the interaction picture operators Q_{int} and Hamiltonian $H_{\text{int}}(t)$ via [15]

$$\langle Q(\tau_0) \rangle = \left\langle \bar{T} \exp \left[i \int_{-\infty(1+i\epsilon)}^{\tau_0} H_{\text{int}}(\tau) a(\tau) d\tau \right] Q_{\text{int}}(\tau_0) T \exp \left[-i \int_{-\infty(1-i\epsilon)}^{\tau_0} H_{\text{int}}(\tau) a(\tau) d\tau \right] \right\rangle . \quad (2.42)$$

The Hamiltonian is given in terms of a Hamiltonian density, $\mathcal{H}_{\text{int}}(\tau, x)$, via

$$H_{\text{int}}(\tau) = \int d^3x a^3(\tau) \mathcal{H}_{\text{int}}(\tau, x) . \quad (2.43)$$

The deformation of the contour by a factor of $(1 \pm i\epsilon)$ defines the Bunch-Davies vacuum and ensures that the integrals converge as $\tau \rightarrow -\infty$. We can make this convergence manifest by Wick rotating the contours on the left and right of the operator by $\tau \rightarrow \pm i\tau_E + \tau_0$ [54, 53]. The resulting expression for the in-in correlators becomes an anti-time ordered integral

$$\langle \mathcal{Q}(\tau_0) \rangle = \left\langle \bar{T} \left(\mathcal{Q}_{\text{int}}(\tau_0) \exp \left[- \int_{-\infty}^{\infty} H_{\text{int}}(i\tau_E + \tau_0) a(i\tau_E + \tau_0) d\tau_E \right] \right) \right\rangle \quad (2.44)$$

This is particularly useful for CFT correlators, where the anti-time order correlators in Euclidean time are given by

$$\langle \mathcal{O}(i\tau_E + \tau_0, \vec{x}) \mathcal{O}(i\tau'_E + \tau_0, \vec{x}') \rangle = \frac{a(i\tau_E + \tau_0)^{-\Delta} a(i\tau'_E + \tau_0)^{-\Delta}}{[(\tau_E - \tau'_E)^2 + (\vec{x} - \vec{x}')^2]^\Delta} \quad (2.45)$$

$$\langle \mathcal{O}(\vec{x}_1, i\tau_1) \mathcal{O}(\vec{x}_2, i\tau_2) \mathcal{O}(\vec{x}_3, i\tau_3) \rangle = \frac{C a(i\tau_1)^{-\Delta} a(i\tau_2)^{-\Delta} a(i\tau_3)^{-\Delta}}{|x_{12}^2 + \tau_{12}^2|^{\Delta/2} |x_{23}^2 + \tau_{23}^2|^{\Delta/2} |x_{31}^2 + \tau_{31}^2|^{\Delta/2}} , \quad (2.46)$$

where $\tau_{ij} = \tau_i - \tau_j$ and $\vec{x}_{ij} = \vec{x}_i - \vec{x}_j$. We left the τ_0 dependence in Equation (2.46) implicit in the interest of space. It is important to notice that all correlators are calculated at equal Lorentzian time, τ_0 , and therefore the τ_0 dependence cancels in τ_{ij} , as shown explicitly in Equation (2.45).

2.B Details of Loop Integration

The explicit calculations of some of the loop integrals in the main text are performed in this appendix. A number of these integrals are divergent but are made finite with dimensional regularization and/or analytic continuation. We will therefore explain the regularization schemes first and then apply it to the integrals needed for the main text.

2.B.1 Dimensional Regularization

Throughout this paper, integrals are regulated by a parameter ε that controls the scaling behavior of the integral. This may or may not be related to the dimension of space-time, as indicated in each section. In Section 2.2, we have general dimension d and an operator of dimension $\Delta = d - \varepsilon$, where d and ε are independent parameters. It is therefore useful to think of the d and Δ dependence of these integrals as independent.

We will often be interested in d -dimensional radial Fourier transform of the correlation functions. As a result, we often have to evaluate the following integral

$$\frac{1}{|\mathbf{x}|^{2\Delta}} = \pi^{\frac{d}{2}} 2^{d-2\Delta} \frac{\Gamma(\frac{d}{2} - \Delta)}{\Gamma(\Delta)} \int \frac{d^d k}{(2\pi)^d} e^{i\mathbf{k}\cdot\mathbf{x}} \frac{1}{|\mathbf{k}|^{d-2\Delta}}. \quad (2.47)$$

This integral is convergent for $2\Delta < d$. We will not be in this regime, but we will define the integral at other values of Δ by analytic continuation of the above formula. This is a standard technique in QFT but is also commonly used as a definition of the Fourier transform. This choice is justified because the divergent contributions we are neglecting are associated with δ -functions in position space (contact terms) and therefore vanish when $x \neq 0$.

For conformal perturbation theory, one is often calculating an integral over a conformal three-point function. Using Equation (3.42) and the convolution theorem, it is straightforward to show that

$$\int \frac{d^d x_3}{(x_{13}^2)^\Delta (x_{32}^2)^\Delta} = \pi^{\frac{d}{2}} \left(\frac{\Gamma(\frac{d}{2} - \Delta)}{\Gamma(\Delta)} \right)^2 \frac{\Gamma(2\Delta - \frac{d}{2})}{\Gamma(d - 2\Delta)} \frac{1}{x_{12}^{4\Delta - d}}. \quad (2.48)$$

This result is again defined by analytic continuation, the divergent contributions are contact terms and vanish when $x_{12} \neq 0$.

2.B.2 de Sitter Conformal Perturbation Theory

The leading correction to the two point correlation function $\langle \mathcal{O} \mathcal{O} \rangle$ in de Sitter space involves the integral (see (2.14))

$$I = -\lambda \mu^\varepsilon C \frac{a(\tau_0)^{-2\Delta}}{x_{12}^\Delta} \int_{-\infty}^{\infty} d\tau_E \int d^3 x_3 \frac{a(i\tau_E + \tau_0)^\varepsilon}{|x_{23}^2 + \tau_E^2|^{\Delta/2} |x_{31}^2 + \tau_E^2|^{\Delta/2}} .$$

Shifting $\vec{x}_3 \rightarrow \vec{x}_3 + \vec{x}_1$, we see that the \vec{x}_3 integral is just a convolution of the function $F(\vec{x}, \tau_E) = (x^2 + \tau_E^2)^{-\Delta/2}$ with itself,

$$\begin{aligned} I &= -\lambda \mu^\varepsilon C \frac{a(\tau_0)^{-2\Delta}}{x_{12}^\Delta} \int_{-\infty}^{\infty} d\tau_E a(i\tau_E + \tau_0)^\varepsilon \int d^3 x_3 \frac{1}{|(\vec{x}_{21} - \vec{x}_3)^2 + \tau_E^2|^{\Delta/2} |x_3^2 + \tau_E^2|^{\Delta/2}} \\ &= -\lambda \mu^\varepsilon C \frac{a(\tau_0)^{-2\Delta}}{x_{12}^\Delta} \int_{-\infty}^{\infty} d\tau_E a(i\tau_E + \tau_0)^\varepsilon \int \frac{d^3 k}{(2\pi)^3} e^{i\vec{k} \cdot \vec{x}_{21}} \tilde{F}(\vec{k}, \tau_E)^2 . \end{aligned}$$

In the last step, we have applied the convolution theorem,

$$\int d^D y F(\vec{x} - \vec{y}) F(\vec{y}) = \int \frac{d^D k}{(2\pi)^D} e^{i\vec{k} \cdot \vec{x}} \tilde{F}(\vec{k})^2 , \quad (2.49)$$

and introduced

$$\tilde{F}(\vec{k}, \tau_E) = \int d^3 x e^{-i\vec{k} \cdot \vec{x}} \frac{1}{(x^2 + \tau_E^2)^{\Delta/2}} = \frac{2\pi^{3/2}}{\Gamma(2 - \frac{\varepsilon}{2})} \left(\frac{k}{2|\tau_E|} \right)^{\frac{1-\varepsilon}{2}} K_{\frac{\varepsilon-1}{2}}(k|\tau_E|) .$$

The full expression is therefore

$$\begin{aligned} I &= -\lambda \mu^\varepsilon C \frac{a(\tau_0)^{-2\Delta}}{x_{12}^\Delta} \int_{-\infty}^{\infty} d\tau_E a(i\tau_E + \tau_0)^\varepsilon \\ &\quad \times \int \frac{d^3 k}{(2\pi)^3} e^{i\vec{k} \cdot \vec{x}_{21}} \frac{4\pi^3}{\Gamma(2 - \frac{\varepsilon}{2})^2} \left(\frac{k}{2|\tau_E|} \right)^{1-\varepsilon} \left(K_{\frac{\varepsilon-1}{2}}(k|\tau_E|) \right)^2 . \end{aligned}$$

Computing the k integral,

$$I = -\lambda \mu^\varepsilon C \frac{a(\tau_0)^{-2\Delta}}{x_{12}^\Delta} \frac{4\pi^2}{\Gamma(2-\frac{\varepsilon}{2})^2} \int_{-\infty}^{\infty} d\tau_E a(i\tau_E + \tau_0)^\varepsilon \\ \times 2^{-5+\varepsilon} |\tau_E|^{-5+2\varepsilon} \Gamma\left(\frac{5}{2}-\varepsilon\right) \Gamma\left(2-\frac{\varepsilon}{2}\right) {}_2\tilde{F}_1\left(\frac{5}{2}-\varepsilon, 2-\frac{\varepsilon}{2}; \frac{5}{2}-\frac{\varepsilon}{2}; -\frac{x_{12}^2}{4\tau_E^2}\right).$$

where ${}_2\tilde{F}_1$ is the regularized hypergeometric function. Carrying out the integral over τ_E and taking the limits $\varepsilon \rightarrow 0$ and $\tau_0 \rightarrow 0$, we get

$$I \approx -\lambda C \frac{a(\tau_0)^{-2\Delta}}{x_{12}^{2\Delta}} 4\pi^2 \left(\frac{1}{\varepsilon} + \log\left(-\frac{\mu x_{12}}{H \tau_0}\right) - \gamma_E + \dots \right). \quad (2.50)$$

2.B.3 Integrals in the $\lambda \phi^4$ theory

The equal time correlation function for the ϕ^2 operator (see Equation (2.25) and Fig. 2.1a) involves the loop integral

$$\int \frac{d^D p}{(2\pi)^D} \frac{1}{|\vec{k} + \vec{p}| p}. \quad (2.51)$$

Usually, one computes loop integrals like this with Feynman parameters. However, there is another way to do this calculation which is particularly useful for unequal times. We notice that the integral (2.51) is just a convolution of the function k^{-1} with itself. Therefore, we can use the convolution theorem in the form

$$\int \frac{d^D p}{(2\pi)^D} \tilde{F}(\vec{k} - \vec{p}) \tilde{F}(\vec{p}) = \int d^D x e^{-i\vec{k}\cdot\vec{x}} F(\vec{x})^2, \quad (2.52)$$

i.e. $\tilde{F} * \tilde{F} \xrightarrow{F.T} F^2$. If $\tilde{F}(\vec{p})$ is radially symmetric we can change $\vec{p} \rightarrow -\vec{p}$ without changing the result. Therefore, all we need to do is find the Fourier transform of k^{-1} and square it. Using (3.42) we see that $2\pi^2 k^{-1} \xrightarrow{F.T} x^{-2+\varepsilon}$ and therefore

$$\int \frac{d^{3-\varepsilon} k}{(2\pi)^{3-\varepsilon}} \frac{1}{|\vec{k} + \vec{p}| p} \stackrel{(2.52)}{=} \int d^{3-\varepsilon} x e^{-i\vec{k}\cdot\vec{x}} \left(\frac{1}{2\pi^2 x^{2-\varepsilon}} \right)^2 \stackrel{(3.42)}{=} c k^{1-\varepsilon},$$

where

$$c = \frac{\Gamma\left(1 - \frac{\varepsilon}{2}\right)^2 \Gamma\left(\frac{\varepsilon-1}{2}\right)}{2^{3-\varepsilon} \pi^{\frac{5-\varepsilon}{2}} \Gamma(2-\varepsilon)} \approx -\frac{1}{4\pi^2} + O(\varepsilon). \quad (2.53)$$

We can use the same strategy to evaluate the loop integral in (2.26),

$$\int \frac{d^{3-\varepsilon} p}{(2\pi)^{3-\varepsilon}} \frac{e^{-|\vec{k}+\vec{p}|\tau_E} e^{-p|\tau_E|}}{2|\vec{k}+\vec{p}|} \frac{1}{2p}. \quad (2.54)$$

Notice that the loop integral is a convolution of the function $\tilde{F}(\vec{k}) = \frac{e^{-k|\tau_E|}}{2k}$ with itself. Moreover

$$\frac{e^{-k|\tau_E|}}{2k} = \int_{-\infty}^{\infty} \frac{d\omega}{2\pi} e^{i\omega\tau_E} \frac{1}{\omega^2 + k^2} \equiv \tilde{F}(\vec{k}),$$

and therefore the Fourier transform of the function $\tilde{F}(\vec{k})$ is

$$\begin{aligned} F(\vec{x}) &= \int \frac{d^D k}{(2\pi)^D} \frac{e^{-k|\tau_E| + i\vec{k}\cdot\vec{x}}}{2k} = \int \frac{d^D k}{(2\pi)^D} \int \frac{d\omega}{2\pi} e^{i\omega\tau_E + i\vec{k}\cdot\vec{x}} \frac{1}{\omega^2 + k^2} \\ &\stackrel{(3.42)}{=} \frac{\Gamma\left(\frac{2-\varepsilon}{2}\right)}{\pi^{\frac{4-\varepsilon}{2}} 2^2} \frac{1}{(x^2 + \tau_E^2)^{\frac{2-\varepsilon}{2}}}. \end{aligned}$$

We can now apply the convolution theorem (2.52) to the loop integral in (2.54) to find

$$\int \frac{d^{3-\varepsilon} p}{(2\pi)^{3-\varepsilon}} \frac{e^{-|\vec{k}+\vec{p}|\tau_E} e^{-p|\tau_E|}}{2|\vec{k}+\vec{p}|} \frac{1}{2p} = \frac{\Gamma^2\left(\frac{2-\varepsilon}{2}\right)}{\pi^{4-\varepsilon} 2^4} \int d^{3-\varepsilon} x \frac{e^{-i\vec{k}\cdot\vec{x}}}{(x^2 + \tau_E^2)^{2-\varepsilon}}. \quad (2.55)$$

This result can be simplified using (3.42) if we turn $d^D x e^{-i\vec{k}\cdot\vec{x}} \rightarrow d^d x e^{-i\mathbf{K}\cdot\mathbf{x}}$ where $\mathbf{K} \equiv (\omega, \vec{k})$ and $\mathbf{x} \equiv (\tau, \vec{x})$. To accomplish this we rewrite

$$\frac{1}{(x^2 + \tau_E^2)^{2-\varepsilon}} = \int_{-\infty}^{\infty} d\tau \delta(\tau - \tau_E) \frac{1}{(x^2 + \tau^2)^{2-\varepsilon}} = \int_{-\infty}^{\infty} d\tau \int_{-\infty}^{\infty} d\omega e^{-i\omega(\tau - \tau_E)} \frac{1}{(x^2 + \tau^2)^{2-\varepsilon}},$$

so that our integral becomes

$$\begin{aligned}
\int d^{3-\varepsilon}x \frac{e^{-i\vec{k}\cdot\vec{x}}}{(x^2 + \tau_E^2)^{2-\varepsilon}} &= \int_{-\infty}^{\infty} d\omega e^{i\omega\tau_E} \int d^{4-\varepsilon}x \frac{e^{-i\mathbf{K}\cdot\mathbf{x}}}{|\mathbf{x}|^{4-2\varepsilon}} \\
&\stackrel{(3.42)}{=} \pi^{\frac{4-\varepsilon}{2}} 2^\varepsilon \frac{\Gamma(\frac{\varepsilon}{2})}{\Gamma(2-\varepsilon)} \int_{-\infty}^{\infty} d\omega \frac{e^{i\omega\tau_E}}{(\omega^2 + k^2)^{\varepsilon/2}} \\
&= \frac{\pi^{\frac{3-\varepsilon}{2}} 2^{\frac{1+\varepsilon}{2}}}{\Gamma(2-\varepsilon)} \left(\frac{k}{|\tau_E|} \right)^{\frac{1-\varepsilon}{2}} K_{\frac{\varepsilon-1}{2}}(k|\tau_E|) ,
\end{aligned}$$

where $K_\nu(z)$ is the modified Bessel function of the second kind. Plugging this back into Equation (2.55), the loop integral turns out to be

$$\int \frac{d^{3-\varepsilon}p}{(2\pi)^{3-\varepsilon}} \frac{e^{-|\vec{k}+\vec{p}||\tau_E|} e^{-p|\tau_E|}}{2|\vec{k}+\vec{p}|} \frac{1}{2p} = M \left(\frac{k}{|\tau_E|} \right)^{\frac{1-\varepsilon}{2}} K_{\frac{\varepsilon-1}{2}}(k|\tau_E|) \quad (2.56)$$

where

$$M = \frac{\Gamma^2(\frac{2-\varepsilon}{2})}{2^{\frac{7-\varepsilon}{2}} \pi^{\frac{5-\varepsilon}{2}} \Gamma(2-\varepsilon)} \stackrel{\varepsilon \rightarrow 0}{=} \frac{1}{\sqrt{128}\pi^5} + O(\varepsilon) . \quad (2.57)$$

2.B.4 Integrals for the Yukawa calculation

In the main text, we found the one-loop correction to the ϕ power spectrum was determined by the correlation function

$$\begin{aligned}
I &= (\lambda\mu^\varepsilon)^2 \int_{-\infty}^{\infty} d\tau_E a^4(\tau) \int_{-\infty}^{\infty} d\tau'_E a^4(\tau') \\
&\quad \langle \overline{T} \left(\overbrace{\phi(\vec{k}, \tau_0) \phi(-\vec{k}, \tau_0)} \overbrace{\phi(-\vec{k}, \tau) \mathcal{O}(\vec{k}, \tau) \phi(\vec{k}, \tau')} \overbrace{\mathcal{O}(-\vec{k}, \tau')} \right) \rangle ,
\end{aligned} \quad (2.58)$$

where we have shown the contractions required for a connected correlator. To evaluate this correlation function we need the anti-time-ordered two-point correlation function of \mathcal{O} . However, unlike a generic operator in a CFT, the normalization of $\mathcal{O} = \bar{\psi}\psi$ is determined by the propagator of the free fermion. With this normalization factor, the power spectrum of this operator is given

by

$$\langle \bar{T}(\mathcal{O}(\vec{k}, \tau) \mathcal{O}(-\vec{k}, \tau')) \rangle = \int d^3x e^{-i\vec{k}\cdot\vec{x}} \langle \bar{T}(\mathcal{O}(x, \tau) \mathcal{O}(0, \tau')) \rangle \quad (2.59)$$

$$= \frac{1}{\pi^4} \int d^3x e^{-i\vec{k}\cdot\vec{x}} \frac{a^{-\Delta}(\tau) a^{-\Delta}(\tau')}{(x^2 + (\tau_E - \tau'_E)^2)^{3-\varepsilon}} \quad (2.60)$$

$$\stackrel{(3.42)}{=} N \int_{-\infty}^{\infty} \frac{d\omega}{2\pi} e^{i\omega(\tau_E - \tau'_E)} (k^2 + \omega^2)^{1-\varepsilon} a(\tau)^{-3+\varepsilon} a(\tau')^{-3+\varepsilon}, \quad (2.61)$$

where, in the second line, the factor of π^{-4} arises for matching to a Dirac fermion and where we have defined

$$N = \frac{1}{2^{2-2\varepsilon} \pi^2} \frac{\Gamma(-1+\varepsilon)}{\Gamma(3-\varepsilon)} \stackrel{\varepsilon \rightarrow 0}{=} -\frac{1}{8\pi} \left(\frac{1}{\varepsilon} - 2\gamma_E + \dots \right) + O(\varepsilon).$$

We now turn our attention to computing (2.35) in two simple cases: (i) In flat space-time and (ii) when $\tau_0 = 0$. Starting with the flat space-time limit,

$$\mathcal{I}(\omega, k) \stackrel{a(\tau) \rightarrow 1}{=} \int_{-\infty}^{\infty} d\tau_E \frac{e^{-k|\tau_E| + i\omega\tau_E}}{2k} = \frac{1}{k^2 + \omega^2},$$

the first order correction (2.58) is

$$I_{\text{flat}} = (\lambda \mu^\varepsilon)^2 N \int_{-\infty}^{\infty} \frac{d\omega}{2\pi} \frac{1}{(k^2 + \omega^2)^{1+\varepsilon}} \stackrel{\varepsilon \rightarrow 0}{\approx} -\frac{\lambda^2}{16\pi^2 k} \left(\frac{1}{\varepsilon} + 2 \log\left(\frac{\mu}{k}\right) - \gamma_E + \dots \right).$$

Next, we return to de Sitter space but set $\tau_0 = 0$ to find

$$\begin{aligned} \mathcal{I}(\omega, k) &= \int_{-\infty}^{\infty} d\tau_E \left(-\frac{1}{H\tau_E} \right)^\varepsilon \frac{e^{-k|\tau_E| + i\omega\tau_E}}{2k} \\ &= \frac{\Gamma(1-\varepsilon)}{H^\varepsilon} \frac{i^\varepsilon (k - i\omega)^{1-\varepsilon} + (-i)^\varepsilon (k + i\omega)^{1-\varepsilon}}{2k (k^2 + \omega^2)^{1-\varepsilon}}. \end{aligned} \quad (2.62)$$

This expression can be simplified using $\exp\left(2i \tan^{-1}\left(\frac{\omega}{k}\right)\right) = \frac{k+i\omega}{k-i\omega}$. Then, the integrand in (2.35) becomes

$$\begin{aligned} & \mathcal{I}(\omega, k) \mathcal{I}(-\omega, k) (k^2 + \omega^2)^{1-\varepsilon} \\ &= \frac{\Gamma(1-\varepsilon)^2}{H^{2\varepsilon} k^2} \cos\left((1-\varepsilon) \tan^{-1}\left(\frac{\omega}{k}\right) + \frac{\pi\varepsilon}{2}\right) \cos\left((1-\varepsilon) \tan^{-1}\left(\frac{\omega}{k}\right) - \frac{\pi\varepsilon}{2}\right) \\ &\stackrel{\varepsilon \rightarrow 0}{\approx} \frac{1}{k^2 + \omega^2} \left(1 + \left(2\gamma_E - 2\log H + 2\frac{\omega}{k} \tan^{-1}\left(\frac{\omega}{k}\right)\right) \varepsilon + O(\varepsilon^2)\right). \end{aligned} \quad (2.63)$$

We can now substitute (2.63) into (2.35) to obtain

$$\begin{aligned} I_0 &= \frac{(\lambda\mu^\varepsilon)^2}{a(\tau_0)^2} N \int_{-\infty}^{\infty} \frac{d\omega}{2\pi} \frac{1}{k^2 + \omega^2} \left(1 + \left(2\gamma_E - 2\log H + 2\frac{\omega}{k} \tan^{-1}\left(\frac{\omega}{k}\right)\right) \varepsilon + O(\varepsilon^2)\right) \\ &\stackrel{\varepsilon \rightarrow 0}{\approx} -\frac{\lambda^2}{16\pi^2 a(\tau_0)^2 k} \left(\frac{1}{\varepsilon} + 2\log\left(\frac{\mu}{H}\right) + \mathcal{A} + \dots\right). \end{aligned} \quad (2.64)$$

In the final step we have used

$$\int_{-\infty}^{\infty} \frac{d\omega}{2\pi} \frac{1}{k^2 + \omega^2} = \frac{1}{2k}$$

and introduced

$$\frac{\mathcal{A}}{k} = \int_{-\infty}^{\infty} \frac{d\omega}{2\pi} \frac{\omega}{k} \frac{\tan^{-1}(\omega/k)}{k^2 + \omega^2} = \frac{1}{2\pi k} \int_{-\pi/2}^{\pi/2} d\theta \theta \tan \theta \quad (2.65)$$

with $\theta = \tan^{-1}\left(\frac{\omega}{k}\right)$. This term is clearly divergent and, as pointed out in the main text, it is a consequence of setting $\tau_0 = 0$.

Chapter 3

Regulating Loops in dS

3.1 Introduction

Inflationary theory [55, 56, 57] posits that the early universe underwent a period of approximately de Sitter (dS) expansion. During this period, inflaton modes of large comoving wavelength leave the horizon, only to re-enter at a later time and seed the structure we see in the night sky. Thus, the quantum dynamics of these super-Hubble fluctuations become ingrained in our cosmological observations. In particular, the equal time in-in correlation functions of light scalar fields encode a great deal of information about the inflationary era that could be revealed by measurements of primordial non-Gaussianity [58]. However, not enough is known about these correlators beyond tree level. This situation becomes untenable as our measurements improve in precision, especially in light of the fact that loop calculations lead to infrared (IR) divergences and unbounded time-dependent ‘secular’ growth [9, 10, 12, 13, 14, 25, 26, 27, 28, 59, 60, 29, 61, 62, 63, 15, 16]. Such secular terms appear at all orders of perturbation theory, and will be our primary concern in this paper.

In this work we develop a method to compute secular divergences associated with scalar field theories on a fixed de Sitter background. It is not easy to calculate these divergences, even for simple 1-loop diagrams [64, 26]. The basic problem is the lack of time translational invariance in dS, which means time appears explicitly in the momentum integrals. Such integrals are not scaleless, hampering our ability to compute them with the usual bag of tricks we employ

in flat space. A solution to this problem was recently introduced in the form of Soft de Sitter Effective Theory (SdSET) [65, 66] where, in the long wavelength limit, the time integrals factorize and separate from integrals over 3-momenta. This returns the scalelessness of the momentum integrals, allowing us to tame the divergences without violating the symmetries of the underlying dS spacetime. However, we still need to match the EFT with the UV theory, and it would be desirable to have a way of regulating loop integrals on the UV side that shares all the nice properties of the regulator we use in the EFT (*dynamical* dimensional regularization). Such a procedure must also be generalizable, so that we don't have to invent a new way of doing the integral for every diagram we encounter.

Our method starts with the following simple observation: dS spacetime has dilatation invariance in place of the time translation invariance of flat space. The latter allows us to Fourier transform the time variable, which suggests that the transform best suited for dS should have, as its basis, the eigenfunctions of the dilatation generator. Mellin transforms have exactly that property [67, 68, 69]. Once we switch to Mellin space, the momentum and time integrals decouple, and the divergences manifest as overlaps of certain poles of the integrand. These overlaps may be removed by introducing tiny shifts to these poles, in much the same way that loops in flat space QFT are regulated by tweaking the number of dimensions [70, 71]. In fact, the connection was first made in [72], and Mellin-Barnes (MB) integrals have been used widely in evaluating sophisticated Feynman diagrams in particle physics [73, 74, 75, 76]. We employ some of the tools developed in these papers in the present work, thereby placing our method on a well-established foundation of computational techniques.

As with dimensional regularization (dimreg), our approach respects the symmetry of the background de Sitter space at every step of the calculation. The end result also bears a strong resemblance to a standard dimreg answer, with the secular growth encoded in diverging Γ functions. Once isolated, such divergences can be interpreted with the machinery of the *dynamical* renormalization group (DRG) [77, 64, 78, 41, 43, 42]. This procedure resums large secular logs in the same way regular RG operates on UV logs in flat space. In the effective theory

language, the DRG evolution of composite operators of a massless scalar naturally leads to the framework of Stochastic Inflation, which describes the probability distribution of the scalar field as a function of time [11, 79, 80, 65, 32, 31, 81]. Stochastic Inflation is the conceptual basis for slow-roll eternal inflation, and even subtle changes to the time dependence in this picture can have a profound impact on the phase transition to eternal inflation. Loop effects introduce such corrections to this framework at higher order, as demonstrated with SdSET [66]. Our method allows us to draw the same conclusion, by performing loop calculations in the full theory itself.

The paper is structured as follows: In sec. 3.2 we outline the transition to Mellin space and explain how divergences are encoded in this representation. Next, we review the MB representation of a 4-pt function in sec. 3.3, and use it to compute the $O(\lambda)$ contribution to $\langle\phi^2\phi^2\rangle$ and $\langle\phi^3\phi\rangle$ in sec. 3.4 and 3.5. We explain the calculations in detail, to be pedagogical, but most of the intermediate steps are mechanical and can be automated [76, 75]. We also identify the issue of requiring more than one parameter to regulate certain integrals, and offer some suggestions to resolve this. By way of a quantitative example we have calculated the anomalous dimension of the ϕ^2 operator over a range of masses and summarized them in table. 3.1. We conclude in sec. 3.6 by reviewing the lessons learnt from our calculations and contemplating future directions.

3.2 dS loops in Mellin space

Perturbative QFT calculations in dS are plagued by a variety of divergences. One particular kind, the secular growth terms, causes the naive perturbation expansion to break down at late times. Such contributions are often furnished by loop integrals, which are difficult to compute in dS. The problem becomes more tractable if we represent the correlation functions in Mellin space.

3.2.1 General structure

Consider a scalar field ϕ with mass m in a fixed dS background with the metric $ds^2 = a(\tau)^2(-d\tau^2 + d\vec{x}^2)$, where $d\vec{x}$ is a line element in D space dimensions, τ is the conformal time and $a(\tau) = -1/H\tau$. For a free scalar field one expands the field in modes according to

$$\phi(\vec{x}, \tau) = \int \frac{d^D k}{(2\pi)^D} e^{i\vec{k}\cdot\vec{x}} \{v_{\vec{k}}(\tau)a_{\vec{k}} + v_{\vec{k}}^*(\tau)a_{\vec{k}}^\dagger\}. \quad (3.1)$$

In the Bunch-Davies vacuum the modes are given by

$$v_{\vec{k}}(\tau) = e^{-\frac{i\pi}{4}} e^{-\frac{\pi\nu}{2}} \frac{\sqrt{\pi}}{2} H^{\frac{D-1}{2}}(-\tau)^{\frac{D}{2}} H_{i\nu}^{(1)}(-k\tau), \quad (3.2)$$

$$v \stackrel{\text{def.}}{=} i\sqrt{\frac{D^2}{4} - \frac{m^2}{H^2}}. \quad (3.3)$$

where $H_{i\nu}^{(1)}$ is the Hankel function of the first kind (we follow the convention in [67]). We are interested in calculating correlation functions of the field at a fixed (late) time using the in-in/Schwinger-Keldysh formalism (see [15, ?] for a review). Such calculations involve integrals of the schematic form

$$\begin{aligned} & \langle \phi_{\vec{k}_1}^\nu(\tau_0) \cdots \phi_{\vec{k}_n}^\nu(\tau_0) \rangle_{\text{in-in}} \\ & \supset \prod_i \int^{\tau_0} d\tau_i a(\tau_i)^{D+1} \prod_j \int \frac{d^D p_j}{(2\pi)^D} \cdots H_{i\nu}(a_m(\vec{k}, \vec{p})\tau_i) H_{i\nu}(a_{m+1}(\vec{k}, \vec{p})\tau_{i+1}) \cdots \end{aligned} \quad (3.4)$$

where $a_m(\vec{k}, \vec{p})$ are some linear combinations of the 3-momenta. The evaluation of this integral is made difficult by the fact that the variables of integration, τ_i and \vec{p}_j , are trapped as arguments of Hankel functions. There are few special values of ν for which $H_{i\nu}(-k\tau)$ has a simpler functional

form, but even in those cases calculations involving loop integrals are cumbersome¹. To make progress, we rely on the following convenient MB representations [82],

$$\begin{aligned}
i\pi e^{\frac{\pi\nu}{2}} H_{i\nu}^{(1)}(z) &= \int_{c-i\infty}^{c+i\infty} \frac{ds}{2\pi i} \Gamma\left(s + \frac{i\nu}{2}\right) \Gamma\left(s - \frac{i\nu}{2}\right) \left(-\frac{iz}{2}\right)^{-2s} \\
-i\pi e^{-\frac{\pi\nu}{2}} H_{i\nu}^{(2)}(z) &= \int_{c-i\infty}^{c+i\infty} \frac{ds}{2\pi i} \Gamma\left(s + \frac{i\nu}{2}\right) \Gamma\left(s - \frac{i\nu}{2}\right) \left(\frac{iz}{2}\right)^{-2s}
\end{aligned} \tag{3.5}$$

where $c > |\nu|$. These representations have been used to study late-time tree level correlation functions in [67, 68]. Building on that work, we will explore whether the same approach is fruitful in analyzing loop integrals in dS. To outline the procedure we begin by substituting (3.5) into (3.4) and changing the order of integration,

$$\begin{aligned}
\langle \phi_{\vec{k}_1}^{\nu}(\tau_0) \cdots \phi_{\vec{k}_n}^{\nu}(\tau_0) \rangle_{\text{in-in}} &\supset \prod_{\ell} \int ds_{\ell} \Gamma(s_{\ell} + \frac{i\nu}{2}) \Gamma(s_{\ell} - \frac{i\nu}{2}) \prod_i \int^{\tau_0} d\tau_i a(\tau_i)^{D+1} (-\tau_i)^{-2s_{\ell}} \\
&\times \prod_j \int \frac{d^D p_j}{(2\pi)^D} \dots a_m(\vec{k}, \vec{p})^{-2s_{\ell}} a_{m+1}(\vec{k}, \vec{p})^{-2s_{\ell'}} \dots \tag{3.6}
\end{aligned}$$

We have ‘released’ the variables τ_i and \vec{p}_j , at the cost of introducing an MB integral for each Hankel function. The Mellin variables s_{ℓ} label the eigenstates of the dilatation generator [69]. In the late-time limit, $\tau_0 \rightarrow 0$, the time integrals reduce to s -conserving delta functions at each vertex [67, 68]; dilatation invariance of de Sitter space leads to conservation of s the same way that translation invariance implies conservation of 3-momenta \vec{k} . We are then left with

$$\begin{aligned}
\langle \phi_{\vec{k}_1}^{\nu}(\tau_0) \cdots \phi_{\vec{k}_n}^{\nu}(\tau_0) \rangle_{\text{in-in}} &\supset \prod_{\ell} \int ds_{\ell} \Gamma(s_{\ell} + \frac{i\nu}{2}) \Gamma(s_{\ell} - \frac{i\nu}{2}) Q(\mathbf{s}) \delta(s_{\ell} + \dots) \delta(s_{\ell'} + \dots) \dots \\
&\times \prod_j \int \frac{d^D p_j}{(2\pi)^D} \dots a_m(\vec{k}, \vec{p})^{-2s_{\ell}} a_{m+1}(\vec{k}, \vec{p})^{-2s_{\ell'}} \dots \tag{3.7}
\end{aligned}$$

¹For instance, the two point function of a conformal mass scalar has the form $\langle \phi \phi \rangle \sim e^{ik(\tau - \tau')}/k$, where the exponential makes it difficult to evaluate the loop integral with techniques we use in flat space calculations (see [64] for more details). Life can be made simpler by imposing a hard cutoff, but this could generate unphysical logs.

where $Q(\mathbf{s}) \equiv Q(s_1, \dots, s_\ell, \dots)$ is some ratio of polynomials of the Mellin variables. The form of the r.h.s. reflects the fact that dilatation and translation do not commute. The momentum integrals are now manifestly scaleless. Evaluating these introduces new s_ℓ -dependent Γ functions,

$$\langle \phi_{k_1}^V(\tau_0) \cdots \phi_{k_n}^V(\tau_0) \rangle_{\text{in-in}} \supset \prod'_\ell \int ds_\ell \Gamma(s_\ell + \frac{i\nu}{2}) \Gamma(s_\ell - \frac{i\nu}{2}) Q(\mathbf{s}) \frac{\Gamma(D - s_\ell - \dots) \cdots}{\Gamma(s_\ell - \dots) \cdots} b_\ell(\vec{k})^{s_\ell} \quad (3.8)$$

where $b_\ell(\vec{k})$ are ratios involving the external momenta, and the prime on \prod'_j indicates that we have applied the delta functions in s . All that remains is the evaluation of a multidimensional MB integral (3.8). Integrals of this form have been studied extensively as a tool to simplify certain Feynman diagrams in particle physics [83, 73, 74, 75, 76]. Drawing on that literature, we turn our attention to extracting and understanding the divergences contained in (3.8).

3.2.2 Divergences in MB integrals

Consider the simple case of an MB integral

$$K(x) = \int_{-i\infty}^{+i\infty} \frac{ds}{2\pi i} \Gamma(s - a) \Gamma(-s) x^{-s}. \quad (3.9)$$

The poles of the integrand are the poles of the Γ functions. These are at $s_\star = a, a - 1, a - 2, a - 3, \dots$ which are the ‘left’ poles and at $s_\star = 0, 1, 2, 3, \dots$ which are the ‘right’ poles. The contour is a straight line that runs parallel to the $\Im(s)$ axis and it must separate all left poles from all right poles. This is the Mellin contour prescription. We may then close the contour on either the left or right half plane, picking up the residues at the poles.

Now consider the case where $a = 0$. This leads to an overlap of the zeroth left and right poles as shown in Fig. 3.1a. In this situation no choice of contour can separate all left poles from the right ones. Instead, if we set $a = -\varepsilon$, where ε is a vanishingly small positive number, we have the situation shown in Fig. 3.1b. The overlap is removed and a contour \mathcal{C} can be driven between the left and right poles. As ε approaches zero the contour is said to be ‘pinched’. The

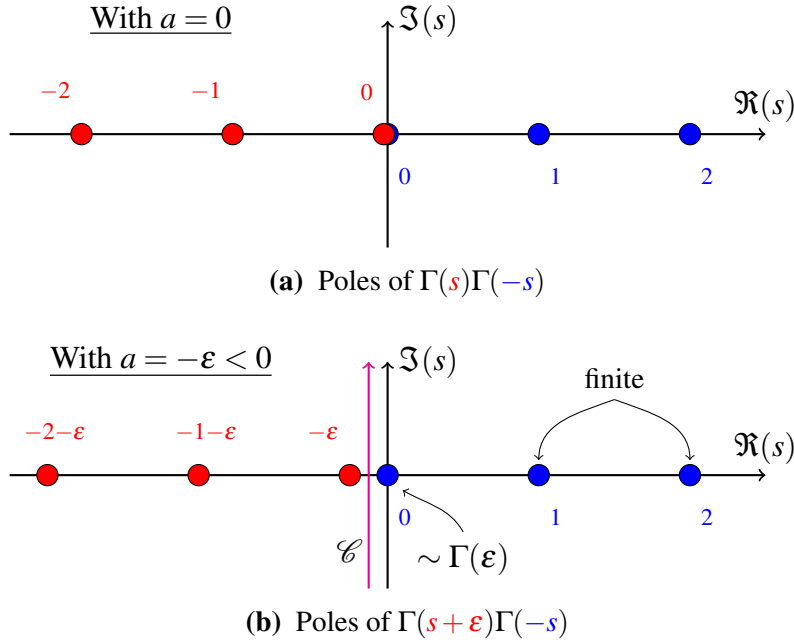


Figure 3.1. Regulating divergences in MB integrals. The overlap of the zeroth left and right poles in (a) makes (3.9) undefined because no contour can separate all the left poles from right ones. In (b) we have shifted the left poles to the left by ε , allowing us to drive a contour between the two kinds of poles. In the limit $\varepsilon \rightarrow 0$ we approach the situation in (a), known as *contour pinching*, which results in a divergence $\Gamma(\varepsilon)$. This is simply the residue at $s_* = 0$, as we close the contour on the RHP. The residues at the other poles are finite in the same limit.

value of the integral at $\varepsilon = 0$ is defined by analytic continuation of the integral at $\varepsilon > 0$.

If we close \mathcal{C} on the RHP we pick up the residues at the right poles. However, notice that the residue at the zeroth right pole $s_* = 0$ is

$$\text{Res}[\Gamma(s+\varepsilon)\Gamma(-s)x^{-s}; s=0] = -\Gamma(\varepsilon), \quad (3.10)$$

which blows up as $\varepsilon \rightarrow 0$. In other words, an overlap of left/right poles signal divergences in the MB integral. Also note how the divergence appears as a $\Gamma(\varepsilon)$, in the same way it does for a flat space loop integral computed with dimreg^2 .

²In fact, the Mellin approach produces the same answer in flat space, that we obtain by the conventional methods. See Ch. 4 of [83] for an instructive example which uses the MB representation of Feynman propagators to compute the one-loop self-energy graph in QED.

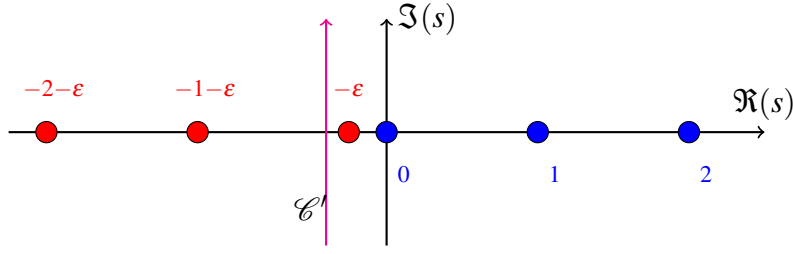


Figure 3.2. A contour that does not separate left/right poles.

What happens if the contour does not separate the left and right poles? Suppose we chose to integrate over a contour \mathcal{C}' that intersects $\Re(s)$ to the left of the pole at $s_* = -\epsilon$, as in Fig. 3.2. Then, this pole must be included in the sum of residues. But that means $K'(x) = \text{Res}[s = -\epsilon] + \text{Res}[s = 0] + \dots = \Gamma(\epsilon) - \Gamma(\epsilon) + \dots$. That is, there is no divergence, even in the limit $\epsilon \rightarrow 0$ when the zeroth poles overlap. The situations in Fig. 3.1b and Fig. 3.2 differ only by the placement of the pole at $s_* = -\epsilon$. Therefore we can write

$$\int_{\mathcal{C}} \frac{ds}{2\pi i} \Gamma(s + \epsilon) \Gamma(-s) x^{-s} = +\text{Res}[s = -\epsilon] + \int_{\mathcal{C}'} \frac{ds}{2\pi i} \Gamma(s + \epsilon) \Gamma(-s) x^{-s}. \quad (3.11)$$

The integral over \mathcal{C}' is a finite and the divergence manifests in the residue at $-\epsilon$. Incidentally, this also suggests an algorithm to identify and separate the divergence from any Mellin integral. If we keep the contour *fixed* in Fig. 3.1b and decrease ϵ , the zeroth left pole will cross over to the right at some point. We then end up in the same situation as Fig. 3.2, except that the contour is still \mathcal{C} . To recover the original integral we'll need to add the residue at $s_* = -\epsilon$, just as we did in (3.11), thereby isolating the divergence as a separate term. This is the basis of the procedure, first introduced in [74], to extract divergences from Mellin integrals over several variables.

3.2.3 N -dimensional MB integrals

By iterating the same basic steps discussed above, we can identify and separate divergences in an N -dimensional MB integral of the general form (cf. (3.8))

$$K(x_1, x_2, \dots, x_N) = \int_{-i\infty}^{i\infty} \frac{ds_1}{2\pi i} \dots \int_{-i\infty}^{i\infty} \frac{ds_N}{2\pi i} \frac{\prod_i \Gamma(U_i(\mathbf{s}))}{\prod_j \Gamma(V_j(\mathbf{s}))} x_1^{-s_1} \dots x_N^{-s_N}, \quad (3.12)$$

where x_n are the ratios of kinematic variables, $\mathbf{s} = (s_1, \dots, s_N)$, and the arguments of the Γ functions in the MB integrand are

$$\begin{aligned} U_i(\mathbf{s}) &\stackrel{\text{def.}}{=} a_i + \sum_{\ell} b_{i\ell} s_{\ell} \\ V_j(\mathbf{s}) &\stackrel{\text{def.}}{=} d'_j + \sum_{\ell} b'_{j\ell} s_{\ell} \end{aligned} \quad (3.13)$$

where the constants $a_i, b_{i\ell}$ etc. are reals. The integral in (3.12) is just an extension of (3.9) to N Mellin variables. The poles of this integral are the poles of the Γ functions in the numerator, that is, those \mathbf{s} where

$$U_i(\mathbf{s}) = -n, \quad n \in \mathbb{Z}_0. \quad (3.14)$$

As before, an MB integral is well-defined if the contours separate the left and right poles. For a multidimensional MB integral like (3.12) this condition is equivalent to the requirement

$$U_i(\mathcal{C}) > 0 \quad \forall i \quad (3.15)$$

where $U_i(\mathcal{C})$ is the real part of U_i evaluated on the contour \mathcal{C} . For example, consider the situation in Fig. 3.3. If $U_1(s) = a + s$, then $U_1(\mathcal{C}) = a + s^{\mathcal{C}} > 0$ if we choose a contour which intersects the $\Re(s)$ axis at $s^{\mathcal{C}} > -a$. Similarly, if $U_2(s) = b - s$ then $U_2(\mathcal{C}) = b - s^{\mathcal{C}} > 0 \implies s^{\mathcal{C}} < b$. Taken together, an integral with both these Γ functions requires $-a < s^{\mathcal{C}} < b$, which is exactly the condition that the contour must separate the left/right poles.

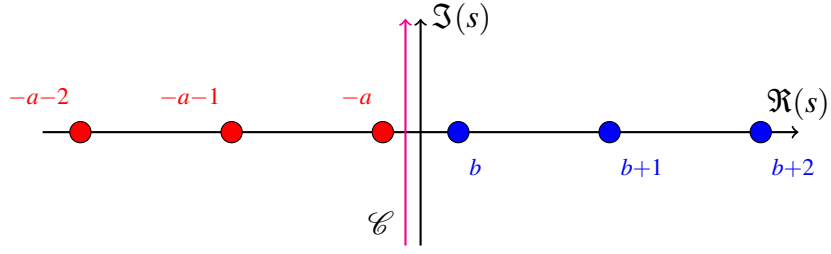


Figure 3.3. Pole structure of an MB integral $\int_{\mathcal{C}} \frac{ds}{2\pi i} \Gamma(a+s)\Gamma(b-s)x^{-s}$. The contour satisfies $a < s^{\mathcal{C}} < b$, which is equivalent to the condition that the arguments of the Γ functions in the integrand are positive when evaluated on the contour (cf. (3.15)).

Generalizing this further, the condition for the n^{th} pole of $\Gamma(U_i)$ to be on the ‘correct’ side is $U_i(\mathcal{C}) + n > 0$. That is, an n^{th} right pole will be on the right side of the contour and an n^{th} left pole will be on the left if this inequality is satisfied. Otherwise it means that the pole has crossed the contour. Thus, we have the following pole crossing condition for the n^{th} pole,

$$U_i(\mathcal{C}) + n < 0. \quad (3.16)$$

The inequalities (3.15) and (3.16) allow us determine where a pole is, even in the N -dimensional case when it becomes difficult to visualize the location of the poles and contours.

3.2.4 Analytic continuation

The MB integral in (3.12) will have divergences if the integrand has overlapping left/right poles. This makes it impossible to choose a set of straight line contours that satisfy (3.15) for all U_i (Fig. 3.4a). We circumvent this issue by introducing parameters ε_k into our integral that shift the poles around until we can meet the conditions (3.15). That is, we change (3.13) to

$$\begin{aligned} U_i(\mathbf{s}) &\rightarrow a_i + \sum_{\ell} b_{i\ell} s_{\ell} + \sum_k c_{ik} \varepsilon_k \\ V_j(\mathbf{s}) &\rightarrow a'_j + \sum_{\ell} b'_{j\ell} s_{\ell} + \sum_k c'_{jk} \varepsilon_k, \end{aligned} \quad (3.17)$$

and choose the initial values $\varepsilon_k = \varepsilon_k^{(0)}$ to make the left/right poles separable with straight line contours (Fig. 3.4b). The original integral, for which $\varepsilon_k = 0$, is defined by analytic continuation of the integral with the modified arguments (3.17). As we take $\varepsilon_k \rightarrow 0$, some of the poles will cross over to the ‘wrong’ side of the contours (Fig. 3.4c), and we separate the residues at those poles as in (3.11). Around $\varepsilon_k \sim 0$ some left/right poles nearly overlap, with the small non-zero values of ε_k keeping them from complete coalescence. The residues at these poles isolate the divergences in the original integral. We can understand these ideas with a rudimentary example. Consider the double integral

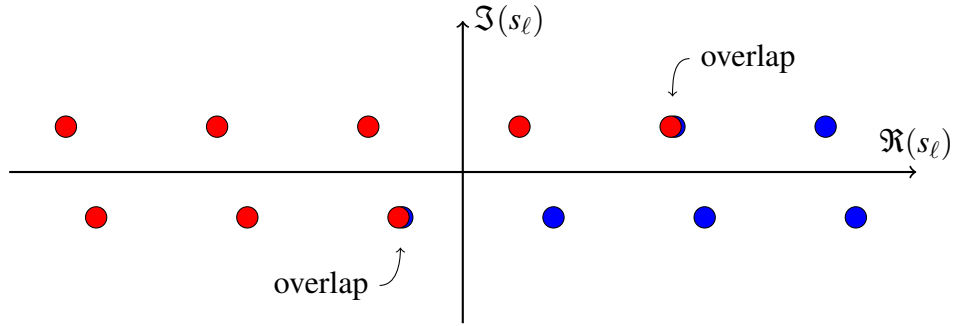
$$K = \int_{\mathcal{C}_z} \frac{dz}{2\pi i} \int_{\mathcal{C}_w} \frac{dw}{2\pi i} \Gamma_1(z, w, \varepsilon) \Gamma_2(z, w, \varepsilon) \dots \Gamma_m(z, w, \varepsilon), \quad (3.18)$$

where $\Gamma_i(z, w, \varepsilon) \equiv \Gamma(U_i(z, w, \varepsilon))$ are Gamma functions with arguments of the form (3.17), and \mathcal{C}_z and \mathcal{C}_w are straight line contours which we close in the right half plane. These contours separate the left/right poles of the integrand at $\varepsilon = \varepsilon_0$. Suppose that, as we decrease $\varepsilon \rightarrow 0$, the first left pole z_* of Γ_1 has crossed to the right of \mathcal{C}_z at $\varepsilon = \varepsilon_1$. Following the discussion around (3.11), we may write

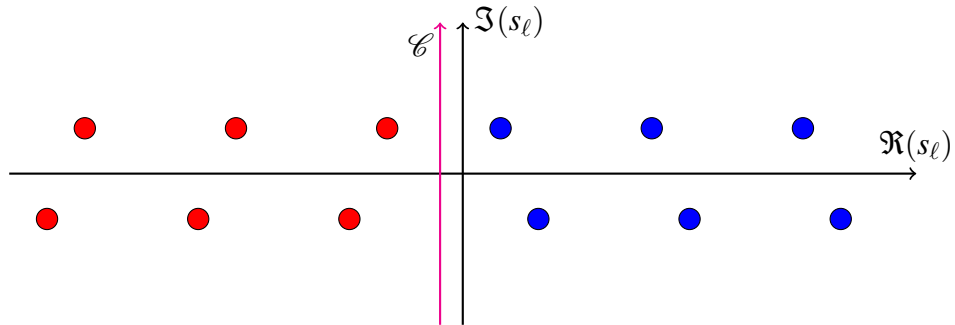
$$\begin{aligned} K &= \text{Res}[\Gamma_1; z_*] \int_{\mathcal{C}_w} \frac{dw}{2\pi i} \Gamma_2(z_*, w, \varepsilon_1) \dots + \int_{\mathcal{C}_z} \frac{dz}{2\pi i} \int_{\mathcal{C}_w} \frac{dw}{2\pi i} \Gamma_1^*(z, w, \varepsilon_1) \Gamma_2(z, w, \varepsilon_1) \dots \\ &\stackrel{\text{def.}}{=} K_1 + K^*. \end{aligned} \quad (3.19)$$

The asterisk on Γ_1^* indicates that the $n = 0$ pole of that function is on the ‘wrong’ side. Therefore, the double integral K^* includes a contribution $-\text{Res}[\Gamma_1; z_*]$ (the minus sign is due to the clockwise direction of the contour), which needs to be compensated with a $+\text{Res}[\Gamma_1; z_*]$ to recover the original integral K . This is exactly the term K_1 , which is the residue of K at the first pole of Γ_1 . If z_* was a right pole that crossed to the left we would have written $\int_{\mathcal{C}_z} \frac{dz}{2\pi i} \Gamma_1(z, w, \varepsilon_1) = -\text{Res}[\Gamma_1; z_*] + \int_{\mathcal{C}_z} \frac{dz}{2\pi i} \Gamma_1^*(z, w, \varepsilon_1)$. Next, we concentrate on the K_1 term³. As we continue

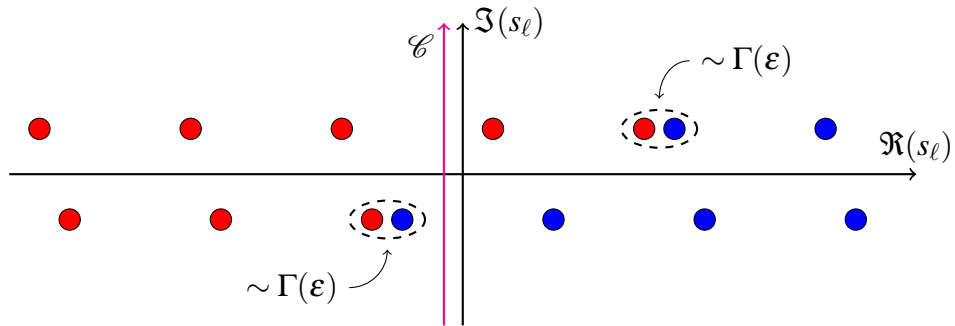
³Note that $\Gamma_2(z_*, w, \varepsilon_1)$ can have a different w dependence than $\Gamma_2(z, w, \varepsilon_1)$.



(a) The original integrand, with all $\varepsilon_k = 0$, has overlapping poles.



(b) The poles are separated initially by setting $\varepsilon_k = \varepsilon_k^{(0)}$.



(c) Some poles end up on the wrong side of the contour and nearly overlap when $\varepsilon_k \sim 0$

Figure 3.4. An MB integral is defined by shifting its poles around till the left/right poles are separated by a straight line contour. Analytic continuation involves reverting these shifts and allowing the poles to cross back to their original position. As a pole crosses the contour, we isolate the contribution at that pole (cf. (3.11)). Some of the left/right poles (encircled) nearly overlap, resulting in divergences. For an N -fold MB integral all this happens across N complex s_ℓ -planes simultaneously. Note: The poles in these figures have been staggered vertically for clarity; they are all real valued in our examples. See sec. 3.2.4 for further explanation.

decreasing ε , suppose a pole w_* of Γ_2 has crossed over at $\varepsilon = \varepsilon_2$. Then,

$$K_1 = \text{Res}[\Gamma_1; z_*] \text{Res}[\Gamma_2(z_*) \dots \Gamma_m(z_*); w_*] + \text{Res}[\Gamma_1; z_*] \int_{\mathcal{C}_w} \frac{dw}{2\pi i} \Gamma_2^*(z_*, w, \varepsilon_2) \dots$$

$$\stackrel{\text{def.}}{=} K_{12} + K_1^*. \quad (3.20)$$

Similarly, if a pole of Γ_2 crosses over in K^* as we decrease ε from ε_1 , we write $K^* = K_2^* + K^{**}$. We will assume that no more poles cross over as we continue down to $\varepsilon \sim 0$. Therefore we can expand the integrals in K_1^* , K_2^* and K^{**} as a Taylor series in ε . It is clear from context which poles are on the wrong side, so we will drop the asterisks on the K 's henceforth⁴. Collecting everything together, we obtain

$$K \rightarrow K_{12} + K_1 + K_2 + K. \quad (3.21)$$

This is just a 2-fold version of (3.11). The break up of K depends on the choice of contours, but the final answer will be the same when everything is added up. Some of the terms in (3.21) will contain $\Gamma(\varepsilon)$'s, from taking residues at nearly overlapping poles (see Fig. 3.4c). These are the divergences we are looking for. Since (3.18) is a 2-fold integral there can be a maximum of two simultaneous pinches, and the leading behavior around $\varepsilon \sim 0$ is at most

$$K \sim \frac{\text{const.}}{\varepsilon^2} + \frac{\text{const.}'}{\varepsilon} + O(\varepsilon^0). \quad (3.22)$$

The extension to the N -dimensional integral (3.12) is straightforward. The procedure described above has been developed into an algorithm in [73, 75, 76]. We will illustrate the steps in the examples below.

⁴The naming convention for the r.h.s. of (3.21) is from [74].

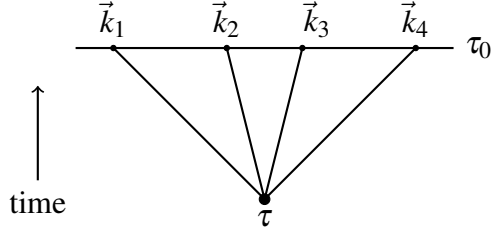


Figure 3.5. The 4-pt correlation function at tree level.

3.3 The tree level 4-point function

The calculations in this paper begin with the contraction of the tree level 4-point function of scalar fields shown in Fig. 5.3 (we are working with a $\lambda \phi^4$ interaction). The MB representation of such functions are detailed in [67]. We will summarize just the basic elements required to set up our loop integrals, using the same conventions as that paper. First, the Mellin-Barnes representation for the dS bulk-to-boundary propagator is

$$F_{\pm, \vec{k}}^{(\nu)}(\tau; \tau_0) = (-\tau)^{\frac{D}{2}-i\nu} \mathcal{N}_\nu(\tau_0) \int_{-i\infty}^{i\infty} \frac{ds}{2\pi i} e^{\delta_\nu^\pm(s)} \Gamma\left(s + \frac{i\nu}{2}\right) \Gamma\left(s - \frac{i\nu}{2}\right) \left(-\frac{\tau k}{2}\right)^{-2s+i\nu} \quad (3.23)$$

where τ is a point in the bulk and the late time $\tau_0 \rightarrow 0$. The contour is a vertical line that intersects the real axis to the right of the pole at $s_* = -\frac{i\nu}{2}$. The other symbols are

$$\delta_\nu^\pm(s) \stackrel{\text{def.}}{=} \mp i\pi \left(s + \frac{i\nu}{2}\right) \quad (3.24)$$

$$\mathcal{N}_\nu(\tau_0) \stackrel{\text{def.}}{=} (-\tau_0)^{\frac{D}{2}+i\nu} \frac{\Gamma(-i\nu) H^{D-1}}{4\pi} \quad (3.25)$$

The $+(-)$ sub-indices indicate the contributions from the (anti)-time-ordered branches of the in-in contour. The four point correlator of Fig. 5.3 is given by

$$\left\langle \phi_{\vec{k}_1}^{(\nu_1)} \phi_{\vec{k}_2}^{(\nu_2)} \phi_{\vec{k}_3}^{(\nu_3)} \phi_{\vec{k}_4}^{(\nu_4)} \right\rangle'_\pm = \pm i \int_{-\infty}^{\tau_0} \frac{d\tau}{(-H\tau)^{D+1}} \prod_{j=1}^4 F_{\vec{k}_j, \pm}^{(\nu_j)}(\tau; \tau_0). \quad (3.26)$$

Substituting (3.23) into this equation gives

$$\begin{aligned} \left\langle \phi_{\vec{k}_1}^{(v_1)} \phi_{\vec{k}_2}^{(v_2)} \phi_{\vec{k}_3}^{(v_3)} \phi_{\vec{k}_4}^{(v_4)} \right\rangle'_{\pm} &= \pm i H^{-D-1} \mathcal{N}_4(\tau_0, k_i) \int [ds]_4 \rho(\mathbf{s}, \mathbf{v}) \prod_{j=1}^4 e^{\delta_{v_j}^{\pm}(s_j)} \left(\frac{k_j}{2}\right)^{-2s_j} \\ &\times \int_{-\infty}^{\tau_0} d\tau (-\tau)^{D-1-2(s_1+s_2+s_3+s_4)}, \end{aligned} \quad (3.27)$$

where $[ds]_N \stackrel{\text{def.}}{=} \prod_{j=1}^N \int \frac{ds_j}{2\pi i}$ and

$$\rho(\mathbf{s}, \mathbf{v}) \stackrel{\text{def.}}{=} \prod_{j=1}^4 \Gamma\left(s_j + \frac{iv_j}{2}\right) \Gamma\left(s_j - \frac{iv_j}{2}\right), \quad (3.28)$$

$$\mathcal{N}_4(\tau_0, k_i) \stackrel{\text{def.}}{=} \prod_{j=1}^4 \left(\frac{k_j}{2}\right)^{iv_j} \mathcal{N}_{v_j}(\tau_0). \quad (3.29)$$

The momentum and time arguments which were previously trapped inside the arguments of Hankel functions are now out in the open. We can do the time integral right away,

$$\int_{-\infty}^{\tau_0} d\tau (-\tau)^{D-1-2(s_1+s_2+s_3+s_4)} = \frac{-(-\tau_0)^{D-2(s_1+s_2+s_3+s_4)}}{D-2(s_1+s_2+s_3+s_4)} \stackrel{\tau_0 \rightarrow 0}{=} i\pi \delta\left(\frac{D}{2} - (s_1+s_2+s_3+s_4)\right) \quad (3.30)$$

which converges⁵ for $\Re\left(\frac{D}{2} - (s_1+s_2+s_3+s_4)\right) < 0$. Applying the delta function constraint and reorganizing a bit allows us to write (3.27) as

$$\left\langle \phi_{\vec{k}_1}^{(v_1)} \phi_{\vec{k}_2}^{(v_2)} \phi_{\vec{k}_3}^{(v_3)} \phi_{\vec{k}_4}^{(v_4)} \right\rangle'_{\pm} = \pm i \frac{H^{-D-1}}{2} e^{\mp i \frac{\pi}{2} (D+i(v_1+v_2+v_3+v_4))} \mathcal{N}_4(\tau_0, k_i) I(\mathbf{k}, \mathbf{v}), \quad (3.31)$$

$$I(\mathbf{k}, \mathbf{v}) \stackrel{\text{def.}}{=} \int [ds]_4 2\pi i \delta\left(\frac{D}{2} - (s_1+s_2+s_3+s_4)\right) \rho(\mathbf{s}, \mathbf{v}) 2^D \prod_{j=1}^4 k_j^{-2s_j}. \quad (3.32)$$

⁵Usually the in-in contours are deformed slightly, such that the lower limit of the forward and return legs are $-\infty(1 \mp i\epsilon)$, to kill the contribution from very early times. The same thing is accomplished here by constraining the real part of the Mellin variables.

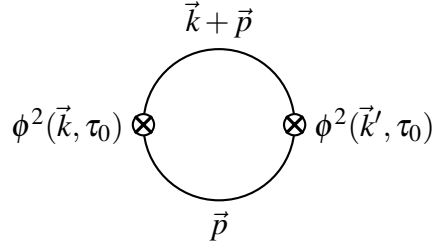


Figure 3.6. $\langle \phi^2 \phi^2 \rangle$ at tree level.

The full 4-point function is the sum of the contributions from the forward and return legs of the in-in contour,

$$\left\langle \phi_{\vec{k}_1}^{(v_1)} \phi_{\vec{k}_2}^{(v_2)} \phi_{\vec{k}_3}^{(v_3)} \phi_{\vec{k}_4}^{(v_4)} \right\rangle' = H^{-D-1} \sin \left(\frac{\pi}{2} (D + i(v_1 + v_2 + v_3 + v_4)) \right) \mathcal{N}_4(\tau_0, k_i) I(\mathbf{k}, \mathbf{v}). \quad (3.33)$$

3.4 The anomalous dimension of ϕ^2

As our first example we compute at 1-loop the anomalous dimension of the ϕ^2 operator, γ_{ϕ^2} . This quantity was computed for the conformal mass case in [64]. We will set up the problem for a scalar field with general mass m and plug in a specific value for m later. We start with the tree level expression for $\langle \phi^2 \phi^2 \rangle$ (see Fig. 3.6),

$$\langle \phi^2 \phi^2 \rangle'_{\text{tree}} = 2 \int \frac{d^D p}{(2\pi)^D} G_{\vec{k}+\vec{p}}^{(v)}(\tau_0) G_{\vec{p}}^{(v)}(\tau_0) \quad (3.34)$$

where $G^{(v)}$ is the late time two point function

$$G_{\vec{k}}^{(v)}(\tau_0) = \lim_{\tau_0 \rightarrow 0} \left\langle \phi_{\vec{k}}^{(v)}(\tau_0) \phi_{\vec{k}'}^{(v)}(\tau_0) \right\rangle' = \frac{H^{D-1}}{4\pi} \Gamma(-iv)^2 (-\tau_0)^{D+2iv} \left(\frac{k}{2} \right)^{2iv}. \quad (3.35)$$

We could, for instance, arrive at this expression by taking the limit $\tau \rightarrow \tau_0 \sim 0$ in (3.23) in which

case the integral is dominated by the pole at⁶ $s_* = -\frac{iv}{2}$. The momentum integral in (3.34) can be computed using the convolution theorem (cf. (3.41)). The result is

$$\langle \phi^2 \phi^2 \rangle'_{\text{tree}} = \frac{2}{(4\pi)^{\frac{D}{2}+2}} \frac{\Gamma(-\frac{D}{2} - 2iv)\Gamma(\frac{D}{2} + iv)^2 \Gamma(-iv)^2}{\Gamma(D + 2iv)} H^{2D-2} (-\tau_0)^{2D+4iv} k^{D+4iv}. \quad (3.36)$$

Next, we calculate the first order correction $\langle \phi^2 \phi^2 \rangle_\lambda$ which is obtained by contracting the legs

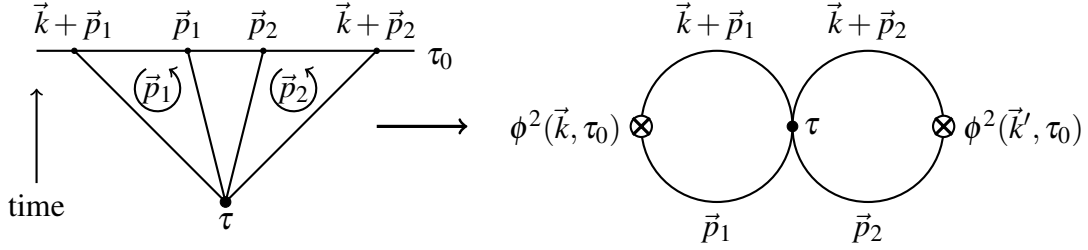


Figure 3.7. The first order correction to $\langle \phi^2 \phi^2 \rangle$.

of the 4-point correlation function (3.33) as shown in Fig. 3.7. This corresponds to setting $\vec{k}_1 = \vec{k} + \vec{p}_1, \vec{k}_2 = \vec{p}_1, \vec{k}_3 = \vec{k} + \vec{p}_2$ and $\vec{k}_4 = \vec{p}_2$ in (3.33) and integrating over \vec{p}_1 and \vec{p}_2 ,

$$\begin{aligned} \langle \phi^2 \phi^2 \rangle'_\lambda &= \int \frac{d^D p_1}{(2\pi)^D} \frac{d^D p_2}{(2\pi)^D} \left\langle \phi_{\vec{k}+\vec{p}_1}^{(v_1)} \phi_{\vec{p}_1}^{(v_2)} \phi_{\vec{k}+\vec{p}_2}^{(v_3)} \phi_{\vec{p}_2}^{(v_4)} \right\rangle' \\ &= C \int [ds]_4 2\pi i \delta\left(\frac{D}{2} - (s_1 + s_2 + s_3 + s_4)\right) \rho(\mathbf{s}, \mathbf{v}) 2^D I_{\text{spec}}(k, \mathbf{s}, \mathbf{v}). \end{aligned} \quad (3.37)$$

Here, I_{spec} is the momentum integral and we have collected the prefactors into the constant C ,

$$I_{\text{spec}}(k, \mathbf{s}, \mathbf{v}) = \int \frac{d^D p_1}{(2\pi)^D} \frac{d^D p_2}{(2\pi)^D} \frac{1}{|\vec{k} + \vec{p}_1|^{2s_1 - iv_1}} \frac{1}{p_1^{2s_2 - iv_2}} \frac{1}{|\vec{k} + \vec{p}_2|^{2s_3 - iv_3}} \frac{1}{p_2^{2s_4 - iv_4}} \quad (3.38)$$

$$C = H^{-D-1} \sin\left(\frac{\pi}{2}(D + i(v_1 + v_2 + v_3 + v_4))\right) \left(\prod_{j=1}^4 \frac{1}{2^{iv_j}} \mathcal{N}_{v_j}(\tau_0)\right). \quad (3.39)$$

We keep the masses distinct for now, leaving open the possibility of using the v_j 's to regulate the divergences in (3.37). The momentum integral (3.38) clearly factorizes into two integrals of the

⁶The integrand in (3.23) also has poles $s_* = \frac{iv}{2} + n$ but these produce analytic terms in k which don't give rise to long-distance correlations. See [67].

form

$$I_{\text{mom}}(a, b) = \int \frac{d^D p}{(2\pi)^D} \frac{1}{|\vec{k} + \vec{p}|^a} \frac{1}{p^b}. \quad (3.40)$$

This presents us with the opportunity to introduce an analytic continuation parameter. To see how, we first note that I_{mom} is just the convolution of the function $\tilde{f}_n(\vec{p}) = 1/p^n$ with itself,

$$I_{\text{mom}}(a, b) = \int \frac{d^D p}{(2\pi)^D} \tilde{f}_a(\vec{k} + \vec{p}) \tilde{f}_b(\vec{p}) = \int d^D y e^{-i\vec{k}\cdot\vec{y}} f_a(\vec{y}) f_b(\vec{y}), \quad (3.41)$$

where $f_n(\vec{y})$ is given by the radial Fourier transform

$$f_n(\vec{y}) = \int \frac{d^D p}{(2\pi)^D} \frac{e^{i\vec{p}\cdot\vec{y}}}{p^n} = \frac{1}{2^n \pi^{D/2}} \frac{\Gamma(\frac{D-n}{2})}{\Gamma(\frac{n}{2})} y^{n-D}. \quad (3.42)$$

Before substituting this into (3.41) we change the integral measure $d^D y \rightarrow d^{\bar{D}} y$ with the promise that we'll take $\bar{D} \rightarrow D$ at the end. We will also introduce a factor of $(-\tau_0)^{D-\bar{D}}$ in front to preserve the overall dimensions, and to ensure that the momenta \vec{k} appears as the product $-k\tau_0$ in the final answer. This way it remains invariant under the rescaling $k \rightarrow \rho^{-1}k$ and $a(\tau) \rightarrow \rho^{-1}a(\tau)$ [64].

With these changes

$$\begin{aligned} \bar{I}_{\text{mom}}(a, b) &= \frac{1}{2^{a+b} \pi^{\bar{D}}} \frac{\Gamma(\frac{D-a}{2}) \Gamma(\frac{D-b}{2})}{\Gamma(\frac{a}{2}) \Gamma(\frac{b}{2})} (-\tau_0)^{D-\bar{D}} \int d^{\bar{D}} y \frac{e^{-i\vec{k}\cdot\vec{y}}}{y^{2D-a-b}} \\ &\stackrel{(3.42)}{=} \frac{1}{(4\pi)^{\frac{2D-\bar{D}}{2}}} \frac{\Gamma(\frac{D-a}{2}) \Gamma(\frac{D-b}{2})}{\Gamma(\frac{a}{2}) \Gamma(\frac{b}{2})} \frac{\Gamma(\frac{a+b}{2} - \frac{2D-\bar{D}}{2})}{\Gamma(D - \frac{a+b}{2})} k^{D-a-b} (-k\tau_0)^{D-\bar{D}} \end{aligned} \quad (3.43)$$

where we have introduced a bar above \bar{I}_{mom} to indicate that we have tampered with the dimension D at an intermediate step. The difference $D - \bar{D}$ can be used as an analytic continuation parameter.

We introduce this parameter into one of the momentum integrals in (3.38) by writing

$$I_{\text{spec}} = \bar{I}_{\text{mom}}(2s_1 - i\nu_1, 2s_2 - i\nu_2) \times I_{\text{mom}}(2s_3 - i\nu_3, 2s_4 - i\nu_4) \quad (3.44)$$

with the other momentum integral obtained by setting $D = \bar{D}$ in (3.43). We may now substitute this into (3.37) and integrate over s_4 to apply the delta function. The result is

$$\begin{aligned}
\langle \phi^2 \phi^2 \rangle'_\lambda &= C \frac{2^D}{(4\pi)^{\frac{3D-\bar{D}}{2}}} (-k\tau_0)^{D-\bar{D}} k^{D+i\Sigma_j v_j} \\
&\times \int [ds]_3 \Gamma\left(\frac{D}{2} - s_1 - s_2 - s_3 + \frac{iv_4}{2}\right) \Gamma\left(s_1 + s_2 + s_3 + \frac{iv_4}{2}\right) \prod_{j=1}^3 \Gamma\left(s_j + \frac{iv_j}{2}\right) \Gamma\left(\frac{D}{2} - s_j + \frac{iv_j}{2}\right) \\
&\times \frac{\Gamma\left(\frac{\bar{D}}{2} - D + s_1 + s_2 - \frac{iv_1}{2} - \frac{iv_2}{2}\right) \Gamma\left(-s_1 - s_2 - \frac{iv_3}{2} - \frac{iv_4}{2}\right)}{\Gamma\left(D - s_1 - s_2 + \frac{iv_1}{2} + \frac{iv_2}{2}\right) \Gamma\left(\frac{D}{2} + s_1 + s_2 + \frac{iv_3}{2} + \frac{iv_4}{2}\right)}. \tag{3.45}
\end{aligned}$$

The divergences are completely encoded in the 3-fold MB integral. To proceed we will need to plug in values for D and v_j .

3.4.1 The conformal mass case

We will first compute γ_{ϕ^2} for a scalar field with conformal mass $m^2 = 2H^2$ in $D = 3$ dimensions. This corresponds to $v = \frac{i}{2}$. Substituting these numbers into (3.36) we obtain the tree level contribution

$$\langle \phi^2 \phi^2 \rangle'_{\text{tree}} = -\frac{1}{8\pi^2} (-H\tau_0)^4 k. \tag{3.46}$$

The first order correction follows from setting

$$\begin{aligned}
v_2 &\rightarrow \frac{i}{2} - i2\alpha \\
v_j &\rightarrow \frac{i}{2}, \quad j \neq 2 \\
\bar{D} &\rightarrow 3 + 2\delta
\end{aligned} \tag{3.47}$$

in (3.45). We have introduced the parameters α and δ to make the MB integral well-defined, that is, to remove any overlaps of left/right poles as required by the Mellin contour prescription⁷. These are the parameters denoted by ϵ_k in (3.17). The actual integral, with $\alpha = 0 = \delta$, will be

⁷It is possible to remove all pole overlaps in this case with just one parameter, as discussed in sec. 3.4.1. We chose to use two here to illustrate some aspects of using multiple parameters.

defined by analytically continuing in these parameters. With these substitutions

$$\langle \phi^2 \phi^2 \rangle'_\lambda = C \frac{8}{(4\pi)^{3-\delta}} k^{1+2\alpha} (-k\tau_0)^{-2\delta} \int [ds]_3 \frac{\Gamma_1 \Gamma_2 \Gamma_3 \Gamma_4 \Gamma_5 \Gamma_6 \Gamma_7 \Gamma_8 \Gamma_9 \Gamma_{10}}{\Gamma_{11} \Gamma_{12}}, \quad (3.48)$$

where we have labelled the Γ -functions,

$$\begin{aligned} \Gamma_1 &= \Gamma(-\tfrac{1}{4} + s_1) \\ \Gamma_2 &= \Gamma(\tfrac{5}{4} - s_1) \\ \Gamma_3 &= \Gamma(-\tfrac{1}{4} + s_2 + \alpha) \\ \Gamma_4 &= \Gamma(\tfrac{5}{4} - s_2 + \alpha) \\ \Gamma_5 &= \Gamma(-\tfrac{1}{4} + s_3) \\ \Gamma_6 &= \Gamma(\tfrac{5}{4} - s_3) \\ \Gamma_7 &= \Gamma(-\tfrac{1}{4} + s_1 + s_2 + s_3) \\ \Gamma_8 &= \Gamma(\tfrac{5}{4} - s_1 - s_2 - s_3) \\ \Gamma_9 &= \Gamma(\tfrac{1}{2} - s_1 - s_2) \\ \Gamma_{10} &= \Gamma(-1 + s_1 + s_2 - \alpha + \delta) \\ \Gamma_{11} &= \Gamma(1 + s_1 + s_2) \\ \Gamma_{12} &= \Gamma(\tfrac{5}{2} - s_1 - s_2 + \alpha). \end{aligned} \quad (3.49)$$

The evaluation of this integral is discussed in detail below. However, most parts of the calculation can be done using the MB Mathematica package by Czakon [76].

Choosing the contours

We shall focus on the MB integral

$$K = \int [ds]_3 \frac{\Gamma_1 \Gamma_2 \Gamma_3 \Gamma_4 \Gamma_5 \Gamma_6 \Gamma_7 \Gamma_8 \Gamma_9 \Gamma_{10}}{\Gamma_{11} \Gamma_{12}}. \quad (3.50)$$

We will integrate this over straight line contours. The integral is well-defined if we can choose contours such that (3.15) is satisfied. This gives the following inequalities:

$$\begin{aligned}
U_{1,2}(\mathcal{C}) > 0 &\implies \frac{1}{4} < s_1^\mathcal{C} < \frac{5}{4} \\
U_{3,4}(\mathcal{C}) > 0 &\implies \frac{1}{4} - \alpha < s_2^\mathcal{C} < \frac{5}{4} + \alpha \\
U_{5,6}(\mathcal{C}) > 0 &\implies \frac{1}{4} < s_3^\mathcal{C} < \frac{5}{4} \\
U_{7,8}(\mathcal{C}) > 0 &\implies \frac{1}{4} < s_1^\mathcal{C} + s_2^\mathcal{C} + s_3^\mathcal{C} < \frac{5}{4} \\
U_9(\mathcal{C}) > 0 &\implies s_1^\mathcal{C} + s_2^\mathcal{C} < \frac{1}{2} \\
U_{10}(\mathcal{C}) > 0 &\implies s_1^\mathcal{C} + s_2^\mathcal{C} > 1 + \alpha - \delta.
\end{aligned} \tag{3.51}$$

These inequalities can be combined to give the condition

$$\max\left(\frac{1}{4}, \frac{3}{4} - \alpha, \frac{5}{4} + \alpha - \delta\right) < s_1^\mathcal{C} + s_2^\mathcal{C} + s_3^\mathcal{C} < \min\left(\frac{5}{4}, \frac{7}{4}, \frac{15}{4} + \alpha\right). \tag{3.52}$$

The contours $s_1^\mathcal{C}$ and $s_2^\mathcal{C}$ have another constraint which follows from $U_{1,3,9}(\mathcal{C}) > 0$,

$$\frac{1}{2} - \alpha < s_1^\mathcal{C} + s_2^\mathcal{C} < \frac{1}{2}. \tag{3.53}$$

This condition can only be satisfied if $\alpha > 0$. This means that for sufficiently small α and δ , (3.52) becomes

$$\frac{5}{4} + \alpha - \delta < s_1^\mathcal{C} + s_2^\mathcal{C} + s_3^\mathcal{C} < \frac{5}{4}, \tag{3.54}$$

which requires $\delta > \alpha$. The inequalities (3.53) and (3.54) indicate that the contours are pinched, with α and $\delta - \alpha$ being the width of the pinches (cf. Fig. 3.3). We will see shortly how these pinches manifest as the divergences of (3.50).

The conditions (3.51) can be satisfied by choosing $\alpha = 0.1$, $\delta = 0.7$, $s_1^\mathcal{C} = s_3^\mathcal{C} = 0.3$ and $s_2^\mathcal{C} = 0.17$. This choice is by no means unique.

Analytic continuation

With the contours fixed we start at $\alpha = 0.1, \delta = 0.7$ and analytically continue to the region around $\alpha, \delta \sim 0$. As we decrease α and δ we keep track of the poles that cross the straight line contours and add the residues at those poles to the integral in (3.50), now evaluated at a smaller value of the parameters α and δ . These residue terms may have poles in the remaining variables which can cross other contours as the parameters are decreased further. Iterating this process we end up with a collection of residue terms, plus the original four fold integral. Some of the residue terms contain factors that diverge as $\alpha, \delta \rightarrow 0$. All remaining integrals can simply be expanded in α, δ under the integral sign since there are no further pole crossings.

The present example is simple enough that we end up with only four residue terms. Decreasing to $\alpha = 0.08$ and $\delta = 0.56$, the first poles to cross the contours are at $s_2 = \frac{1}{4} - \alpha$ and $s_2 = 1 - s_1 + \alpha - \delta$ which are the zeroth poles of Γ_3 and Γ_{10} . Following the pattern in (3.11) and (3.21), we can write

$$K \rightarrow K_3 + K_{10} + K, \quad (3.55)$$

where the K on the r.h.s. is evaluated at the new values of α and δ , and

$$K_3 = \int \frac{ds_1}{2\pi i} \frac{ds_3}{2\pi i} \frac{\Gamma_1 \Gamma_2 \Gamma_4 \Gamma_5 \Gamma_6 \Gamma_7 \Gamma_8 \Gamma_9 \Gamma_{10}}{\Gamma_{11} \Gamma_{12}} \Big|_{s_2 = \frac{1}{4} - \alpha}, \quad (3.56)$$

$$K_{10} = \int \frac{ds_1}{2\pi i} \frac{ds_3}{2\pi i} \frac{\Gamma_1 \Gamma_2 \Gamma_3 \Gamma_4 \Gamma_5 \Gamma_6 \Gamma_7 \Gamma_8 \Gamma_9}{\Gamma_{11} \Gamma_{12}} \Big|_{s_2 = 1 - s_1 + \alpha - \delta}. \quad (3.57)$$

The Γ functions of K_3 and K_{10} will have a different dependence on α and δ once s_2 is eliminated. Reducing the parameters further we find that the zeroth pole of Γ_9 , at $s_1 = \frac{1}{4} + \alpha$, crosses over in K_3 prompting us to write $K_3 \rightarrow K_{39} + K_3$. At the same time the pole $s_3 = \frac{1}{4} - \alpha + \delta$ of Γ_8 crosses over in K_{10} leading to the split $K_{10} \rightarrow K_{10,8} + K_{10}$. There are no further pole crossings as

$\alpha, \delta \rightarrow 0$. All in all we end up with

$$K \rightarrow K_{39} + K_{10,8} + K_3 + K_{10} + K. \quad (3.58)$$

The term K_{39} is

$$\frac{2\Gamma(\alpha)\Gamma(1-\alpha)\Gamma(2\alpha+1)\Gamma(-\frac{1}{2}-\alpha+\delta)}{\sqrt{\pi}\Gamma(\alpha+2)} \int_{0.3-i\infty}^{0.3+i\infty} \frac{ds_3}{2\pi i} \Gamma(\frac{3}{4}-s_3)\Gamma(\frac{5}{4}-s_3)\Gamma(-\frac{1}{4}+s_3)\Gamma(\frac{1}{4}+s_3). \quad (3.59)$$

The left/right poles in the s_3 integral are separated by the contour. Therefore we can evaluate this integral using Barnes's first lemma⁸ to obtain

$$K_{39} = -2\pi\Gamma(\alpha) + O(1). \quad (3.61)$$

Next, the integral $K_{10,8}$ is

$$K_{10,8} = \frac{\Gamma(\delta-\alpha)\Gamma(1+\alpha-\delta)\Gamma(-\frac{1}{2}-\alpha+\delta)}{\Gamma(\frac{3}{2}+\delta)\Gamma(2+\alpha-\delta)} \times \int_{0.3-i\infty}^{0.3+i\infty} \frac{ds_1}{2\pi i} \Gamma(\frac{5}{4}-s_1)\Gamma(-\frac{1}{4}+s_1)\Gamma(\frac{1}{4}+s_1+\delta)\Gamma(\frac{3}{4}-s_1+2\alpha-\delta). \quad (3.62)$$

The poles of the of the s_1 integral are well separated by the straight line contour around $\alpha, \delta \sim 0$.

Therefore we can once again use (3.60) to obtain

$$K_{10,8} = -2\pi\Gamma(\delta-\alpha) + O(1). \quad (3.63)$$

The remaining terms K_3, K_{10} and K in (3.58) are at most⁹ $O(1)$ and can be ignored. Putting the

⁸Barnes's first lemma states

$$\int_{-i\infty}^{+i\infty} \frac{dz}{2\pi i} \Gamma(\lambda_1+z)\Gamma(\lambda_2+z)\Gamma(\lambda_3-z)\Gamma(\lambda_4-z) = \frac{\Gamma(\lambda_1+\lambda_3)\Gamma(\lambda_1+\lambda_4)\Gamma(\lambda_2+\lambda_3)\Gamma(\lambda_2+\lambda_4)}{\Gamma(\lambda_1+\lambda_2+\lambda_3+\lambda_4)}, \quad (3.60)$$

where the contour is a vertical line that separates the left/right poles of the Γ functions in the integrand.

⁹ $O(1)$ terms are those which do not blow up as the analytic continuation parameters approach 0.

pieces together we have

$$K = -2\pi [\Gamma(\alpha) + \Gamma(\delta - \alpha)] + O(1), \quad (3.64)$$

which completes the evaluation of (3.50). Substituting the above result into (3.48),

$$\langle \phi^2 \phi^2 \rangle'_\lambda = \lim_{\alpha, \delta \rightarrow 0} C \frac{8}{(4\pi)^{3-\delta}} k^{1+2\alpha} (-k\tau_0)^{-2\delta} \times -2\pi [\Gamma(\alpha) + \Gamma(\delta - \alpha)]. \quad (3.65)$$

We evaluate the prefactor C defined in (3.39) with the v_j from (3.47) and¹⁰ $D = 3$,

$$C = \frac{H^4}{2^{6+2\alpha} \pi^{5/2}} \cos(\pi\alpha) \Gamma(\frac{1}{2} - 2\alpha) (-\tau_0)^{4+2\alpha} \sim \frac{H^4}{64\pi^2} (-\tau_0)^{4+2\alpha}. \quad (3.66)$$

Then, at leading order in α and δ we have

$$\langle \phi^2 \phi^2 \rangle'_\lambda = \frac{(-H\tau_0)^4}{512\pi^5} k \times -2\pi \left[\frac{1}{\alpha} + \frac{1}{\delta - \alpha} - 2\gamma_E + \dots \right] (-k\tau_0)^{2\alpha - 2\delta}. \quad (3.67)$$

As expected the divergences are directly related to the width of the pinches. However, we do not know the exact relationship between α and δ except that they are both infinitesimal and $\delta > \alpha$ (this condition, which follows from (3.54), fixes the sign of the $\frac{1}{\delta - \alpha}$ divergence and we must adhere to it throughout the analytic continuation process). It is ‘reasonable’ to make the width of the pinches equal by setting $\delta - \alpha = \alpha$. Then,

$$\boxed{\langle \phi^2 \phi^2 \rangle'_\lambda = -\frac{(-H\tau_0)^4}{128\pi^4} k \left[\frac{1}{\alpha} - 2\log(-k\tau_0) + \dots \right]}. \quad (3.68)$$

¹⁰The number of space dimensions in (3.39) is $D = 3$ and not the $\bar{D} = 3 + 2\delta$ introduced in (3.43).

An alternate parameterization

It is possible to define (3.50) with a single parameter instead of the α and δ we introduced in (3.47). This time we will set all $v_j \rightarrow \frac{i}{2}$ and $\bar{D} = D = 3$ but modify the time integral (3.30) to

$$(-\tau_0)^{-2\varepsilon} \int_{-\infty}^{\tau_0} d\tau (-\tau)^{D-1-2(s_1+s_2+s_3+s_4)+2\varepsilon} \stackrel{\tau_0 \rightarrow 0}{\equiv} (-\tau_0)^{-2\varepsilon} \times i\pi\delta\left(\frac{D}{2} - (s_1 + s_2 + s_3 + s_4) + \varepsilon\right) \quad (3.69)$$

where ε is the new parameter in which we will analytically continue. We have used a factor of $(-\tau_0)^{-2\varepsilon}$ to keep the dimensions correct, just as we did in (3.43). Introducing these changes into (3.45) and repeating the calculation we get

$$\langle \phi^2 \phi^2 \rangle'_\lambda = -\frac{(-H\tau_0)^4}{128\pi^4} k \left[\frac{1}{\varepsilon} - 2\log(-k\tau_0) + \dots \right], \quad (3.70)$$

in agreement with (3.68). There is no ambiguity about the relationship between analytic continuation parameters here since there is only one of them. We also see that it was correct to require the width of the pinches match, for, any other choice would have led to a different answer. This piece of insight will be useful in the next example where it is impossible to make the MB integral well-defined with just one parameter.

Dynamical renormalization

The expression (3.68), with its $1/\alpha$ pole and the associated log, resembles a standard 1-loop result in flat space, computed by continuing the number of spacetime dimensions¹¹. The term $\log(-k\tau_0) \equiv \log(k/(aH))$ blows up at late times, $\tau_0 \rightarrow 0$, jeopardizing the validity of the perturbation series. This indicates that our series expansion was too simple-minded to begin with, and a more careful treatment is required to handle these secular growth terms. The Dynamical Renormalization Group (DRG) [77, 78] provides the required fix. To review quickly, we start by

¹¹We can push the analogy further, to see that resumming the logs at all orders will simply change the scaling dimension of the ϕ^2 operator (cf. (3.72)). The parallel between DRG and RG is explored in greater detail in [64].

combining (3.46) and (3.68),

$$\begin{aligned}\langle\phi^2\phi^2\rangle' &= \langle\phi^2\phi^2\rangle'_{\text{tree}} - \lambda\langle\phi^2\phi^2\rangle'_\lambda + O(\lambda^2) \\ &= -\frac{1}{8\pi^2}(-H\tau_0)^4 k \left[1 - \frac{\lambda}{16\pi^2} \left(\frac{1}{\alpha} - 2\log(-k\tau_0) + \dots \right) + O(\lambda^2) \right].\end{aligned}\quad (3.71)$$

We now remove the divergence with a counterterm, which also introduces a new ratio of scales $k_*/(aH)_*$ (see [77, 64] for more details). Noticing that the correlation function must be independent of this ratio, we obtain a differential equation for $\langle\phi^2\phi^2\rangle$, the solution of which resums the secular logs to

$$\begin{aligned}\langle\phi^2\phi^2\rangle' &= -\frac{1}{8\pi^2}(-H\tau_0)^4 k \exp\left(\frac{\lambda}{8\pi^2}\log(-k\tau_0) + \dots\right) (1 + \dots) \\ &= -\frac{1}{8\pi^2}(-H\tau_0)^4 k (-k\tau_0)^{2\gamma_{\phi^2}} (1 + O(\lambda^2)) \\ &= -\frac{1}{8\pi^2} \frac{H^{-2\gamma_{\phi^2}}}{a(\tau_0)^{2\Delta_{\phi^2} + 2\gamma_{\phi^2}}} k^{1+2\gamma_{\phi^2}} (1 + O(\lambda^2)).\end{aligned}\quad (3.72)$$

Thus, treating the secular dependence with DRG induces an anomalous dimension for the ϕ^2 operator, namely

$$\gamma_{\phi^2} = \frac{\lambda}{16\pi^2}.\quad (3.73)$$

This anomalous scaling is a product of subhorizon effects, as we demonstrate in sec. 3.5.1. For now, we note that the treatment of secular growth in dS closely resembles the handling of UV divergences in flat space. This connection holds for all scalar fields of general mass, except when the field is massless; massless scalars in dS have no flat space analogue.

3.4.2 γ_{ϕ^2} for other masses

The calculation above was repeated for a few other light scalars with masses in the range $0 < m^2 < (\frac{D}{2})^2 H^2$. The results are summarized in Table 3.1, and plotted in Fig. 3.8. An interesting feature of this graph is the sharp rise in the value of γ_{ϕ^2} as we approach the massless

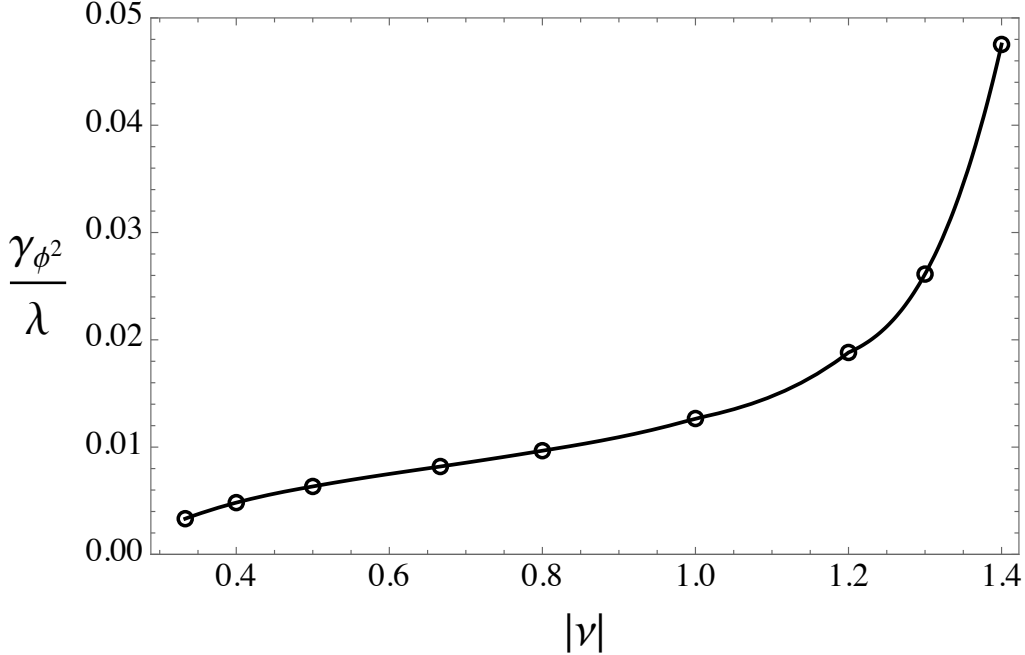


Figure 3.8. Anomalous dimension of ϕ^2 for different masses. Larger values of $|\nu|$ correspond to smaller masses (see (3.3)). The encircled points are given in table 3.1.

limit, $\nu \rightarrow i3/2$. This indicates another divergence creeping in as we decrease the mass to zero. If we set all $\nu_j = i3/2 - i2\alpha$ and $D = 3$ in (3.45), and examine the Γ functions, we will find *four* pairs of nearly overlapping zeroth poles which can lead to a maximum of three simultaneous contour pinches¹². That means $\langle \phi^2 \phi^2 \rangle_\lambda$ diverges as $\sim \alpha^{-3}$ where 2α is the width of each pinch. Of these, one factor of α^{-1} is already present at the tree level (cf. (3.36) and [84]) and another factor of α^{-1} comes from the loop integral, just like in (3.68). The remaining α^{-1} is roughly due to time evolution of the long wavelength modes; this intuition is made precise by the effective field theory treatment of such modes in [65, 66]. Such divergences are a well-known feature of massless fields in dS and their careful resummation leads to Starobinsky’s Stochastic Inflation framework [80, 32].

¹²A very similar phenomenon happens with the massless two-loop calculation in sec. 3.5.1. The divergence structure of the MB integral is explained in greater detail there.

Table 3.1. Anomalous dimension of ϕ^2 for different masses.

$ \mathbf{v} $	γ_{ϕ^2}/λ
1/3	0.00333
2/5	0.00483
1/2	$\frac{1}{16\pi^2}$
2/3	0.00819
4/5	0.00967
1	$\frac{1}{8\pi^2}$
6/5	0.01882
13/10	0.02612
7/5	0.04753

3.5 Mixing of ϕ^3 and ϕ

As our second example, we compute the order λ contribution to $\langle\phi^3\phi\rangle$. The dynamics of a massless scalar, as described by Stochastic Inflation, receives an NNLO correction from this term [66]. It is easiest to see this in the Soft de Sitter Effective Theory (SdSET), wherein Stochastic Inflation is a direct consequence of EFT power counting (see sec. 5.2 of [65]). The calculation below produces the same divergence structure for $\langle\phi^3\phi\rangle_\lambda$ in the full theory as that computed in the SdSET, verifying the correctness of the effective theory approach.

We start with (3.33) and contract three of the legs together resulting in the two loop diagram of Fig. 3.9,

$$\begin{aligned}
 \langle\phi^3\phi\rangle'_\lambda &= \int \frac{d^D p_1}{(2\pi)^D} \frac{d^D p_2}{(2\pi)^D} \left\langle \phi_{\vec{p}_1}^{(v_1)} \phi_{\vec{p}_2}^{(v_2)} \phi_{\vec{k}-\vec{p}_1-\vec{p}_2}^{(v_3)} \phi_{\vec{k}}^{(v_4)} \right\rangle' \\
 &= C \int [ds]_4 2\pi i \delta\left(\frac{D}{2} - (s_1 + s_2 + s_3 + s_4)\right) \rho(\mathbf{s}, \mathbf{v}) 2^D I_{\text{sun}}(k, \mathbf{s}, \mathbf{v})
 \end{aligned} \tag{3.74}$$

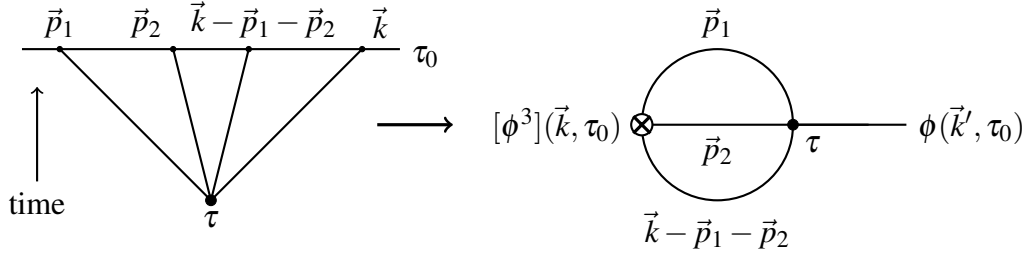


Figure 3.9. The leading contribution to $\langle \phi^3 \phi \rangle$.

where C is the prefactor defined in (3.39) and I_{sun} is the momentum integral

$$I_{\text{sun}}(k, \mathbf{s}, \mathbf{v}) = \int \frac{d^D p_1}{(2\pi)^3} \frac{d^D p_2}{(2\pi)^3} \frac{1}{p_1^a p_2^b (\vec{k} - \vec{p}_1 - \vec{p}_2)^c k^d}, \quad (3.75)$$

with $a = 2s_1 - iv_1$, $b = 2s_2 - iv_2$, $c = 2s_3 - iv_3$ and $d = 2s_4 - iv_4$. Once again, this integral can be evaluated by noting that it is a convolution in momentum space (cf. (3.41)). We'll also take this opportunity to introduce an analytic continuation parameter $D - \bar{D}$, just as we did in (3.43).

The result is

$$I_{\text{sun}}(k, \mathbf{s}, \mathbf{v}) = \frac{1}{(4\pi)^{\frac{3D-\bar{D}}{2}}} \frac{(-k\tau_0)^{D-\bar{D}}}{k^{\sum_{j=1}^3 (2s_j - iv_j) - 2D}} \prod_{j=1}^3 \frac{\Gamma\left(\frac{D}{2} - s_j + \frac{iv_j}{2}\right)}{\Gamma\left(s_j - \frac{iv_j}{2}\right)} \frac{\Gamma\left(s_1 + s_2 + s_3 - i(\mathbf{v}_1 + \mathbf{v}_2 + \mathbf{v}_3)/2 - \frac{3D-\bar{D}}{2}\right)}{\Gamma\left(\frac{3D}{2} - s_1 - s_2 - s_3 + i(\mathbf{v}_1 + \mathbf{v}_2 + \mathbf{v}_3)/2\right)}. \quad (3.76)$$

We can substitute this into (3.74) and apply the delta function. In order to proceed we must plug in some actual numbers for the masses and dimension.

3.5.1 The massless case

We'll now restrict our attention to the case of massless scalar fields. It is not possible to make (3.74) well-defined with a single parameter. So we will do the calculation in two different parameterizations, first by floating the masses and then by tweaking the time integral and number

of dimensions, and compare the results. We set

$$\begin{aligned}
v_j &= i\frac{3}{2} - i2\alpha_j, \quad j = 1, 2, 3 \\
v_4 &= i\frac{3}{2} - i2\alpha_4 \\
D &= 3 \\
\bar{D} &= 3 + 2\delta
\end{aligned} \tag{3.77}$$

where we have introduced three parameters to satisfy (3.15). We could have chosen a different α_j for each v_j , to get $v_j = i\frac{3}{2} - i2\alpha_j$. However these parameters will always show up together as the sum $\alpha_1 + \alpha_2 + \alpha_3$, which make sense since the s_j variables associated with the legs carrying loop momenta are interchangeable. So $\alpha_1 + \alpha_2 + \alpha_3$ is really just one parameter which we have identified as 3α and distributed equally between v_1, v_2 and v_3 . The fourth leg, which does not participate in the loop integral, is given its own α_4 . We end up with

$$\langle \phi^3 \phi \rangle'_\lambda = C \frac{8}{(4\pi)^{3-\delta}} \frac{(-k\tau_0)^{-2\delta}}{k^{3-6\alpha-2\alpha_4}} \int [ds]_3 \frac{\Gamma_1 \Gamma_2 \Gamma_3 \Gamma_4 \Gamma_5 \Gamma_6 \Gamma_7 \Gamma_8 \Gamma_9}{\Gamma_{10}}, \tag{3.78}$$

where

$$\begin{aligned}
\Gamma_1 &= \Gamma\left(\frac{9}{4} - s_1 - s_2 - s_3 - \alpha_4\right) \\
\Gamma_2 &= \Gamma\left(\frac{3}{4} - s_1 - s_2 - s_3 + \alpha_4\right) \\
\Gamma_3 &= \Gamma\left(-\frac{3}{4} + s_1 + s_2 + s_3 - 3\alpha + \delta\right) \\
\Gamma_4 &= \Gamma\left(\frac{3}{4} - s_1 + \alpha\right) \\
\Gamma_5 &= \Gamma\left(-\frac{3}{4} + s_1 + \alpha\right) \\
\Gamma_6 &= \Gamma\left(\frac{3}{4} - s_2 + \alpha\right) \\
\Gamma_7 &= \Gamma\left(-\frac{3}{4} + s_2 + \alpha\right) \\
\Gamma_8 &= \Gamma\left(\frac{3}{4} - s_3 + \alpha\right) \\
\Gamma_9 &= \Gamma\left(-\frac{3}{4} + s_3 + \alpha\right) \\
\Gamma_{10} &= \Gamma\left(\frac{9}{4} - s_1 - s_2 - s_3 + 3\alpha\right).
\end{aligned} \tag{3.79}$$

We will now focus on evaluating the MB integral in (3.78),

$$K = \int [ds]_3 \frac{\Gamma_1 \Gamma_2 \Gamma_3 \Gamma_4 \Gamma_5 \Gamma_6 \Gamma_7 \Gamma_8 \Gamma_9}{\Gamma_{10}}. \tag{3.80}$$

Anticipating the answer

At a glance (3.80) looks very similar to (3.50) but it is in fact hiding a much more intricate divergence structure. This is already apparent if we examine the arguments of the Γ functions above. For instance, the zeroth left pole of Γ_4 is at a distance 2α from the zeroth right pole of Γ_5 . As we take $\alpha \rightarrow 0$ these poles pinch the contour and generate a $1/2\alpha$ divergence. There are four such pairs of Γ functions in the list which together can generate up to a cubic order divergence. Thus, without actually evaluating (3.80), we may deduce the following form of the answer:

$$K \sim \frac{c_3}{\alpha^3} + \frac{c_2}{\alpha^2} + \frac{c_1}{\alpha} + O(\alpha^0), \tag{3.81}$$

where α denotes some linear combination of the parameters α, α_4 and δ , all of which are nearly zero, and c_i collects together the remaining factors. Also note that, for a massive scalar ($|v| < 3/2$) there would be fewer simultaneous contour pinches, and the leading small α behavior would be less singular than (3.81). This is another example of our observation from Fig. 3.8: massless scalars in dS are saddled with more IR divergences than their massive counterparts.

The Mellin variables s_j carry physical meaning, as eigenvalues of the dilatation operator. Therefore, it is worth understanding which poles contribute to the terms in (3.81). To do so we consider a simpler 2-fold toy integral, with the same features as (3.80):

$$K_{\text{toy}} = \int [ds]_2 \Gamma(\frac{3}{4} - s_1 - s_2 + \alpha) \Gamma(-\frac{3}{4} + s_1 + s_2 + \alpha) \prod_{j=1}^2 \Gamma(\frac{3}{4} - s_j + \alpha) \Gamma(-\frac{3}{4} + s_j + \alpha). \quad (3.82)$$

As $\alpha \rightarrow 0$ this integrand generates three contour pinches, of which at most two manifest simultaneously. Thus, the answer has the form

$$K_{\text{toy}} \sim \frac{\bar{c}_2}{\alpha^2} + \frac{\bar{c}_1}{\alpha} + O(\alpha^0). \quad (3.83)$$

We can examine the singular structure of K_{toy} on a $\Re(s_1) - \Re(s_2)$ plane (Fig. 3.10). The poles of our integrand are real and these are represented by straight lines in Fig. 3.10a and Fig. 3.10b. These lines are the graphs $U_i(\mathbf{s}) = -n$ (cf. (3.14)). For example, the red lines represent the poles of $\Gamma(3/4 - s_j + \alpha)$, which are at $s_{j*} = 3/4 + \alpha + n$ with $n \in \mathbb{Z}_0$ and $j = 1, 2$. Similarly, we map:

$$\begin{aligned} \frac{3}{4} - s_j + \alpha &= -n \text{ (red lines)} \\ -\frac{3}{4} + s_j + \alpha &= -n \text{ (blue lines)} \\ \frac{3}{4} - s_1 - s_2 + \alpha &= -n \text{ (orange lines)} \\ -\frac{3}{4} + s_1 + s_2 + \alpha &= -n \text{ (green lines)}. \end{aligned}$$

In applying Cauchy's theorem we compute residues at the intersections of these lines and add

them up in specific ways [85]. The real parts of the straight line contours are represented by a point \mathcal{C} in these plots.

We define the integral by choosing a value of α such that the left/right poles are well separated by contours, as shown in Fig. 3.10a (see also Fig. 3.4b). As we decrease $\alpha \rightarrow 0$ some of the $n = 0$ poles (blue and orange) cross over to the other side, and come within 2α distance of $n = 0$ poles of the opposite nature (red and green lines). The crossed poles are indicated by dashed lines in Fig. 3.10b, and the intersections at which we take residues are marked with dots. Due to their proximity to other poles, the residues along each dashed line will contain a factor of $\Gamma(2\alpha)$ (cf. (3.10)); residues computed at intersections of two dashed lines generate $\Gamma(2\alpha)^2$. Residues computed at all other intersections, which don't involve any dashed lines, contribute to the $O(\alpha^0)$ term in (3.83).

It is clear from Fig. 3.10 that only a small subset of all possible poles contribute divergences to the answer. This is just a 2-dimensional generalization of what we observed in (3.11). However, there is something else going on: only a *finite* number of intersections produce an α^{-2} term, whereas an infinity of them diverge as α^{-1} . The poles which generate the α^{-2} capture the leading behavior of the mode functions in the long wavelength limit (see discussion under (3.35)). In fact, the EFT description of such soft modes reproduces this divergence exactly, without any UV matching [66]. On the other hand, an infinite number of residues have to be summed over to fully account for the α^{-1} term, indicating that it is tracking much more than just $k \ll (aH)$ effects. In other words, this term encodes subhorizon physics. A similar analysis on the example from sec. 3.4.1 would show that the α^{-1} term there is also derived from summing over an infinite number of intersections (this is apparent from (3.59) and (3.62)), which means the anomalous scaling we found there was truly a UV effect.

Diagrams like Fig. 3.10 have special significance in the evaluation of multidimensional MB integrals by the method of residues [86]. The straight lines we studied above become hypersurfaces for an N -fold MB integral, and we take residues over the polyhedra formed by these surfaces. For a field theory calculation, this leads to a multiple series in powers and

logarithms of the kinematic parameters. The convergence of such a series has a geometrical connection to the aforementioned polyhedra [85, 87]. While we focus only on the divergent contributions in this work, it would be worth investigating whether the ideas in these references can be used to understand the properties of dS loops in various kinematic limits.

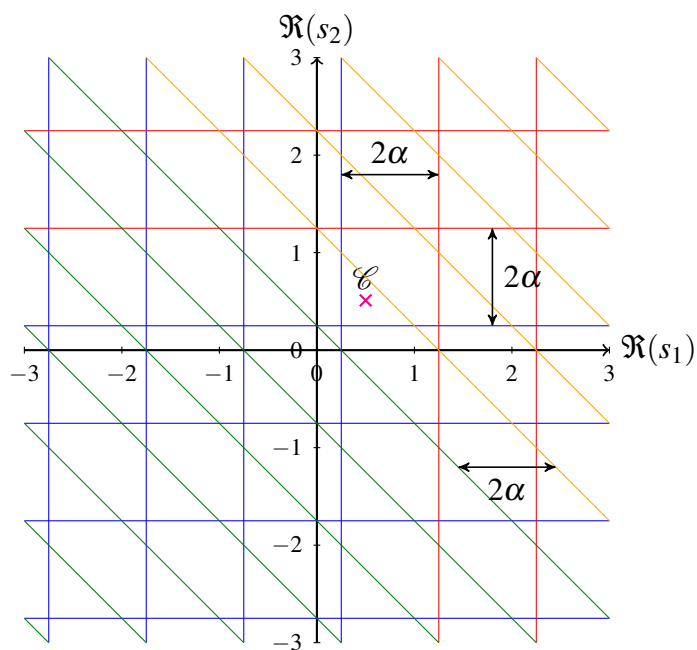
Choosing the contours

We now return to the task of computing (3.80). The initial values of the parameters α , α_4 and δ are chosen to satisfy (3.15), by the same process as in sec. 3.4.1. One possible choice is $\delta = 0.06$, $\alpha = 0.26$, $\alpha_4 = 0.76$ with contours $s_1^{\mathcal{C}} = s_2^{\mathcal{C}} = s_3^{\mathcal{C}} = 0.495$. We have placed the contours at the same position in the s_1, s_2 and s_3 planes to leverage the symmetry of the integral under the exchange of these variables. In practice this choice leads to simultaneous pole crossings, which requires special care [75]. A simple solution that works for the present calculation is to stagger the contours by a little bit, by choosing say $s_1^{\mathcal{C}} = 0.5$, $s_2^{\mathcal{C}} = 0.495$ and $s_3^{\mathcal{C}} = 0.492$.

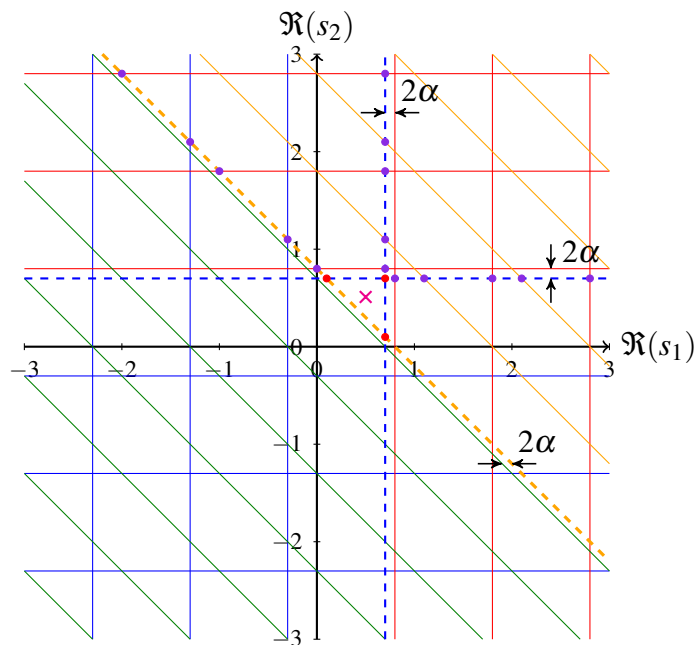
The conditions $U_{4,5}(\mathcal{C}) > 0$ etc., $U_{2,3}(\mathcal{C}) > 0$, and $U_{1,5,7,9}(\mathcal{C}) > 0$ produce pinches similar to (3.53) and (3.54),

$$\begin{aligned} \frac{3}{4} - \alpha < s_j^{\mathcal{C}} < \frac{3}{4} + \alpha, \quad j = 1, 2, 3 \\ \frac{3}{4} + 3\alpha - \delta < s_1^{\mathcal{C}} + s_2^{\mathcal{C}} + s_3^{\mathcal{C}} < \frac{3}{4} + \alpha_4 \\ \frac{9}{4} - 3\alpha < s_1^{\mathcal{C}} + s_2^{\mathcal{C}} + s_3^{\mathcal{C}} < \frac{9}{4} - \alpha_4 \end{aligned} \tag{3.84}$$

from which we infer that $\alpha > 0$, $3\alpha - \delta < \alpha_4$ and $3\alpha > \alpha_4$. We should honor these relationships throughout, lest we end up with incorrect signs for the divergences. It should be noted that the last pinch above does not give a divergence, because the poles of Γ_1 are very nearly the same as those of the Γ_{10} in the denominator, and they cancel. In other words, it does not correspond to an overlap of poles in the unregulated integral, for which α , α_4 and δ are zero.



(a) Prior to analytic continuation, when the left/right poles are separated (cf. Fig. 3.4b).



(b) At the end of continuation, with the dashed lines indicating crossed poles (cf. Fig. 3.4c).

Figure 3.10. The poles of the integrand are represented by straight lines on a $\Re(s_1) - \Re(s_2)$ plane. Residues are computed at the intersections of these lines. Poles that cross over to the other side are represented by dashed lines in (b). The residues at \bullet contain a $\Gamma(\alpha)^2$ divergence whereas those at \bullet give a $\Gamma(\alpha)$. The latter encode subhorizon physics, as explained in sec. 3.5.1.

Analytic continuation

We now begin our journey to $\alpha, \alpha_4, \delta \sim 0$ to determine (3.80) for a massless theory. The first poles to cross at those of Γ_5, Γ_7 and Γ_9 . We separate the residues at those poles and write

$$K \rightarrow K_5 + K_7 + K_9 + K_{57} + K_{59} + K_{79} + K_{579} + K. \quad (3.85)$$

Γ_5, Γ_7 and Γ_9 are the same upto an exchange of s_j , and so are the terms K_5, K_7 and K_9 as well as K_{57}, K_{59} and K_{79} . Therefore, the above breakup is really $K \rightarrow 3K_5 + 3K_{57} + K_{579} + K$. We focus now on each of these terms. First, K_{579} is the residue of K at the three poles $s_j = \frac{3}{4} - \alpha$ and it involves no integrals. Next, K_{57} is a single integral which further breaks up, in stages, into $K_{57} \rightarrow K_{572} + K_{572'} + K_{57}$ as the parameters are taken to zero. The prime in $K_{572'}$ indicates that the residue is taken at $n = 1$ pole of Γ_2 (cf. (3.16)). At the same time, the double integral K_5 further breaks up into $K_5 \rightarrow K_{527'} + K_{52} + K_5$. Finally, the K in the r.h.s. of (3.85) is a triple integral which separates as $K \rightarrow K_2 + K$. The analytic continuation is now complete, with

$$K = 3(K_{527'} + K_{52} + K_5) + 3(K_{572} + K_{572'} + K_{57}) + K_{579} + K_2 + K. \quad (3.86)$$

Evaluation of the terms

We will evaluate a few of the terms in (3.86) to demonstrate the steps involved. The easiest ones are those involving residues in all three variables. For e.g.

$$K_{579} = \frac{\Gamma_1 \Gamma_2 \Gamma_3 \Gamma_4 \Gamma_6 \Gamma_8}{\Gamma_{10}} \Big|_{s_j = \frac{3}{4} - \alpha} = \frac{\Gamma(2\alpha)^3 \Gamma(3\alpha - \alpha_4) \Gamma(-\frac{3}{2} + 3\alpha + \alpha_4) \Gamma(\frac{3}{2} - 6\alpha + \delta)}{\Gamma(6\alpha)}. \quad (3.87)$$

There are also terms with a single integral, like

$$\begin{aligned}
K_{52} &= \int_{\mathcal{C}_3} \frac{ds_3}{2\pi i} \frac{\Gamma_1 \Gamma_3 \Gamma_4 \Gamma_6 \Gamma_7^{**} \Gamma_8 \Gamma_9^*}{\Gamma_{10}} \Big|_{s_1=\frac{3}{4}-\alpha, s_2=-s_3+\alpha+\alpha_4} \\
&= \Gamma(2\alpha)\Gamma(-3\alpha + \alpha_4 + \delta) \frac{\Gamma(\frac{3}{2} - 2\alpha_4)}{\Gamma(\frac{3}{2} + 3\alpha - \alpha_4)} \\
&\quad \times \int_{\mathcal{C}_3} \frac{ds_3}{2\pi i} \Gamma(\frac{3}{4} + s_3 - \alpha_4) \Gamma^*(-\frac{3}{4} + s_3 + \alpha) \Gamma(\frac{3}{4} - s_3 + \alpha) \Gamma^{**}(-\frac{3}{4} - s_3 + 2\alpha + \alpha_4).
\end{aligned} \tag{3.88}$$

The symbol Γ^* indicates that the first pole of that Γ function has crossed over. Γ^{**} means the first two poles have crossed, and so on (see sec. 3.2.4). The s_3 integral by itself does not produce any new divergence since the overlapping poles are on the other side of the contour (see Fig. 3.2). Since the prefactor is already $O(\alpha^{-2})$ as $\alpha \rightarrow 0$, we need to retain the α dependence inside the s_3 integral to compute the $O(\alpha^{-1})$ contribution to K . We can Taylor expand the integrand to linear order in α, α_4 and write

$$\begin{aligned}
&\int_{\mathcal{C}_3} \frac{ds_3}{2\pi i} \Gamma(\frac{3}{4} + s_3) \Gamma^*(-\frac{3}{4} + s_3) \Gamma(\frac{3}{4} - s_3) \Gamma^{**}(-\frac{3}{4} - s_3) \\
&\quad \times \left(1 + \alpha\psi(-\frac{3}{4} + s_3) + \alpha\psi(\frac{3}{4} - s_3) + (2\alpha + \alpha_4)\psi(-\frac{3}{4} - s_3) - \alpha_4\psi(\frac{3}{4} + s_3) \right)
\end{aligned} \tag{3.89}$$

where $\psi(x) \equiv \frac{\Gamma'(x)}{\Gamma(x)}$ is the digamma function. This integral can be computed using corollaries of Barnes's first lemma (3.60), like those given in appendix D of [83]. The answer is

$$\begin{aligned}
K_{52} &= \Gamma(2\alpha)\Gamma(-3\alpha + \alpha_4 + \delta) \frac{\Gamma(\frac{3}{2} - 2\alpha_4)}{\Gamma(\frac{3}{2} + 3\alpha - \alpha_4)} \left(-2\pi + \frac{4\pi}{3} [\gamma_E + \psi(\frac{3}{2})] \right. \\
&\quad \left. - \alpha \frac{2\pi}{3} \left[(2\gamma_E^2 + \pi^2 + 9\psi(-\frac{1}{2}) - 3\psi(\frac{1}{2}) - 6\psi(-\frac{3}{2})\psi(\frac{3}{2}) + \gamma_E(-6 - 6\psi(-\frac{3}{2}) + 2\psi(\frac{3}{2}))) \right] \right. \\
&\quad \left. - \alpha_4 \frac{2}{3} \pi \left[-8 + \pi^2 - 2\gamma_E\psi(-\frac{3}{2}) + 3\psi(-\frac{1}{2}) - 3\psi(\frac{1}{2}) + 2\gamma_E\psi(\frac{3}{2}) - 2\psi(-\frac{3}{2})\psi(\frac{3}{2}) + 2\psi(\frac{3}{2})^2 \right] \right)
\end{aligned} \tag{3.90}$$

Next, there are terms in (3.86) which involve double integrals. For instance,

$$\begin{aligned}
K_5 &= \int_{\mathcal{C}_2} \frac{ds_2}{2\pi i} \int_{\mathcal{C}_3} \frac{ds_3}{2\pi i} \frac{\Gamma_1 \Gamma_2^* \Gamma_3 \Gamma_4}{\Gamma_{10}} \frac{\Gamma_6 \Gamma_7^* \Gamma_8 \Gamma_9^*}{\Gamma_{10}} \Big|_{s_1 = \frac{3}{4} - \alpha} \\
&= \Gamma(2\alpha) \int_{\mathcal{C}_2} \frac{ds_2}{2\pi i} \Gamma(\frac{3}{4} - s_2) \Gamma^*(-\frac{3}{4} + s_2) \int_{\mathcal{C}_3} \frac{ds_3}{2\pi i} \Gamma(\frac{3}{4} - s_3) \Gamma^*(-\frac{3}{4} + s_3) \Gamma^*(-s_{23}) \Gamma(s_{23})
\end{aligned} \tag{3.91}$$

where $s_{23} \stackrel{\text{def.}}{=} s_2 + s_3$. We have retained only the leading order contribution from the double integral since the prefactor is at most $O(\alpha^{-1})$. Once again these are evaluated using corollaries to (3.60), and we get

$$K_5 = \Gamma(2\alpha) \frac{2\pi}{3} \left[3\gamma_E^2 + \pi^2 + 6\gamma_E \psi(\frac{3}{2}) + 3\psi(\frac{3}{2})^2 - 12 \right]. \tag{3.92}$$

Finally, the K in the r.h.s. of (3.80) is what is left of the original K after all the divergent residues have been extracted. It produces at most an $O(1)$ contribution and may be ignored. All other terms in (3.86) can be evaluated in the manner shown above.

The problem of too many parameters

It is clear from (3.87), (3.90) and (3.92) that K will have the structure we anticipated in (3.81). However, the answer involves three parameters α , α_4 and δ , and we need to establish a relationship between these to extract a meaningful result from (3.86). So far, all we have are the inequalities $\alpha > 0$, $3\alpha - \delta < \alpha_4$ and $3\alpha > \alpha_4$ (cf. (3.84)). We encountered a similar problem in (3.67) and resolved it by insisting that all pinches have the same width. Said differently, all divergent Γ functions in K must have the same argument. In the present case such a requirement furnishes the condition (cf. (3.90))

$$-3\alpha + \alpha_4 + \delta = 2\alpha. \tag{3.93}$$

Next, we see that (3.87) has a $\Gamma(3\alpha - \alpha_4)$ in the numerator but, as noted under (3.84), this does not lead to a divergence due to the $\Gamma(6\alpha)$ in the denominator. So it makes little sense to equate $3\alpha - \alpha_4$ with the pinch width 2α . Thus we are still one constraint shy of being able to express δ and α_4 in terms of α . To proceed we'll make yet another 'reasonable' assumption: we'll choose $\alpha_4 = -3\alpha$ to make $\Gamma(3\alpha - \alpha_4)$ cancel $\Gamma(6\alpha)$ exactly. Then,

$$\langle \phi^3 \phi \rangle'_\lambda \approx \frac{H^4}{512\pi^5} \frac{(-k\tau_0)^{-16\alpha}}{k^3} \left[\frac{\pi}{3\alpha^3} - \frac{8\pi(\gamma_E - 2 + \log(4))}{3\alpha^2} + \frac{4\pi(3\pi^2 - 32 + 8(\gamma_E - 2 + \log(4))^2)}{3\alpha} + O(\alpha^0) \right] \quad (3.94)$$

where we have used (3.93) to eliminate δ .

An alternate parameterization

We will now redo the calculation using a different parameterization and compare with the above result. This will help us justify our choice of α_4 at the end of the previous section.

It is possible to make (3.80) well-defined with just two parameters instead of three. The first of these parameters, ε , is introduced by modifying the time integral as in (3.69). The second parameter κ is a shift in the number of space dimensions, $D = 3 + 2\kappa$. Finally we set all $v_j \rightarrow i\frac{3}{2}$, and $\bar{D} = 3$ in (3.76). Applying the conditions (3.15) on this new integral we identify the pinches

$$\begin{aligned} \frac{3}{4} < s_j^\varepsilon < \frac{3}{4} + \kappa; \quad j = 1, 2, 3 \\ \frac{3}{4} + 2\kappa < s_1^\varepsilon + s_2^\varepsilon + s_3^\varepsilon < \frac{3}{4} + \kappa + \varepsilon \\ \frac{9}{4} < s_1^\varepsilon + s_2^\varepsilon + s_3^\varepsilon < \frac{9}{4} + \kappa + \varepsilon. \end{aligned} \quad (3.95)$$

Comparing this with (3.84) we see that the width of the first three pinches are now κ instead of 2α , the second pinch is $-\kappa + \varepsilon$ wide, and the parameters must satisfy $\varepsilon > \kappa > 0$. The last inequality in (3.95) does not represent a true pinch because the divergence associated with it is cancelled by the Γ_{10} in the denominator, exactly as in the previous parameterization.

However, the important difference is that equating the pinch widths establishes an unambiguous relationship, $\varepsilon = 2\kappa$, between all two parameters. This also sets $\Gamma_1/\Gamma_{10} \rightarrow 1$, which is exactly what the choice $\alpha_4 = -3\alpha$ accomplished in the last calculation. Proceeding with the analytic continuation, and setting $\varepsilon = 2\kappa$, we arrive at

$$\langle \phi^3 \phi \rangle'_\lambda \approx \frac{H^4 (-H\tau_0)^{4\kappa}}{512\pi^5} \frac{(-k\tau_0)^{-2\kappa}}{k^{3+2\kappa}} \left[\frac{8\pi}{3\kappa^3} - \frac{16\pi(2\gamma_E - 5 + 2\log(4))}{3\kappa^2} + \frac{4\pi(40 + 3\pi^2 - 16(\gamma_E - 2 + \log(4)) + 16(\gamma_E - 2 + \log(4))^2)}{3\kappa} + O(\kappa^0) \right] \quad (3.96)$$

The leading coefficient of $\log(-k\tau_0)$ is the same in both (3.94) and (3.96), upto a renaming of $\alpha \rightarrow \kappa$,

$$-\frac{H^4}{96\pi^4 k^3 \alpha^2}. \quad (3.97)$$

A more careful renormalization is required to make the subleading terms match. The important takeaway is that the divergence structure of $\langle \phi^3 \phi \rangle'_\lambda$ in the full theory matches what we calculated in the SdSET [66], with a regulator that also characterizes divergences with $1/\alpha$ poles. Thus, the calculation in this section confirms that the SdSET correctly reproduces the IR divergences of the full theory.

In closing, we note that the sample calculations in this paper were ‘simple’, in that we went no farther than $O(\lambda)$, and the MB integrands did not contain terms of the form $p_i^{s_j}$, where p_i denotes a momentum variable. While it is certainly worth pushing the method to do higher loops, we believe the two examples considered above sufficiently illustrate the usefulness of the method both as a computational tool, and as a way to glean qualitative insights about the IR behavior of fields in dS.

3.6 Conclusions

In this paper we advanced a method to identify and extract divergences in dS loop calculations. Motivated by the dilatation invariance of dS, we worked with the Mellin-Barnes

representation of dS correlation functions [67, 68]. This allowed us to import the techniques developed in [72, 73, 74, 75, 76], for flat space Feynman diagrams, to the calculation of loop integrals in dS. The resulting expressions have the familiar structure of a dimreg answer (cf. (3.68) and (3.94)), and we can resum the divergences with dynamical RG by way of extracting meaningful physics. While the examples we considered in this work were simple, they illustrate a few important aspects of loop calculations in dS that are worth highlighting once again:

1. The divergences in dS correlation functions manifest as pole overlaps in the Mellin space; the problem of isolating divergences becomes a matter of locating these pole overlaps in a hyperspace spanned by the complex Mellin variables $\{s_\ell\}$.
2. Our method works for loop integrals involving scalar fields of any mass. In particular, the calculations of sec. 3.4 reveal that *all* massive scalars are afflicted with secular growth, with additional divergences introduced as we approach the massless limit (see Fig. 3.8). Stochastic Inflation provides a non-perturbative resolution of these IR issues for massless scalars. The technique developed in this paper allows us to compute higher order corrections to the stochastic description, directly from the full theory.
3. Dynamical RG resums the secular logs from dS loop integrals, just as regular RG treats UV logs in flat space. However, it is not clear whether DRG resums logarithmic corrections at all orders, as regular RG does. The bulk of the difficulty in addressing this problem lies in the evaluation of higher loop integrals. However, if we can extract the general properties of such loops, without doing the calculations explicitly (see for e.g. (3.81)), perhaps we could improve the underpinnings of DRG itself. Alternatively, the fact that the SdSET correctly reproduces IR divergences of the full theory can be taken as evidence that the DRG works. From that perspective, investigating higher loops in dS could further strengthen the validity of SdSET.
4. When Mellin representations are used to simplify Feynman integrals in flat space, the

variables $\{s_\ell\}$ serve as little more than auxiliary parameters to be integrated over. But in dS , these variables carry physical meaning, as the eigenvalues of the dilatation generator. Furthermore, as we noted in sec. 3.5.1, multidimensional MB integrals can be computed with the method of residues using a geometrical procedure on the hyperplanes $U_i(\mathbf{s}) = -n$. We used these facts to identify that certain secular behaviors originate from subhorizon dynamics. We are left with the distinct impression that there may be deeper physical insights hidden away in the geometry of the aforementioned planes.

Mellin space is fertile ground for the study of correlation function in dS , as many authors have noted before. It is our hope that the observations in this work reinforce that view, and encourages further investigation of these tools.

Acknowledgements:

We are grateful to Daniel Green and Tim Cohen for providing valuable guidance and encouragement throughout this project. We also thank Charlotte Sleight and Chia-Hsien Shen for comments on the manuscript, and John McGreevy for insightful discussions. A.P. was supported by the US Department of Energy under grant no. DE-SC0019035.

This chapter, in full, is a reprint of the material as it appears in Akhil Premkumar, arXiv: 2110.12504. The dissertation author was the primary investigator and author of this paper.

Chapter 4

Stochastic Inflation at NNLO

4.1 Introduction

The study of quantum fields in de Sitter (dS) space provides insight into the foundations of inflationary cosmology. In particular, the equal-time in-in correlation functions of light scalar fields form the theoretical underpinnings of the predictions for the observed density fluctuations sourced during inflation [7, 15, 16]. These correlators encode a wealth of information about the inflationary era that could be revealed by measurements of primordial non-Gaussianity [58]. Yet, despite their importance, our understanding of cosmological correlators beyond tree level is quite limited. For light scalars, explicit loop calculations have revealed the presence of infrared (IR) divergences and unbounded time-dependent “secular” growth [9, 10, 12, 13, 14, 25, 84, 26, 27, 28, 59, 60, 29, 61, 62, 63].

Stochastic Inflation [11, 79, 80] is a framework for treating the IR dynamics of a massless scalar field in a dS background, and has long been suspected to provide the non-perturbative resolution to the IR issues associated with massless fields in dS [88, 89, 43, 90, 91, 30, 31, 32, 81, 65, 92, 93]. The idea is to reframe the problem in terms of the probability distribution for the scalar field as a function of time, resulting in a Fokker-Planck equation that depends on the scalar field potential. There are two contributions to the evolution, resulting from quantum noise induced by fluctuations of the field as it crosses the dS horizon and classical drift due to the potential. This framework forms the conceptual basis for slow-roll eternal inflation [94, 95, 96]

and can be used to describe the onset of eternal inflation quantitatively [97]. Moreover, these results hint at the physical meaning of the dS entropy [98, 99, 100], which remains a significant unsolved problem [5].

Notwithstanding the conceptual and technical appeal of Stochastic Inflation, it is necessarily approximate. For example, we expect that there are non-Gaussian contributions to the quantum noise that result from the UV interaction, which are not modeled by Stochastic Inflation. Furthermore, the Fokker-Planck formalism obscures the connection to cosmological correlators, and it is not a priori obvious how to incorporate higher-order corrections. It would be ideal if we could understand how the success of Stochastic Inflation relates to other results regarding the IR behavior of fields in dS, such as the freeze-out of superhorizon metric fluctuations which has been shown to all orders in perturbation theory [23, 20, 19], or the loop generated anomalous scaling for the time-evolution of massive fields [53, 64]. One of our goals in exploring the corrections to Stochastic Inflation is to understand how they fit into the broader context of quantum field theory in dS.

A framework that accomplishes this ambitious goal is the Soft de Sitter Effective Theory (SdSET) [65]. By following the standard Effective Field Theory (EFT) playbook, this approach isolates the dynamics that persist in the superhorizon limit, yielding more efficient calculations of loop corrections to long wavelength cosmological correlators. Taking a real scalar field in dS as the UV description, SdSET describes the IR limit of this model by relying on two degrees of freedom that correspond to the growing and decaying modes which are familiar from the solving the Klein-Gordon equation classically in a dS background. This representation admits a power counting prescription that systematically expands about the long wavelength limit in terms of a local Lagrangian. Loop dependence on time and space is manifestly factorized throughout the calculation, allowing an efficient isolation of the time dependent IR divergent logs. Such logs lead to secular growth for both massive and light fields, and appear in SdSET as contributions to the anomalous dimensions of local operators. In the case of light fields, an infinite number of operators become degenerate and Starobinsky's model of Stochastic Inflation is equivalent

to the leading order (LO) dynamical renormalization group (RG) that governs their mixing as a function of time.¹ This implies that corrections to Stochastic Inflation can be computed by simply extending the RG analysis to higher orders.

Taking the UV description to be massless $\lambda\phi^4$ theory, the endpoint of this RG flow is a non-trivial fixed point where the field values are $\phi \sim H\lambda^{-1/4}$. Corrections to this description around this fixed point must account for this non-perturbative scaling with λ . In this paper, we will calculate the evolution of operators to next-to-next-to leading order (NNLO) in this power counting. At NLO, our results reproduce previous calculations [31, 92]; as we will show, these contributions can be attributed to field definitions within SdSET. In contrast, at NNLO we find a universal correction in the form of a two-loop anomalous dimension that introduces the first higher derivative correction to Stochastic Inflation. In the process, we perform the full one-loop matching in SdSET, which further elucidates the relationship between the EFT and the UV descriptions.

One novel feature of SdSET is that consistently matching a UV theory onto the EFT requires specifying both Wilson coefficients and (time-independent) initial conditions. Deriving the RG that yields Stochastic Inflation at NNLO requires performing this matching explicitly at one-loop order. This provides a highly non-trivial check of the SdSET formalism, and these results can be utilized for a wide variety of correlator calculations. We will also use this calculation as an opportunity to demonstrate the power of the symmetry preserving “dynamical dimensional regularization” technique introduced in [65].

This paper is organized as follows. We begin with a review of Stochastic Inflation in Sec. 4.2, with an emphasis on its origins as a Markovian process, which provides a framework with which we can organize corrections. Then Sec. 4.3 reviews the most salient aspects of the SdSET formalism. The new calculations begin in Sec. 4.4, where we present the one-loop matching results that are relevant for our applications here. These are then applied in Sec. 4.5,

¹The dynamical RG flow described here should not be confused with the RG flow that appears in a holographic dual via dS/CFT [5, 4, 6, 7, 45]. The key difference is that our dynamical RG applies directly to the in-in correlators and not to the wavefunction of the universe.

where we compute the composite operator anomalous dimensions that feed into Stochastic Inflation up to NNLO, and leads to the main result of this work in Eq. (4.144). We then explore the implications of this formula in Sec. 4.6, and finally conclude in Sec. 5.6. An appendix on the relevant, but somewhat technical, six-point function matching is provided in Sec. 4.A, and the hard cutoff version of the main calculations are given in Sec. 4.B.

4.2 Stochastic Inflation

In a theory of a massless scalar field ϕ in a dS background with Hubble constant H , the field's value will fluctuate by $O(H)$ as each momentum mode crosses the dS horizon. An equivalent point of view is that these stochastic fluctuations are the result of the non-zero temperature within dS. This effect has a natural interpretation as a random walk, an idea that was made precise by Starobinsky [11] and led the formalism known as Stochastic Inflation. In this section, we discuss this approach, and emphasize the structure of higher order corrections.

For concreteness, we will assume the canonical example of $\lambda\phi^4$ theory in a dS background, whose UV description in terms of a scalar field ϕ is

$$S_{\text{UV}} = \int d^4x \sqrt{-g} \left[-\frac{1}{2} g_{\mu\nu} \partial^\mu \phi \partial^\nu \phi + \frac{1}{2} m^2 \phi^2 + \frac{1}{4!} \lambda \phi^4 \right], \quad (4.1)$$

where $g_{\mu\nu}$ is the dS metric and $g \equiv \det g_{\mu\nu}$ as usual. The essential formalism developed here holds for general models. However, we will not be able to derive corrections to Stochastic Inflation generically, and so we will work with this simple and well studied example when we calculate explicit corrections.

In the process of discussing the general structure of corrections to Stochastic Inflation, we will arrive at a natural interpretation for higher-order corrections in terms of the transition amplitudes for the field ϕ . Unfortunately, how to determine the corrections directly is not transparent in this description. In Sec. 4.3.5 we will show how the corrections discussed in this Section arise from operator mixing, and the remainder of the paper is devoted to deriving these

corrections and their implications using SdSET.

Before moving on, we emphasize that the formalism we develop in this section will rely on the assumption that the late time evolution of ϕ can be modeled as a Markovian system (as described in Sec. 4.2.2 below). This will be justified by the concrete calculation of the dynamical renormalization group using the SdSET that is developed later in this paper. It ultimately is due to the fact that the dynamics of the SdSET degrees of freedom are governed by a first order equation, which is a consequence of the EFT power counting.

4.2.1 Leading Order

The framework of Stochastic Inflation results in a probability distribution $P(\phi, t)$ for the field ϕ at a time t . To leading order, $P(\phi, t)$ obeys a Fokker-Planck equation

$$\frac{\partial}{\partial t} P(\phi, t) = \frac{H^3}{8\pi^2} \frac{\partial^2}{\partial \phi^2} P(\phi, t) + \frac{1}{3H} \frac{\partial}{\partial \phi} [V'(\phi) P(\phi, t)], \quad (4.2)$$

where the first term captures the stochastic noise from the inherent quantum variance of ϕ , while the second term is due to the classical drift induced by the potential where $V'(\phi) \equiv \partial V / \partial \phi$. One interesting application of this equation is to solve for the fixed point that the scalar field would reach if it lived in an eternal dS background. To find the fixed point, we enforce that $\partial P_{\text{eq}} / \partial t = 0$ for the equilibrium solution P_{eq} , which implies

$$\frac{\partial^2}{\partial \phi^2} P_{\text{eq}}(\phi) = -\frac{8\pi^2}{3H^4} \frac{\partial}{\partial \phi} [V'(\phi) P_{\text{eq}}(\phi)]. \quad (4.3)$$

Integrating both sides of this equation twice leads to the solution

$$P_{\text{eq}}(\phi) = C e^{-8\pi^2 V(\phi) / 3H^4}. \quad (4.4)$$

We can use this leading order solution to organize corrections to Stochastic Inflation as a perturbative series in the UV coupling.

4.2.2 Beyond Leading Order

Having reviewed the leading order formalism and its consequence for pure dS, we now turn to exploring the form we can expect corrections to take. In order to generalize this Fokker-Planck equation, we return to its origins. The underlying assumption is that the system is Markovian, in that the time slice of interest is entirely determined by the information contained in the previous step. In other words, a Markovian system has no “memory.” Since this assumption holds for the spectrum of scalar field fluctuations at horizon crossing, the resulting formalism will tell us what kinds of corrections to Stochastic Inflation we can expect.

The Markovian assumption leads directly to the Chapman-Kolmogorov equations, which describe a probability distribution $P(\phi, t + dt)$ that is fully determined by $P(\phi, t)$:

$$\frac{\partial}{\partial t} P(\phi, t) = \int d\phi' \left[P(\phi', t) W(\phi|\phi') - P(\phi, t) W(\phi'|\phi) \right], \quad (4.5)$$

where $W(\phi|\phi')$ is a “transition rate” in that it sets the rate for transitioning to ϕ from another value ϕ' in a differential amount of time. This equation simply expresses that the probability distribution for ϕ at $t + dt$ is fully determined by the weighted sum of the possible transitions that yield ϕ minus the sum of all the weighted transitions for ϕ to change value.

Next, we will reorganize Eq. (4.5) using what is known as the Kramers-Moyal expansion, visualized in Fig. 4.1. This is effectively the assumption that the transitions are dominated by “local” jumps [101]. The first step is to make a substitution of $\Delta\phi = \phi - \phi'$ in the first term and $\Delta\phi = \phi' - \phi$ in the second term. In other words, when ϕ is in the final state, then $\phi' = \phi - \Delta\phi$ and when ϕ' is in the final state $\phi' = \phi + \Delta\phi$. This yields

$$\frac{\partial}{\partial t} P(\phi, t) = \int d\Delta\phi \left[P(\phi - \Delta\phi, t) W(\phi|\phi - \Delta\phi) - P(\phi, t) W(\phi + \Delta\phi|\Delta\phi) \right], \quad (4.6)$$

where we have included two compensating relative minus signs, one from the different changes of variables for the two terms, and another due to needing to flip the limits of integration after

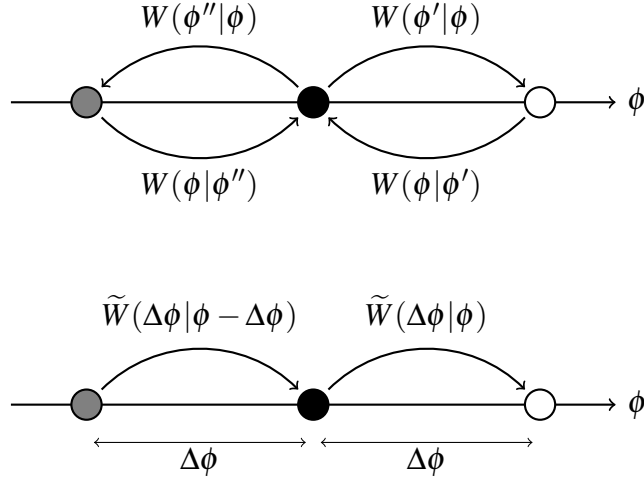


Figure 4.1. Visualization of the Kramers-Moyal expansion. The top panel shows the probability of “hopping” from ϕ to ϕ' , $W(\phi'|\phi)$ or from ϕ' to ϕ , $W(\phi|\phi')$, or equivalently any other point such as ϕ'' . On the bottom, we see the process in terms of the probability $\tilde{W}(\Delta\phi|\phi)$ to hop from a specific starting point ϕ by a distance $\Delta\phi$.

switched the integration variable $\Delta\phi \rightarrow -\Delta\phi$ in the second term. Since we are assuming the main support of W comes from local jumps, we want to Taylor expand the first term for fixed ϕ . To make performing this expansion transparent, it is then useful to redefine W using

$$\tilde{W}(y,x) \equiv W(x+y|x), \quad (4.7)$$

so that Eq. (5.56) becomes

$$\frac{\partial}{\partial t} P(\phi, t) = \int d\Delta\phi \left[P(\phi - \Delta\phi, t) \tilde{W}(\Delta\phi, \phi - \Delta\phi) - P(\phi, t) \tilde{W}(\Delta\phi, \phi) \right]. \quad (4.8)$$

Then Taylor expanding the first term about a fixed value of ϕ yields

$$\begin{aligned} \int d\Delta\phi P(\phi - \Delta\phi, t) \tilde{W}(\Delta\phi, \phi - \Delta\phi) &= \int d\Delta\phi \sum_{n=0}^{\infty} \frac{1}{n!} \left(-\Delta\phi \frac{\partial}{\partial \phi} \right)^n P(\phi, t) \tilde{W}(\Delta\phi, \phi) \\ &= \sum_{n=0}^{\infty} \frac{1}{n!} \frac{\partial^n}{\partial \phi^n} \int d\Delta\phi (-\Delta\phi)^n P(\phi, t) \tilde{W}(\Delta\phi, \phi), \end{aligned} \quad (4.9)$$

where in the last line, we used the fact that $\Delta\phi$ is independent of ϕ to pull the derivatives outside of the integral. Plugging this expansion into Eq. (4.8), we see that the $n = 0$ term cancels so that

$$\frac{\partial}{\partial t}P(\phi, t) = \sum_{n=1}^{\infty} \frac{1}{n!} \frac{\partial^n}{\partial \phi^n} \Omega_n(\phi) P(\phi, t), \quad (4.10)$$

where

$$\Omega_n(\phi) \equiv \int d\Delta\phi (-\Delta\phi)^n W(\phi + \Delta\phi | \Delta\phi), \quad (4.11)$$

and we have used Eq. (4.7) to write this expression in terms of the original transition rate W . Note that all terms in this expansion are total derivatives, as required for the conservation of the total probability. We also see that $\Omega_n(\phi)$ encodes the ϕ -dependence of the n^{th} moment of the distribution. For the theories of interest here, $\Omega_n(\phi)$ will admit a polynomial expansion in ϕ :

$$\Omega_n(\phi) = \sum_{m=0}^{\infty} \frac{1}{m!} \Omega_n^{(m)} \phi^m, \quad (4.12)$$

for some coefficients $\Omega_n^{(m)}$.

Thus far, all of this discussion was very general. If we specialize to the case of leading order Stochastic Inflation, we can compare this expanded result with Eq. (4.2) to identify that the $n = 1$ “drift” term is proportional to the derivative of the potential,

$$V = \sum_{\ell} \frac{1}{\ell!} c_{\ell} \phi^{\ell}. \quad (4.13)$$

so that matching with Eq. (4.2) implies

$$\Omega_1^{(m)} = \frac{1}{3H} c_{m+1}. \quad (4.14)$$

Hence, for $n = 1$, m tracks the polynomial interactions that could appear in a generic potential.

Moving to the $n = 2$ “noise” term, we again can compare to Eq. (4.2) to find

$$\Omega_2^{(0)} = \frac{H^3}{4\pi^2}. \quad (4.15)$$

In this case, the $m > 0$ terms correspond to higher order corrections.

To summarize, if we assume that the UV theory has only a $\lambda\phi^4$ interaction, we conclude that the generalized evolution equation that describes Stochastic Inflation takes the form

$$\frac{\partial}{\partial t} P(\phi, t) = \sum_{n=2}^{\infty} \frac{1}{n!} \frac{\partial^n}{\partial \phi^n} \left[\sum_{m=0}^{\infty} \frac{1}{m!} \Omega_n^{(m)} \phi^m P(\phi, t) \right] + \frac{1}{3H} \frac{\partial}{\partial \phi} \left[V'(\phi) P(\phi, t) \right], \quad (4.16)$$

where V' is the ϕ derivative of the potential, which includes the matching corrections required to obtain the accuracy of interest.

To develop some intuition for what the Ω_n corrections are capturing, we can interpret $W(\phi + \Delta\phi | \Delta\phi)$ as the probability distribution of transitions of size $\Delta\phi$. Then $\Omega_n(\phi)$ is simply the n^{th} moment of this distribution; the first and second moments $\Omega_1(\phi)$ and $\Omega_2(\phi)$ are the complete set of inputs for a Gaussian distribution. Furthermore, if Ω_2 has non-trivial ϕ dependence, i.e., $\Omega_2^{(m \neq 0)} \neq 0$, then the variance of the noise depends on the starting location of the jump. Finally, if $\Omega_{n=3}(\phi) \neq 0$, then we know our distribution is non-Gaussian. More generally, we interpret the $n > 2$ terms in the generalized equation governing Stochastic Inflation in Eq. (4.16) as encoding contributions from non-Gaussian noise generated by the UV $\lambda\phi^4$ interaction. Therefore, we conclude that corrections to Eq. (4.2) are of three types:

- Higher order “noise” terms captured by $\partial^n / \partial \phi^n$ with $n > 2$, see Eq. (5.58).
- Higher polynomial terms in Ω_n , see Eq. (4.12).
- Higher order terms in the potential V via corrections to coefficients and the generation of higher polynomial ϕ terms.

Next, we will argue for how to relate the expansion in each of these quantities to the expansion

in the UV quartic coupling λ as it corrects the equilibrium solution in Eq. (4.4).

Organizing Corrections Systematically

Due to the underlying $\lambda \phi^4$ potential, we expect that the statistics of ϕ are neither Gaussian nor independent of the background value of the field. We therefore expect corrections to the equation for Stochastic Inflation of the form discussed previously. In this section, we will take the equilibrium solution in Eq. (4.4) and apply it to a UV theory with

$$V(\phi) = \frac{1}{4!} \lambda \phi^4 \quad \implies \quad P_{\text{eq}}(\phi) = C e^{-8\pi^2 \lambda \phi^4 / (3 \cdot 4! H^4)} \equiv C e^{-(\phi/\phi_{\text{eq}})^4}. \quad (4.17)$$

where $\phi_{\text{eq}}^4 = 9H^4/(\pi^2 \lambda)$. This distribution has support over a field range $|\phi| \lesssim \phi_{\text{eq}}$ such that

$$\langle \phi^4 \rangle = \frac{1}{4} \Gamma\left[\frac{5}{4}\right] \times \phi_{\text{eq}}^4 = \frac{9}{4\pi^2} \Gamma\left[\frac{5}{4}\right] \frac{H^4}{\lambda}. \quad (4.18)$$

Therefore, we will organize the possible corrections by assuming the equilibrium scaling

$$\phi \simeq \phi_{\text{eq}} \sim H \lambda^{-1/4}. \quad (4.19)$$

We will further assume that the corrections are generated as an expansion in perturbation theory, so that

$$\Omega_2^{(2m)} \sim \lambda^m; \quad \Omega_3^{(2m+1)} \sim \lambda^{m+1}; \quad \Omega_4^{(2m)} \sim \lambda^{m+1}; \quad \text{and} \quad c_{2\ell} \sim \lambda^{\ell-1}, \quad (4.20)$$

which we will see agrees with the explicit calculations presented below. Putting all of this together allows us to determine the order in λ for each term that appears in Eq. (4.16). Note that we will assume the $\phi \rightarrow -\phi$ UV symmetry is preserved, which explains the absence of many terms. These contributions are as follows.

Leading Order (LO): Stochastic Inflation at leading order is given by Eq. (4.2):

$$\frac{\partial}{\partial t}P(\phi, t) = \frac{H^3}{8\pi^2} \frac{\partial^2}{\partial \phi^2} P(\phi, t) + \frac{1}{3H} \frac{\partial}{\partial \phi} \left[\frac{1}{3!} \lambda \phi^3 P(\phi, t) \right], \quad (4.21)$$

where we have used the known leading order results $\Omega_2^{(0)} = H^3/(4\pi^2)$ and $V'(\phi) = \lambda \phi^3/3!$. Both terms on the right hand side of this equation are $O(\lambda^{1/2}) \times P(\phi, t)$, which defines what we mean by ‘‘LO.’’

Next-to-leading Order (NLO): Accounting for both $\Omega_n^{(m)}$ and corrections to the potential, we can determine that the next-to-leading corrections to Stochastic Inflation should take the form

$$\frac{\partial}{\partial t}P(\phi, t) = O(\lambda^{1/2}) + \frac{\partial^2}{\partial \phi^2} \left[\Omega_2^{(2)} \phi^2 P(\phi, t) \right] + \frac{1}{3H} \frac{\partial}{\partial \phi} \left[\frac{1}{5!} c_6 \phi^5 P(\phi, t) \right], \quad (4.22)$$

where the correction to the noise term $\Omega_2^{(2)} \sim \lambda$ and the correction to the potential $c_6 \sim \lambda$ will both be determined below, and $\Omega_2^{(1)} = 0$ due to the $\phi \rightarrow -\phi$ symmetry. We see that these NLO terms are $O(\lambda) \times P(\phi, t)$. These corrections have been previously calculated in [31, 92].

Next-to-next-to-leading Order (NNLO): Following the same logic, we can find the form that the next order terms take:

$$\begin{aligned} \frac{\partial}{\partial t}P(\phi, t) = & O(\lambda^{1/2}) + O(\lambda) + \frac{H^3}{8\pi^2} \frac{\partial^2}{\partial \phi^2} \left(\Omega_2^{(4)} \phi^4 P(\phi, t) \right) \\ & + \frac{1}{3H} \frac{\partial}{\partial \phi} \left[\frac{1}{7!} c_8 \phi^7 P(\phi, t) \right] + \frac{\partial^3}{\partial \phi^3} \left(\Omega_3^{(1)} \phi P(\phi, t) \right), \end{aligned} \quad (4.23)$$

where $\Omega_2^{(4)} \sim \lambda^2$ and $\Omega_3^{(1)} \sim \lambda$ will be determined by operator mixing in the next section and $c_8 \sim \lambda^3$, and $\Omega_3^{(0)} = 0$ due to the $\phi \rightarrow -\phi$ symmetry. These NNLO terms are $O(\lambda^{3/2}) \times P(\phi, t)$.

Note that in addition to these corrections, we must also include subleading corrections to the parameters that already appear at lower order; these do not change the structure of the equation, but will of course be accounted for as we perform the calculation. The rest of this paper is devoted to determining these coefficients systematically using the framework of SdSET,

with a brief discussion of the physical implications of working with NNLO Stochastic Inflation.

4.3 Soft de Sitter Effective Theory

Stochastic Inflation, and corrections to it, are the consequence of quantum field theory in dS for scalar particles with masses $m^2 \ll H^2$. This can be seen directly at leading order, where a variety of methods have been used to derive the Fokker-Planck equation [11, 79, 80, 88, 89, 43, 90, 91, 30, 31, 32, 81, 65, 92, 93]. However, many of these methods become cumbersome beyond leading order and often obscure how corrections arise.

Soft de Sitter Effective Theory offers a method to compute the equations of Stochastic Inflation systematically to any order. The key advantage offered by SdSET is that power counting is manifest, thereby making corrections easy to identify. Furthermore, loop integrals are scaleless and regulated by (dynamical) dim reg and thus preserve the power counting that is manifest in the action. In addition to fixing the values of the SdSET Wilson coefficients, the UV theory sets the initial conditions for the effective theory fields. We will be specifically interested in understanding the corrections to Stochastic Inflation for the concrete example of $\lambda\phi^4$ theory in dS, where the UV action is given above in Eq. (4.1).

In this section, we will review the machinery of SdSET and how it arises from a given UV theory. In the subsequent sections, we will use this technology to match SdSET to $\lambda\phi^4$ theory and then use it to derive the equations of Stochastic Inflation at NNLO.

4.3.1 In-In Correlators

As we will see below, Stochastic Inflation is equivalent to the renormalization group equations that govern how composite operators mix. One approach to determining the operator mixing is to compute the divergences of in-in correlation functions involving composite operators. This section is devoted to setting up the relevant framework. We work in the interaction picture, where fields are quantized using the solutions to their quadratic equations of motion. A free

scalar fields in dS can be expressed as a mode expansion:

$$\phi(\vec{x}, \tau) = \int \frac{d^3k}{(2\pi)^3} e^{i\vec{k}\cdot\vec{x}} \left(\bar{\phi}(\vec{k}, \tau) a_{\vec{k}}^\dagger + \bar{\phi}^*(\vec{k}, \tau) a_{-\vec{k}} \right), \quad (4.24)$$

where $\tau = -1/[aH]$ is the conformal time, and $a_{\vec{k}}^\dagger$ and $a_{\vec{k}}$ are the canonical creation and annihilation operators respectively that satisfy

$$\left[a_{\vec{k}}^\dagger, a_{\vec{k}'} \right] = (2\pi)^3 \delta(\vec{k} - \vec{k}'). \quad (4.25)$$

In the Bunch-Davies vacuum, one finds the positive frequency modes are given by

$$\bar{\phi}(\vec{k}, \tau) = -i e^{i(\nu + \frac{1}{2})\frac{\pi}{2}} \frac{\sqrt{\pi}}{2} H(-\tau)^{3/2} H_\nu^{(1)}(-k\tau) \quad \text{with} \quad \nu = \sqrt{\frac{9}{4} - \frac{m^2}{H^2}}, \quad (4.26)$$

so that $\nu = 3/2$ corresponds to a massless field (see e.g. [102] for review). The observables of this theory are equal-time in-in correlation functions, which are computed via

$$\begin{aligned} \langle \text{in} | Q(t) | \text{in} \rangle &= \sum_{N=0}^{\infty} i^N \int_{-\infty}^t dt_1 \int_{-\infty}^{t_1} dt_2 \dots \int_{-\infty}^{t_{N-1}} dt_N \\ &\times \left\langle \left[H_{\text{int}}(t_N), [H_{\text{int}}(t_{N-1}), \dots [H_{\text{int}}(t_1), Q_{\text{int}}(t)] \dots] \right] \right\rangle, \end{aligned} \quad (4.27)$$

using

$$H_{\text{int}}(t) = \int d^3x \sqrt{-g} \frac{\lambda}{4!} \phi^4(\vec{x}, t). \quad (4.28)$$

We will be interested in multi-field correlators in the long wavelength limit, so that $Q(t) = \phi(\vec{k}_1, t) \dots \phi(\vec{k}_n, t)$. In general, this expression must be generalized to allow for the $i\epsilon$ prescription that projects the initial state onto the interacting vacuum, but this form is the most useful starting point for understanding the superhorizon evolution.

For illustration, we can compute the tree-level four point correlation function as

$$\left\langle \phi(\vec{k}_1) \phi(\vec{k}_2) \phi(\vec{k}_3) \phi(\vec{k}_4) \right\rangle'_{\text{tree}} = i \frac{\lambda}{4!} \int^t dt_1 d^3x a(t)^3 \left\langle \left[\phi^4(\vec{x}, t_1), \phi(\vec{k}_1) \dots \phi(\vec{k}_4) \right] \right\rangle', \quad (4.29)$$

where the $\phi(\vec{k})$ fields are all evaluated at the same time t , and we have introduced the notation

$$\langle \dots \rangle = (2\pi)^3 \delta^3(\sum \vec{k}_i) \langle \dots \rangle'. \quad (4.30)$$

At tree-level, we can simply use the massless mode functions,²

$$\bar{\phi}(\vec{k}, \tau) \rightarrow \frac{H}{\sqrt{2k^3}} (1 - ik\tau) e^{ik\tau}, \quad (4.31)$$

to evaluate this expression

$$\begin{aligned} \left\langle \phi(\vec{k}_1) \phi(\vec{k}_2) \phi(\vec{k}_3) \phi(\vec{k}_4) \right\rangle'_{\text{tree}} &= \lambda \, 2\text{Im} \int^\tau \frac{d\tau_1}{(-H\tau_1)^4} \prod_{i=1}^4 \frac{(1 - ik_i\tau_1)(1 + ik_i\tau)}{2k_i^3} e^{ik_i(\tau_1 - \tau)} \\ &= \frac{\lambda}{8(k_1 k_2 k_3 k_4)^3} \left[\frac{1}{3} \left(\sum_i k_i^3 \right) \left(\log \frac{k_t}{[aH]} + \gamma_E + \frac{1}{3} - 2 \right) - \frac{k_1 k_2 k_3 k_4}{k_t} - \frac{1}{9} k_t^3 \right. \\ &\quad \left. + 2 \sum_{i < j < \ell} k_i k_j k_\ell + \frac{1}{3} k_t \left(\sum_i k_i^2 - \sum_{i < j} k_i k_j \right) \right], \end{aligned} \quad (4.32)$$

where $k_t = k_1 + k_2 + k_3 + k_4$. In the final step, we have used $\tau = -1/[aH]$, have kept the $\log[aH]$ and time-independent contributions, and have not included terms that vanish as $[aH] \rightarrow \infty$. In deriving this expression, we have expressed the commutator as the imaginary part of the integral, which holds for real fields at first order in the H_{int} expansion, namely

$$i \left(\langle H_{\text{int}}(t_1) Q(t) \rangle - \langle Q(t) H_{\text{int}}(t_1) \rangle \right) = 2\text{Im} \langle Q(t) H_{\text{int}}(t_1) \rangle, \quad (4.33)$$

for a real operator $Q(t)$.

²We will use $\frac{3}{2} - \nu \equiv \alpha \neq 0$ as a regulator when we encounter loops.

4.3.2 Taking the Long Wavelength Limit

In this section, we review how to determine in-in correlators in the soft limit using SdSET. The starting point is to decompose the UV fields according to

$$\phi_S(\vec{k}, \tau) = H \left([a(\tau)H]^{-\alpha} \varphi_+(\vec{k}, \tau) + [a(\tau)H]^{-\beta} \varphi_-(\vec{k}, \tau) \right). \quad (4.34)$$

where $\phi(\vec{x}, \tau) = \phi_S(\vec{x}, \tau) + \Phi_H(\vec{x}, \tau)$ is split into soft (superhorizon) and hard (subhorizon) modes, and we have introduced a dimensionless time variable $\tau \equiv Ht$ so that the mass dimension of operators tracks the EFT power counting. The parameters α and β are subject to the constraint $\alpha + \beta = 3$. This is straightforward to derive from the top down, as these parameters are determined by the mass via $\alpha = 3/2 - \nu$ and $\beta = 3/2 + \nu$, where ν is defined in Eq. (4.26).

The decomposition of ϕ_S into φ_+ and φ_- is exact in the free theory. Taking the limit $k\tau \ll 1$ and using $\tau = -1/[aH]$ in Eq. (4.26), we find

$$\varphi_+(\vec{x}, t) = \int \frac{d^3k}{(2\pi)^3} e^{i\vec{k}\cdot\vec{x}} \bar{\varphi}_+(\vec{k}, t) \tilde{a}_{\vec{k}} \quad (4.35a)$$

$$\varphi_-(\vec{x}, t) = \int \frac{d^3k}{(2\pi)^3} e^{i\vec{k}\cdot\vec{x}} \bar{\varphi}_-(\vec{k}, t) \tilde{b}_{\vec{k}}, \quad (4.35b)$$

where

$$\bar{\varphi}_+ = C_\alpha \frac{1}{\sqrt{2}k^{\frac{3}{2}-\alpha}}, \quad \text{and} \quad \bar{\varphi}_- = D_\beta \frac{1}{\sqrt{2}k^{\frac{3}{2}-\beta}}, \quad (4.36)$$

and

$$C_\alpha = 2^{1-\alpha} \frac{\Gamma(\frac{3}{2}-\alpha)}{\sqrt{\pi}}, \quad \text{and} \quad D_\beta = -2^{1-\beta} \frac{\sqrt{\pi}}{\cos(\pi\beta)\Gamma(\beta-\frac{1}{2})}. \quad (4.37)$$

The operators $\tilde{a}_{\vec{k}}$ and $\tilde{b}_{\vec{k}}$ are given in terms of the UV creation and annihilation operators of the

form

$$\tilde{a}_{\vec{k}} = e^{i\delta_v} a_{\vec{k}}^\dagger + e^{-i\delta_v} a_{-\vec{k}}, \quad \text{and} \quad \tilde{b}_{\vec{k}} = i \left(e^{-i\delta_v} a_{\vec{k}}^\dagger - e^{i\delta_v} a_{-\vec{k}} \right). \quad (4.38)$$

From the UV theory, we determine that the operators commute with themselves

$$\left[\tilde{a}_{\vec{k}}^\dagger, \tilde{a}_{\vec{k}} \right] = \left[\tilde{b}_{\vec{k}}^\dagger, \tilde{b}_{\vec{k}} \right] = 0. \quad (4.39)$$

Nevertheless, these operators still have non-zero correlation function

$$\left\langle \tilde{a}_{\vec{k}} \tilde{a}_{\vec{k}'} \right\rangle = (2\pi)^3 \delta(\vec{k} + \vec{k}') \quad (4.40a)$$

$$\left\langle \tilde{b}_{\vec{k}} \tilde{b}_{\vec{k}'} \right\rangle = (2\pi)^3 \delta(\vec{k} + \vec{k}') , \quad (4.40b)$$

where $\langle \dots \rangle \equiv \langle 0 | \dots | 0 \rangle$, and $|0\rangle$ is the vacuum that is annihilated by $a_{\vec{k}}$. This gives rise to classical statistical power spectra

$$\left\langle \varphi_+(\vec{k}) \varphi_+(\vec{k}') \right\rangle = \frac{C_\alpha^2}{2} \frac{1}{k^{3-2\alpha}} (2\pi)^3 \delta(\vec{k} + \vec{k}') \quad (4.41a)$$

$$\left\langle \varphi_-(\vec{k}) \varphi_-(\vec{k}') \right\rangle = \frac{D_\beta^2}{2} \frac{1}{k^{3-2\beta}} (2\pi)^3 \delta(\vec{k} + \vec{k}') , \quad (4.41b)$$

where C_α and D_β are defined in Eq. (4.37) above. Note that in the massless limit $\alpha \rightarrow 0$, we reproduce the famous scale invariant power spectrum.

The corrections to this mapping can be systematically accounted for by matching between the UV theory and the EFT, see Sec. 4.4. The fields φ_+ and φ_- have well defined power counting; they carry operator dimension α and β respectively. After utilizing field redefinitions, on-shell conditions, and power counting to remove redundant operators, the low energy effective action is

given by

$$S_{\pm} = \int d^3x dt \left[-v(\dot{\varphi}_+ \varphi_- - \varphi_+ \dot{\varphi}_-) - \sum_{n \geq 2}^{\infty} [aH]^{3-n\alpha-\beta} \frac{c_{n,1}}{n!} \varphi_+^n \varphi_- \right], \quad (4.42)$$

where the $c_{n,1}$ are dimensionless Wilson coefficients. Note that \mathfrak{t} carries dimension zero by SdSET power counting, so marginal operators are dimension three. This explains why we have only included operators with a single factor of φ_- since these are the only terms that become marginal in the massless limit ($\alpha \rightarrow 0$). Additionally, we have not included any terms with $\vec{\partial}$, which start at dimension five and are therefore power suppressed by at least $k^2/[aH]^2$.

In addition to an action, SdSET requires specifying *initial conditions* for the fields φ_+ and φ_- that are acquired from the time evolution prior to horizon crossing. These initial conditions are random such that, to leading order, φ_+ behaves as a classical stochastic variable with correlations fixed by matching

$$\left\langle \varphi_+(\vec{k}_1) \dots \varphi_+(\vec{k}_N) \right\rangle_{\text{IC}^{(n)}} = \mathcal{K}^{-3(N-1)+N\alpha} F_{(n)}(\{\vec{q}_i\}) (2\pi)^3 \delta\left(\sum \vec{k}_i\right), \quad (4.43)$$

where \mathcal{K} is a reference momentum scale, $F_{(n)}(\{\vec{q}_i\})$ encode the dependence on the rescaled momenta $\vec{q}_i = \vec{k}_i/\mathcal{K}$, and the (n) subscripts track the order in the λ perturbative expansion for each contribution; the two point correlators in Eq. (4.41) should be viewed as $\langle \dots \rangle_{\text{IC}^{(0)}}$. Because φ_+ is time independent to leading order in the EFT, the initial conditions are determined by matching the time independent terms.

We evaluate time integrals in the EFT using

$$\int_{-\infty}^{\mathfrak{t}} dt' [a(\mathfrak{t}')H]^{\gamma} = \frac{1}{\gamma} [a(\mathfrak{t})H], \quad (4.44)$$

where we assume that this holds even when $\gamma < 0$. This analytic continuation enforces that the contributions from early times vanish, thereby ensuring that power law divergences associated with physics at horizon crossing are automatically absorbed into the initial conditions (in close

analogy with how dim reg treats power law divergences).

Cosmological correlators are determined in SdSET using the same in-in formalism as applied to the UV theory, see Sec. 4.3.1. For illustration, we can compute the tree-level trispectrum using Eq. (4.27) and the canonical commutator

$$\left[\varphi_+(\vec{x}, \tau), \varphi_-(\vec{x}', \tau) \right] = -\frac{i}{2\nu} \delta(\vec{x} - \vec{x}'). \quad (4.45)$$

Performing the time integrals using Eq. (4.44), we find

$$\begin{aligned} \left\langle \varphi_+(\vec{k}_1) \varphi_+(\vec{k}_2) \varphi_+(\vec{k}_3) \varphi_+(\vec{k}_4) \right\rangle &= \left\langle \left[\varphi_+(\vec{k}_1) \varphi_+(\vec{k}_2) \varphi_+(\vec{k}_3) \varphi_+(\vec{k}_4), \right. \right. \\ &\quad \left. \left. (-i) \frac{c_{3,1}}{3!} \int d\tau' d^3x' [a(\tau')H]^{-2\alpha} \varphi_+^3 \varphi_-(\vec{x}', \tau') \right] \right\rangle \\ &= -\frac{c_{3,1}}{2\nu} \left\langle \varphi_+(\vec{k}_2) \varphi_+(\vec{k}_3) \varphi_+(\vec{k}_4) \int d^3x' \varphi_+^3 \right\rangle \int d\tau' [a(\tau')H]^{-2\alpha} + \text{permutations} \\ &= \frac{c_{3,1}}{2\nu} \frac{C_\alpha^6 \sum_i k_i^{3-2\alpha}}{(k_1 k_2 k_3 k_4)^{3-2\alpha}} \left(\frac{[aH]^{-2\alpha}}{2\alpha} \right), \end{aligned} \quad (4.46)$$

where $c_{3,1}$ is the Wilson coefficient for the $\varphi_+^3 \varphi_-$ operator, see Eq. (4.42), and we used Eq. (4.41a) to evaluate the field contractions. In addition, we must include any trispectrum associated with the initial conditions.

4.3.3 (Dynamical) Renormalization

Loops corrections are calculated in the SdSET using dynamical dimensional regularization (dynamical dim reg). Rather than varying the spacetime dimension, we instead float the dynamical exponents α , and evaluate loop integrals by analytic continuation in α . Then when we encounter divergences as $\alpha \rightarrow 0$, they will be accompanied by log corrections to the time evolution, in exact analogy with conventional dim reg. To keep the units fixed as we vary α , we will introduce the necessary powers of $[aH]$ such that φ_+ stays dimensionless. Then we take

$\alpha = 0$ at the end of the calculation, so that:

$$\phi_S(\vec{k}, \tau) \rightarrow H \left(\varphi_+(\vec{k}, \tau) + [a(\tau)H]^{-3} \varphi_-(\vec{k}, \tau) \right), \quad (4.47)$$

so that φ_+ corresponds to a massless mode.

Since we are working within the EFT, we will typically encounter vanishing scaleless integrals. Then we can isolate the UV divergence in the usual way by regulating the IR with a dimensionful parameter K :

$$\begin{aligned} \langle \mathcal{O} \dots \rangle &\propto [aH]^{-2\alpha} \int \frac{d^3 p}{(2\pi)^3} \frac{1}{p^{3-2\alpha}} \\ &\rightarrow [aH]^{-2\alpha} \int \frac{d^3 p}{(2\pi)^3} \frac{1}{(p^2 + K^2)^{3/2-\alpha}} = [aH]^{-2\alpha} \frac{1}{8\pi^{3/2}} \frac{\Gamma[-\alpha]}{\Gamma[3/2-\alpha]} K^{2\alpha} \\ &\rightarrow -\frac{1}{2\pi^2} \left(\frac{1}{2\alpha} + \log \frac{K}{[aH]} - \log 2 \right), \end{aligned} \quad (4.48)$$

where we have taken the limit $\alpha \rightarrow 0$ in the third line. Having isolated these UV divergent contributions, we can use them to determine the (dynamical) RG flow, which resums a series in $\log[aH]$.

Having regulated the divergence, we can then absorb it into the renormalization of the operator

$$\mathcal{O} = Z_{\mathcal{O}} \mathcal{O}_R \quad \text{with} \quad Z_{\mathcal{O}} - 1 \propto -\frac{1}{2\pi^2} \left(\frac{1}{2\alpha} + \log \frac{K_{\star}}{[aH]_{\star}} \right), \quad (4.49)$$

so that

$$\langle \mathcal{O}_R \dots \rangle \propto \frac{1}{2\pi^2} \log \frac{[aH]_{\star}}{[aH]} + \log \frac{K}{K_{\star}}, \quad (4.50)$$

where $[aH]_{\star}$ and K_{\star} are energy and momentum scales we have invented to make the logs small, i.e., subtraction points. By definition the bare operator \mathcal{O} is independent of these arbitrary

parameters, and thus

$$\frac{d}{d \log[aH]_\star} \mathcal{O} = 0 \iff \frac{d}{d \log[aH]_\star} \mathcal{O}_R = -\frac{d \log Z_\mathcal{O}}{d \log[aH]_\star} \mathcal{O}_R \equiv \gamma \mathcal{O}_R, \quad (4.51)$$

where the anomalous dimension γ is independent of $[aH]$. We are working with a scheme where $Z_\mathcal{O}$ is diagonal at the scale $[aH]_\star$. In general, $\gamma \rightarrow \gamma_{ij}$ is a matrix that acts on the space of operators, and which encodes both the anomalous scaling and mixing of these operators.

4.3.4 Matching and Initial Conditions

SdSET provides an effective description for the time evolution of scalar modes that have crossed the Hubble horizon. Their state at the time of horizon crossing cannot be computed within the EFT, and instead has to be provided as an additional input. This is why SdSET requires matching for both the initial conditions and the EFT Wilson coefficients. This is not unique to SdSET, but is necessarily part of any EFT description of the post inflationary universe as well, see e.g. [103].

When defined using dynamical dim reg, SdSET is a so-called continuum EFT [104]. Concretely, the time integrals include arbitrary early times, even though the EFT does not provide a model of the subhorizon physics, since it relies on the use of the long-wavelength mode functions at all times. Importantly, as with all continuum EFT, these early time integrals only make scaleless (and therefore vanishing) contributions. Thus we can integrate over all times, such that the regulated integrals respect the low energy symmetries and the EFT power counting. Underlying the validity of this procedure is the fact that the subhorizon physics only alters the initial conditions and thus we can fully account for all subhorizon evolution by matching a UV theory onto SdSET.

One can demonstrate how matching separates into Wilson coefficient and initial condition corrections more directly using a hard cutoff to evaluate time and momentum integrals, i.e., treating the theory as a Wilsonian EFT [104]. Let k_i denote the magnitudes of the momenta

appearing in the cosmological correlator, and let the cutoff of the momentum integrals Λ be much greater than any of the k_i . In addition, we denote the time cutoff by t_Λ ; this is the time when all the EFT modes are in the superhorizon limit, and thus it specifies when we set the initial conditions for the EFT.

Before t_Λ , a subset of EFT modes are subhorizon, and so one must use the UV theory to describe them. To match onto the EFT, it is useful to split the full theory time evolution into pieces before and after t_Λ . Let $U_I(t, t')$ represent the interaction picture propagator, and $|\Omega\rangle$ be the UV vacuum state. This decomposition can then be written as

$$\begin{aligned} \langle \Omega | \phi(\vec{k}_1, t) \dots \phi(\vec{k}_n, t) | \Omega \rangle &= \langle \Omega | U_I^\dagger(t, -\infty) \phi_I(\vec{k}_1, t) \dots \phi_I(\vec{k}_n, t) U_I(t, -\infty) | \Omega \rangle \\ &= \langle \Omega | U_I^\dagger(t_\Lambda, -\infty) U_I^\dagger(t, t_\Lambda) \phi_I(\vec{k}_1, t) \dots \phi_I(\vec{k}_n, t) U_I(t, t_\Lambda) U_I(t_\Lambda, -\infty) | \Omega \rangle, \end{aligned} \quad (4.52)$$

where ϕ_I is the interaction picture field.

One can trivially re-write Eq. (4.52) as an expectation value of $|\psi\rangle = U_I(t_\Lambda, -\infty) |\Omega\rangle$, the state of the full theory fields at t_Λ . One can then integrate out the modes whose wave vector magnitudes satisfy $k > \Lambda$, so that the remaining modes are superhorizon after t_Λ . It was shown in [65] that, after integrating out these so-called hard modes, the resulting action for the superhorizon modes φ_+ and φ_- is local. We can then evolve these modes from t_Λ to t using the unitary time evolution operators defined within the SdSET itself:

$$\begin{aligned} \langle \Omega | \phi(\vec{k}_1, t) \dots \phi(\vec{k}_n, t) | \Omega \rangle &= \\ &= \langle \psi_{\text{EFT}}(t_\Lambda) | U_{I, \text{EFT}}^\dagger(t, t_\Lambda) \phi_S(\vec{k}_1, t) \dots \phi_S(\vec{k}_n, t) U_{I, \text{EFT}}(t, t_\Lambda) | \psi_{\text{EFT}}(t_\Lambda) \rangle, \end{aligned} \quad (4.53)$$

where $U_{I, \text{EFT}}$ is the interaction picture propagator obtained from Eq. (4.42), and ϕ_S is given by Eq. (4.47). The state $|\psi_{\text{EFT}}(t_\Lambda)\rangle$ is the EFT state inherited from $|\psi\rangle$ that results from integrating out the hard modes; this state encodes the initial conditions for φ_+ and φ_- .

One then fixes the EFT parameters in Eq. (4.42) and the initial state $|\psi_{\text{EFT}}(t_\Lambda)\rangle$ by

matching to full theory correlators. In practice, the full form of $|\psi_{\text{EFT}}(t_\Lambda)\rangle$ is more information than is needed to derive the late time behavior of n -point correlation functions of ϕ . Instead, it is sufficient to determine a finite number of n -point functions,

$$\langle \psi_{\text{EFT}}(t_\Lambda) | \varphi_+(\vec{k}_1) \dots \varphi_+(\vec{k}_n) | \psi_{\text{EFT}}(t_\Lambda) \rangle, \quad (4.54)$$

from matching. Furthermore, this shows that all of the contributions from $t < t_\Lambda$ are encoded in the state $|\psi_{\text{EFT}}(t_\Lambda)\rangle$ or, equivalently, in the initial conditions set at t_Λ . Finally, since t_Λ is an unphysical cutoff parameter, no physical results can depend on it. In particular, the initial conditions can be identified as the *time-independent* contribution from the UV correlators. This implies that we do not need to rely on hard cutoff to derive the initial conditions. In what follows, we will regulate the theory using dynamical dim reg, and will derive the initial conditions by identifying the time-independent contributions to correlators that appear when matching.

To illustrate the matching procedure, it is useful to first consider a simple example. By expanding Eq. (4.27) to leading order in $c_{3,1}$ and setting $|\text{in}\rangle = |\psi_{\text{EFT}}\rangle$ we find that the tree-level EFT prediction for the four point function of ϕ is

$$\begin{aligned} \langle \Omega | \phi(\vec{k}_1, t) \dots \phi(\vec{k}_4, t) | \Omega \rangle &= \left(\frac{\tau}{\tau_\Lambda} \right)^{4\alpha} \left[\langle \psi_{\text{EFT}}(t_\Lambda) | \varphi_+(\vec{k}_1) \dots \varphi_+(\vec{k}_4) | \psi_{\text{EFT}}(t_\Lambda) \rangle \right. \\ &\quad \left. + 2ic_{3,1} \int_{\tau_\Lambda}^{\tau} \frac{d\tau_1}{\tau_1^{1+2\alpha}} \int d^3x \langle \psi_{\text{EFT}}(t_\Lambda) | [\varphi_+(\vec{k}_1) \dots \varphi_+(\vec{k}_4), \varphi_+^3 \varphi_-(\vec{x}, \tau_1)] | \psi_{\text{EFT}}(t_\Lambda) \rangle \right]. \quad (4.55) \end{aligned}$$

As in all perturbative SdSET calculations, the time dependence and field contractions factorize at the integrand level. The EFT prediction is then parameterized by the coupling $c_{3,1}$ and two expectation values of $|\psi_{\text{EFT}}\rangle$.

The expectation values parameterize the subhorizon evolution of the EFT modes before t_Λ . If the full theory is perturbative, then the subhorizon evolution is approximately Gaussian.

Assuming the UV theory is given by $\lambda\phi^4$, then to $O(\lambda)$ we can write

$$\begin{aligned} \langle \psi_{\text{EFT}}(t_\Lambda) | \varphi_{I,+}(\vec{k}_1) \dots \varphi_{I,+}(\vec{k}_4) | \psi_{\text{EFT}}(t_\Lambda) \rangle &= \left(\langle \varphi_{I,+}(\vec{k}_1) \varphi_{I,+}(\vec{k}_2) \rangle_{\text{IC}^{(0)}} \langle \varphi_{I,+}(\vec{k}_3) \varphi_{I,+}(\vec{k}_4) \rangle_{\text{IC}^{(0)}} \right. \\ &+ 2 \langle \varphi_{I,+}(\vec{k}_1) \varphi_{I,+}(\vec{k}_2) \rangle_{\text{IC}^{(0)}} \langle \varphi_{I,+}(\vec{k}_3) \varphi_{I,+}(\vec{k}_4) \rangle_{\text{IC}^{(1)} + \text{perms}} \left. + \langle \varphi_{I,+}(\vec{k}_1) \dots \varphi_{I,+}(\vec{k}_4) \rangle_{\text{IC}^{(1)}} \right), \end{aligned} \quad (4.56)$$

where the final term on the RHS encodes the non-Gaussian contribution to the subhorizon evolution of the modes. There is a similar formula for the expectation value on the second line of Eq. (4.55). However, since it is already multiplied by $c_{3,1}$, we only need the $\langle \dots \rangle_{\text{IC}^{(0)}}$ contribution to the expectation value at this order.

The SdSET two point functions derived from the free theory are given in Eq. (4.41). To include the impact of the UV interaction on the EFT, we compute $\langle \varphi_{I,+}(\vec{k}_1) \dots \varphi_{I,+}(\vec{k}_4) \rangle_{\text{IC}}$ and $c_{3,1}$ by matching to the full theory. The superhorizon evolution between t_Λ and t generates the term proportional to $c_{3,1}$, and so we can isolate the initial conditions contribution by evaluating both sides of Eq. (4.55) at t_Λ , giving

$$\langle \varphi_{I,+}(\vec{k}_1) \dots \varphi_{I,+}(\vec{k}_4) \rangle_{\text{IC}} = \langle \Omega | \phi(\vec{k}_1, t_\Lambda) \dots \phi(\vec{k}_4, t_\Lambda) | \Omega \rangle_{\text{connected}}, \quad (4.57)$$

where the ‘‘connected’’ subscript refers to the fact that this does not include the contributions from products of lower point contractions. The RHS of Eq. (4.57) can be computed using Eq. (4.27), where H_I is given by the full theory interaction Hamiltonian and the time integrals extend from $-\infty$ to t_Λ . Since the integral’s main region of support occurs when the modes are subhorizon, we cannot replace the mode functions with their late time behavior, and instead have to use their full UV form given in Eq. (4.26). The UV mode functions simplify for scalars whose mass is much lighter than the Hubble constant and can be approximated by Eq. (4.31).

One can then fix $c_{3,1}$ by demanding that Eq. (4.55) reproduces the full theory prediction for the correlator in the regime $t > t_\Lambda$. While the split between subhorizon ($t < t_\Lambda$) and super-

horizon ($t > t_\Lambda$) evolution is manifest in the EFT, this split has to be inputted by hand in the full theory, as was done in Eq. (4.52); this is effectively making a choice of scheme. Practically, one can decompose the time integrals in Eq. (4.27) into regions before and after t_Λ . In our four point example, subhorizon contribution is already taken care of by the initial conditions, i.e., Eq. (4.57), while the second term in Eq. (4.55) must reproduce the superhorizon evolution. The Wilson coefficient $c_{3,1}$ is fixed by this condition.

Since the split time t_Λ is arbitrary from the perspective of the full theory, all full-theory and EFT predictions of the ϕ correlators must be independent of it. This provides an additional check on the matching calculation in the hard cutoff scheme. Fortunately, when we calculate with dynamical dim reg, the time integrals are manifestly independent of t_Λ , while still maintaining the split between initial conditions and time-evolution. In this sense, the hard-cutoff scheme proves the validity of dynamical dim reg, while dynamical dim reg makes it manifest that we can implement this procedure without breaking symmetries. This matches the more intuitive argument that our treatment of initial conditions and time evolution in SdSET is identical to the continuum EFT approach.

4.3.5 Stochastic Inflation from SdSET

From the point of view of our EFT, Stochastic Inflation can be understood as a consequence of operator mixing. Specifically, for light fields for which $\alpha \rightarrow 0$, the composite operators ϕ_+^n are degenerate to leading order (in that they have the same dimension as determined by the EFT power counting). Assuming the correlations of these fields are only due to the Gaussian contribution given in Eq. (4.41), one encounters a UV divergence from a one-loop contraction

$$\begin{aligned} \langle \phi_+^n(\vec{x}) \dots \rangle &\supset \langle \phi_+^{n-2}(\vec{x}) \dots \rangle \times \binom{n}{2} \frac{C_\alpha^2}{2} \int \frac{d^3 p}{(2\pi)^3} \frac{H^{2-2\alpha}}{p^{3-2\alpha}} \\ &\supset \langle \phi_+^{n-2}(\vec{x}) \dots \rangle \times \binom{n}{2} \frac{C_\alpha^2}{4\pi^2} \log[aH]. \end{aligned} \quad (4.58)$$

The dynamical RG associated with this operator mixing can be written as

$$\frac{\partial}{\partial \mathfrak{t}} \langle \varphi_+^n(\vec{x}) \dots \rangle = \frac{n(n-1)}{8\pi^2} \langle \varphi_+^{n-2}(\vec{x}) \dots \rangle - \frac{n}{3} \sum_{m>1} \frac{c_{m,1}}{m!} \langle \varphi_+^{n-1}(\vec{x}) \varphi_+^m(\vec{x}) \dots \rangle, \quad (4.59)$$

where the second term arises from the classical time evolution. This equation contains the same information as Starobinsky's formulation of Stochastic Inflation. Specifically, we can use the Fokker-Planck equation given in Eq. (4.2) to see that these two approaches are equivalent:

$$\begin{aligned} \frac{\partial}{\partial \mathfrak{t}} \langle \varphi_+^n \rangle &= \frac{\partial}{\partial \mathfrak{t}} \int d\varphi_+ \varphi_+^n P(\varphi_+, \mathfrak{t}) \\ &= \int d\varphi_+ \varphi_+^n \left(\frac{1}{8\pi^2} \frac{\partial^2}{\partial \varphi_+^2} P(\varphi_+, \mathfrak{t}) + \frac{1}{3} \frac{\partial}{\partial \varphi_+} \left[\sum_{m>1} \frac{c_{m,1}}{m!} \varphi_+^m P(\varphi_+, \mathfrak{t}) \right] \right) \\ &= \int d\varphi_+ \left(\frac{n(n-1)}{8\pi^2} \varphi_+^{n-2} P(\varphi_+, \mathfrak{t}) - \frac{n}{3} \varphi_+^{n-1} \sum_{m>1} \frac{c_{m,1}}{m!} \varphi_+^m P(\varphi_+, \mathfrak{t}) \right) \\ &= \frac{n(n-1)}{8\pi^2} \langle \varphi_+^{n-2} \rangle - \frac{n}{3} \sum_{m>1} \frac{c_{m,1}}{m!} \langle \varphi_+^{n-1} \varphi_+^m \rangle, \quad (4.60) \end{aligned}$$

where in the second line we plugged in Eq. (4.2), $Ht = \mathfrak{t}$, the $\alpha = 0$ relation $\phi|_{\varphi_-=0} \rightarrow H\varphi_+$, and

$$V'(\phi) \rightarrow \frac{\partial}{\partial \varphi_-} V(\varphi_+, \varphi_-) \Big|_{\varphi_-=0} = \sum_{m>1} \frac{c_{m,1}}{m!} \varphi_+^m. \quad (4.61)$$

This shows that Eq. (4.59) is equivalent to the leading order equation for Stochastic Inflation Eq. (4.2). Therefore, calculating corrections to Stochastic Inflation has been reduced to the straightforward task of computing the higher order dynamical RG equation using SdSET. Concretely, we would expect to find mixing between composite operators φ_+^n and all possible

φ_+^n such that

$$\begin{aligned} \frac{\partial}{\partial \tau} \langle \varphi_+^n \rangle &= -\frac{n}{3} \sum_{m>1}^{\text{odd}} \frac{c_{m,1}}{m!} \langle \varphi_+^{n+m-1} \rangle + \binom{n}{2} \sum_{m=0}^{\infty} b_m \langle \varphi_+^{n+2m-2} \rangle \\ &\quad - \binom{n}{3} \sum_{m=0}^{\infty} d_m \langle \varphi_+^{n+2m-2} \rangle + \binom{n}{4} \sum_{m=0}^{\infty} e_m \langle \varphi_+^{n+2m-4} \rangle + \dots \end{aligned} \quad (4.62)$$

Note the role of the binomial coefficient which will originate from the number of fields inside φ_+^n whose contractions are responsible for mixing with a given operator, leading to a single log divergence. Repeating the above argument, we see that this dynamical RG is equivalent to

$$\begin{aligned} \frac{\partial}{\partial \tau} P(\varphi_+, \tau) &= \frac{1}{3} \frac{\partial}{\partial \varphi_+} \left[\partial_{\varphi_-} V(\varphi_+, \varphi_-) |_{\varphi_- = 0} P(\varphi_+, \tau) \right] + \frac{\partial^2}{\partial \varphi_+^2} \left[\sum_{m=0}^{\infty} \frac{b_m}{2!} \varphi_+^{2m} P(\varphi_+, \tau) \right] \\ &\quad + \frac{\partial^3}{\partial \varphi_+^3} \left(\varphi_+ \sum_{m=0}^{\infty} \frac{d_m}{3!} \varphi_+^{2m} P(\varphi_+, \tau) \right) + \frac{\partial^4}{\partial \varphi_+^4} \left(\sum_{m=0}^{\infty} \frac{e_m}{4!} \varphi_+^{2m} P(\varphi_+, \tau) \right) + \dots, \end{aligned} \quad (4.63)$$

where we see that number of derivatives is related to the binomial coefficient of the associated mixing term. Comparing with Sec. 4.2.2, we see that the NLO corrections are determined by $c_{5,1}$ and b_1 while the NNLO coefficients are $c_{7,1}$, b_2 and d_0 . Achieving NNLO accuracy requires matching $\lambda \phi^4$ theory onto the SdSET at one loop, the subject of the next section. Note, however, that we have described Stochastic Inflation in terms of φ_+ rather than the UV field ϕ . This distinction will be important because the equations of Stochastic Inflation are not invariant under field redefinitions. We will address these issues in detail in Sec. 4.5.3. Finally, we note that this result demonstrates the Markovian assumption which led to Eq. (4.16) does in fact hold as a consequence of SdSET power counting. Specifically, the fact that the φ_- dynamics are irrelevant to the evolution of the φ_+ correlators implies that the evolution of the system is indeed linear, and thus it has no “memory.”

4.4 Matching $\lambda\phi^4$ Onto SdSET at One-Loop

In this section we will show how to match correlators of ϕ to correlators of ϕ_+ in the SdSET to determine the EFT parameters in terms of UV data. This then serves as input for any calculation of cosmological correlators for $\lambda\phi^4$ theory in the long wavelength limit, including the corrections to Stochastic Inflation we will discuss in subsequent sections. Furthermore, by extending this program to one-loop order for the first time, this calculation will serve as a non-trivial check of the SdSET framework.

Unlike conventional EFTs, we match both the couplings of SdSET and the stochastic initial conditions, the former results from studying the time-dependent terms in the EFT while the latter is fixed at the time of horizon crossing. As a result, consistent matching of time-dependence of the UV correlators is non-trivial and requires that the SdSET is a complete representation of the long wavelength dynamics. In contrast, time-independent contributions to a given correlator can always be absorbed into the initial conditions (up to composite operators as discussed in Sec. 4.4.3). As a result, for tree and one-loop matching we will be particularly focused on time-dependent UV contributions.

4.4.1 Tree-level Matching and Field Redefinitions

Tree-level matching in the interacting theory is non-trivial due to the impact on the initial conditions. We will need to introduce non-Gaussian initial conditions in order to match higher point correlation functions as calculated by the UV theory.

We can understand many important aspects of matching by Taylor expanding the UV calculation in the long wavelength limit. As a simple demonstration, we can explore the superhorizon behavior of the operator ϕ . At first order in the coupling, we can apply the

definition of the in-in correlator given in Eq. (4.27) with $Q(t) = \phi$, which gives

$$\begin{aligned} [\phi]_\lambda(\vec{x}, \tau) &= i \int^\tau d\tau_1 \left[H_{\text{int}}(\tau_1), \phi_{\text{in}}(\vec{x}, \tau) \right] \\ &= \frac{\lambda}{3!} \int^\tau \frac{d\tau_1}{(-H\tau_1)^4} \int d^3x_1 \phi_{\text{int}}(\vec{x}_1, \tau_1)^3 i \left[\phi_{\text{int}}(\vec{x}_1, \tau_1), \phi_{\text{int}}(\vec{x}, \tau) \right], \end{aligned} \quad (4.64)$$

where ϕ_{int} are the interaction picture fields. Because the time integral runs over all times, this includes both the regime where the modes are hard (UV) and the long wavelength limit where the EFT applies. Nevertheless, if we expand in the long wavelength limit and evaluate the integrals with dynamical dim reg, we will only get contributions from late times. Since ϕ_{in} are the free field operators, we can use the map given in Eq. (4.34) to determine the long wavelength behavior of the full theory:³

$$\phi_{\text{int}} \rightarrow H \left([aH]^{-\alpha} \varphi_+ + [aH]^{-3+\alpha} \varphi_- \right). \quad (4.65a)$$

Then using $\tau = -1/[aH]$ and keeping only terms that survive as $[aH] \rightarrow \infty$, one finds

$$\begin{aligned} [\phi]_\lambda(\vec{x}, \tau) &\rightarrow \frac{\lambda}{3!} H \int^\tau dt_1 \int d^3x_1 [a(t_1)H]^{-2\alpha} \varphi_+^3(\vec{x}_1) \\ &\quad i \left(\left[\varphi_-(\vec{x}_1), \varphi_+(\vec{x}) \right] + \frac{[a(t_1)H]^3}{[a(t)H]^3} \left[\varphi_+(\vec{x}_1), \varphi_-(\vec{x}) \right] \right) \\ &= \frac{\lambda}{3!} \frac{H}{3} \left(- \left(-\frac{1}{2\alpha} + \log[a(t)H] \right) + \frac{1}{3} \right) \varphi_+^3(\vec{x}), \end{aligned} \quad (4.66)$$

where in the last line we expanded in $\alpha \ll 1$. Note that the scaling dimension of φ_+ is still α and thus will provide the necessary distance scale to make the log dimensionless inside of a correlator, as is familiar from conventional dim reg.

Now we turn to exploring the same effect within the EFT direction by calculating the

³Note we are not working in the EFT yet, because we have not integrated out the hard modes. All we are doing here is taking the long wavelength limit.

time evolution of φ_+ using SdSET. Using Eq. (4.34) with $Q = \varphi_+$ and $\mathcal{H}_{\text{int}} = c_{3,1} \varphi_+^3 \varphi_- / 3!$ we have

$$\begin{aligned} [\varphi_+]_\lambda(\vec{x}, \tau) &= \frac{c_{3,1}}{3!} \int^{\tau} d\tau_1 \int d^3x_1 [aH(\tau_1)]^{-2\alpha} \varphi_+^3(\vec{x}_1) i \left[\varphi_-(\vec{x}_1), \varphi_+(\vec{x}) \right] \\ &= -\frac{c_{3,1}}{3!} \frac{1}{3} \left(-\frac{1}{2\alpha} + \log[a(\tau)H] \right) \varphi_+^3(\vec{x}), \end{aligned} \quad (4.67)$$

where it is trivial to match the tree-level UV interaction to the EFT interaction, such that

$$c_{4,0} = c_{3,1} = \dots = \lambda + O(\lambda^2). \quad (4.68)$$

The equality between $c_{n,0}$ and $c_{n-m,m}$ found in matching is also fixed by the reparametrization invariance of SdSET. We see that the EFT is capturing the first term in the Taylor expansion of the UV theory given in Eq. (4.66), but not the second.

The origin of the missing term is two-fold. First, we are only considering correlations of φ_+ instead of the full UV field, which also includes φ_- . This alone would not matter, since φ_- is suppressed by $[aH]^{-3}$. However, in order to organize the interactions within the EFT, we removed the $c_{4,0} \varphi_+^4 / 4!$ term by a field redefinition. Specifically, to remove the $c_{n,0} \varphi_+^n / n!$ operator, we take

$$\varphi_- \rightarrow \varphi_- + \frac{c_{n,0}}{9(n-1)!} [aH]^{3-(n-1)\alpha} \varphi_+^{n-1}. \quad (4.69)$$

Therefore, keeping track of the field redefinition implies that we should use

$$\underline{\varphi}_{\text{EFT}} \equiv \underline{\varphi} = H \left([aH]^{-\alpha} \varphi_+ + [aH]^{-\beta} \varphi_- + \frac{c_{4,0}}{9} \frac{1}{3!} [aH]^{-3\alpha} \varphi_+^3 + \dots \right), \quad (4.70)$$

with $\alpha \rightarrow 0$ and $\beta \rightarrow 3$. Now the quantities on the RHS live purely in the EFT. As a result φ_- will not contribute to correlation functions of $\underline{\varphi}$ because they are suppressed by powers of

$[aH]^{-3}$. Combining this with Eq. (4.67), we find

$$[\underline{\varphi}]_\lambda = \varphi_+ + \frac{1}{3!} \frac{H}{3} \left(c_{3,1} \left(\frac{1}{2\alpha} - \log[aH] \right) + \frac{c_{4,0}}{3} \right) \varphi_+^3(\vec{x}), \quad (4.71)$$

where we dropped terms suppressed by powers of $[aH]$. Now we see that this matches the UV expression in Eq. (4.66) when we use the tree-level matching relations $c_{3,1} = c_{4,0} = \lambda$ given in Eq. (4.68).

This result also provides the map between SdSET and Refs. [32, 93], which derived the soft behavior by explicitly expanding the UV in-in correlator in the superhorizon limit. The tree-like structure they observe is a consequence of our power counting as only $c_{n,1}$ is marginal and hence interactions only include a single factor of φ_- . The nested set of commutators in Eq. (4.27) ensures that the marginal operators always have a tree-like structure. In SdSET, this is manifest from dynamical RG, and all the additional finite terms arise from the field redefinitions.

By similar considerations, we must apply the field redefinition to match the UV potential onto $V(\varphi_+, \varphi_-)$ in the EFT. Although $\lambda \varphi_+^4$ has been removed, this procedure introduces higher order terms, such as

$$\frac{c_{3,1}}{3!} \varphi_+^3 \varphi_- \rightarrow \frac{c_{3,1} c_{4,0}}{9(3!)^2} [aH]^3 \varphi_+^6 \quad (4.72a)$$

$$\frac{c_{2,2}}{4} [aH]^{-3} \varphi_+^2 \varphi_-^2 \rightarrow \frac{c_{2,2} c_{4,0}}{18(3!)} \varphi_+^5 \varphi_- . \quad (4.72b)$$

Removing the first term will introduce a $\varphi_+^7 \varphi_-$ interaction at order λ^3 and so on. As a result, our field redefinition requires that

$$V(\varphi_+, \varphi_-) \supset \frac{1}{3!} \varphi_- \left(c_{3,1} \varphi_+^3 + \frac{c_{2,2} c_{4,0}}{18} \varphi_+^5 + \frac{c_{2,2} c_{3,1} c_{4,0}}{162} \varphi_+^7 + \dots \right) . \quad (4.73)$$

Finally, using $c_{2,2} = c_{3,1} = c_{4,0} = \lambda$ from matching, we arrive at

$$V(\varphi_+, \varphi_-) \supset \frac{\lambda}{3!} \varphi_- \left(\varphi_+^3 + \frac{\lambda}{18} \varphi_+^5 + \frac{\lambda^2}{162} \varphi_+^7 + \dots \right). \quad (4.74)$$

or $c_{5,1} = \frac{\lambda^2}{18} \frac{5!}{3!}$ and $c_{7,1} = \frac{\lambda^3}{162} \frac{7!}{(3!)}$.

The correction to $c_{5,1}$ is equivalent to the NLO corrections to the effective potential calculated in Refs. [31] and [92] using complementary techniques. While these two references approach this problem from different perspectives, the wavefunction of the universe and the dS static patch respectively, both effectively integrate out the decaying mode φ_- which leads to an additional term in the potential. Instead, when φ_- is included, our corrections arise from insuring φ_- does not mix with φ_+ at higher orders in perturbation theory. As the dimensions of φ_+ and φ_- are well separate for $\alpha \rightarrow 0$, removing mixing can always be achieved by such a field redefinition. Additionally, it is easy to determine the correction to $c_{2n+1,1} \propto \lambda^n$ by repeated application of Eq. (4.69). Most importantly, we do not integrate out φ_- to ensure we have a local action, rather than an open EFT for the growing mode alone [30].

What we have accomplished thus far is to determine the correct basis of operators to match the EFT and UV descriptions. We have ensured that the superhorizon limit of ϕ and $\underline{\varphi}$ agree as operators at higher orders in λ . However, in order to match the correlators of the UV theory, which include the subhorizon evolution, we will need to determine the stochastic initial conditions beyond the Gaussian limit.

In order to correctly match the four-point function, we write the EFT trispectrum to order

λ as⁴

$$\begin{aligned}
\left\langle \underline{\varphi}(\vec{k}_1) \underline{\varphi}(\vec{k}_2) \underline{\varphi}(\vec{k}_3) \underline{\varphi}(\vec{k}_4) \right\rangle'_C &= \left\langle [\underline{\varphi}]_\lambda(\vec{k}_1) \varphi_+(\vec{k}_2) \varphi_+(\vec{k}_3) \varphi_+(\vec{k}_4) \right\rangle'_C + \text{permutations} \\
&\quad + \left\langle \underline{\varphi}(\vec{k}_1) \underline{\varphi}(\vec{k}_2) \underline{\varphi}(\vec{k}_3) \underline{\varphi}(\vec{k}_4) \right\rangle'_{\text{IC}^{(1)}} \\
&= \frac{\lambda H^4}{8(k_1 k_2 k_3 k_4)^3} \sum_i \frac{k_i^3}{3} \left(c_{3,1} \left(\frac{1}{2\alpha} + \log \frac{k_i}{[aH]} \right) + \frac{c_{4,0}}{3} \right) \\
&\quad + \left\langle \underline{\varphi}(\vec{k}_1) \underline{\varphi}(\vec{k}_2) \underline{\varphi}(\vec{k}_3) \underline{\varphi}(\vec{k}_4) \right\rangle'_{\text{IC}^{(1)}}, \tag{4.75}
\end{aligned}$$

where $c_{3,1} = c_{4,0} = \lambda$ as before, and the subscript ‘‘C’’ denotes that this is only the connected contributions. Matching this EFT expression to the UV result in Eq. (4.32) fixes the non-Gaussian contribution to the initial conditions:

$$\begin{aligned}
\left\langle \underline{\varphi}(\vec{k}_1) \underline{\varphi}(\vec{k}_2) \underline{\varphi}(\vec{k}_3) \underline{\varphi}(\vec{k}_4) \right\rangle'_{\text{IC}^{(1)}} &= \frac{\lambda H^4}{8(k_1 k_2 k_3 k_4)^3} \left[\frac{\sum_i k_i^3 \left(-\frac{1}{2\alpha} + \gamma_E - 2 + \log \frac{k_t}{k_i} \right)}{3} \right. \\
&\quad \left. - \frac{k_1 k_2 k_3 k_4}{k_t} - \frac{1}{9} k_t^3 + 2 \sum_{h < i < j} k_h k_i k_j + \frac{1}{3} k_t \left(\sum_i k_i^2 - \sum_{i < j} k_i k_j \right) \right], \tag{4.76}
\end{aligned}$$

where $k_t = k_1 + k_2 + k_3 + k_4$. Most significantly, all the time-dependence of the full UV trispectrum is already captured by the EFT and, as expected, the initial conditions are only required for matching the time-independence contributions. This result is extended to the six-point function in Sec. 4.A as expected from general arguments.

Matching Derivative Operators: Before moving on the loop-level matching, let us briefly comment on the case where the UV theory is itself an effective theory. Specifically, we are only considering the case of a $\lambda \phi^4$ interaction in the UV, while in principle there could be a variety of higher derivative (irrelevant) interactions as well. The first such operator we can write down is

⁴For convenience, we take $C_\alpha \rightarrow 1$ for the light fields and have dropped the additional constants that arise from expanding $C_\alpha = 1 + \alpha(\gamma_E - 2 + \log 2) + O(\alpha^2)$. While this choice has no impact on the physics (since the correct constants will appear in the initial conditions by matching), it will simplify the algebra significantly.

$(\nabla_\mu \phi \nabla^\mu \phi)^2/M^4$. The full tree level trispectrum was calculated in Ref. [105] and is given by

$$\begin{aligned}
\langle \phi(\vec{k}_1) \phi(\vec{k}_2) \phi(\vec{k}_3) \phi(\vec{k}_4) \rangle_{\nabla^4} &= (2\pi)^3 \delta\left(\sum_i \vec{k}_i\right) \frac{1}{M^4} \frac{H^8}{\prod_i 2k_i^3} \\
&\times \left[-\frac{144k_1^2 k_2^2 k_3^2 k_4^2}{k_t^5} - 4 \left(\frac{12k_1 k_2 k_3 k_4}{k_t^5} + \frac{3 \prod_{i < j < l} k_i k_j k_l}{k_t^4} \right. \right. \\
&\quad \left. \left. + \frac{\prod_{i < j} k_i k_j}{k_t^3} + \frac{1}{k_t} \right) \left((\vec{k}_1 \cdot \vec{k}_2) (\vec{k}_3 \cdot \vec{k}_4) + 2 \text{ perms} \right) \right. \\
&\quad \left. + (\vec{k}_1 \cdot \vec{k}_2) \left(\frac{4k_3^2 k_4^2}{k_t^3} + \frac{12(k_1 + k_2) k_3^2 k_4^2}{k_t^4} + \frac{48k_1 k_2 k_3^2 k_4^2}{k_t^5} \right) \right. \\
&\quad \left. + 5 \text{ perms} \right]. \tag{4.77}
\end{aligned}$$

What we notice right away is that this gives us a completely time-independent result. It can therefore only be absorbed into the initial conditions of φ_+ :

$$\langle \varphi_+(\vec{k}_1) \varphi_+(\vec{k}_2) \varphi_+(\vec{k}_3) \varphi_+(\vec{k}_4) \rangle_{\text{IC}} \supset H^{-4} \langle \phi(\vec{k}_1) \phi(\vec{k}_2) \phi(\vec{k}_3) \phi(\vec{k}_4) \rangle_{\nabla^4}. \tag{4.78}$$

This result illustrates a broader feature of physics in dS: higher derivatives decouple at long wavelength and thus contribute, at most, time-independent correlation functions. This property is made manifest in SdSET and must hold in matching. As a result, a variety of possible UV theories only impact the initial conditions and not the long wavelength dynamics. In this sense, our choice to focus $\lambda \phi^4$ is not missing more complicated superhorizon evolution. Instead, higher derivative terms are trivially matched in SdSET and thus do not further illuminate the structure of the EFT.

4.4.2 One-loop Matching

When calculating loops in the UV theory, rather than the EFT, our EFT regulator (dynamical dim reg) is not effective.⁵ Loop calculations in the UV are not scaleless and therefore we will need to regulate them differently than the EFT approach. This difference will be absorbed into the matching calculating. In Sec. 4.B, we match using a hard cutoff in both theories for an example with consistent regulators in both and find identical results, up to scheme dependent coefficients. To avoid the usual challenges of working with a hard cutoff, we will use dimensional regularization in the UV theory via

$$\langle \phi(\vec{k}, \tau) \phi(-\vec{k}, \tau') \rangle = \frac{\pi}{4} H^{d-1} (-\tau)^{\frac{d}{2}} (-\tau')^{\frac{d}{2}} H_\nu(-k\tau) H_\nu^*(-k\tau'), \quad (4.79)$$

where $\nu = \sqrt{d^2/4 - m^2/H^2}$. To simplify calculations, we can fix $\nu = 3/2$ for any dimension, and then can regulate integrals that appear via an analytic continuation in d . We note that while this will regulate the one-loop divergences that appear in this section, dim reg alone is not sufficient in general, as we will see below.

We will begin with the one-loop power spectrum of the growing mode, illustrated in the left side of Fig. 4.2. In the UV theory, a standard in-in calculations gives us

$$\langle \phi(\vec{k}) \phi(\vec{k}') \rangle'_{(1)} = \frac{\lambda}{4k^3} \frac{H^2}{3} \left(\frac{1}{\epsilon} + \log \frac{2k}{[aH]} + \gamma_E - 2 \right) \left[[aH]^{-\epsilon} \int \frac{d^d p}{(2\pi)^d} \frac{1}{2p^3} \right]. \quad (4.80)$$

Regulating the IR by substituting $p^2 \rightarrow p^2 + K^2$ in the denominator, we get

$$\langle \phi(\vec{k}) \phi(\vec{k}') \rangle'_{(1)} = \frac{\lambda}{8\pi^2 k^3} \frac{H^2}{3} \left(\frac{1}{\epsilon} + \log \frac{2k}{[aH]} + \gamma_E - 2 \right) \left[\frac{1}{\epsilon} - \log \frac{K}{[aH]} + \frac{1}{2} (\log 4\pi - \gamma_E) \right]. \quad (4.81)$$

⁵In a forthcoming paper [106], it will be shown that when these integrals are transformed to Mellin space, then it is indeed possible to implement dynamical dim reg in the full theory.

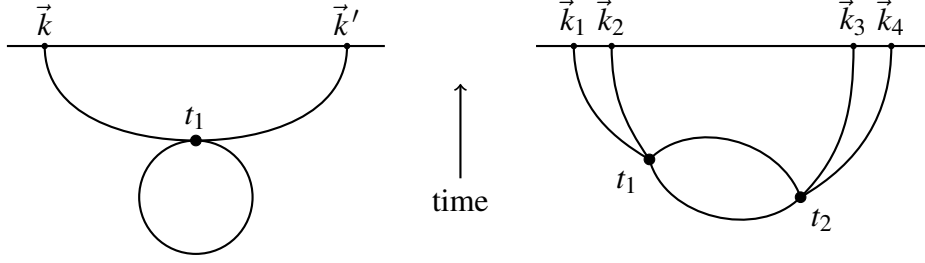


Figure 4.2. Diagrams for the one-loop matching, as computed in the UV theory. The horizontal line indicates a surface on constant conformal time τ_0 on which our in-in correlators are evaluated. *Left:* One-loop power spectrum. *Right:* One-loop trispectrum.

This is the complete one-loop power spectrum of the UV theory.

In SdSET, the one-loop power spectrum is given by several terms

$$\begin{aligned} \langle \underline{\varphi}(\vec{k}) \underline{\varphi}(\vec{k}') \rangle'_{(1)} &= H^2 [aH]^{-2\alpha} \langle \varphi_+(\vec{k}) \varphi_+(\vec{k}') \rangle'_{(1)} + H^2 [aH]^{-2\alpha} \langle \varphi_+(\vec{k}) \varphi_+(\vec{k}') \rangle'_{\delta\alpha^{(1)}} \\ &\quad + 2 \frac{c_{4,0}}{9} \frac{1}{3!} H^2 [aH]^{-4\alpha} \langle \varphi_+(\vec{k}) \varphi_+^3(\vec{k}') \rangle'_{(0)} + \langle \underline{\varphi}(\vec{k}) \underline{\varphi}(\vec{k}') \rangle'_{\text{IC}^{(1)}}, \end{aligned} \quad (4.82)$$

where $c_{4,0} \sim \lambda$, and $\underline{\varphi}$ is given in Eq. (4.70). The subscript (n) labels the order in λ in which correlator is calculated and $\delta\alpha^{(m)}$ is the contribution to the correlator from a shift in the value of α at order λ^m . The first term is the one-loop power spectrum in the EFT,

$$\begin{aligned} [aH]^{-2\alpha} \langle \varphi_+(\vec{k}) \varphi_+(\vec{k}') \rangle'_{(1)} &= -[aH]^{-4\alpha} \frac{1}{2\nu} \left(-\frac{1}{2\alpha} \right) \frac{\lambda}{4k^{3-2\alpha}} \int \frac{d^3p}{(2\pi)^3} \frac{1}{p^{3-2\alpha}} \\ &\rightarrow -\frac{1}{6\pi^2} \frac{\lambda}{4k^3} \left(-\frac{1}{2\alpha} - \log \frac{k}{[aH]} \right) \left(-\frac{1}{2\alpha} - \log \frac{K}{[aH]} \right). \end{aligned} \quad (4.83)$$

We must also allow for the possibility that, due to matching, we will need to correct the value of α from its free-field value. Substituting $\alpha \rightarrow \alpha + \delta\alpha^{(1)}$ in Eq. (4.41a) and expanding to linear

order, we have

$$H^2 [aH]^{-2\alpha} \left\langle \varphi_+(\vec{k}) \varphi_+(\vec{k}') \right\rangle'_{\delta\alpha^{(1)}} = \left\langle \underline{\varphi}(\vec{k}) \underline{\varphi}(\vec{k}') \right\rangle_{(0)} \left(1 + 2\delta\alpha^{(1)} \log \frac{k}{[aH]} \right), \quad (4.84)$$

where we have absorbed the $[aH]^{-2\delta\alpha}$ into the definition of this term to derive the dimensionless argument of the log. From the EFT point of view, $\delta\alpha^{(1)}$ is an unknown constant of order λ to be fixed by matching. Finally, we have the contribution to the $\underline{\varphi}$ power spectrum from the field redefinition:

$$2 \frac{c_{4,0}}{9} \frac{1}{3!} H^2 [aH]^{-4\alpha} \left\langle \varphi_+(\vec{k}) \varphi_+^3(\vec{k}') \right\rangle'_{(0)} \rightarrow \frac{c_{4,0}}{9} \frac{1}{2k^3} \frac{1}{2\pi^2} \left(-\frac{1}{2\alpha} - \log \frac{K}{[aH]} + \log 2 \right). \quad (4.85)$$

We emphasize that since the coefficient of φ_+^3 in the definition of $\underline{\varphi}$ is fixed by matching the superhorizon six-point function, there is no additional freedom within this term that can be used to match the 1-loop power spectrum.

The final term $\delta \left\langle \underline{\varphi}(\vec{k}) \underline{\varphi}(\vec{k}') \right\rangle'_{\text{IC}}$ is time independent and is determined by matching the time-independent part of the UV calculation. Combining these results and using $c_{4,0} \rightarrow \lambda$, we find

$$\begin{aligned} H^2 \left\langle \underline{\varphi}(\vec{k}) \underline{\varphi}(\vec{k}') \right\rangle'_{(1)} &= \frac{H^2}{6\pi^2} \frac{\lambda}{4k^3} \left(\frac{1}{-2\alpha} + \log \frac{[aH]}{k} + \frac{2}{3} \right) \left(\frac{1}{-2\alpha} + \log \frac{[aH]}{K} \right) \\ &\quad + \delta\alpha^{(1)} \frac{H^2}{k^3} \log \frac{k}{a} + \frac{\lambda}{9} \frac{1}{2k^3} \frac{1}{2\pi^2} \log 2 + \left\langle \underline{\varphi}(\vec{k}) \underline{\varphi}(\vec{k}') \right\rangle'_{\text{IC}(1)}. \end{aligned} \quad (4.86)$$

Comparing this result to Eq. (4.81), we see that the time-dependence of the UV and EFT agree after matching the single log coefficient with

$$\delta\alpha^{(1)} = \frac{\lambda}{8\pi^2} \frac{1}{3} \left(\gamma_E - \frac{7}{3} + \log 2 - \frac{1}{2} (\log 4\pi - \gamma_E) \right). \quad (4.87)$$

This is a non-trivial result as we only have a single free parameter to match the full time-

dependence on the UV result. All the time-independent contributions can be matched by adjusting the initial conditions, $\text{IC}^{(1)}$, which in this case is just a renormalization of the amplitude of the two point function, namely a shift in C_α .

One-loop Trispectrum

Now we move on to the one-loop trispectrum, as illustrated in the right side of Fig. 4.2. For our purposes here, it suffices to simply match the UV divergent terms which result in time dependent $\log[aH]$ factors.⁶ This will result in a correction to the $c_{3,1}$ Wilson coefficient in the EFT. While the initial conditions also receive corrections from matching the trispectrum, these would contribute to Stochastic Inflation beyond NNLO, and so we will not compute them here.

For convenience, we break the UV calculation into two terms

$$\mathcal{I}_4 = \left\langle \phi^{(2)}(\vec{k}_1) \phi^{(1)}(\vec{k}_2) \phi^{(2)}(\vec{k}_3) \phi^{(1)}(\vec{k}_4) \right\rangle + \text{permutations} \quad (4.88a)$$

$$\mathcal{K}_4 = \left\langle \phi^{(3)}(\vec{k}_1) \phi^{(1)}(\vec{k}_2) \phi^{(1)}(\vec{k}_3) \phi^{(1)}(\vec{k}_4) \right\rangle + \text{permutations}, \quad (4.88b)$$

where

$$\phi^{(2)}(\vec{k}, t) = i \int^t dt_1 \left[H_{\text{int}}(t_1), \phi(\vec{k}, t) \right] \quad (4.89a)$$

$$\phi^{(3)}(\vec{k}, t) = - \left[\int^{t_1} dt_2 H_{\text{int}}(t_2), \left[\int^t dt_1 H_{\text{int}}(t_1), \phi(\vec{k}, t) \right] \right], \quad (4.89b)$$

where H_{int} is given in Eq. (4.28). In what follows, we will show that \mathcal{I}_4 is UV finite, while \mathcal{K}_4 is UV divergent. Then we will match this divergent contribution between the UV theory and the EFT to derive the one-loop correction to $c_{3,1}$.

⁶We remind the reader that the ‘‘UV divergences’’ that we are isolating here take their origins from the IR divergences of the full theory that are resummed by Stochastic Inflation. The expansions being done to simplify the integrals that appear on the UV theory side of this matching calculation amount to decomposing the correlator via the method of regions [107, 108].

We begin by evaluating \mathcal{S}_4 . Expanding in the limit $p \gg k_i$, we have

$$\begin{aligned} \mathcal{S}_4 &= \frac{1}{k_2^3 k_4^3} \int_{-\tau}^{\tau} \frac{d\tau_1}{(-\tau_1)^4} \int \frac{d^3 p}{(2\pi)^3} G(\vec{k}_1, \tau, \tau_1) \frac{(1 - ip\tau_1)^2}{p^3} e^{i2p\tau_1} \\ &\quad \times \int_{-\tau}^{\tau} \frac{d\tau_2}{(-\tau_2)^4} \int \frac{d^3 p}{(2\pi)^3} G(\vec{k}_3, \tau, \tau_2) \frac{(1 + ip\tau_2)^2}{p^3} e^{-i2p\tau_2} \\ &\quad + \text{permutations}. \end{aligned} \tag{4.90}$$

The integrals over τ_1 and τ_2 are independent and we can evaluate them as usual. Expanding in $k_i \tau_i \ll 1$, we have

$$\begin{aligned} \int_{-\tau}^{\tau} \frac{d\tau_1}{(-\tau_1)^4} G(\vec{k}_1, \tau, \tau_1) (1 - ip\tau_1)^2 e^{i2p\tau_1} &\rightarrow -\frac{1}{3} \int_{-\tau}^{\tau} \frac{d\tau_1}{(-\tau_1)^4} (\tau^3 - \tau_1^3) (1 - ip\tau_1)^2 e^{i2p\tau_1} \\ &= \frac{(-i)}{3} \left(\log p\tau - \frac{11}{12} \right). \end{aligned} \tag{4.91}$$

Putting this together yields

$$\mathcal{S}_4 \simeq \frac{1}{k_2^3 k_4^3} \int \frac{d^3 p}{(2\pi)^3} \frac{1}{p^6} \left(\log p\tau - \frac{11}{12} \right)^2. \tag{4.92}$$

This integral will not lead to any UV divergences. Furthermore, this result is exact in $p\tau$ since we have only expanded in k/p . Therefore all the subleading terms will be more UV convergent, and correspond to higher power corrections in the EFT. This shows that all we need to include when matching $c_{3,1}$ is the correction due to \mathcal{H}_4 .

The second term, \mathcal{H}_4 , gives rise to more interesting UV behavior. Again expanding for

large loop momentum $p \gg k_i$, we have

$$\begin{aligned} \mathcal{K}_4 \simeq & \frac{H^4}{32(k_2 k_3 k_4)^3} \int \frac{d^d p}{(2\pi)^d} \int^\tau \frac{d\tau_1}{(-\tau_1)^{d+1}} G(\vec{k}_1, \tau, \tau_1) \\ & \times 2\text{Im} \int^{\tau_1} \frac{d\tau_2}{(-\tau_2)^4} \frac{1}{p^6} (1 + ip\tau_1)^2 (1 - ip\tau_2)^2 e^{-i2p(\tau_1 - \tau_2)} \\ & + \text{permutations}. \end{aligned} \quad (4.93)$$

We have expressed the commutator acting on the loop momenta in $\phi^{(3)}$ in terms of the imaginary part to simplify the calculation. In this form, the time integrals can be evaluated exactly, giving

$$\begin{aligned} \mathcal{K}_4 \simeq & \frac{H^4 \lambda^2}{16(k_2 k_3 k_4)^3} \int \frac{d^d p}{(2\pi)^d} \frac{1}{p^3} \left[\frac{10}{81} - \frac{1}{27} \gamma_E (2 + 3\gamma_E) - \frac{5}{36} \pi^2 \right. \\ & \left. + \frac{1}{9} \left(\log \frac{2p}{[aH]} \right)^2 + (1 + 3\gamma_E) \log \frac{2p}{[aH]} + \frac{4}{9} \log \frac{k}{[aH]} \right] + \text{permutations} \\ = & \frac{H^4 \lambda^2}{8(k_2 k_3 k_4)^3} \frac{1}{4\pi^2} \left(\frac{2}{\varepsilon} + \log \frac{k}{[aH]} + \log \frac{K^2}{4\pi} - \gamma_E \right) \\ & \times \left[\frac{10}{81} - \frac{1}{27} \gamma_E (2 + 3\gamma_E + 6 \log 2) - \frac{5}{36} \pi^2 + \frac{2 \log 2 + 3 \log^2 2}{27} \right] \\ & + O\left((\log[aH])^2\right) + \text{permutations}. \end{aligned} \quad (4.94)$$

In the last line, we are only writing the terms that are linear in $\log[aH]$ since this is what determines the contribution to the RG.

We can see the appearance of higher powers of log from the perturbative EFT contribution

to the one-loop trispectrum

$$\begin{aligned}
\langle \varphi_+(\vec{k}_1) \dots \varphi_+(\vec{k}_4) \rangle' &\supset \frac{C_\alpha^6 \sum_i k_i^3}{8(k_1 k_2 k_3 k_4)^{3-2\alpha}} \frac{1}{9} \\
&\times \int^t dt_1 \int^{t_1} dt_2 ([a(t_1)H][a(t_2)H])^{-2\alpha} \int \frac{d^3 p}{(2\pi)^3} \frac{C_\alpha^2}{2p^{3-2\alpha}} \\
&\rightarrow \frac{\sum_i k_i^3}{8(k_1 k_2 k_3 k_4)^{3-2\alpha}} \frac{1}{9} \frac{1}{2} \left(-\frac{1}{2\alpha} + \log[aH] \right)^2 \\
&\times \frac{1}{2\pi^2} \left(-\frac{1}{2\alpha} - \log \frac{K}{[aH]} + \log 2 \right), \tag{4.95}
\end{aligned}$$

where the compensating dimensionful factors that appear inside the $\log[aH]$ term come from expanding the prefactor in the small α limit. One can check that this term matches the coefficient of the \log^3 divergence of the UV calculation.

In order to match the linear log term, we need to keep track of the EFT field redefinition to order λ^2 . Specifically, we need

$$\underline{\varphi} = H \left([aH]^{-\alpha} \varphi_+ + [aH]^{-\beta} \varphi_- + \frac{\lambda}{9} \frac{1}{3!} [aH]^{-3\alpha} \varphi_+^3 + \frac{\lambda^2}{81} \frac{1}{3!} [aH]^{-5\alpha} \varphi_+^5 \right). \tag{4.96}$$

to remove the φ_+^6 operator from the EFT potential. This $O(\lambda^2)$ term contributes to the trispectrum at one loop:

$$\langle \underline{\varphi}(\vec{k}_1) \underline{\varphi}(\vec{k}_2) \underline{\varphi}(\vec{k}_3) \underline{\varphi}(\vec{k}_4) \rangle' \supset \frac{\sum_i k_i^3}{(k_1 k_2 k_3 k_4)^3} \frac{\lambda^2}{81} \frac{5!}{3!2} \int \frac{d^3 p}{(2\pi)^3} \frac{1}{p^{3-2\alpha}}, \tag{4.97}$$

which matches the leading UV term in Eq. (4.94), namely the log term proportional to a factor of $10/81$. After matching this term, we see a fairly complicated expression remains for the linear log. This can be absorbed into the $c_{3,1}$ Wilson coefficient in the potential using Eq. (4.46), such that

$$c_{3,1} \rightarrow \lambda - \frac{\lambda^2}{2\pi^2} \left(\frac{1}{9} \gamma_E (2 + 3\gamma_E + 6\log 2) + \frac{5}{12} \pi^2 - \frac{2\log 2 + 3\log^2 2}{9} \right). \tag{4.98}$$

This is the one-loop matching correction to an EFT Wilson coefficient, in analogy with Eq. (4.87) above. A priori, one might think that we have to consider the divergence from the mixing of the operators φ_+ and φ_+^3 . In later sections, we will see that such a mixing is equivalent to a shift in the potential of the form in Eq. (4.98), and therefore these two interpretations of the logarithmic growth are related to each other by a field redefinition.

4.4.3 Initial Conditions for Composite Operators

The above matching procedure is sufficient to regulate the correlation function of ϕ and match φ_+ correlators at separated points. Composite operators are defined when some of these operators are at coincident points. In Fourier space, this involves a convolution integral which can produce divergences that require renormalizing the composite operator itself.

Composite operators can be defined in this way purely within the EFT. Since we are regulating loops in the EFT with dynamical dim reg, this implies that we will need to know initial conditions for general α . Fortunately, we will be interested in limits where the momenta are hierarchical (UV divergences of the momentum integrals), which simplifies the matching considerably.

We will start by taking the tree-level initial conditions for the trispectrum, and tying two of the legs together to form a $\varphi_+^2[\vec{x} = 0]$ composite operator:

$$\left\langle \varphi_+^2[0] \varphi_+(\vec{k}_1) \varphi_+(\vec{k}_2) \right\rangle'_{\text{IC}} = \int \frac{d^3 p}{(2\pi)^3} \left\langle \varphi_+(\vec{p}) \varphi_+(-\vec{p} - \vec{k}_1 - \vec{k}_2) \varphi_+(\vec{k}_1) \varphi_+(\vec{k}_2) \right\rangle'_{\text{IC}}, \quad (4.99)$$

where we are interested in determining the integrand of the right hand side in the limit $p \gg k_i$. For $\alpha = 0$, we determined the initial conditions exactly in Eq. (4.76). In order to regulate the UV divergence that comes from tying the two legs together, we want to evaluate this for general α , while isolating the term of interest, which is proportional to $P_+(k_1)P_+(k_2)$, where P_+ is defined by

$$\left\langle \varphi_+(\vec{k}) \varphi_+(\vec{k}') \right\rangle = P_+(k)(2\pi)^3 \delta(\vec{k} + \vec{k}'), \quad (4.100)$$

so that $(P_+(k))_{\text{tree}} = (2k^3)^{-1}$. Since $k \ll p$, the initial conditions will arise at the horizon crossing of the modes carrying momentum p when the k_i -modes are superhorizon. As discussed in Sec. 4.4.2, we therefore match using massive mode functions for only the k_i fields, where we can also Taylor expand in $k\tau \ll 1$. As a result, the initial conditions are given by

$$\begin{aligned} \left\langle \varphi_+(\vec{p}) \varphi_+(-\vec{p} - \vec{k}_1 - \vec{k}_2) \varphi_+(\vec{k}_1) \varphi_+(\vec{k}_2) \right\rangle'_{\text{IC}^{(1)}} &\simeq \lambda P_+(k_1) P_+(k_2) \\ &\times \lim_{\tau_0 \rightarrow 0} 2\text{Im} \int^{\tau_0} \frac{d\tau}{(-H\tau)^4} [aH]^{-2\alpha} \frac{1}{4p^2} (1 - ip\tau)^2 (1 + ip\tau_0)^2 e^{i2p(\tau - \tau_0)}, \end{aligned} \quad (4.101)$$

where $[aH]^{-2\alpha} = (-\tau)^{2\alpha}$. The RHS of this expression is the calculation in the UV theory with the appropriate choice of masses for the mode functions. We are implicitly evaluating the correlation function at a time τ_0 and extracting the τ_0 -independent piece in the $\tau_0 \rightarrow 0$ limit. Evaluating the integral, we find

$$\begin{aligned} \left\langle \varphi_+(\vec{p}) \varphi_+(\vec{p} - \vec{k}_1 - \vec{k}_2) \varphi_+(\vec{k}_1) \varphi_+(\vec{k}_2) \right\rangle'_{\text{IC}^{(1)}} &\simeq \\ &\lambda P_+(k_1) P_+(k_2) \frac{(1 + 2\alpha)\Gamma[-1 + 2\alpha] \sin\left(\frac{\pi}{2}(1 - 2\alpha)\right)}{2^{2\alpha} p^{3+2\alpha}}. \end{aligned} \quad (4.102)$$

Corrections to this result are suppressed by powers of k_i/p which will not contribute to the one-loop divergences that we will use to determine the RG for composite operator mixing below in Sec. 4.5.1.

For two-loop divergences, one must determine the initial conditions (see Sec. 4.5.2 below):

$$\begin{aligned} \left\langle \varphi_+^3[0] \varphi_+(\vec{k}) \right\rangle'_{\text{IC}^{(1)}} &= \\ &\int \frac{d^3 p_1}{(2\pi)^3} \int \frac{d^3 p_2}{(2\pi)^3} \left\langle \varphi_{+\alpha_1}(\vec{p}_1) \varphi_{+\alpha_2}(\vec{p}_2) \varphi_{+\alpha_3}(-\vec{k} - \vec{p}_1 - \vec{p}_2) \varphi_+(\vec{k}) \right\rangle'_{\text{IC}^{(1)}}, \end{aligned} \quad (4.103)$$

where we will take the limit $p_i \gg k$, such that $-\vec{k} - \vec{p}_1 - \vec{p}_2 \simeq -\vec{p}_1 - \vec{p}_2$. We calculate this contribution for general α_i by matching to the full theory:

$$\begin{aligned} \left\langle \phi_{\alpha_1}(\vec{p}_1) \phi_{\alpha_2}(\vec{p}_2) \phi_{\alpha_3}(\vec{p}_3) \phi(\vec{k}) \right\rangle'_{(1)} &= 2\text{Im} \left[u_{\nu_1}^*(\vec{p}_1, \tau) u_{\nu_2}^*(\vec{p}_2, \tau) u_{\nu_3}^*(\vec{p}_3, \tau) u_{3/2}^*(\vec{k}, \tau) \right. \\ &\quad \left. \times \int^\tau \frac{d\tau_1}{(-\tau_1)^4} u_{\nu_1}(\vec{p}_1, \tau_1) u_{\nu_2}(\vec{p}_2, \tau_1) u_{\nu_3}(\vec{p}_3, \tau_1) u_{3/2}(\vec{k}, \tau_1) \right], \end{aligned} \quad (4.104)$$

where

$$u_\nu(\vec{k}, \tau) = -i e^{i(\nu + \frac{1}{2})\frac{\pi}{2}} \frac{\sqrt{\pi}}{2} H(-\tau)^{3/2} \mathbf{H}_\nu^{(1)}(-k\tau), \quad (4.105)$$

is the positive frequency mode for a field with $\alpha = \frac{3}{2} - \nu$. Again, since the mode functions at horizon crossing behave as if they are effectively massless, this contribution can be determined using massless mode function of $p\tau_1$, but we must use the massive mode functions for $p\tau$. The result of integrating over τ_1 is

$$\left\langle \varphi_+(\vec{p}_1) \varphi_+(\vec{p}_2) \varphi_+(\vec{p}_3) \varphi_+(\vec{k}) \right\rangle'_{\text{IC}(1)} = \lambda \frac{\prod_{i=1}^3 C_{\alpha_i} p_i^{\alpha_i}}{12(p_1 p_2 p_3)^3} \left(\sum_i \kappa_i p_i^3 - p_1 p_2 p_3 + \sum_{i \neq j} p_i^2 p_j \right), \quad (4.106)$$

where the correlators were matched at time τ ,

$$\kappa_i = \frac{1}{3} \left(-\frac{1}{2\alpha} + \gamma_E - 2 + \log \frac{p_t}{p_i} \right), \quad (4.107)$$

and $p_t = p_1 + p_2 + p_3$.

Finally, we must also determine the tree-level six-point initial conditions, illustrated in Fig. 4.3. We are specifically interested in the correlator

$$\left\langle \varphi_+(\vec{p}) \varphi_+(-\vec{p} - \vec{k}_t) \varphi_+(\vec{k}_1) \dots \varphi_+(\vec{k}_4) \right\rangle, \quad (4.108)$$

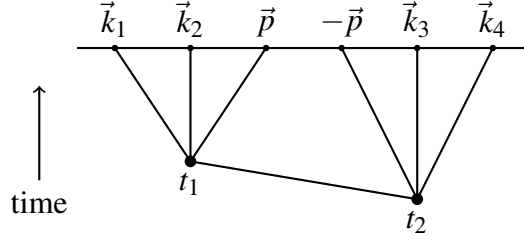


Figure 4.3. Tree level pentaspectrum

in the limit $p \gg k_i$, where $\vec{k}_t \equiv \sum_{i=1}^4 \vec{k}_i$. As in the case of the trispectrum, we will isolate the term

$$\left\langle \varphi_+(\vec{p}) \varphi_+(-\vec{p} - \vec{k}_t) \varphi_+(\vec{k}_1) \dots \varphi_+(\vec{k}_4) \right\rangle_{\text{IC}(2)} \supset \lambda^2 \Gamma_{2,4}(p) P_+(k_1) \dots P_+(k_4), \quad (4.109)$$

such that

$$\begin{aligned} \Gamma_{2,4}(p) = & \int^{\tau} \frac{d\tau_1}{(-\tau_1)^{4-2\alpha}} \int^{\tau} \frac{d\tau_2}{(-\tau_2)^{4-2\alpha}} \left\langle \phi^2(p, \tau_1) \phi^2(p, \tau) \phi^2(p, \tau_2) \right\rangle \\ & - 2\text{Re} \int^{\tau} \frac{d\tau_1}{(-\tau_1)^{4-2\alpha}} \int^{\tau_1} \frac{d\tau_2}{(-\tau_2)^{4-2\alpha}} \left\langle \phi^2(p, \tau) \phi^2(p, \tau_1) \phi^2(p, \tau_2) \right\rangle. \end{aligned} \quad (4.110)$$

By direct calculation we find that

$$\begin{aligned} \Gamma_{2,4}(p) = & \frac{1}{216p^{3+4\alpha}} \left[16 + 4\gamma_E(-11 + 3\gamma_E) + 3\pi^2 + 4(-11 + 6\gamma_E + 3\log 2)\log 2 \right. \\ & \left. + O\left(\log \frac{p}{[aH]}\right) \right]. \end{aligned} \quad (4.111)$$

4.5 Composite Operator Mixing

From our above discussion, we argued that corrections to Stochastic Inflation are uniquely determined by the correlation functions of composite operators; computing those that are relevant to correcting Stochastic Inflation up to NNLO is the topic of this section. We will start by setting up the problem of calculating composite operator renormalization. We are interested in operators

of the form $\varphi_+^n(\vec{x})$. These are well-defined purely within the EFT, so we must be able to discuss their correlation functions and renormalizations given only the EFT data. Of course, the crucial information is the initial conditions, which therefore depend on first matching to the UV.

In general, given the EFT field operator $\varphi_+(\vec{x}, \tau)$, we can always define a composite operator

$$\varphi_+^n(\vec{x}) = \prod_{i=1}^n \int \frac{d^3 p_i}{(2\pi)^3} e^{-i\vec{p}_i \cdot \vec{x}} \varphi_+(\vec{p}_i). \quad (4.112)$$

In a free theory, we find the structure:

$$\begin{aligned} \langle \varphi_+^n(\vec{x}) \varphi_+(\vec{k}_1) \dots \varphi_+(\vec{k}_n) \rangle &= n! \prod_{i=1}^n \int \frac{d^3 p_i}{(2\pi)^3} e^{-i\vec{p}_i \cdot \vec{x}} (2\pi)^3 \delta(\vec{k}_i + \vec{p}_i) P_+(k_i) \\ &= n! e^{i\sum \vec{k}_i \cdot \vec{x}} P_+(k_1) \dots P_+(k_n), \end{aligned} \quad (4.113)$$

where P_+ is defined in Eq. (4.100). Taking the Fourier transform,

$$\varphi_+^n(\vec{k}) = \int d^3 x e^{i\vec{k} \cdot \vec{x}} \varphi_+^n(\vec{x}), \quad (4.114)$$

we have

$$\langle \varphi_+^n(\vec{k}) \varphi_+(\vec{k}_1) \dots \varphi_+(\vec{k}_n) \rangle = n! P_+(k_1) \dots P_+(k_n) \delta\left(\vec{k} + \sum \vec{k}_i\right). \quad (4.115)$$

For simplicity, it will often be easiest to use $\varphi_+^n(\vec{x} = 0) \equiv \varphi_+^n[0]$ to avoid the extra δ -function.

Given this definition, we see that we should be able to define all such correlators of composite operators as simply integrals over the correlators of φ_+ . For example,

$$\langle \varphi_+^n[\vec{x} = 0] \varphi_+(\vec{k}_1) \dots \varphi_+(\vec{k}_m) \rangle = \prod_{i=1}^n \int \frac{d^3 p_i}{(2\pi)^3} \langle \varphi_+(\vec{p}_1) \dots \varphi_+(\vec{p}_n) \varphi_+(\vec{k}_1) \dots \varphi_+(\vec{k}_m) \rangle. \quad (4.116)$$

A very important feature of this formula is that the integrand on the RHS is free of divergences, in the sense that we should have already regulated and renormalized the expression. As a result, all of the renormalization of the composite operator itself (and hence the matrix of anomalous

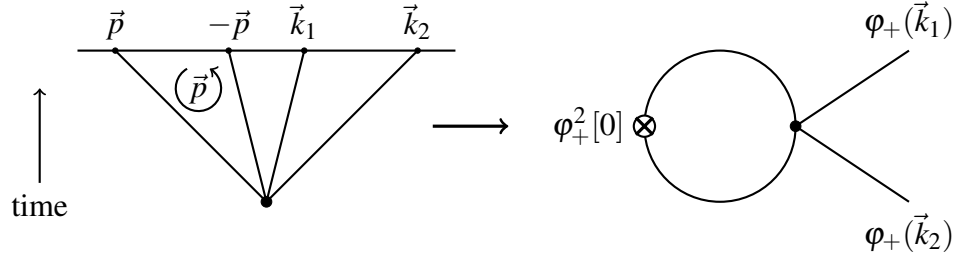


Figure 4.4. One loop correction to φ_+^2 that looks like an anomalous dimension ($\varphi_+^2 \rightarrow \varphi_+^2$). We start from the tree level trispectrum and integrate over two of the fields to form the composite operator φ_+^2 . *Left:* The Witten diagram with a boundary at future infinity. *Right:* The Feynman diagram with the same momentum flow.

dimensions) has to be associated with integrals over \vec{p}_i as opposed to the loop integrals that appear in the calculation of $\langle \varphi_+(\vec{p}_1) \dots \varphi_+(\vec{p}_n) \varphi_+(\vec{k}_1) \dots \varphi_+(\vec{k}_m) \rangle$ itself.

4.5.1 One-loop Corrections

Trispectrum

We will start by computing b_1 , which is determined from the four-point function via

$$\langle \varphi_+^2[0] \varphi_+(\vec{k}_1) \varphi_+(\vec{k}_2) \rangle = \int \frac{d^3 p}{(2\pi)^3} \langle \varphi_+(\vec{p}) \varphi_+(-\vec{p} - \vec{k}_1 - \vec{k}_2) \varphi_+(\vec{k}_1) \varphi_+(\vec{k}_2) \rangle'. \quad (4.117)$$

The relationship between this loop contribution and the tree-level trispectrum is illustrated in Fig. 4.4. The contribution to the four-point function from the time evolution already yields a $\log[aH]$. Therefore, any anomalous scaling (which should also only be a single log) must arise from the initial conditions. The relevant contribution was calculated in Eq. (4.102).

Performing the integration over p using dynamical dim reg, we find

$$\begin{aligned} \langle \varphi_+^2[0] \varphi_+(\vec{k}_1) \varphi_+(\vec{k}_2) \rangle &= \lambda P_+(k_1) P_+(k_2) \\ &\times \frac{(1+2\alpha)\Gamma[-1+2\alpha] \sin\left(\frac{\pi}{2}(1-2\alpha)\right) K^{-2\alpha} \pi^{3/2} \Gamma[\alpha]}{2^{2\alpha} \Gamma\left[\frac{3}{2} + \alpha\right]}. \end{aligned} \quad (4.118)$$

Expanding for $\alpha \rightarrow 0$ we have

$$\begin{aligned} \langle \varphi_+^2[0] \varphi_+(\vec{k}_1) \varphi_+(\vec{k}_2) \rangle &= \lambda P_+(k_1) P_+(k_2) \left(\frac{1}{48\pi^2 \alpha^2} + \frac{(4 - 3\gamma_E - 3 \log K)}{72\pi^2 \alpha} + \text{finite} \right) \\ &\rightarrow \frac{\lambda}{36\pi^2} P_+(k_1) P_+(k_2) (4 - 3\gamma_E) \left(\frac{1}{2\alpha} - \log \frac{[aH]}{k_i} \right) + \dots \quad (4.119) \end{aligned}$$

We can repeat this calculation with $\varphi_+^n[0]$ to determine the one-loop anomalous dimension for all n . Keeping track of combinatorics, one finds

$$\begin{aligned} \langle \varphi_+^n[0] \varphi_+(\vec{k}_1) \dots \varphi_+(\vec{k}_n) \rangle &\supset \frac{\lambda}{36\pi^2} \binom{n}{2} n! P_+(k_1) \dots P_+(k_n) \\ &\times \sum_i (4 - 3\gamma_E) \left(\frac{1}{2\alpha} - \log \frac{[aH]}{k_i} + \mathcal{O}\left(\frac{1}{\alpha^2}\right) + \text{finite} \right). \quad (4.120) \end{aligned}$$

This NLO $\log[aH]$ dependence can be resummed by including the following correction in the dynamical RG:

$$b_1 = -\frac{\lambda}{36\pi^2} (4 - 3\gamma_E). \quad (4.121)$$

Six-point

Our next task is to compute b_2 , which we determine by evaluating the six point function,

$$\langle \varphi_+^2[0] \varphi_+(\vec{k}_1) \dots \varphi_+(\vec{k}_4) \rangle = \int \frac{d^3 p}{(2\pi)^3} \langle \varphi_+(\vec{p}) \varphi_+\left(-\vec{p} - \sum_{i=1}^4 \vec{k}_i\right) \varphi_+(\vec{k}_1) \dots \varphi_+(\vec{k}_4) \rangle', \quad (4.122)$$

with $p \gg k_i$. The relationship between this one-loop contribution and the tree-level six-point function is illustrated in Fig. 4.5. As before, only the initial conditions arising from

$$\langle \varphi_+(\vec{p}) \varphi_+(-\vec{p} - \vec{k}_i) \varphi_+(\vec{k}_1) \dots \varphi_+(\vec{k}_4) \rangle' \supset \lambda^2 \Gamma_{2,4}(p) P_+(k_1) \dots P_+(k_4), \quad (4.123)$$

will contribute to the operator mixing, where $\Gamma_{2,4}(p)$ was calculated in Eq. (4.111). Performing the momentum integration using dynamical dim reg, we find

$$\lambda^2 \int \frac{d^3 p}{(2\pi)^3} \Gamma_{2,4}(p) = \left(\frac{1}{8\pi^2 \alpha} - \frac{1}{2\pi^2} + \dots \right) \left[b_{2,4} + \mathcal{O}\left(\frac{1}{\alpha}\right) \right] + \text{finite}, \quad (4.124)$$

where

$$b_{2,4} = \frac{\lambda^2}{216} \left[16 + 4\gamma_E(3\gamma_E - 11) + 3\pi^2 + 4\log 2(6\gamma_E + 3\log 2 - 11) \right]. \quad (4.125)$$

Now we restore the factor $(k_1 k_2 k_3 k_4)^\alpha [aH]^{-4\alpha}$ associated with $P(k_i)$ for general α and take the limit $\alpha \rightarrow 0$ to get

$$\left\langle \varphi_+^2[0] \varphi_+(\vec{k}_1) \dots \varphi_+(\vec{k}_4) \right\rangle \supset b_{2,4} P_+(k_1) \dots P_+(k_4) \left[\frac{1}{8\pi^2 \alpha} + \frac{1}{2\pi^2} \sum_{i=1}^4 \frac{1}{4} \log \frac{k_i}{[aH]} \right]. \quad (4.126)$$

Repeating this calculation for φ_+^n we have

$$\begin{aligned} \left\langle \varphi_+^n[0] \varphi_+(\vec{k}_1) \dots \varphi_+(\vec{k}_{n+2}) \right\rangle &\supset b_{2,4} \binom{n}{2} (n+2)! P_+(k_1) \dots P_+(k_{n+2}) \\ &\times \left[\frac{1}{8\pi^2 \alpha} + \frac{1}{2\pi^2} \sum_{i=1}^4 \frac{1}{4} \log \frac{k_i}{[aH]} \right]. \end{aligned} \quad (4.127)$$

This NLO $\log[aH]$ dependence can be resummed by including the following correction in the dynamical RG:

$$b_2 = \frac{1}{2\pi^2} \frac{\lambda^2}{216} \left[16 + 4\gamma_E(3\gamma_E - 11) + 3\pi^2 + 4\log 2(6\gamma_E + 3\log 2 - 11) \right]. \quad (4.128)$$

4.5.2 Two-loop Corrections

Next, we move to the calculation of the two-loop anomalous dimension that generates the NNLO non-Gaussian noise term for Stochastic Inflation. This represents a novel contribution

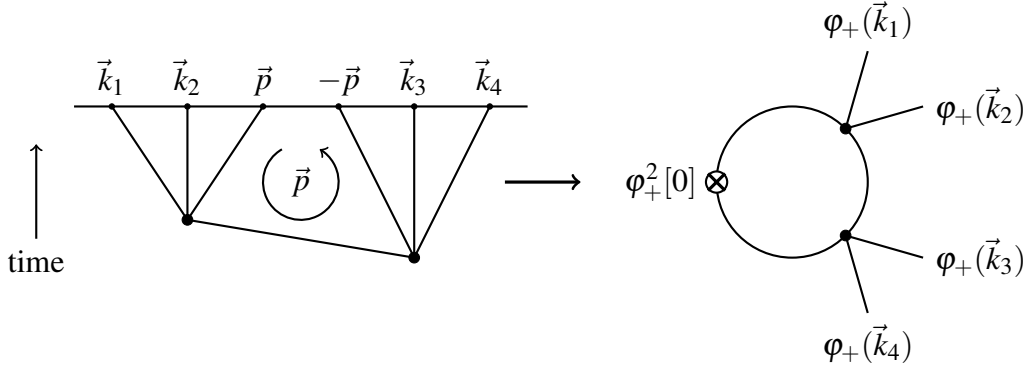


Figure 4.5. Diagram of contribution one loop contribution to $\Gamma_{2,4} (\varphi_+^2 \rightarrow \varphi_+^4)$. We start from the tree level pentaspectrum (6 points function) and integrate over two of the fields to form the composite operator φ_+^2 . *Left:* The Witten diagram with a boundary at future infinity. *Right:* The Feynman diagram with the same momentum flow.

which is calculated here for the first time. In particular, our goal is to calculate:

$$\langle \varphi_+^3[0] \varphi_+(\vec{k}) \rangle = \int \frac{d^3 p_1 d^3 p_2 d^3 p_3}{(2\pi)^9} \langle \varphi_+(\vec{p}_1) \varphi_+(\vec{p}_2) \varphi_+(\vec{p}_3) \varphi_+(\vec{k}) \rangle, \quad (4.129)$$

where $p_{1,2,3} \gg k$. The relationship between this two-loop contribution and the tree-level trispectrum is illustrated in Fig. 4.6. The correlation function on the RHS was calculated in Eq. (4.106) for general α_i (for each p_i) such that we can regulate the integral with dynamical dim reg. Making the above substitution

$$\langle \varphi_+^3[0] \varphi_+(\vec{k}) \rangle \supset P_+(k) \int \frac{d^3 p_1 d^3 p_2}{(2\pi)^6} \lambda \frac{\prod_{i=1}^3 C_{\alpha_i} p_i^{\alpha_i}}{12(p_1 p_2 p_3)^3} \left(\kappa \sum_i p_i^3 - p_1 p_2 p_3 + \sum_{i \neq j} p_i^2 p_j \right), \quad (4.130)$$

where κ is fixed by the full calculation for the reasons described above, see Eq. (4.107). We note, that this result will require us to calculate several integrals of the form

$$I_3 = \int \frac{d^3 p_1 d^3 p_2}{(2\pi)^6} \frac{1}{(p_1^2)^a (p_2^2)^b ((\vec{p}_1 + \vec{p}_2)^2)^c}, \quad (4.131)$$

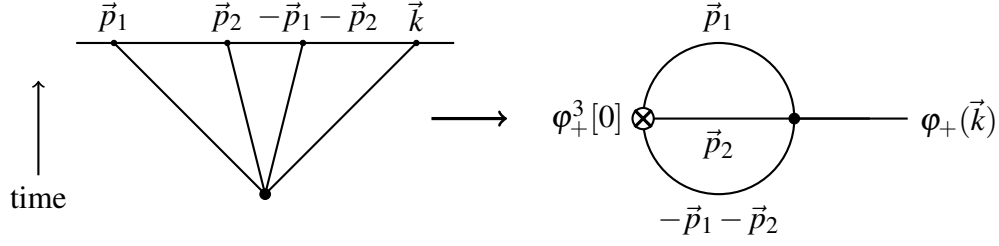


Figure 4.6. Diagram of contribution two loop contribution to the mixing $\varphi_+^3 \rightarrow \varphi_+$. We start from the tree level trispectrum and integrate over *three* of the fields to form the composite operator φ_+^3 . We first drew this as a Witten diagram with a boundary at future infinity. At the bottom we have shown the Feynman diagram with the same momentum flow.

where a, b and c are half integers when $\alpha = 0$. We can evaluate this integral as follows:

$$\begin{aligned}
I_3 &= \frac{\Gamma[b+c]}{\Gamma[b]\Gamma[c]} \int_0^1 dx \int \frac{d^3 p_1}{(2\pi)^3} \frac{1}{p_1^{2a}} \int \frac{d^3 \bar{p}_2}{(2\pi)^3} \frac{x^{b-1}(1-x)^{c-1}}{(\bar{p}_2^2 + x(1-x)p_1^2)^{b+c}} \\
&= \frac{\Gamma[b+c-\frac{3}{2}]}{\Gamma[b]\Gamma[c]} \frac{1}{(4\pi)^{3/2}} \int \frac{d^3 p_1}{(2\pi)^3} \frac{1}{p_1^{2a+2b+2c-3}} \int dx \frac{x^{b-1}(1-x)^{c-1}}{(x(1-x))^{b+c-3/2}} \\
&= \frac{\Gamma[b+c-\frac{3}{2}]}{\Gamma[b]\Gamma[c]} \frac{\Gamma[\frac{3}{2}-b]\Gamma[\frac{3}{2}-c]}{\Gamma[3-b-c]} \frac{1}{(4\pi)^3} \frac{\Gamma[a+b+c-3]}{\Gamma[a+b+c-\frac{3}{2}]} K^{6-2a-2b-2c}, \quad (4.132)
\end{aligned}$$

where we introduced an IR regulator K as we did for our 1-loop divergence. This IR regulator is only needed when $a+b+c \simeq 3$ (the integral vanishes by dynamical dim reg otherwise). One should also notice that enforcing $a+b+c \rightarrow 3$ restores the invariance under permutations of a, b and c .

We always have at least one log from $\Gamma[a+b+c-3]$. Therefore, the only contributions that are not \log^2 (or higher) are those where all the other Γ functions are finite. Up to permutations, there are three relevant cases (i) $a = 3/2, b = 3/2, c = 0$, (ii) $a = 3/2, b = 1, c = 1/2$, and (iii) $a = b = c = 1$. Only (iii) is a single log as expected from above. Isolating just the single log term, for example using $a = 1 - \alpha/2$ with $b = c = 1$, we get

$$\left\langle \varphi_+^3[0] \varphi_+(\vec{k}) \right\rangle_{(1)} = -P_+(k) \frac{\lambda}{12} \frac{1}{16\pi^2} \left(-\frac{1}{\alpha} + \log \frac{[aH]}{k} + \log \frac{k}{K} + \dots \right) + O\left(\frac{1}{\alpha^2}\right). \quad (4.133)$$

Repeating this calculation for φ_+^n we have

$$\begin{aligned} \left\langle \varphi_+^n [0] \varphi_+(\vec{k}_1) \dots \varphi_+(\vec{k}_{n-2}) \right\rangle_{(1)} &\supset -\frac{\lambda}{192\pi^2} \binom{n}{3} (n-2)! P_+(k_1) \dots P_+(k_{n-2}) \\ &\times \sum_i \left(-\frac{1}{\alpha} - \sum_i \log \frac{k_i}{[aH]} \right). \end{aligned} \quad (4.134)$$

This NNLO $\log[aH]$ dependence can be resummed by including the following correction in the dynamical RG:

$$d_0 = \frac{\lambda}{192\pi^2}. \quad (4.135)$$

4.5.3 Stochastic Inflation at NNLO

Now we have computed all the necessary pieces. To summarize our results, we have found that at NNLO, the Fokker-Planck equation for Stochastic Inflation becomes

$$\begin{aligned} \frac{\partial}{\partial \tau} P(\varphi_+, \tau) &= \frac{1}{3} \frac{\partial}{\partial \varphi_+} \left[\partial_{\varphi_-} V(\varphi_+, \varphi_-) \Big|_{\varphi_- = 0} P(\varphi_+, \tau) \right] \\ &+ \frac{1}{2} \frac{\partial^2}{\partial \varphi_+^2} \left[(b_0 + b_1 \varphi_+^2 + b_2 \varphi_+^4) P(\varphi_+, \tau) \right] + \frac{1}{3!} \frac{\partial^3}{\partial \varphi_+^3} \left(d_0 \varphi_+ P(\varphi_+, \tau) \right), \end{aligned} \quad (4.136)$$

where

$$V(\varphi_+, \varphi_-) = \frac{\lambda}{3!} \varphi_- \left(\varphi_+^3 + \frac{\lambda}{18} \varphi_+^5 + \frac{\lambda^2}{162} \varphi_+^7 + \dots \right) \quad (4.137a)$$

$$b_0 = \frac{1}{4\pi^2} \quad (4.137b)$$

$$b_1 = -\frac{\lambda}{36\pi^2} (4 - 3\gamma_E) \quad (4.137c)$$

$$b_2 = \frac{1}{2\pi^2} \frac{\lambda^2}{216} \left[16 + 4\gamma_E(3\gamma_E - 11) + 3\pi^2 + 4\log 2(6\gamma_E + 3\log 2 - 11) \right] \quad (4.137d)$$

$$d_0 = \frac{\lambda}{192\pi^2}. \quad (4.137e)$$

The rest of this section is devoted to expressing this result in a particularly simple basis. As we have emphasized above, the coefficient b_1 and b_2 are basis dependent, in the sense that they can be changed by taking a field redefinition. For the purposes of solving for the NNLO equilibrium distribution, we will find it useful to first perform a field redefinition that moves their effects into the potential. For contrast, we note that the coefficient d_0 is basis independent, and furthermore field redefinitions of this $(\partial/\partial\varphi_+)^3$ term will only induce higher order (NNNLO) terms that we will neglect.

Concretely, we want to redefine the field $\tilde{\varphi}_+ = f(\varphi_+)$ such that $\tilde{b}_1 = \tilde{b}_2 = 0$. Using $P = (d\tilde{\varphi}_+/d\varphi_+)\tilde{P}$ under such a field redefinition, we see that

$$\begin{aligned} \frac{1}{2} \frac{\partial^2}{\partial\varphi_+^2} \left[(b_0 + b_1\varphi_+^2 + b_2\varphi_+^4)P(\varphi_+, \tau) \right] &\rightarrow \\ \frac{1}{2} \frac{\partial^2}{\partial\tilde{\varphi}_+^2} \left[\left(\frac{d\tilde{\varphi}_+}{d\varphi_+} \right)^2 (b_0 + b_1\varphi_+^2 + b_2\varphi_+^4)P(\tilde{\varphi}_+, \tau) \right] & \\ - \frac{1}{2} \frac{\partial}{\partial\tilde{\varphi}_+} \left[\frac{d^2\tilde{\varphi}_+}{d\varphi_+^2} \frac{d\tilde{\varphi}_+}{d\varphi_+} (b_0 + b_1\varphi_+^2 + b_2\varphi_+^4)P(\tilde{\varphi}_+, \tau) \right] &. \end{aligned} \quad (4.138)$$

Next, in order to set $\tilde{b}_1 = \tilde{b}_2 = 0$, we define $\tilde{\varphi}_+$ so that

$$\left(\frac{d\tilde{\varphi}_+}{d\varphi_+} \right)^2 (b_0 + b_1\varphi_+^2 + b_2\varphi_+^4) = b_0, \quad (4.139)$$

We can integrate this equation to determine

$$\tilde{\varphi}_+ = \varphi_+ - \frac{b_1}{6b_0}\varphi_+^3 + \frac{3b_1^2 - 4b_0b_2}{4b_0^2}\varphi_+^5 \quad \rightarrow \quad \varphi_+ \simeq \tilde{\varphi}_+ + \frac{b_1}{6b_0}\tilde{\varphi}_+^3. \quad (4.140)$$

The remaining term is then determined to be

$$\begin{aligned} \frac{d^2 \tilde{\varphi}_+}{d\varphi_+^2} \frac{d\tilde{\varphi}_+}{d\varphi_+} (b_0 + b_1 \varphi_+^2 + b_2 \varphi_+^4) &= -\frac{1}{2} \frac{b_0}{b_0 + b_1 \varphi_+^2 + b_2 \varphi_+^4} (2b_1 \varphi_+ + 4b_2 \varphi_+^3) \\ &\simeq -b_1 \tilde{\varphi}_+ - \left(2b_2 - \frac{5b_1^2}{6b_0} \right) \tilde{\varphi}_+^3. \end{aligned} \quad (4.141)$$

This basis change also impacts the effective potential that appears in the Fokker-Planck equation:

$$\begin{aligned} V'_{\text{eff}}(\tilde{\varphi}_+) &= \partial_{\varphi_-} V(\varphi_+, \varphi_-) \Big|_{\varphi_- = 0} + \frac{3}{4} \frac{b_0}{b_0 + b_1 \varphi_+^2 + b_2 \varphi_+^4} (2b_1 \varphi_+ + 4b_2 \varphi_+^3) \\ &\rightarrow \frac{3}{2} b_1 \tilde{\varphi}_+ + \left(\frac{c_{3,1}}{3!} + 3b_2 - \frac{5b_1^2}{4b_0} \right) \tilde{\varphi}_+^3 + \dots \end{aligned} \quad (4.142)$$

The first term, $\frac{3}{2} b_1 \tilde{\varphi}_+$, simply provides an $O(\lambda)$ correction to α , i.e., the quadratic term in the potential $c_{1,1}$ can always be removed by redefining α , just as we did above when matching the 1-loop matching power spectrum, see Eq. (4.87). The new contribution to the second term, $b_2 = O(\lambda^2)$, is simply a correction to the definition $c_{3,1}$, again just as was computed above when matching to the 1-loop trispectrum, see Eq. (4.98). The same is true for higher powers of φ_+ that we have dropped. In short, we see that b_1 and b_2 simply shift the definition of the couplings within SdSET at higher order in λ but do not introduce any new terms. As a result, we may simply define

$$\lambda_{\text{eff}} = \lambda + 18b_2 + 3! \delta c_{3,1} \quad (4.143a)$$

$$\delta c_{3,1} = -\frac{\lambda^2}{2\pi^2} \left(\frac{1}{9} \gamma_E (2 + 3\gamma_E + 6 \log 2) + \frac{5}{12} \pi^2 - \frac{2 \log 2 + 3 \log^2 2}{9} \right), \quad (4.143b)$$

where $\delta c_{3,1}$ is the correction from one-loop matching in Eq. (4.98). For the other contributions to Stochastic Inflation, $\lambda_{\text{eff}} = \lambda$ is sufficient to achieve NNLO accuracy. In this sense, the coefficients of the NLO and NNLO corrections to the potential are independent of redefinitions of λ . This same argument explains the scheme-independence of β -functions up to two loops.

Putting this all together and relabeling $\tilde{\varphi}_+ \rightarrow \varphi_+$, we arrive at a canonical form for the NNLO equation:

$$\begin{aligned} \frac{\partial}{\partial \tau} P(\varphi_+, \tau) = & \frac{1}{3} \frac{\partial}{\partial \varphi_+} [V'_{\text{eff}}(\varphi_+) P(\varphi_+, \tau)] + \frac{1}{8\pi^2} \frac{\partial^2}{\partial \varphi_+^2} P(\varphi_+, \tau) \\ & + \frac{\lambda_{\text{eff}}}{1152\pi^2} \frac{\partial^3}{\partial \varphi_+^3} (\varphi_+ P(\varphi_+, \tau)) \end{aligned} \quad (4.144a)$$

$$V'_{\text{eff}} = \frac{\lambda_{\text{eff}}}{3!} \left(\varphi_+^3 + \frac{\lambda_{\text{eff}}}{18} \varphi_+^5 + \frac{\lambda_{\text{eff}}^2}{162} \varphi_+^7 + \dots \right). \quad (4.144b)$$

Presumably this freedom to put these equations into such a canonical form can be recast in terms of a covariant description in field space [109, 110], and multi-field generalizations thereof.

4.6 Implications

Having derived novel corrections to the equations that govern the Markovian evolution of the probability distribution for φ_+ , we now turn to solving them. In particular, this section will explore the physical implications of these new terms by calculating the NNLO equilibrium distribution for φ_+ , assuming a static dS background. Then we will extend this to account for the dynamics of the system as it relaxes to the equilibrium state. To this end, we will set up the formalism to calculate the “relaxation eigenvalues,” and will numerically solve for these quantities to $O(\lambda^{3/2})$.

4.6.1 Equilibrium Probability Distribution

Starting with the canonical form of the NNLO equation governing Stochastic Inflation, we can understand the impact on the equilibrium probability distribution $P_{\text{eq}}(\varphi_+)$, which by definition satisfies $\frac{\partial}{\partial \tau} P_{\text{eq}}(\varphi_+) = 0$. We can solve the problem non-perturbatively in the absence

of the higher derivative term proportional to d_0 . Therefore, our strategy will be to find the solution in terms of general V'_{eff} , and then include the correction from d_0 as a perturbation.

The equilibrium contribution from V_{eff} can be determined non-perturbatively following Sec. 4.2.1. The equilibrium solution satisfies

$$\frac{\partial^2}{\partial \varphi_+^2} P_{\text{eq}}^V(\varphi_+) = -\frac{8\pi^2}{3} \frac{\partial}{\partial \varphi_+} V'_{\text{eff}}(\varphi_+) P_{\text{eq}}^V(\varphi_+). \quad (4.145)$$

where $V'_{\text{eff}}(\varphi_+) \equiv \partial_{\varphi_-} V_{\text{eff}}(\varphi_+, \varphi_-)|_{\varphi_-=0}$ and P_{eq}^V is defined as being a solution to this equation.⁷

Integrating twice gives the solution

$$P_{\text{eq}}^V(\varphi_+) = C e^{-8\pi^2 V_{\text{eff}}(\varphi_+)/3}, \quad (4.146)$$

where we defined

$$V_{\text{eff}}(\varphi_+) \equiv \int^{\varphi_+} d\tilde{\varphi}_+ V'_{\text{eff}}(\tilde{\varphi}_+). \quad (4.147)$$

Note that V_{eff} is only a function of φ_+ and should not be confused with $V(\varphi_+, \varphi_-)$ in Eq. (4.74). Since this solution holds for any V_{eff} , it gives the answer at both LO and NLO provided we include the NLO contributions to V_{eff} .

At NNLO, in addition to the correction to V_{eff} , we must include $d_0 = \lambda_{\text{eff}}/(192\pi^2)$ which alters the equation for the equilibrium solution

$$\frac{d_0}{3!} \frac{\partial^3}{\partial \varphi_+^3} (\varphi_+ P_{\text{eq}}(\varphi_+)) + \frac{\partial^2}{\partial \varphi_+^2} P_{\text{eq}}(\varphi_+) = -\frac{8\pi^2}{3} \frac{\partial}{\partial \varphi_+} V'_{\text{eff}}(\varphi_+) P_{\text{eq}}(\varphi_+). \quad (4.148)$$

We can integrate this equation once to get

$$\frac{1}{P_{\text{eq}}(\varphi_+)} \left(\frac{d_0}{3!} \frac{\partial^2}{\partial \varphi_+^2} \varphi_+ P_{\text{eq}}(\varphi_+) + \frac{\partial}{\partial \varphi_+} P_{\text{eq}}(\varphi_+) \right) = -\frac{8\pi^2}{3} V'_{\text{eff}}(\varphi_+). \quad (4.149)$$

⁷Note that $P_{\text{eq}}^V(\varphi_+)$ includes any higher order correction in V'_{eff} but not does not including higher derivative terms that arise at NNLO and beyond. In this sense P_{eq}^V is not to be confused with the LO solution, as it contains some (but not all) contributions at every order.

This can be solved using separation of variables, so we will make the ansatz

$$P_{\text{eq}}(\varphi_+) = P_{\text{eq}}^V(\varphi_+)Q(\varphi_+), \quad (4.150)$$

where P_{eq}^V is given in Eq. (4.146), including the NNLO corrections to V_{eff} . Plugging this ansatz into Eq. (4.149) gives

$$\frac{d_0}{3!} \frac{1}{Q(\varphi_+)P_{\text{eq}}^V(\varphi_+)} \frac{\partial^2}{\partial \varphi_+^2} (\varphi_+ P_{\text{eq}}^V(\varphi_+) Q(\varphi_+)) + \frac{1}{Q(\varphi_+)} \frac{\partial}{\partial \varphi_+} Q(\varphi_+) = 0. \quad (4.151)$$

We can solve this equation perturbatively in Q . The zeroth order term is $Q = \text{constant}$. At the next order, clearly Q' is order d_0 so we can neglect derivatives of Q in the first terms such that

$$\begin{aligned} \frac{1}{Q(\varphi_+)} \frac{\partial}{\partial \varphi_+} Q(\varphi_+) &= -\frac{d_0}{3! P_{\text{eq}}^V(\varphi_+)} \frac{\partial^2}{\partial \varphi_+^2} (\varphi_+ P_{\text{eq}}^V(\varphi_+)) \\ &= -\frac{d_0}{3!} \left(-\frac{16\pi^2}{3} V'_{\text{eff}}(\phi) + \varphi_+ \left(\frac{8\pi^2}{3} V'_{\text{eff}}(\phi) \right)^2 - \frac{8\pi^2}{3} \varphi_+ V''_{\text{eff}}(\phi) \right), \end{aligned} \quad (4.152)$$

such that the solution becomes

$$\log Q = \frac{d_0}{3!} \left[\frac{16\pi^2}{3} V_{\text{eff}}(\phi) - \int d\varphi_+ \left(\varphi_+ \left(\frac{8\pi^2}{3} V'_{\text{eff}}(\phi) \right)^2 - \frac{8\pi^2}{3} \varphi_+ V''_{\text{eff}}(\phi) \right) \right]. \quad (4.153)$$

Finally, we use $d_0 = \lambda_{\text{eff}}/(192\pi^2)$ and $V_{\text{eff}} \simeq \lambda_{\text{eff}}\varphi_+^4/4!$, which consistently captures effects up to NNLO accuracy. We then evaluate the integrals and simplify the expression to find

$$Q(\varphi_+) = \exp \left[\frac{\lambda_{\text{eff}}^2 \varphi_+^4}{1152} \left(\frac{5}{9} - \frac{2\pi^2}{81} \lambda_{\text{eff}} \varphi_+^4 \right) \right]. \quad (4.154)$$

Using the fact that $\lambda_{\text{eff}}\varphi_+^4 = O(1)$ for the LO equilibrium solution, we see that both terms in Q are $O(\lambda_{\text{eff}})$, as expected for NNLO accuracy. Recall the NLO and one additional contribution at

NNLO are encoded in $V_{\text{eff}}(\phi_+)$ and are included in $P_{\text{eq}}^V(\phi)$. Combining these terms and writing $P_{\text{eq}} = CP_{\text{LO}}(\phi_+)P_{\text{NLO}}(\phi_+)P_{\text{NNLO}}(\phi_+)$, we have

$$P_{\text{LO}} = \exp\left(-\frac{\pi^2}{9}\lambda_{\text{eff}}^2\phi_+^4\right) \quad (4.155a)$$

$$P_{\text{NLO}} = \exp\left(-\frac{\pi^2}{243}\lambda_{\text{eff}}^2\phi_+^6\right) \quad (4.155b)$$

$$P_{\text{NNLO}} = \exp\left(\frac{5}{10368}\lambda_{\text{eff}}^2\phi_+^4 - \frac{17\pi^2}{46656}\lambda_{\text{eff}}^3\phi_+^8\right). \quad (4.155c)$$

In the regime where $\log P_{\text{LO}} = O(1)$, we have $\log P_{\text{NLO}} = O(\lambda_{\text{eff}}^{1/2})$ and $\log P_{\text{NNLO}} = O(\lambda_{\text{eff}})$.

4.6.2 Relaxation Eigenvalues

In this section, we will explore the implications for the time dependence of $P(\phi_+, \tau)$. This can be characterized by computing the so-called ‘‘relaxation eigenvalues’’ as we explain below. In the previous section, we could calculate the analytic NNLO equilibrium probability distribution where we only had to treat the $(\partial/\partial\phi_+)^3$ term perturbatively. Here, we must resort to a numerical evaluation of the perturbative expansion, which requires that we treat *all* higher order corrections as perturbations.

To begin, we return to the full NNLO equation that governs Stochastic Inflation given in Eq. (4.144a), and rewrite it as a Euclidean Schrödinger equation [80, 32]:

$$\frac{\partial}{\partial\tau}P(\phi_+, \tau) = \frac{1}{3}\frac{\partial}{\partial\phi_+}\left[V'_{\text{eff}}(\phi_+)P(\phi_+, \tau)\right] + \frac{1}{8\pi^2}\frac{\partial^2}{\partial\phi_+^2}P(\phi_+, \tau), \quad (4.156)$$

where $V'_{\text{eff}}(\phi_+) \equiv \partial_{\phi_-}V_{\text{eff}}(\phi_+, \phi_-)|_{\phi_- = 0}$. This equation can be solved using separation of variables

$$P(\phi_+, \tau) = \exp\left[-\frac{4\pi^2}{3}V_{\text{eff}}(\phi_+)\right] \sum_{n=0}^{\infty} \Phi_n(\phi_+)e^{-\Lambda_n\tau}, \quad (4.157)$$

where $V_{\text{eff}}(\phi_+)$ is defined in Eq. (4.147), we have assumed $t_0 = 0$, and Φ_n are the eigenfunctions

of [80, 32]

$$\frac{\partial^2}{\partial \varphi_+^2} \Phi_n(\varphi_+) - U(\varphi_+) \Phi_n(\varphi_+) = -8\pi^2 \Lambda_n \Phi_n(\varphi_+), \quad (4.158)$$

where Λ_n are the non-negative ‘‘relaxation eigenvalues,’’ and the Schrödinger potential is

$$U(\varphi_+) = \left(\frac{4\pi^2}{3} V'_{\text{eff}}(\varphi_+) \right)^2 - \frac{4\pi^2}{3} \frac{\partial}{\partial \varphi_+} V'_{\text{eff}}(\varphi_+). \quad (4.159)$$

The lowest eigenvalue is zero with the eigenfunction $\Phi_0(\varphi_+) \propto \exp \left[-\frac{4\pi^2}{3} V_{\text{eff}}(\varphi_+) \right]$. Since all other Λ_n are positive, at late times the distribution $P(\varphi_+, t)$ relaxes to the fixed point

$$P(\varphi_+, \tau) = N \exp \left[-\frac{8\pi^2}{3} V_{\text{eff}}(\varphi_+) \right]. \quad (4.160)$$

This reproduces the static result above in Eq. (4.146). However, for the numerical evaluations we take $V'_{\text{eff}}(\varphi_+) = \frac{\lambda_{\text{eff}}}{3!} \varphi_+^3$, and treat the additional correction to the potential as perturbations. In addition, for the remainder of this section, we will drop subscript ‘eff’ on the coupling, $\lambda_{\text{eff}} \rightarrow \lambda$, for brevity.

To explore the effect of the NNLO correction we need to determine the eigenvalues Λ_n of Eq. (4.144a) for $n \geq 1$. We can find the eigenvalues and eigenfunctions of Eq. (4.144a) as perturbative expansions in powers of $\sqrt{\lambda}$,

$$\Lambda_n = \lambda^{1/2} \Lambda_n^{(0)} + \lambda \Lambda_n^{(1)} + \lambda^{3/2} \Lambda_n^{(2)} + \dots \quad (4.161a)$$

$$\Phi_n = \Phi_n^{(0)} + \lambda^{1/2} \Phi_n^{(1)} + \lambda \Phi_n^{(2)} + \dots \quad (4.161b)$$

$$U = \lambda^{1/2} U^{(0)} + \lambda U^{(1)} + \lambda^{3/2} U^{(2)} + \dots, \quad (4.161c)$$

where $\Lambda_n^{(0)}$ and $\Phi_n^{(0)}$ are the solutions of Eq. (4.158) with Schrödinger potential $U = U^{(0)}$. This potential is obtained from Eq. (4.159) by setting $V'_{\text{eff}}(\varphi_+) = \frac{\lambda}{3!} \varphi_+^3$, the leading term in

Eq. (4.144b). Explicitly,

$$\frac{\partial^2}{\partial \varphi_+^2} \Phi_n^{(0)}(\varphi_+) - \left[\frac{4\pi^4}{81} \lambda^2 \varphi_+^6 - \frac{2\pi^2}{3} \lambda \varphi_+^2 \right] \Phi_n^{(0)}(\varphi_+) = -8\pi^2 \lambda^{\frac{1}{2}} \Lambda_n^{(0)} \Phi_n^{(0)}(\varphi_+) \quad (4.162)$$

Since $\varphi_+ \sim \lambda^{-1/4}$ we see that the Schrödinger potential, the term in square brackets, indeed scales as $O(\lambda^{1/2})$. This equation can be solved numerically by the shooting method[111]. Higher order terms in Eq. (4.144b) as well as the NNLO term $\partial_{\varphi_+}^3(\varphi_+ P)$ can be treated as perturbative corrections to Eq. (4.162). That is, if we substitute Eq. (4.157) into Eq. (4.144a) and keep terms up to $O(\lambda^{3/2})$, the eigenfunctions Φ_n must solve

$$\frac{\partial^2}{\partial \varphi_+^2} \Phi_n - \left[\lambda^{1/2} U^{(0)} + \lambda U^{(1)} + \lambda^{3/2} U^{(2)} \right] \Phi_n = -8\pi^2 \left[\lambda^{1/2} \Lambda_n^{(0)} + \lambda \Lambda_n^{(1)} + \lambda^{3/2} \Lambda_n^{(2)} \right] \Phi_n, \quad (4.163)$$

where

$$\lambda^{1/2} U^{(0)} = \frac{4\pi^4}{81} \lambda^2 \varphi_+^6 - \frac{2\pi^2}{3} \lambda \varphi_+^2 \quad (4.164a)$$

$$\lambda U^{(1)} = \frac{4\pi^4}{729} \lambda^3 \varphi_+^8 - \frac{5\pi^2}{81} \lambda^2 \varphi_+^4 \quad (4.164b)$$

$$\begin{aligned} \lambda^{3/2} U^{(2)} = & \frac{79\pi^4}{104976} \lambda^4 \varphi_+^{10} - \frac{53\pi^2}{5832} \lambda^3 \varphi_+^6 - \frac{5}{1728} \lambda^2 \varphi_+^2 + \left(\frac{\pi^2}{7776} \lambda^3 \varphi_+^7 - \frac{5}{1728} \lambda^2 \varphi_+^3 \right) \partial_{\varphi_+} \\ & + \left(-\frac{1}{1728} \lambda^2 \varphi_+^4 + \frac{\lambda}{384\pi^2} \right) \partial_{\varphi_+}^2 + \frac{\lambda}{1152\pi^2} \varphi_+ \partial_{\varphi_+}^3. \end{aligned} \quad (4.164c)$$

Finally, the perturbative corrections to the eigenvalues are computed numerically using

$$8\pi^2 \Lambda_n^{(1)} = \langle \Phi_n^{(0)} | U^{(1)} | \Phi_n^{(0)} \rangle \quad (4.165a)$$

$$8\pi^2 \Lambda_n^{(2)} = \langle \Phi_n^{(0)} | U^{(2)} | \Phi_n^{(0)} \rangle + \frac{\lambda^{1/2}}{8\pi^2} \sum_{k \neq n} \frac{|\langle \Phi_k^{(0)} | U^{(1)} | \Phi_n^{(0)} \rangle|^2}{\Lambda_n^{(0)} - \Lambda_k^{(0)}}. \quad (4.165b)$$

The first few relaxation eigenvalues are (recall that $\lambda = \lambda_{\text{eff}}$ here)

n	Λ_n
1	$0.03630 \lambda^{1/2} + 0.00076 \lambda + 0.00049 \lambda^{3/2}$
2	$0.11814 \lambda^{1/2} + 0.00338 \lambda + 0.00138 \lambda^{3/2}$
3	$0.21910 \lambda^{1/2} + 0.00795 \lambda + 0.00316 \lambda^{3/2}$

The contribution to the eigenvalues at $O(\lambda^{3/2})$ includes both corrections to the equations of Stochastic Inflation at NNLO as well as perturbative corrections to the eigenvalues from the LO and NLO equations. Working with the full NNLO equations was crucial to obtaining the detailed numeric values. We note that the NNLO contribution to V_{eff} in Eq. (4.144b) dominates; the small numerical coefficient of $d_0 \simeq 9 \times 10^{-5} \lambda$ suppresses its impact on these eigenvalues. As the form of V_{eff} is determined by SdSET field redefinitions to all orders, it may prove useful in future studies to simply include higher order corrections to the potential as an approximation. We expect this minor impact of d_0 is due to the fact that we are assuming the UV theory is $\lambda \phi^4$ such that the non-Gaussian noise and corrections to the potential are determined by the same parameter. In contrast, if one were to consider inflationary models with primordial non-Gaussianity, these two effects are controlled by independent parameters, such that the non-Gaussian contribution to the noise could become important [58]. In either case, this investigation is only possible because we have framework in which all corrections to Stochastic Inflation, including contributions from non-Gaussian noise, can be systematically computed.

4.7 Conclusions

Understanding the nature of quantum dS space is one of the most basic conceptual problems in cosmology [5]. Stochastic Inflation [11, 79, 80] informs much of the physical intuition for how we think about accelerating cosmologies, particularly as we approach the eternally inflating regime that is dominated by quantum fluctuations [94, 95, 97, 96]. Yet, Stochastic Inflation is itself an approximation whose regime of validity, and corrections thereof, should follow from a more basic starting point. Ultimately, a complete description should include dynamical gravity, although the simpler case of quantum field theory in a fixed dS background studied here already provides a non-trivial challenge.

In this paper, we demonstrated precisely how corrections to Stochastic Inflation arise from quantum field theory in dS, namely as a natural consequence of dynamical renormalization group flow within the EFT that emerges in the superhorizon limit. By working with SdSET, the origin of the stochastic description is a direct consequence of EFT power counting, which also explains why this effect is only relevant for light (massless) scalars. (This same power counting scheme also explains the all orders conservation of the adiabatic mode [65].) By matching $\lambda\phi^4$ theory onto SdSET up to one loop, we could then calculate the log enhanced corrections to the mixing of EFT operators up to two loops. This allowed us to derive the corrections to the equations of Stochastic Inflation at NNLO accuracy. These results include the first higher derivative correction to the framework, which is the leading signature of the non-Gaussian contribution to the noise as modes cross the horizon.

This work extends derivations of Stochastic Inflation from quantum field theory in dS at LO [30, 32, 65, 93] and NLO [31, 81, 92] to NNLO. Yet, even at NLO, we showed that the “universal” correction to the effective potential follows from a field redefinition and can be extended to all orders. This result agrees with Refs. [31, 81, 92], which arrive at this NLO correction by (effectively) integrating-out the decaying mode at tree-level. Furthermore, the first appearance of non-Gaussianity in the stochastic noise appears at NNLO and requires a

genuine two-loop calculation. Higher-loop calculations of inflationary correlators are notoriously difficult, but they are made manageable by working with SdSET, which facilitates the use of the symmetry preserving dynamical dimensional regularization. Most importantly, SdSET reduces the problem of calculating any corrections to Stochastic Inflation to the determination of the matrix of anomalous dimensions. Rather than being a mysterious feature of dS space, we now see that the derivation of Stochastic Inflation and corrections thereof is conceptually and technically similar to calculating the scaling dimensions of operators at the Wilson-Fisher fixed point in $d = 4 - \epsilon$ dimensions. Finally, there is an intriguing connection that could be made with a thermodynamic interpretation of the equilibrium probability distributions, $P_{LO} \sim \exp(-\beta E)$, where the inverse temperature is $\beta = 2\pi/H$. It would be interesting to understand the meaning of the NNLO corrections derived here from this point of view.

Phenomenologically, Stochastic Inflation is an important tool for understanding the predicted non-Gaussianity in multi-field inflation [23, 112, 113, 114, 115, 116], where superhorizon evolution can give rise to non-trivial correlations. Previous work has included the non-Gaussian contributions for the non-linear superhorizon evolution, but thus far the effects of non-Gaussian noise has been missing. It will be interesting to explore models where both effects are simultaneously important. For example, one might hope this techniques would elucidate the physics of the small mass regime of quasi-single field inflation [117], which is known to produce large logs.

Conceptually, Stochastic Inflation serves as the basis for much of our understanding of slow-roll eternal inflation. This description requires coupling a light scalar field to gravity, yet much of the structure is determined by the quantum noise in the Fokker-Planck equation. Specifically, the regime of slow roll eternal inflation is the limit where the potential becomes flat and the quantum noise dominates the time evolution until inflation ends. While understanding this regime is often considered a conceptual problem, it may have important consequences for cosmological solutions to hierarchy problems, such as [118, 119, 120, 121].

Finally, underlying our results on Stochastic Inflation is a demonstration that SdSET is a consistent description of dS quantum field theory at loop level. Calculations in a wide variety of

cosmological settings are beset with challenges stemming from the underlying time evolution and lack of consistent regulator. The successful implementation of SdSET as an organizing principle for calculating quantum correlators in dS offers hope that more of these cosmological problems may be organized and simplified when described with the right degrees of freedom. The emergence of Stochastic Inflation as a simple consequence of EFT power counting is a non-trivial example of these principles in action.

Acknowledgements

We are grateful to Daniel Baumann, Matthew Baumgart, Raphael Flauger, Tom Hartman, Mehrdad Mirbabayi, Gui Pimentel, Eva Silverstein, and Raman Sundrum for helpful discussions. T. C. is supported by the US Department of Energy, under grant no. DE-SC0011640. D. G., A. P. and A. R. were supported by the US Department of Energy under grant no. DE-SC0019035.

This chapter, in full, is a reprint of the material as it appears in Timothy Cohen, Daniel Green, Akhil Premkumar, Alexander Ridgway, *Journal of High Energy Physics* **09** (2021) 159. The dissertation author was one of the primary investigators and authors of this paper.

4.A Matching the Six-point Function

In this appendix, we provide some details for matching the tree-level six-point function, as illustrated in Fig. 4.7. This serves as an input to the one-loop corrections, see Fig. 4.5, and also provides a non-trivial check on the matching the EFT operator $\underline{\varphi}$ to the UV field ϕ .

Assuming the UV interaction is $\lambda \phi^4$, the six-point function first arises at second order in perturbation theory. Using the commutator form of the in-in correlator, see Eq. (4.27), we can write the full six-point function as

$$\left\langle \phi(\vec{k}_1) \phi(\vec{k}_2) \phi(\vec{k}_3) \phi(\vec{k}_4) \phi(\vec{k}_5) \phi(\vec{k}_6) \right\rangle_{\text{tree}} = A_6 + B_6, \quad (4.166)$$

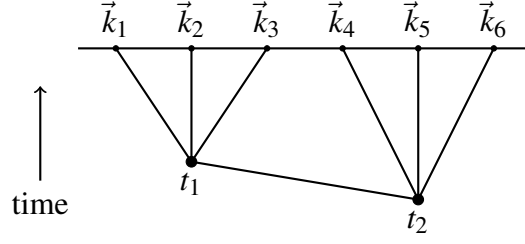


Figure 4.7. The tree level in-in six-point function.

where

$$A_6 = \left\langle \left(i \int dt_1 [H_{\text{int}}(t_1), \phi(\vec{k}_1)] \right) \left(i \int dt_2 [H_{\text{int}}(t_2), \phi(\vec{k}_2)] \right) \phi(\vec{k}_3) \phi(\vec{k}_4) \phi(\vec{k}_5) \phi(\vec{k}_6) \right\rangle + \text{permutations}, \quad (4.167)$$

and

$$B_6 = \left\langle \phi(\vec{k}_1) \phi(\vec{k}_2) \phi(\vec{k}_4) \phi(\vec{k}_4) \phi(\vec{k}_5) i^2 \int dt_1 \int^{t_1} dt_2 [H_{\text{int}}(t_2), [H_{\text{int}}(t_1), \phi(\vec{k}_6)]] \right\rangle + \text{permutations}. \quad (4.168)$$

Our goal is to match this expression onto the EFT, so we need to take the limit where all of the fields are superhorizon. The additional contributions that arise from the subhorizon region, $k_i \tau_j = O(1)$, will be absorbed into the initial conditions, which we do not need to calculate explicitly for our purposes in this work.

To match the superhorizon behavior, we can again expand the operator using Eq. (4.66) to find

$$[\phi]_\lambda = i \int^t dt_1 [H_{\text{int}}(t_1), \phi(\vec{k}_1)] = \frac{\lambda}{3!} \frac{1}{3} \left(- \left(-\frac{1}{2\alpha} + \log[aH] \right) + \frac{1}{3} \right) \varphi_+^3(\vec{x}). \quad (4.169)$$

It is easy to see that the superhorizon contribution to A_6 is determined by $[\phi]_\lambda$,

$$A_6 = \left\langle [\phi]_\lambda(\vec{k}_1) [\phi]_\lambda(\vec{k}_2) \phi(\vec{k}_3) \phi(\vec{k}_4) \phi(\vec{k}_5) \phi(\vec{k}_6) \right\rangle + \text{permutations}.$$

This shows that by matching the trispectrum with Eq. (4.71), we can also match A_6 .

Clearly we cannot determine B_6 using $[\phi]_\lambda$. The most straightforward way to determine the superhorizon contribution is to write

$$B_6 = \frac{\lambda^2}{3!2} \left\langle \phi(\vec{k}_1) \phi(\vec{k}_2) \phi(\vec{k}_4) \phi(\vec{k}_4) \phi(\vec{k}_5) \int_{-\infty}^t dt_1 a^3(t_1) G(\vec{k}_6, t_1, t) \int d^3x_1 \phi^2(\vec{x}_1, t_1) \right. \\ \left. \times \int_{-\infty}^{t_1} dt_2 a^3(t_2) G(\vec{k}_{123}, t_2, t_1) \int d^3x_2 \phi^3(\vec{x}_2, t_2) \right\rangle. \quad (4.170)$$

where

$$G(\vec{k}, t', t) = i \left\langle \left[\phi(\vec{k}, t'), \phi(\vec{k}', t) \right] \right\rangle' \simeq \frac{H}{3} \left([a(t')H]^{-3} - [a(t)H]^{-3} \right). \quad (4.171)$$

Integrating this expression using dynamical dim reg, we find the superhorizon contribution is

$$B_6 = \lambda^2 \frac{H^6 \sum_i k_i^3}{2^5 (k_1 k_2 k_3 k_4 k_5 k_6)^3} \frac{5!}{(3!)^2} \int^t dt_1 \frac{[a(t_1)H]^{-2\alpha}}{3} \left(-1 + \frac{[a(t_1)H]^3}{[a(t)H]^3} \right) \\ \times \int^{t_1} dt_2 \frac{[a(t_2)H]^{-2\alpha}}{3} \left(-1 + \frac{[a(t_2)H]^3}{[a(t_1)H]^3} \right) \\ = \frac{\lambda^2 H^6 \sum_i k_i^3}{2^5 (k_1 k_2 k_3 k_4 k_5 k_6)^3} \left[\frac{10}{9} \left(\frac{1}{2\alpha} - \log[aH] + \frac{1}{3} \right) \left(\frac{1}{4\alpha} - \log[aH] + \frac{1}{3} \right) + \frac{10}{81} \right]. \quad (4.172)$$

Next, we would like to see how this formula arises in SdSET. First, we calculate the contribution to the six-point function at second order in $c_{3,1}$. We take the same commutator structure as B_6 , where one $[\phi_+, \phi_-]$ acts on the external line and the other on an internal

commutator. The result is

$$\begin{aligned}
B_{3,1} &= c_{3,1}^2 \frac{5!}{(3!)2} \frac{H^6}{2^5(k_1..k_6)^{3-2\alpha}} \sum_i k_i^{3-2\alpha} \int^{t_1} dt_1 \frac{1}{3} [a(t_1)H]^{2\alpha} \int^{t_1} dt_2 \frac{1}{3} [a(t_2)H]^{2\alpha} \\
&= c_{3,1}^2 \frac{10}{9} \sum_i k_i^{3-2\alpha} \frac{C_\alpha^{10}}{(k_1..k_6)^{3-2\alpha}} \frac{[aH]^{4\alpha}}{8\alpha^2}, \quad (4.173)
\end{aligned}$$

where the additional factors of $1/3$ are from the commutator $i[\varphi_+, \varphi_-] = \delta(\vec{x} + \vec{x}')/3$ when $\alpha = 0$. In addition, we have the contribution from the time evolution of $\underline{\varphi}$ at order $c_{3,1}$ from Eq. (4.70) and Eq. (4.71), which yields

$$\begin{aligned}
\underline{\varphi} \supset \frac{c_{4,0}}{9} \frac{H}{3!} [aH]^{-3\alpha} \varphi_+^3 &\rightarrow \frac{c_{4,0}}{3} \frac{1}{3!} [aH]^{-3\alpha} \varphi_+^2 [\varphi_+]_\lambda \\
&\rightarrow \frac{H}{3!^2} \frac{c_{4,0} c_{3,1}}{9} \left(\frac{1}{2\alpha} - \log[aH] \right) \varphi_+^5(\vec{x}). \quad (4.174)
\end{aligned}$$

This contribution is in addition, to the φ_+^5 term in $\underline{\varphi}$ in Eq. (4.96), that we determined from our field redefinition,

$$\underline{\varphi} \supset \frac{\lambda^2}{81} \frac{1}{3!} [aH]^{-5\alpha} \varphi_+^5. \quad (4.175)$$

Combining these two terms in $\underline{\varphi}$, we get the contribution to the six-point function:

$$B_{\underline{\varphi}} = \frac{\lambda^2 H^6 \sum_i k_i^3}{2^5 (k_1 k_2 k_3 k_4 k_5 k_6)^3} \left[\frac{10}{27} \left(\frac{1}{2\alpha} - \log[aH] \right) + \frac{20}{81} \right]. \quad (4.176)$$

Finally, from the field redefinition we found in Eq. (4.74), we also have a correction to the effective potential via $c_{5,1} = \frac{\lambda^2 5!}{18 3!}$. This contributions to the six-point function at linear order in $c_{5,1}$:

$$\begin{aligned}
B_{5,1} &= \frac{c_{5,1}}{2\nu} \frac{[aH]^{-4\alpha}}{4\alpha} \frac{H^6}{2^5 k_1^{3-2\alpha} .. k_6^{3-2\alpha}} \sum_i k_i^{3-2\alpha} \\
&\rightarrow \lambda^2 \frac{10}{27} \frac{H^6 \sum_i k_i^{3-2\alpha}}{2^5 k_1^{3-2\alpha} .. k_6^{3-2\alpha}} \left(\frac{1}{4\alpha} - \log[aH] \right). \quad (4.177)
\end{aligned}$$

Combining these terms and using $c_{3,1} = c_{4,0} = \lambda$, we match the UV six-point function

$$B_6 = B_{3,1} + B_{\underline{\phi}} + B_{5,1}. \quad (4.178)$$

Note that there is some ambiguity in the constant term due to scheme dependence associated with regulating our (divergent) time integrals. Although our expression matches the constant as well, in some other schemes, the initial conditions may play a role in matching. On the other hand, all powers of $\log aH$ must match in any scheme, as we find here.

4.B Hard Cutoff Calculations

In the main text, we used dynamical dim reg for the EFT loop calculations. Loops in the UV calculations were, in some cases, regulated with dim reg rather than dynamical dim reg. These regulators offer some technical advantages but one might worry about using different regulators in the matching calculation. We can therefore gain further conceptual insight by redoing these calculations with a hard cutoff. This regulator can be easily implemented in both the UV and EFT and also makes the origin of divergences more transparent. Furthermore, we can work directly with the massless mode functions, thereby avoiding the complications of working with massive modes. In this appendix we will repeat the calculations from the main text using a hard cutoff, reproducing all the above results up to differences in scheme dependent coefficients.

4.B.1 Matching

In this section, we compute the matching for $\lambda\phi^4$ onto the SdSET up to one-loop order. We will use a hard cutoff for both momentum and time integrals. Specifically, we regulate the momentum integral with a UV cutoff $\Lambda = [aH]$ and an IR cutoff K . For time integrals, noting that the UV region of integration does not contribute due to our $i\epsilon$ prescription, we simply regulate the IR with a cutoff τ_* , which corresponds to the time of horizon crossing for a mode k .

Power Spectrum

The one-loop power spectrum in the UV theory is given by a standard in-in calculation,

$$\left\langle \phi(\vec{k}) \phi(\vec{k}') \right\rangle'_{(1)} = \frac{\lambda}{4k^3} \frac{H^2}{3} \left(\log \frac{2k}{[aH]} + \gamma_E - 2 \right) \int \frac{d^3 p}{(2\pi)^3} \frac{1}{p^3}, \quad (4.179)$$

where the primed correlator is defined in Eq. (4.30) above. The resulting power spectrum is

$$\left\langle \phi(\vec{k}) \phi(\vec{k}') \right\rangle'_{(1)} = \frac{\lambda}{4k^3} \frac{H^2}{3} \left(\log \frac{2k}{[aH]} + \gamma_E - 2 \right) \frac{1}{2\pi^2} \log \frac{[aH]}{K}. \quad (4.180)$$

We can calculate the one-loop power spectrum in the EFT using

$$\begin{aligned} \left\langle \underline{\varphi}(\vec{k}) \underline{\varphi}(\vec{k}') \right\rangle'_{(1)} &= H^2 \left\langle \varphi_+(\vec{k}) \varphi_+(\vec{k}') \right\rangle'_{(1)} + H^2 \left\langle \varphi_+(\vec{k}) \varphi_+(\vec{k}') \right\rangle'_{\delta\alpha(1)} \\ &\quad + 2 \frac{c_{4,0}}{9} \frac{1}{3!} H^2 \left\langle \varphi_+(\vec{k}) \varphi_+^3(\vec{k}') \right\rangle'_{(0)} + \left\langle \underline{\varphi}(\vec{k}) \underline{\varphi}(\vec{k}') \right\rangle'_{\text{IC}(1)}, \end{aligned} \quad (4.181)$$

where we have set $\alpha = 0$ for the UV mode functions. The second term allows for the possibility that $\alpha = \delta\alpha$ is generated by matching and the third term is generated by performing the EFT field redefinition given in Eq. (4.70). Using the leading order matching relation for the Wilson coefficient $c_{4,0} = c_{3,1} = \lambda + O(\lambda^2)$, we find

$$\begin{aligned} H^2 \left\langle \varphi_+(\vec{k}) \varphi_+(\vec{k}') \right\rangle'_{(1)} &= -\frac{H^2}{3} \log \frac{[aH]}{k} \frac{\lambda}{4k^3} \int \frac{d^3 p}{(2\pi)^3} \frac{1}{p^3} \\ &= -\frac{H^2}{3} \log \frac{[aH]}{k} \frac{\lambda}{4k^3} \frac{1}{2\pi^2} \log \frac{[aH]}{K}, \end{aligned} \quad (4.182)$$

where we evaluated the time integral with a hard cutoff at the time of horizon crossing, $[aH]_* = k$,

$$\int_{t_*}^t dt' = \log[aH] - \log[aH]_* = \log \frac{[aH]}{k}. \quad (4.183)$$

As with the main text, the contribution from a shift in α is given by

$$H^2 \langle \varphi_+(\vec{k}) \varphi_+(\vec{k}') \rangle'_{\delta\alpha^{(1)}} = \langle \underline{\varphi}(\vec{k}) \underline{\varphi}(\vec{k}') \rangle_{(0)} \left(1 + 2\delta\alpha \log \frac{k}{[aH]} \right), \quad (4.184)$$

and from the field redefinition is

$$\begin{aligned} 2 \times \frac{\lambda H^2}{9 \cdot 3!} \langle \varphi_+(\vec{k}) [\varphi_+^3](\vec{k}') \rangle_{(0)} &= \frac{\lambda}{9} \frac{1}{2k^3} \int \frac{d^3p}{(2\pi)^3} \frac{1}{2p^3} \\ &= \frac{\lambda H^2}{9} \frac{1}{2k^3} \frac{1}{4\pi^2} \log \frac{[aH]}{K}. \end{aligned} \quad (4.185)$$

Combing these results we have

$$H^2 \langle \underline{\varphi}(\vec{k}) \underline{\varphi}(\vec{k}') \rangle'_{(1)} = \frac{H^2}{3} \left(\log \frac{k}{[aH]} + \frac{1}{3} \right) \frac{\lambda}{4k^3} \frac{\log[aH]/K}{2\pi^2} + H^2 \langle \underline{\varphi}(\vec{k}) \underline{\varphi}(\vec{k}') \rangle'_{\text{IC}^{(1)}}. \quad (4.186)$$

Comparing the UV expression given in Eq. (4.180) with the combined EFT results, Eq. (4.186), we see that we need

$$\delta\alpha^{(1)} = \frac{\lambda}{24\pi^2} \left(\gamma_E - \frac{7}{3} + \log 2 \right). \quad (4.187)$$

This expression differs from our result with dynamical dim reg, Eq. (4.87). This is not entirely surprising as the precise definitions of the parameters in the UV are scheme dependent and thus this scheme dependence is also inherited through matching.

Trispectrum

Next, we will perform the calculation to match the trispectrum taking $\alpha = 0$ on all legs and regulating all integrals with a hard cutoff. As was argued above, \mathcal{H}_4 is the only term that can

generate log divergences from the loop momentum integrals. Taking $p \gg k_i$ we have

$$\begin{aligned}
\mathcal{H}_4 &\simeq \frac{1}{(k_2 k_3 k_4)^3} \int \frac{d^3 p}{(2\pi)^3} \int^\tau \frac{d\tau_1}{(-\tau_1)^4} G(\vec{k}_1; \tau, \tau_1) \\
&\quad \times 2\text{Im} \int^{\tau_1} \frac{d\tau_2}{(-\tau_2)^4} \frac{G(\vec{p}, \tau_1, \tau_2)}{p^3} (1 + ip\tau_1)(1 - ip\tau_2) e^{-ip(\tau_1 - \tau_2)} + \text{permutations} \\
&\simeq \frac{H^4 \lambda^2}{16(k_2 k_3 k_4)^3} \int \frac{d^3 p}{(2\pi)^d} \frac{1}{p^3} \left[\frac{10}{81} - \frac{1}{27} \gamma_E (2 + 3\gamma_E) - \frac{5}{36} \pi^2 \right. \\
&\quad \left. + \frac{1}{9} \left(\log \frac{2p}{[aH]} \right)^2 + (1 + 3\gamma_E) \log \frac{2p}{[aH]} + \frac{4}{9} \log \frac{k}{[aH]} \right] + \text{permutations} \\
&= \frac{H^4 \lambda^2}{8(k_2 k_3 k_4)^3} \frac{1}{2\pi^2} \log \frac{[aH]}{K} \left[\frac{10}{81} - \frac{1}{27} \gamma_E (2 + 3\gamma_E + 6 \log 2) - \frac{5}{36} \pi^2 + \frac{2 \log 2 + 3 \log^2 2}{27} \right] \\
&\quad + O\left((\log[aH])^2\right) + \text{permutations}. \tag{4.188}
\end{aligned}$$

As we did in the main text, we are focused on the single $\log[aH]/K$ term because it cannot be absorbed into the initial conditions and the RG implies that higher powers of log should be products of logs already present in lower order diagrams.

In order to compare this to the EFT, we need to keep track of our field redefinition to order λ^2 . Specifically, we need

$$\underline{\varphi} \equiv H \left([aH]^{-\alpha} \varphi_+ + [aH]^{-\beta} \varphi_- + \frac{\lambda}{9} \frac{1}{3!} [aH]^{-3\alpha} \varphi_+^3 + \frac{\lambda^2}{81(3!)} [aH]^{3-5\alpha} \varphi_+^5 \right). \tag{4.189}$$

to remove the φ_+^6 operator in the EFT Lagrangian. This additional term contributes to the trispectrum at one loop:

$$\begin{aligned}
\langle \underline{\varphi}(\vec{k}_1) \dots \underline{\varphi}(\vec{k}_4) \rangle' &\supset \frac{\sum_i k_i^3}{(k_1 k_2 k_3 k_4)^3} \frac{\lambda^2}{81} \frac{5!}{3!2} \int \frac{d^3 p}{(2\pi)^3} \frac{1}{p^3} \\
&= \frac{\sum_i k_i^3}{(k_1 k_2 k_3 k_4)^3} \frac{\lambda^2}{81} \frac{5!}{3!2} \frac{1}{2\pi^2} \log \frac{[aH]}{K}, \tag{4.190}
\end{aligned}$$

which matches the leading term in the UV expression, namely the factor of $10/81$. After

matching this term, we see a fairly complicated expression remains for the linear log. This can be absorbed into the $c_{3,1}$ using Eq. (4.46), such that

$$c_{3,1} \rightarrow \lambda - \frac{\lambda^2}{2\pi^2} \left(\frac{1}{9} \gamma_E (2 + 3\gamma_E + 6 \log 2) + \frac{5}{12} \pi^2 - \frac{2 \log 2 + 3 \log^2 2}{9} \right). \quad (4.191)$$

This agrees with Eq. (4.98), which was computed using dynamical dim reg.

4.B.2 Composite Operator Mixing

We continue to demonstrate how the calculations proceed using a hard cutoff regulator. In this section, we will compute the correlators that yield composite operator mixing, thereby determining the dynamical RG equations.

One Loop

The first (and simplest) non-trivial calculation to do is the anomalous dimension of φ_+^2 , which we derive from

$$\begin{aligned} \langle \varphi_+^2[0] \varphi_+(\vec{k}_1) \varphi_+(\vec{k}_2) \rangle &= \int \frac{d^3 p_1 d^3 p_2}{(2\pi)^6} \langle \varphi_+(\vec{p}_1) \varphi_+(\vec{p}_2) \varphi_+(\vec{k}_1) \varphi_+(\vec{k}_2) \rangle \\ &= \int \frac{d^3 p}{(2\pi)^3} \langle \varphi_+(\vec{p}) \varphi_+(-\vec{p} - \vec{k}_1 - \vec{k}_2) \varphi_+(\vec{k}_1) \varphi_+(\vec{k}_2) \rangle'. \end{aligned} \quad (4.192)$$

Since our goal is to reproduce the $O(\lambda)$ log divergence we found above in the main text, we can compute the correlator in terms of φ_+^2 as opposed to using $\underline{\varphi}$. Using φ_+ , there is already a term proportional to $\log k/[aH]$ from the tree-level time evolution that would only give a \log^2 term after integrating over p . Instead, we are interested in the contribution from the initial

conditions:

$$\begin{aligned} \left\langle \varphi_+(\vec{k}_1) \dots \varphi_+(\vec{k}_4) \right\rangle'_{\text{IC}(1)} &= \frac{\lambda}{8(k_1 k_2 k_3 k_4)^3} \left[\frac{(\gamma_E - 2)}{3} \sum_i k_i^3 - \frac{k_1 k_2 k_3 k_4}{k_t} \right. \\ &\quad \left. - \frac{1}{9} k_t^3 + 2 \sum_{h < i < j} k_h k_i k_j + \frac{1}{3} k_t \left(\sum_i k_i^2 - \sum_{i < j} k_i k_j \right) \right]. \end{aligned} \quad (4.193)$$

Taking $k_1 \simeq k_2 = p$ and expanding in $k_3, k_4 \ll p$, we find

$$\begin{aligned} \left\langle \varphi_+^2[0] \varphi_+(\vec{k}_1) \varphi_+(\vec{k}_2) \right\rangle &\simeq P_+(k_1) P_+(k_2) \int \frac{d^3 p}{(2\pi)^3} \frac{1}{2p^3} \frac{2}{3} (\gamma_E - 2) \\ &= \frac{2}{3} (\gamma_E - 2) \frac{1}{2\pi^2} \log \frac{[aH]}{K} P_+(k_1) P_+(k_2). \end{aligned} \quad (4.194)$$

We can then apply the same steps to evaluate a correlator with an arbitrary composite operator to find

$$\begin{aligned} \left\langle \phi^n[0] \phi(\vec{k}_1) \dots \phi(\vec{k}_n) \right\rangle &\supset \frac{n!}{2^n (k_1 \dots k_n)^3} \lambda \int \frac{d^3 p}{(2\pi)^3} \frac{n(n-1)}{4p^6} \\ &\quad \times 2 \text{Im} \int \frac{d\tau_1}{(-\tau_1)^4} (1 - ip\tau)^2 (1 + ip\tau_1)^2 e^{i2p(\tau - \tau_1)} \\ &\supset \frac{n!}{2^n (k_1 \dots k_n)^3} \lambda \binom{n}{2} \frac{1}{3} \left(\log \frac{2k}{aH} + \gamma_E - 2 \right) \int \frac{d^3 p}{(2\pi)^3} \frac{1}{2p^3} \cdot \\ &\supset \frac{n!}{2^n (k_1 \dots k_n)^3} \lambda \binom{n}{2} \frac{1}{6\pi^2} \left(\log \frac{2k}{aH} + \gamma_E - 2 \right) \log \frac{[aH]}{K}. \end{aligned} \quad (4.195)$$

The term of interest in this expression is the log divergence, which is multiplied $\binom{n}{2}$. We see this coefficient is scheme dependent as this result differs slightly from the result using dynamical dim reg in Eq. (4.120).

We can extend this to order λ^2 using

$$\left\langle \varphi_+^2[0] \varphi_+(\vec{k}_1) \dots \varphi_+(\vec{k}_4) \right\rangle = \int \frac{d^3 p}{(2\pi)^3} \left\langle \varphi_+(\vec{p}) \varphi_+(-\vec{p}) \varphi_+(\vec{k}_1) \dots \varphi_+(\vec{k}_4) \right\rangle. \quad (4.196)$$

We will evaluate this expression for $k_i \ll p$, which is a different limit of the 6-point function as compared to the previous calculation. We also want to isolate the piece proportional to $P_+(k_1) \dots P_+(k_4)$, so we can simply isolate a subgraph that looks just like two mass insertions:

$$\left\langle \varphi_+(\vec{p}) \varphi_+(-\vec{p}) \varphi_+(\vec{k}_1) \dots \varphi_+(\vec{k}_4) \right\rangle \supset \Gamma_{2,4}(p) P_+(k_1) \dots P_+(k_4), \quad (4.197)$$

with

$$\begin{aligned} \Gamma_{2,4}(p) &= \int^\tau \frac{d\tau_1}{(-\tau_1)^4} \int^\tau \frac{d\tau_2}{(-\tau_2)^4} \left\langle \phi^2(p, \tau_1) \phi^2(p, \tau) \phi^2(p, \tau_2) \right\rangle \\ &\quad - 2\text{Re} \int^\tau \frac{d\tau_1}{(-\tau_1)^4} \int^{\tau_1} \frac{d\tau_2}{(-\tau_2)^4} \left\langle \phi^2(p, \tau) \phi^2(p, \tau_1) \phi^2(p, \tau_2) \right\rangle. \end{aligned} \quad (4.198)$$

By direct calculation we find that

$$\begin{aligned} \Gamma_{2,4}(p) &= \frac{1}{216p^3} \left[16 + 4\gamma_E(-11 + 3\gamma_E) + 3\pi^2 + 4(-11 + 6\gamma_E + 3\log 2) \log 2 \right. \\ &\quad \left. + O\left(\log \frac{p}{[aH]}\right) \right], \end{aligned} \quad (4.199)$$

which agrees with Eq. (4.128) above. This calculation is illustrated in terms of Witten and Feynman diagrams as shown in Fig. 4.5. Performing the momentum integral, we find

$$\int \frac{d^3p}{(2\pi)^3} \Gamma_{2,4}(p) = \frac{1}{2\pi^2} \log \frac{aH}{K} \left[b_{2,4} + O\left(\log \frac{aH}{K}\right) \right] + \text{finite}, \quad (4.200)$$

where

$$b_{2,4} = \frac{\lambda^2}{216} \left[16 + 4\gamma_E(3\gamma_E - 11) + 3\pi^2 + 4\log 2(6\gamma_E + 3\log 2 - 11) \right]. \quad (4.201)$$

Two Loops

The two-loop mixing of φ_+^3 and φ_+ is calculated using

$$\langle \varphi_+^3[0] \varphi_+(\vec{k}) \rangle = \int \frac{d^3 p_1 d^3 p_2 d^3 p_3}{(2\pi)^9} \langle \varphi_+(\vec{p}_1) \varphi_+(\vec{p}_2) \varphi_+(\vec{p}_3) \varphi_+(\vec{k}) \rangle, \quad (4.202)$$

see Eq. (4.129). When we use a hard cutoff as the regulator, we may use the tree-level four-point function with all massless fields:

$$\begin{aligned} \langle \varphi_+(\vec{p}_1) \varphi_+(\vec{p}_2) \varphi_+(\vec{p}_3) \varphi_+(\vec{k}) \rangle'_{\text{IC}(1)} &\simeq \frac{\lambda}{8(p_1 p_2 p_3 k)^3} \left[\left(\sum_i p_i^3 \right) \frac{1}{3} \left(\log \frac{p_t}{p_i} + \gamma_E + \frac{1}{3} - 2 \right) \right. \\ &\quad \left. - \frac{1}{9} p_t^3 + 2 \sum_{i < j < \ell} p_i p_j p_\ell + \frac{1}{3} p_t \left(\sum p_i^2 - \sum_{i < j} p_i p_j \right) \right]. \end{aligned}$$

where $p_t \equiv p_1 + p_2 + p_3$. Here we have assumed $k/p_i \ll 1$ and kept only the leading terms in this expansion since higher orders will not contribute to the mixing. Expanding this out and (implicitly) imposing the momentum conserving δ -function so that $\vec{p}_3 = -\vec{p}_1 - \vec{p}_2$ we get

$$\langle \varphi_+^3[0] \varphi_+(\vec{k}) \rangle \simeq \lambda P_+(k) \int \frac{d^3 p_1 d^3 p_2}{(2\pi)^6} \frac{1}{12(p_1 p_2 p_3)^3} \left(\sum_i \kappa_i p_i^3 - p_1 p_2 p_3 + \sum_{i \neq j} p_i^2 p_j \right), \quad (4.203)$$

where $\kappa_i = \log p_t/p_i + \gamma_E + 1/3 - 2$. The first term (proportional to κ) factorizes into two logarithmically divergent integrals. The only single log comes from the second term, which can be evaluated using a change of variables

$$\int \frac{d^3 p_1 d^3 p_2}{(2\pi)^6} = \int \frac{d^3 p_1}{(2\pi)^3} p_1^3 \frac{3!}{(2\pi)^2} \int_{1/2}^1 dx_2 \int_{1-x_2}^{x_2} dx_3 x_2 x_3, \quad (4.204)$$

where $x_2 = p_2/p_1$ and $x_3 = p_3/p_1$. We then get

$$\begin{aligned}
\langle \varphi_+^3[0] \varphi_+(\vec{k}) \rangle &\supset -\frac{\lambda}{12} P_+(k) \int \frac{d^3 p_1}{(2\pi)^3} \frac{1}{p_1^3} \frac{3!}{(2\pi)^2} \int_{1/2}^1 dx_2 \int_{1-x_2}^{x_2} dx_3 \frac{1}{x_2 x_3} \\
&= -\frac{\lambda}{12} \frac{3!}{(2\pi)^2} \frac{\pi^2}{12} P_+(k) \int \frac{d^3 p_1}{(2\pi)^3} p_1^3 \\
&= -\frac{\lambda}{192\pi^2} P_+(k) \left(\log \frac{[aH]}{K} \right). \tag{4.205}
\end{aligned}$$

We see this result matches the result using dynamical dim reg from the main text given in Eq. (4.133). This is a further confirmation that the d_0 coefficient in Eq. (4.135) is scheme independent.

Finally, we will argue that the third term in Eq. (4.203) will produce a \log^2 in this description, and therefore does not contribute to the RG. If we define

$$\rho(a, b, c) = \int \frac{d^3 p_1 d^3 p_2}{(2\pi)^6} \frac{1}{p_1^{2a} p_2^{2b} p_3^{2c}}, \tag{4.206}$$

then the final term corresponds to taking $a = 3/2$, $b = 1$ and $c = 1/2$, plus permutations thereof.

We can use the methods discussed in the main text to calculate $\rho(a, b, c)$ as

$$\int \frac{d^3 p_1 d^3 p_2}{(2\pi)^6} = \int \frac{d^3 p_1}{(2\pi)^3} p_1^3 \frac{3!}{(2\pi)^2} \int_{1/2}^{1-\varepsilon} dx_2 \int_{1-x_2}^{x_2} dx_3 x_2 x_3 \frac{1}{x_2^{2b} x_3^{2c}}, \tag{4.207}$$

where we have included an additional regulator ε to address additional divergences that do not appear in the p_1 integral.

$$\rho(3/2, 1, 1/2) + \text{permutations} = \frac{1}{2\pi^2} \log([aH]/K) \times \log \varepsilon \propto (\log aH)^2. \tag{4.208}$$

The sum over permutations is essential in this calculation as the split into p_1 , x_2 and x_3 breaks the manifest permutation invariance of the measure of integration, which is only valid if the integrand itself is permutation invariant. This calculation reproduces the result from the main

text where this contribution is \log^2 , although the need for two separate regulators makes this less transparent.

Chapter 5

A Tail of Eternal Inflation

5.1 Introduction

Developing a complete picture of physics in de Sitter space remains one of the great unsolved problems in theoretical physics [5, 122, 123]. The issues appear in many guises. On the practical side, we do not have a rigorous (non-perturbative) definition of cosmological observables [5, 124]. More conceptually, confusions abound when attempting to characterize the eternal inflating phase [94, 95, 96]. Meanwhile, these significant challenges do not seem to impede our ability to make quantitative predictions for the universe we inhabit. Weak coupling allows us to calculate and understand the structure of observable correlation functions as a controlled approximation. Yet, our goal in this paper is to demonstrate, for the first time, that there are fundamental questions about our own patch of the universe whose answers are not calculable in perturbation theory, *e.g.* the possibility that our universe is eternally inflating.

Cosmological observations suggest that the large scale structures in our universe were seeded during inflation, a period of quasi-de Sitter expansion [125, 126, 127]. The observable implications of inflation can be captured by an Effective Field Theory (EFT) framework [128, 129]. Much progress has been made in understanding how to calculate the statistical predictions of inflation perturbatively [130, 102]. A notable recent advance is the cosmological bootstrap, which aims to reconstruct inflationary observables directly from locality and causality [48, 68, 131, 132, 133, 134, 135]. Much of the interest in the structure of cosmological correlators centers

on the possible signatures of primordial non-Gaussianity, since this provides an observational window into the particle content and interactions that played a role during inflation [58].

The fact that the observational and conceptual aspects of cosmology are decoupled is a simple consequence of dimensional analysis, which additionally underlies the validity of the EFT of Inflation approach. There is a significant separation between the two energy scales H and f_π that characterize inflation [136] (see also [137, 129, 138, 139, 140, 44, 141, 142, 143, 144, 145, 146, 1]), as illustrated in Fig. 5.1. The EFT of Inflation can be framed in terms of the spontaneous breaking of time translation symmetry, where the associated Goldstone boson π describes the scalar density fluctuations. The universal scale describing the dynamics of the fluctuations is $f_\pi^2 \simeq |\dot{\phi}|$, where $\dot{\phi} \neq 0$ is the order parameter for the breaking of time translation invariance, and ϕ is a fundamental scalar in most concrete UV models. Typical de Sitter fluctuations are produced with a characteristic energy set by the Hubble parameter during inflation H , which results in there being a de Sitter temperature $2\pi T_{\text{dS}} = H$. In more detail, an emergent scalar degree of freedom ζ experiences adiabatic fluctuations, whose amplitude is $2\pi^2 A_s \equiv \Delta_\zeta = H^4 / (2f_\pi^4)$. In our patch of the universe, measurements of the cosmic microwave background imply $A_s = 2.1 \simeq 10^{-9}$ [147], and so we can infer $f_\pi \simeq 59H$. This tells us that $f_\pi \gg H$ is a good approximation in our universe. As we explore the physics of de Sitter space and the relation to eternal inflation in this work, we will also consider f_π and H to be free parameters, for example the parameter space where $f_\pi \simeq H$.

Primordial non-Gaussianity in single-field inflation arises through derivative interactions that are suppressed by some dimensionful UV scale Λ .¹ While the precise relationship to the amplitude of equilateral non-Gaussianity $f_{\text{NL}}^{\text{eq}}$ varies among different possible models, the scaling relation $f_{\text{NL}}^{\text{eq}} \simeq f_\pi^2 / \Lambda^2$ is universal. Given the current constraints from Planck, $f_{\text{NL}}^{\text{eq}} = -26 \pm 47$ (68% confidence interval) [2], the region of parameter space where $\Lambda^2 \ll f_\pi^2$ remains a viable

¹Here we are assuming scale invariant non-Gaussianity. Scale dependent signals [148], such as models of resonant non-Gaussianity [149], are also possible. As these model also leave signatures in the power spectrum [150, 54, 151], we will not consider them further to ensure a clean separation between the Gaussian and non-Gaussian effects.

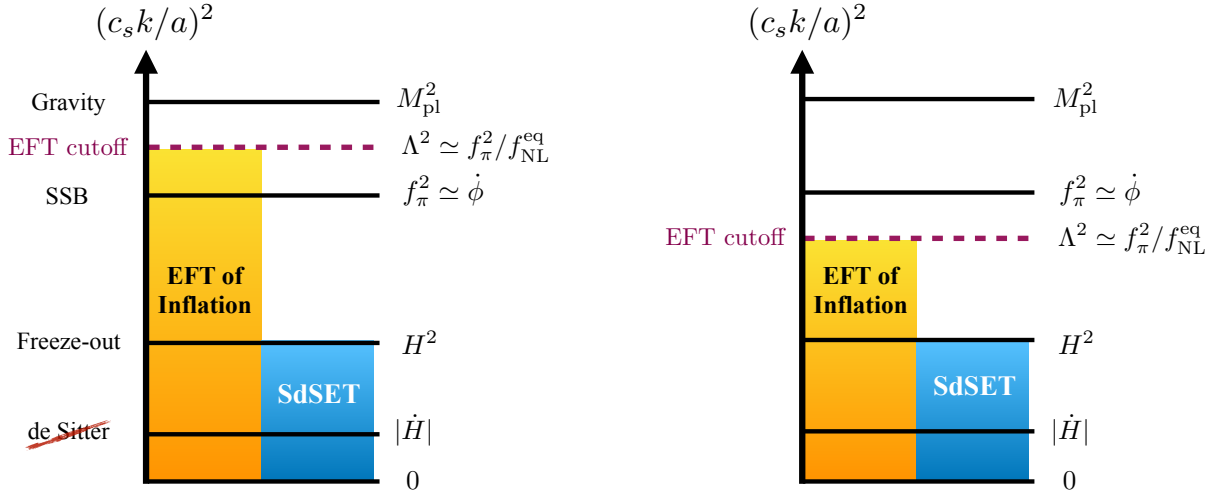


Figure 5.1. The relevant energy scales for single field inflation and the regimes of validity of the EFT of Inflation [orange] and Soft de Sitter Effective Theory (SdSET) [blue]. The background time evolution leads to a scale f_π , below which the time translation symmetry is spontaneously broken (SSB). Primordial non-Gaussianity arises from interactions that are suppressed by the EFT cutoff scale Λ , which is related to the amplitude for equilateral non-Gaussianity $f_{\text{NL}}^{\text{eq}}$ by $\Lambda^2 \simeq f_\pi^2/f_{\text{NL}}^{\text{eq}}$. Requiring the EFT of Inflation is weakly coupled at horizon crossing allows both $\Lambda > f_\pi$ [left] and $\Lambda < f_\pi$ [right]. Deviations from a de Sitter background arise at $|\dot{H}| \ll H^2$.

possibility. On the other hand, canonical models of slow roll inflation require that $f_{\text{NL}}^{\text{eq}} < 1$ so that the background evolution $\dot{\phi}$ is calculable in the weakly coupled regime [152, 143, 144]. Nevertheless, a number of compelling models such as DBI inflation [8], models that utilize non-trivial field space curvature [153, 154], and those involving interactions with massive fields [155, 117] can easily produce $f_{\text{NL}}^{\text{eq}} \gg 1$ self-consistently. It is only essential that $\Lambda > H$ in order to reliably calculate the observational predictions using perturbation theory [136]. In this work, we revisit whether $\Lambda > H$ is sufficient to ensure perturbative control over all quantities of interest.

For cosmological correlators, all of the thorny issues of observables in de Sitter are under control as long as one is in the perturbative regime where H^2/M_{pl}^2 , H^2/f_π^2 , and H^2/Λ^2 are all small. To an excellent approximation, inflation is described by a fixed background geometry in which the scalar fluctuations evolve. In the absence of non-Gaussianity, even the onset of slow-roll eternal inflation is calculable and arises when $\Delta_\zeta \geq \pi^2/3$ [97]. Building on this,

one might expect then that the phase transition to eternal inflation in models with primordial non-Gaussianity can also be calculated as a perturbative expansion in H^2/Λ^2 . Remarkably, this intuition is wrong. We will show that there are corrections to the expansion that scale as f_π^2/Λ^2 , even when $f_\pi^2 \gg H^2$ ($\Delta_\zeta \ll 1$) where we might expect eternal inflation does not occur. This implies that when $\Lambda \ll f_\pi$, there are important observables associated with the inflationary epoch that are incalculable in the EFT of Inflation [128, 129]. Furthermore, this incalculability is not simply due to the breakdown of the EFT itself, since all the N -point correlators are calculable in perturbation theory. Our goal is to demonstrate this result and explain why it occurs.

At a qualitative level, the onset of slow-roll eternal inflation occurs when the amplitude of quantum fluctuations exceeds that of classical motion of the field [94, 95]. In canonical slow-roll inflation $f_\pi^2 = \dot{\phi}$, so that the classical distance moved in a Hubble time ($\Delta t = H^{-1}$) is $(\Delta\phi)_{\text{classical}} \simeq f_\pi^2/H$. Meanwhile, the Gaussian *quantum* fluctuation introduce an effective noise in the motion of the field with an amplitude set by the expansion rate, $(\Delta\phi)_{\text{noise}} \simeq H$. Slow-roll eternal inflation occurs when these two types of field excursions are of the same order, $(\Delta\phi)_{\text{classical}} \simeq (\Delta\phi)_{\text{noise}}$, which happens when $H^2 \simeq f_\pi^2$ or equivalently when $\Delta_\zeta \simeq 1$. However, implicit to this argument is that the rate for generating fluctuations that are larger than H is negligible. If instead there was a non-negligible rate for quantum fluctuations from the tail of the distribution such that $(\Delta\phi)_{\text{tail}} \simeq f_\pi^2/H$ with $f_\pi > H$, these larger quantum fluctuations could be the dominant effect that would determine the onset of eternal inflation. The probability of such a large fluctuation is exponentially small for Gaussian theories. However, primordial non-Gaussianity could, in principle, increase the rate of these large fluctuations such that they dominate the onset of eternal inflation. Noting that the energy scale associated with such non-Gaussian quantum fluctuations is $(\dot{\phi})_{\text{tail}} \simeq H(\Delta\phi)_{\text{tail}} \simeq f_\pi^2$, these fluctuations would correspond to physics above the UV cutoff for models with $\Lambda < f_\pi$.

In this paper, we use Soft de Sitter Effective Theory² (SdSET) [65, 66] to calculate

²While the EFT of Inflation and SdSET have overlapping regions of validity, SdSET makes manifest the long wavelength behavior of the fluctuations in the universe, particularly with regards to IR divergences and their resummation via the dynamical renormalization group (RG). This property of SdSET is essential for deriving the

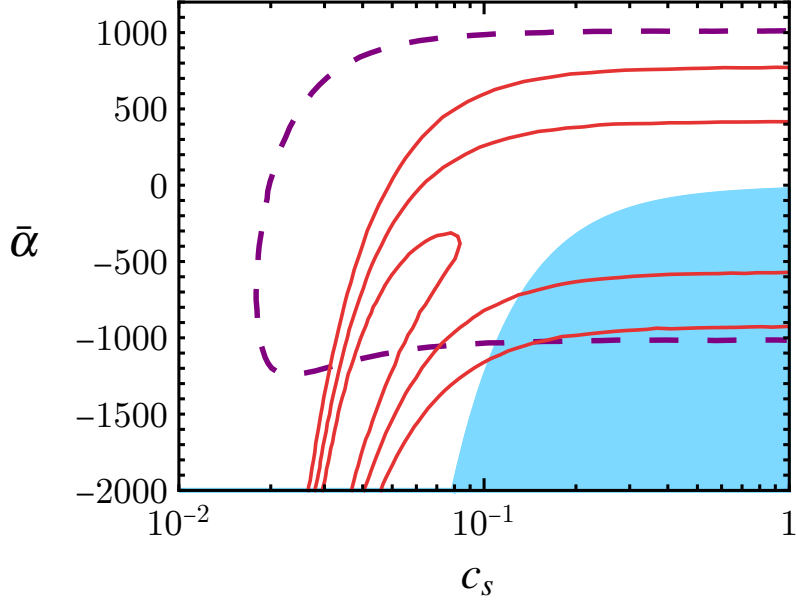


Figure 5.2. The solid blue region shows where primordial non-Gaussianity naively implies eternal inflation, suggesting a breakdown of Stochastic Inflation and/or the EFT of Inflation. The region allowed by perturbative unitarity at horizon crossing, derived in [1], corresponds to the region enclosed by the dashed purple line. The current 1-,2- and 3- σ limits from Planck [2] are shown as solid red lines. We see there is a significant region where the calculation of the transition to external inflation is breaking down, that is nonetheless consistent with the theory being weakly coupled at horizon crossing (as determined by unitarity) and current observations. The parameters $\bar{\alpha}$ and c_s are related to the two allowed cubic couplings in the EFT of Inflation, as defined in Sec. 5.3. Perturbative unitarity as defined in [1] is particularly conservative and may explain why regions of parameter space allowed by Planck are excluded. We simply wish to emphasize that there are regions of parameter space in blue that are perturbative even by that definition.

corrections to Stochastic Inflation [11] (see also [79, 156, 23, 80, 112, 33, 113, 114, 157, 115, 116, 111, 110]), which allows us to demonstrate that the onset of eternal inflation is incalculable when $\Lambda < f_\pi$. This occurs because large field variations (corresponding to the tail of the probability distribution) are probes of high energy physics during inflation. When $\Lambda < f_\pi$, the onset of eternal inflation is sensitive to the regime where the EFT does not apply. Concretely, the blue shaded region in Fig. 5.2 naively corresponds to eternal inflation in our universe and signals this breakdown. Interestingly, this parameter space overlaps the regions allowed by current

results in this paper.

observations and weak coupling at horizon crossing. The source of the issue is that correctly modeling the tails of the probability distributions requires a non-perturbative calculation of the transition probabilities that go beyond the perturbative contributions that are included in the Stochastic Inflation framework. We interpret the blue region as providing a sharp bound, akin to a perturbative unitarity bound at the energy scale f_π . Otherwise, as we show below, the EFT predictions would be inconsistent with interpreting the de Sitter entropy [158] as resulting from a finite number of degrees of freedom (see *e.g.* [122, 99, 100, 159, 123, 160, 161]).

This work adds a novel direction to the vast literature on the perturbative regime inflationary fluctuations [137, 138, 139, 140, 44, 136, 141, 142, 143, 144, 145, 146, 1] and the implications for eternal inflation [162, 98, 35, 163, 164, 165]. Prior discussions of eternal inflation are relevant for the parameter space with $f_\pi \simeq H$ ($\Delta_\zeta = \mathcal{O}(1)$), as this is the only regime of canonical slow-roll inflation where eternal inflation can occur. In any parameter regime, it is a necessary condition that the theory is weakly coupled at horizon crossing, $\Lambda > H$, for calculations to be under control. In the context of previous discussions of eternal inflation where $f_\pi \simeq H$, the breakdown of weak coupling at horizon crossing is indistinguishable from the breakdown of the Stochastic framework. In contrast, most of the discussion in our paper applies to our own observable universe where $f_\pi \simeq 59H$ ($\Delta_\zeta \simeq 4.1 \times 10^{-8}$), and where the theories of inflation of interest are weakly coupled at horizon crossing. One would not expect eternal inflation in this regime. However, although much is known about the structure of Stochastic Inflation in canonical slow roll models [11, 79, 156, 23, 80, 112, 33, 113, 114, 157, 115, 116, 111, 110], before this work it was not known how to include the non-Gaussian corrections into the Stochastic Inflation framework. These are exactly the new ingredients that are required to ask questions about the phase transition to eternal inflation.

Our concrete results will show that there is a breakdown in the calculation that is signaled by the apparent onset of eternal inflation in the regime $f_\pi \gg H$. This failure of Stochastic Inflation is only relevant when attempting to predict the tail of the distribution of scalar fluctuations and is distinct from having control over perturbative calculations at horizon crossing. While it is

known that the tails of the distribution can break down using typical perturbative methods (see *e.g.* [166]), Stochastic Inflation is a resummation of the perturbative results [65, 66] that has been used to calculate the tail of the probability distribution in a variety of models (see *e.g.* [167] for review). For example, the tail of the distribution of a particular class of two-field models was calculated using stochastic inflation in [168, 169]; yet, it is also known that this class of two field models reduces to the single field models we will discuss below when the second field is massive. In this precise sense, the unusual behavior of the tail of the distribution we will demonstrate in this paper is not a generic issue of perturbative calculations, but is instead a failure of a Stochastic Inflation in a regime where it had previously been successfully employed [136].

The paper is organized as follows. In Sec. 5.2, we calculate the first higher derivative correction to Stochastic Inflation from primordial non-Gaussianity in Single-Field Inflation. In Sec. 5.3, we solve these corrected equations and use the results to compute the onset of eternal inflation. We apply these results to interpretation of the de Sitter entropy in Sec. 5.4. In Sec. 5.5, we interpret the surprising dependence on non-Gaussian fluctuation as a breakdown of Stochastic Inflation requiring a UV calculation of the underlying transition amplitudes. We conclude in Sec. 5.6. Two appendices give background for these results. In Sec. 5.A, we review aspects of single field inflation that are essential for understanding the key results in this paper. In Sec. 5.B, we provide an alternate derivation of our solution to the corrected Fokker-Planck equation using the Fourier transform and the method of steepest descents.

5.2 Non-Gaussian Corrections to Stochastic Inflation

Light scalar fields in quasi de Sitter space, such as the inflaton, undergo random quantum fluctuations. In perturbation theory, these fluctuations give rise to large infrared (IR) effects, which can be resummed using the framework known as Stochastic Inflation [11, 79, 80]. This gives rise to a Fokker-Planck equation that determines the evolution of the probability distribution for the local value of the field.

The canonical formation of Stochastic Inflation provides a leading order prediction for the field's evolution. Interactions correct the Fokker-Planck equation at higher orders, which can be represented on general grounds as [66] (see also [31, 92])

$$\frac{\partial}{\partial t} P(\phi, t) = \sum_{n=2}^{\infty} \frac{1}{n!} \frac{\partial^n}{\partial \phi^n} \left[\sum_{m=0}^{\infty} \frac{1}{m!} \Omega_n^{(m)} \phi^m P(\phi, t) \right] + \frac{1}{3H} \frac{\partial}{\partial \phi} [V'(\phi) P(\phi, t)] . \quad (5.1)$$

The term proportional to $V'(\phi)$ is just the classical evolution of the field, and the rest of the terms account for the quantum fluctuations. The original formulation due to Starobinski applies to leading order in the coupling,³ in which case the quantum noise is given by $\Omega_2^{(m=0)} = H^3/(8\pi^2)$ with all other $\Omega_n^{(m)} = 0$.

Given the intuitive description of Stochastic Inflation, it might seem surprising that calculating these higher order corrections remained elusive until recently [31, 92, 66]. It had often been suggested that the Stochastic framework is related to IR divergences in dS [88, 89, 43, 90, 91, 30, 31, 32, 81, 65, 92, 93]. Leveraging this insight to systematically improve the framework naturally results in the SdSET approach [65]. The SdSET converts the full theory IR divergences into EFT UV divergences in the usual sense (see *e.g.* [170]). This allows one to resum full theory IR divergences using the usual RG playbook within the EFT. Specifically, Stochastic Inflation is equivalent to the (dynamical) RG for SdSET composite operators. The contributions from the quantum noise can be extracted from operator mixing under time evolution, which takes the generic form

$$\frac{\partial}{\partial \mathfrak{t}} \langle \varphi_+^N \rangle = \sum_{m=0}^{\infty} \sum_{n=1}^{N+m} \tilde{\Omega}_n^{(m)} (-1)^n \binom{N}{n} \langle \varphi_+^{N-n+m} \rangle , \quad (5.2)$$

where for a massless scalar field ϕ , we identify φ_+ as the growing mode mode such that $\phi \rightarrow H\varphi_+$. We also defined $\mathfrak{t} = Ht$ and $\tilde{\Omega}_n^{(m)} = H^{m-n-1} \Omega_n^{(m)}$ to simplify the expression in terms of φ_+ . Finally, $V'(\phi)$ is replaced by $\tilde{\Omega}_1^{(m)}$, which also receives corrections at higher orders.

³See *e.g.* [66] for a derivation of the power counting for Stochastic Inflation.

5.2.1 Stochastic Inflation for Single Field Inflation

The first higher-derivative correction to this framework was calculated in [66] assuming the UV model was $\lambda\phi^4$ in fixed dS. We will now extend these results to single-field inflation. This is a non-trivial generalization both because the metric fluctuates (the background is no longer fixed dS), and these fluctuations are subject to additional constraints from the diffeomorphism invariance. The corrections to Stochastic Inflation are most transparent when expressed in terms of the scalar metric fluctuation ζ . This choice is particularly useful because ζ transforms non-linearly under large diffeomorphisms [7, 24, 171, 22]

$$D_{\text{NL}} : \delta\zeta = -1 - \vec{x} \cdot \vec{\partial}_{\vec{x}} \zeta \tag{5.3a}$$

$$K_{\text{NL}}^i : \delta\zeta = -2x^i - 2x^i \left(\vec{x} \cdot \vec{\partial}_{\vec{x}} \zeta \right) + x^2 \partial^i \zeta . \tag{5.3b}$$

The Ward identities associated with these symmetries [172, 173] impose constraints on correlation functions that are also known as the single field consistency conditions [7, 24]. The above transformation uniquely fixes the definition of ζ , and it ensures our results will be free from field redefinition ambiguities and scheme dependence [174]. The important implication for our purposes here is that these non-linearly realized symmetries fix the form of possible corrections to the Stochastic Inflation framework. This is already known for the properties of $\zeta(\vec{x})$ at separated points, where it leads to the all-orders conservation of $\zeta(\vec{k})$, namely $\zeta(\vec{k}) \rightarrow 0$ as an operator statement in the limit $k/(aH) \rightarrow 0$ [23, 20, 19, 65]. From Eq. (5.2), we see that applying these symmetries to Stochastic Inflation is the same as extending the operator statements to products of ζ 's at coincident points, *i.e.*, composite operators built from ζ .

By power counting in the SdSET, the dynamical RG of any light field is necessarily ultra-local in space, in that it contains no derivatives. This implies that the most general possible

result must take the form

$$\frac{\partial}{\partial \mathbf{t}} \zeta^N(\vec{x}, \mathbf{t}) = \sum_M \Gamma_M^N(\mathbf{t}) \zeta^M(\vec{x}, \mathbf{t}) . \quad (5.4)$$

Applying D_{NL} from Eq. (5.3a) to the both sides of the equation implies

$$\frac{\partial}{\partial \mathbf{t}} N \zeta^{N-1}(\vec{x}, \mathbf{t}) = \sum_M M \Gamma_M^N(\mathbf{t}) \zeta^{M-1}(\vec{x}, \mathbf{t}) . \quad (5.5)$$

Substituting Eq. (5.4) on the left-hand side yields

$$N \sum_M \Gamma_M^{N-1}(\mathbf{t}) \zeta^M(\vec{x}, \mathbf{t}) = \sum_M M \Gamma_M^N(\mathbf{t}) \zeta^{M-1}(\vec{x}, \mathbf{t}) . \quad (5.6)$$

Matching the powers of ζ , we find

$$(N+1)\Gamma_M^N = (M+1)\Gamma_{M+1}^{N+1} . \quad (5.7)$$

We demand $\Gamma_M^N = 0$ if $N < 0$ or $M < 0$, since operators with fields in the denominator are unphysical. If we assume $N > 0$ and the existence of a first non-zero anomalous dimension $\Gamma_0^n \equiv \gamma_n \neq 0$ for some n , the solution to Eq. (5.7) becomes

$$\Gamma_M^N = \gamma_n \delta_{M, N-n} \prod_{\ell=n+1}^N \frac{\ell}{\ell-n} = \binom{N}{n} \gamma_n \delta_{M, N-n} . \quad (5.8)$$

Summing over all possible γ_n , we have

$$\frac{\partial}{\partial \mathbf{t}} \zeta^N(\vec{x}, \mathbf{t}) = \sum_n \gamma_n \binom{N}{n} \zeta^{N-n}(\vec{x}, \mathbf{t}) . \quad (5.9)$$

Finally, we apply the relation between the operator mixing language and Stochastic Inflation (see

e.g. [66]), which leads to the following general form for the time evolution of the probability distribution of ζ :

$$\frac{\partial}{\partial \tau} P(\zeta, \tau) = \sum_{n \geq 2} (-1)^n \frac{\gamma_n}{n!} \frac{\partial^n}{\partial \zeta^n} P(\zeta, \tau). \quad (5.10)$$

This result makes intuitive sense: in order to preserve the nonlinear symmetry, the generalization of the Fokker-Planck equation can only depend on derivatives of ζ (no explicit factors of ζ appear).

We see from the above result, that we can calculate all corrections to Stochastic Inflation from the mixing coefficients $\zeta^n \rightarrow \mathbb{1}$, where $\mathbb{1}$ is the identity operator. For $n = 2$, this is the usual Gaussian (quantum) noise contribution to Stochastic Inflation such that

$$\int \frac{d^3 k}{(2\pi)^3} \langle \zeta(\vec{k}) \zeta(\vec{k}') \rangle = 2\gamma_2 \log aH/K \quad \rightarrow \quad \gamma_2 = \frac{\Delta_\zeta}{4\pi^2}, \quad (5.11)$$

where K is an IR regulator and Δ_ζ is the amplitude of the power spectrum,⁴

$$\langle \zeta(\vec{k}) \zeta(\vec{k}') \rangle = \Delta_\zeta k^{-3+(n_s-1)} (2\pi)^3 \delta(\vec{k} + \vec{k}'). \quad (5.12)$$

Previous studies of stochastic effects in single-field inflation were limited to this contribution and the classical drift from the potential.

We are interested in computing the leading non-Gaussian contribution, which starts at $n = 3$. As we are simply calculating the mixing of operators under dynamical RG, the coefficient of the $n = 3$ term is determined by the logarithmic divergence in the two point function of ζ^3 and $\mathbb{1}$, *i.e.*, the one-point function of ζ^3 . This can be calculated, as illustrated in Fig. 5.3, from the bispectrum (three-point function) via

$$\langle \zeta^3(\vec{x} = 0) \rangle = \int \frac{d^3 k_1 d^3 k_2 d^3 k_3}{(2\pi)^3} \langle \zeta(\vec{k}_1) \zeta(\vec{k}_2) \zeta(\vec{k}_3) \rangle. \quad (5.13)$$

⁴Here we are defining Δ_ζ so that $\Delta_\zeta = 2\pi^2 A_s$ [175].

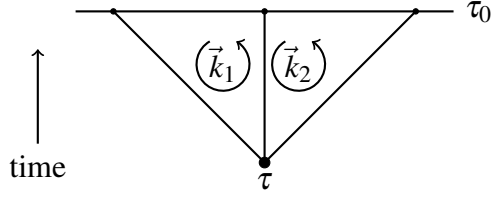


Figure 5.3. Illustration of the correlation function $\langle \zeta^3(\vec{x} = 0) \rangle$ represented as an integral over the bispectrum $B(k_1, k_2, k_3)$ computed at tree-level. The momentum integration is analogous to a two-loop integral.

In single-field inflation, there are two contributions to this three-point function arising from the $\dot{\zeta} \partial_i \zeta \partial^i \zeta$ and $\dot{\zeta}^3$ interactions, which are given by [176]

$$B_{\dot{\zeta}(\partial_i \zeta)^2}(k_1, k_2, k_3) = -\frac{1}{4} \left(1 - \frac{1}{c_s^2}\right) \Delta_\zeta^2 \times \frac{(24K_3^6 - 8K_2^2 K_3^3 K_1 - 8K_2^4 K_1^2 + 22K_3^3 K_1^3 - 6K_2^2 K_1^4 + 2K_1^6)}{K_3^9 K_1^3}, \quad (5.14)$$

and

$$B_{\dot{\zeta}^3}(k_1, k_2, k_3) = \left[6(c_s^2 - 1) + 8\frac{c_3}{c_s^2}\right] \Delta_\zeta^2 \frac{1}{K_3^3 K_1^3}, \quad (5.15)$$

where we have defined

$$\langle \zeta(\vec{k}_1) \zeta(\vec{k}_2) \zeta(\vec{k}_3) \rangle = B(k_1, k_2, k_3) (2\pi)^3 \delta(\vec{k}_1 + \vec{k}_2 + \vec{k}_3), \quad (5.16a)$$

$$B = B_{\dot{\zeta}(\partial_i \zeta)^2} + B_{\dot{\zeta}^3}, \quad (5.16b)$$

$$K_1 \equiv k_1 + k_2 + k_3, \quad K_2 \equiv (k_1 k_2 + k_2 k_3 + k_3 k_1)^{1/2}, \quad K_3 \equiv (k_1 k_2 k_3)^{1/3}. \quad (5.16c)$$

Defining $x_i = k_i/k_1$ and changing variables, we find

$$\begin{aligned} \langle \zeta^3(\vec{x} = 0) \rangle &= \int \frac{d^3 k_1}{(2\pi)^3} \frac{1}{k_1^3} \frac{3!}{(2\pi)^2} \int_{1/2}^1 dx_2 x_2 \int_{1-x_2}^{x_2} dx_3 x_3 B(1, x_2, x_3) \\ &= \frac{\log aH/K}{2\pi^2} \times \frac{\Delta_\zeta^2}{16\pi^2} \left(\left(1 - \frac{1}{c_s^2}\right) (9 + 3c_s^2) + \frac{c_3}{c_s^2} \right), \end{aligned} \quad (5.17)$$

where we have simply introduced a hard UV cutoff $k_1 = aH$ and an IR cutoff as $k_1 = K$ to regulate the log-divergence. This simple regulator breaks the symmetries of dS, and so we provide Sec. 5.A.2, which shows how to derive the same result using the symmetry preserving dynamical dimensional regularization approach.

The coefficient γ_3 is determined from the factor multiplying the log:

$$\gamma_3 = \frac{\Delta_\zeta^2}{32\pi^4} \left(\left(1 - \frac{1}{c_s^2}\right) (9 + 3c_s^2) + \frac{c_3}{c_s^2} \right), \quad (5.18)$$

so that

$$\frac{\partial}{\partial \tau} P_{\text{NG}}(\zeta, \tau) = \left(\frac{\Delta_\zeta}{8\pi^2} \frac{\partial^2}{\partial \zeta^2} - \frac{\Delta_\zeta^2}{192\pi^4} \left(\left(1 - \frac{1}{c_s^2}\right) (9 + 3c_s^2) + \frac{c_3}{c_s^2} \right) \frac{\partial^3}{\partial \zeta^3} \right) P_{\text{NG}}(\zeta, \tau). \quad (5.19)$$

This result is consistent with the interpretation that it is a small non-Gaussian correction: a typical fluctuation in the Gaussian limit is $\zeta \simeq \Delta_\zeta^{1/2}$, so if we assume $\partial/\partial\zeta \sim \Delta_\zeta^{-1/2}$, the first term is $\mathcal{O}(1)$ and the second term is $\mathcal{O}(\Delta_\zeta^{1/2}/c_s^2)$. We can rewrite this estimate in terms of the cutoff scale, using the relation $\Lambda = f_\pi c_s$:

$$\Delta_\zeta = \frac{1}{2} \frac{H^4}{f_\pi^4} \quad \Rightarrow \quad \gamma_3 \frac{\partial^3}{\partial \zeta^3} \simeq \frac{\Delta_\zeta^{1/2}}{c_s^2} = \frac{1}{\sqrt{2}} \frac{H^2}{\Lambda^2}. \quad (5.20)$$

This tells us that for typical fluctuations, the higher order corrections are suppressed by H^2/Λ^2 as one would expect.

5.3 Eternal Inflation and Non-Gaussian Tails

Now that we have the leading corrections to the Fokker-Planck equation in the presence of a non-trivial bispectrum, we want to apply this formalism to see how it impacts the onset of eternal inflation and the implications for the de Sitter entropy. Even without appealing to a microscopic description, we can define an order parameter for the end of inflation ϕ . Within the

EFT of Inflation, there is a natural choice [141]

$$\phi \equiv f_\pi^2(t + \pi) \simeq \frac{f_\pi^2}{H}(\tau - \zeta) , \quad (5.21)$$

where π is the Goldstone boson of the EFT of Inflation (see Appendix 5.A.1 for review) defined such that $\zeta = -H\pi + \mathcal{O}(\varepsilon\pi^2)$, where ε is the slow roll parameter, and f_π^2 is the decay constant for π . By construction $\langle \dot{\phi} \rangle = f_\pi^2$. Since we will be working in the limit $\varepsilon \rightarrow 0$, we can treat Eq. (5.21) as an exact relation to define ζ in terms of ϕ :

$$\zeta \equiv \tau - \frac{H}{f_\pi^2}\phi . \quad (5.22)$$

Here ϕ will be the field that defines the end of inflation so that $\phi \in (-\infty, 0)$ corresponds to the inflationary regime with inflation ending when $\phi = 0$. (Ending inflation at $\phi = 0$ simplifies expressions, but of course nothing can depend on this arbitrary choice).

To set the stage, we will review how one determines the onset of eternal inflation in the Gaussian case, $\gamma_3 = 0$. The evolution equation for ζ is

$$\frac{\partial}{\partial \tau} P_G(\zeta, \tau) = \frac{\Delta_\zeta}{4\pi^2} \frac{\partial^2}{\partial \zeta^2} P_G(\zeta, \tau) , \quad (5.23)$$

whose solutions are given by a Gaussian:

$$P_G(\zeta, \tau, \zeta_0) = \frac{1}{\sqrt{2\pi\sigma^2\tau}} e^{-(\zeta - \zeta_0)^2/(2\sigma^2\tau)} , \quad (5.24)$$

for any choice of the constant ζ_0 , and with $\sigma^2 \equiv \Delta_\zeta/(2\pi^2)$. We impose the initial condition $P_G(\zeta, \tau = 0, \zeta_i) = \delta(\zeta - \zeta_i)$ so that $\zeta = \zeta_i > 0$ ($\phi < 0$) at $\tau = 0$ in order to be consistent with Eq. (5.22). Since inflation ends when $\phi \geq 0$, we set $P(\phi[\zeta] \geq 0; \tau) = 0$ by hand. However, we must also impose the boundary condition that $P_G(\zeta, \tau, \zeta_i)$ is continuous at $\phi[\zeta] = 0$. Note that every choice of ζ_0 in the solution Eq. (5.24) gives a δ -function $\delta(\zeta - \zeta_0)$ at $\tau = 0$. In order

to impose our boundary condition at $\phi = 0$, we must add additional solutions in the region $\phi[\zeta] < 0$ with different values of $\zeta_0 < 0$ so that they naively produce a δ -function for $\phi > 0$ at $\tau = 0$. However, since we are imposing $P_G(\phi > 0, \tau) = 0$ by hand, adding these additional terms remains consistent with our initial conditions. A natural guess is that the solution takes the form

$$P_G(\phi[\zeta] < 0, \tau, \zeta_i) = \frac{1}{\sqrt{2\pi\sigma^2\tau}} \left[e^{-(\zeta - \zeta_i)^2/(2\sigma^2\tau)} - e^{-4\zeta_i/(2\sigma^2)} e^{-(\zeta + \zeta_i)^2/(2\sigma^2\tau)} \right], \quad (5.25)$$

where $\phi = 0$ corresponds to $\zeta = \tau$. This way of imposing the boundary conditions is typically called the method of images.

Now that we have the probability distribution, we can apply it to compute the onset of eternal inflation. Following [97], the probability that reheating occurs at time τ is determined by

$$p_{R,G}(\tau) = -\frac{d}{d\tau} \int_{-\infty}^0 d\phi P_G(\phi; \tau) \propto e^{-\tau/(2\sigma^2)}, \quad (5.26)$$

where we used the Fokker-Planck equation Eq. (5.23) and integrated by parts. From here we can calculate the average volume of the reheating surface,

$$\langle V \rangle_G = L^3 \int_0^\infty d\tau e^{3\tau} p_{R,G}(\tau) \simeq L^3 \int_0^\infty d\tau e^{\tau(3-1/(2\sigma^2))}. \quad (5.27)$$

where L^3 is the size of the initial patch at $\tau = 0$. The onset of eternal inflation occurs when this quantity diverges:

$$\sigma^2 = \frac{\Delta\zeta}{2\pi^2} > \frac{1}{6}. \quad (5.28)$$

In canonical slow-roll inflation, the perturbative description remains weakly coupled up to the phase transition and therefore this determination of the critical value of $\Delta\zeta$ is meaningful [97].

Now let us repeat this analysis for theories with primordial non-Gaussianity, $\gamma_3 \neq 0$. The

evolution is described by (see Eq. (5.10))

$$\frac{\partial}{\partial t} P_{\text{NG}}(\zeta, t) = \frac{\sigma^2}{2} \frac{\partial^2}{\partial \zeta^2} P_{\text{NG}}(\zeta, t) - \frac{\gamma_3}{3!} \frac{\partial^3}{\partial \zeta^3} P_{\text{NG}}(\zeta, t). \quad (5.29)$$

Building off the solution in Eq. (5.24), we can make the ansatz for the solution to this modified Fokker-Planck equation:

$$P_{\text{NG}}(\zeta, t, \zeta_0) = \exp\left(\frac{\kappa(t)}{3!} \frac{\partial^3}{\partial \zeta^3}\right) P_{\text{G}}(\zeta, t, \zeta_0). \quad (5.30)$$

Substituting this ansatz into Eq. (5.29) gives

$$\frac{d}{dt} \kappa(t) = -\gamma_3 \rightarrow \kappa(t) = -\gamma_3 t + \kappa_0. \quad (5.31)$$

We again impose the initial condition at $t = 0$, $\zeta = \zeta_i < 0$, and $P(\phi \geq 0) = 0$, so the solution takes the form

$$P_{\text{NG}}(\zeta, t, \zeta_i) = \exp\left(-\frac{\gamma_3 t}{3!} \frac{\partial^3}{\partial \zeta^3}\right) P_{\text{G}}(\zeta, t, \zeta_i) + \text{images}, \quad (5.32)$$

where the images are solutions with $\zeta_0 > 0$. While this can be solved in principle, a closed form solution to these equations is both unnecessary and beyond our scope. Specifically, the phase transition is determined by the behavior at $\phi = 0$ or $\zeta \rightarrow t$ in the limit $t \rightarrow \infty$. In this limit, we have

$$\frac{\partial^n}{\partial \zeta^n} P_{\text{G}}(\zeta, t, \zeta_0) \Big|_{\zeta=t} = \left(\frac{(-1)^n}{\sigma^{2n}} + \mathcal{O}(t^{-1})\right) P_{\text{G}}(\zeta, t, \zeta_0) \quad (5.33)$$

so that the Gaussian behaves as an eigenfunction of the derivative operator in the $t \rightarrow \infty$ limit. In this regime, the probability distribution for ζ becomes

$$\exp\left(-\frac{\gamma_3 t}{3!} \frac{\partial^3}{\partial \zeta^3}\right) P_{\text{G}}(\zeta; t, \zeta_0) \rightarrow \exp\left[\frac{\gamma_3}{3!} t \left(\frac{(\zeta - \zeta_0)}{\sigma^2 t}\right)^3 - \frac{(\zeta - \zeta_0)^2}{2\sigma^2 t}\right]. \quad (5.34)$$

This solution is also derived in Sec. 5.B using the method of steepest descents.

This probability distribution for ζ tells us that the large τ behavior for the probability of reheating is

$$p_{\text{R,NG}}(\tau) \propto \exp \left[-\tau \left(\frac{1}{2\sigma^2} - \frac{\gamma_3}{3!} \frac{1}{\sigma^6} \right) \right]. \quad (5.35)$$

Repeating the same argument from above to derive the onset of eternal inflation, we see that $\langle V \rangle_{\text{NG}}$ diverges when

$$\frac{1}{2\sigma^2} - \frac{\gamma_3}{3!} \frac{1}{\sigma^6} < 3. \quad (5.36)$$

Note that this result depends on the sign of γ_3 , which is not fixed. Using the explicit form of γ_3 given in Eq. (5.18) and $\sigma^2 = \Delta_\zeta / (2\pi^2)$, eternal inflation occurs when

$$\frac{1}{2} - \frac{1}{48} \left(\left(1 - \frac{1}{c_s^2} \right) (9 + 3c_s^2) + \frac{c_3}{c_s^2} \right) < \frac{3\Delta_\zeta}{2\pi^2}. \quad (5.37)$$

At this point, we notice something surprising. One might have expected that the Gaussian term would dominate when $H^2/\Lambda^2 \ll 1$. However, if we recall that $\Lambda = f_\pi c_s$, we can rewrite this expression as

$$\frac{1}{2} - \frac{1}{48} \frac{f_\pi^2}{\Lambda^2} \left((c_s^2 - 1) (9 + 3c_s^2) + c_3 \right) < \frac{3\Delta_\zeta}{2\pi^2}. \quad (5.38)$$

When computing the onset of eternal inflation, we see the corrections scale as $f_\pi^2/\Lambda^2 \gg H^2/\Lambda^2$. Taken at face value, this implies that for $c_s = 1$ ($c_s \ll 1$), eternal inflation occurred in our universe for $c_3 < 24$ ($c_3 < -9$). In Fig. 5.2, we compare this region to current observational constraints from Planck denoted by the red contours in Fig. 5.2 on the parameter space (taking $\Delta_\zeta \simeq 0$), in terms of c_s and

$$\bar{\alpha}_1 \equiv -\frac{4}{3} \frac{c_3}{c_s^2} - \frac{1}{2} \frac{(1 - c_s^2)^2}{c_s^2}. \quad (5.39)$$

The figure also shows conservative bounds on these parameters from perturbative unitarity at horizon crossing, derived in [1] (see Appendix 5.A.3 for a review of perturbative unitarity constraints on the EFT of Inflation).

Since the correction we calculated scales as f_π^2/Λ^2 it is natural to guess we have become sensitive to the cutoff scale for the EFT of Inflation. This suggests that we would become sensitive to even higher derivative corrections. We can estimate the size of these terms by dimensional analysis, using their relation to the connected correlators of ζ . Using our normalization of higher dimension operators in terms of Λ , we have

$$\gamma_n \simeq \sigma^n \left(\frac{H}{\Lambda} \right)^{2n-4}. \quad (5.40)$$

Extending the ansatz in Eq. (5.30) to include higher derivatives, we find

$$P(\zeta; \mathfrak{t}, \zeta_0) = \exp \left(\sum_{n>2} (-1)^n \frac{\gamma_n \mathfrak{t}}{n!} \frac{\partial^n}{\partial \zeta^n} \right) P_G(\zeta; \mathfrak{t}, \zeta_i) + \text{images}, \quad (5.41)$$

so that

$$p_R(\mathfrak{t}) \propto \exp \left[-\mathfrak{t} \left(\frac{1}{2\sigma^2} + \sum_{n>2} \frac{\gamma_n}{n!} \frac{1}{\sigma^{2n}} \right) \right]. \quad (5.42)$$

Again, we see that in the $\mathfrak{t} \rightarrow \infty$ limit, all the γ_n corrections contribute to coefficient of the exponential decay but do not change powers of \mathfrak{t} in the exponent. As a result, the reheating volume diverges when

$$\frac{1}{2} + \sum_{n>2} (-1)^n \frac{\gamma_n}{n!} \frac{1}{\sigma^{2n-2}} < 3\sigma^2. \quad (5.43)$$

Now we notice that the n^{th} term in the sum is

$$\frac{\gamma_n}{n!} \frac{1}{\sigma^{2n-2}} \simeq \frac{1}{n!} \frac{1}{\sigma^{n-2}} \left(\frac{H}{\Lambda} \right)^{2n-4} \frac{1}{\Delta_\zeta^{(n-1)/2}} \simeq \left(\frac{f_\pi}{\Lambda} \right)^{2n-4}. \quad (5.44)$$

Therefore, the series is under control for typical couplings when $\Lambda > f_\pi$.

On the other hand, when $\Lambda < f_\pi$, it is possible, in principle, to tune the coefficients of the higher order terms so that γ_3 is the dominant contribution. Yet, the fact that our results naturally organize into an expansion in f_π/Λ suggests that something more drastic is occurring

in the parameter space where $\Lambda < f_\pi$ that cannot be resolved by fine tuning. We will revisit this interpretation in Sec. 5.5.

5.4 The de Sitter Entropy and Microstate Counting

The interpretation of these corrections in the context of eternal inflation becomes even more more drastic when we apply them [122, 99, 100] to our interpretation of the de Sitter entropy [158],

$$S_{\text{dS}} = \frac{\pi}{H^2 G_{\text{N}}} = \frac{8\pi^2 M_{\text{pl}}^2}{H^2}, \quad (5.45)$$

where G_{N} is Newton's constant. During inflation, the de Sitter entropy is slowly changing as $H(t)$ decreases, such that

$$\frac{dS_{\text{dS}}}{dt} = \frac{dS_{\text{dS}}}{H dt} = -\frac{16\pi^2 M_{\text{pl}}^2 \dot{H}}{H^4} = \frac{4\pi^2}{c_s \Delta_\zeta}. \quad (5.46)$$

In analogy with the entropy of a black hole, it is natural to interpret this entropy as reflecting a finite number of degrees of freedom describing the microphysics of (quasi) de Sitter space. One crude test of this hypothesis is to compare the de Sitter entropy to the entropy of the fluctuations that are observable after inflation ends, following [122]. The number of Fourier modes that are being “created” (*i.e.*, crossing the horizon) per e-fold is simply the expansion rate

$$\frac{d \log N_{\text{modes}}}{dt} = 3. \quad (5.47)$$

If the de Sitter entropy is to be interpreted as resulting from the size of the Hilbert space describing the modes that live in de Sitter, $S_{\text{dS}} \propto \log N_{\text{states}}$, then we should be prevented from observing more than a de Sitter entropy's worth of Fourier modes, so that $N_{\text{modes}} < N_{\text{states}}$, which

implies

$$\int dt \frac{d \log N_{\text{modes}}}{dt} < \int dt \frac{dS_{\text{dS}}}{dt} . \quad (5.48)$$

Our general expectation is that $N_{\text{modes}} \ll N_{\text{states}}$ since the semi-classical fluctuations should capture only a small fraction of the gravitational microstates.

In the models of interest here, the integrands are nearly constant so that Eq. (5.48) holds at the level of the integrand:

$$\frac{d \log N_{\text{modes}}}{dt} = 3 < \frac{dS_{\text{dS}}}{dt} = \frac{4\pi^2}{c_s \Delta_\zeta} . \quad (5.49)$$

Naively, one can imagine violating this interpretation by taking

$$\Delta_\zeta > \frac{4\pi^2}{3c_s} . \quad (5.50)$$

However, to derive a contradiction, it should be unambiguous that all N_{modes} are independent and observable. This would be verifiable if inflation ended everywhere in the universe, allowing us a vantage point from which to reconstruct all of inflation. However, if inflation never ends, *i.e.*, we are eternally inflating, then these modes are not accessible to an observer. In canonical slow-roll inflation ($c_s = 1$ and $c_3 = 0$), the onset of eternal inflation was determined in Eq. (5.28). Therefore, a finite period of inflation always satisfies the inequality

$$\Delta_\zeta < \frac{\pi^2}{3} < \frac{4\pi^2}{3} . \quad (5.51)$$

As a result, we never encounter a regime where more than $e^{S_{\text{dS}}}$ modes are produced while maintaining control of the background in canonical slow-roll inflation.

In the presence of non-Gaussianity, the onset of eternal inflation is modified, potentially allowing a contradiction with this interpretation of the de Sitter entropy. In particular, demanding

a finite inflationary volume while violating our de Sitter entropy bound is possible when

$$\frac{\pi^2}{3} - \frac{\pi^2}{72} \left(\left(1 - \frac{1}{c_s^2}\right) (9 + 3c_s^2) + \frac{c_3}{c_s^2} \right) > \Delta_\zeta > \frac{4\pi^2}{3c_s}. \quad (5.52)$$

When $c_s \ll 1$, the left hand side of this equality scales as $1/c_s^2$, which easily allows a window where $\Delta_\zeta > 4\pi^2/(3c_s)$ without transitioning to eternal inflation. If we set $c_3 = 0$, this equality can be satisfied for any

$$c_s < 0.095. \quad (5.53)$$

When $c_3 \neq 0$ and $c_s \ll 1$, we can satisfy the inequality for $c_3 < 9$.

Rather than seeing this as a breakdown of the relation between the de Sitter entropy and the microstate counting, it is natural to interpret this as a breakdown of the EFT of Inflation. The likely possibility is that $c_s < 0.095$ is in the strongly coupled regime of the EFT of Inflation, telling us that we cannot trust the calculation of the onset of eternal inflation. Concretely, we can again rewrite this equality in terms of $\Lambda = c_s f_\pi$ as

$$\frac{\pi^2}{3} + \frac{\pi^2 f_\pi^2}{72 \Lambda^2} \left((1 - c_s^2) (9 + 3c_s^2) - c_3 \right) > \Delta_\zeta > \frac{4\pi^2}{3c_s}. \quad (5.54)$$

We can again only satisfy this inequality when $\Lambda^2 < f_\pi^2$, and in the case $c_s \ll 1$ we require $\Lambda^2 \ll f_\pi^2$. However, eternal inflation occurs when $\Delta_\zeta > 4\pi^2/(3c_s)$:

$$\frac{H^4}{f_\pi^4} > \frac{8\pi^2}{3c_s}. \quad (5.55)$$

This is only satisfied for $f_\pi < H$ and therefore the regime of interest is where $\Lambda^2 \ll H^2$. This strongly suggests that we cannot see more than a de Sitter entropy's worth of modes in the regime that is under control within the EFT of Inflation. We might even interpret $c_s > 0.095$ (when $\Delta_\zeta > \frac{4\pi^2}{3c_s}$) as a bound on the regime of validity of the EFT defined by the de Sitter entropy. We compare this to the bound from naively applying perturbative unitarity in Appendix 5.A.3 and

find good agreement. One may hope that a further exploration of the de Sitter entropy will bound the range of parameters in the EFT of Inflation directly from the cosmological background, complementing other approaches more similar to QFT in flat space [144, 177, 178].

5.5 On the Breakdown of Stochastic Inflation

By direct calculation, we have shown that the presence of primordial non-Gaussianity leads to a series of large corrections that can dramatically modify the onset of eternal inflation when $\Lambda < f\pi$. Our goal here is to make the case that this should be interpreted as a breakdown of Stochastic Inflation akin to the breakdown of the EFT of Inflation in the strong coupling regime. This should not prevent us from calculating the phase transition in a UV complete model. We can understand both issues by returning to the origins of Stochastic Inflation.

The Stochastic framework follows as a consequence of general Markovian evolution. For a scalar field ϕ , this evolution is described by

$$\frac{\partial}{\partial t}P(\phi, t) = \int d\Delta\phi \left[P(\phi - \Delta\phi, t)W(\phi|\phi - \Delta\phi) - P(\phi, t)W(\phi + \Delta\phi|\Delta\phi) \right], \quad (5.56)$$

where $W(\phi|\phi')$ is the transition amplitude for the field to jump from ϕ' to ϕ during the time dt . If these transition amplitudes are sufficiently “local,” we can Taylor expand Eq. (5.56) to get

$$\frac{\partial}{\partial t}P(\phi, t) = \sum_{n=1}^{\infty} \frac{1}{n!} \frac{\partial^n}{\partial \phi^n} \Omega_n(\phi) P(\phi, t), \quad (5.57)$$

where

$$\Omega_n(\phi) \equiv \int d\Delta\phi (-\Delta\phi)^n \tilde{W}(\Delta\phi, \phi), \quad (5.58)$$

and $\tilde{W}(y, x) \equiv W(x + y|x)$. For approximately Gaussian transition amplitudes, the moments of the distribution should be well defined, leading to a reasonable derivative expansion. Indeed, for the case of $\lambda\phi^4$ theory [66] and inflation (Sec. 5.2 above), we have verified that these coefficients are calculable by explicitly evaluating them.

Scalar metric fluctuations ζ are constrained by an additional non-linearly realized symmetry (Eq. (5.3)), which enforces that $W(\zeta|\zeta') = W(\zeta - \zeta')$ or $\tilde{W}(y,x) \equiv \tilde{W}(y)$. Using the expected scaling behavior for γ_n given in Eq. (5.40), we write

$$\gamma_n = g_n \sigma^n \left(\frac{H}{\Lambda} \right)^{2n-4}, \quad (5.59)$$

so that $g_n = \mathcal{O}(1)$ and

$$\frac{\partial}{\partial \mathfrak{t}} P(\zeta, \mathfrak{t}) = \left(\frac{\sigma^2}{2} \frac{\partial^2}{\partial \zeta^2} + \frac{\Lambda^4}{H^4} \sum_{n=3}^{\infty} (-1)^n \frac{1}{n!} g_n \left(\sigma \frac{H^2}{\Lambda^2} \frac{\partial}{\partial \zeta} \right)^n \right) P(\zeta, \mathfrak{t}), \quad (5.60)$$

This is the scaling behavior we would get from a transition amplitude of the form

$$W(\Delta\zeta) = \frac{1}{\sqrt{2\pi^2\sigma^2}} \exp \left[-\frac{(\Delta\zeta)^2}{2\sigma^2} \left(1 + \sum_{n>2} (-1)^n g_n \left(\frac{2\pi f_\pi^2(\Delta\zeta)}{\Lambda^2} \right)^{n-2} \right) \right], \quad (5.61)$$

where $\Delta\zeta \equiv \zeta - \zeta'$. This series expansion will break down when

$$\Delta\zeta > \frac{\Lambda^2}{2\pi f_\pi^2}, \quad (5.62)$$

or, using $\Delta\zeta = H\Delta\phi/f_\pi^2$,

$$H\Delta\phi > \frac{\Lambda^2}{2\pi}. \quad (5.63)$$

Notice that the expression on the left is $H\Delta\phi \simeq \dot{\phi}$. It is natural to interpret the large changes in the field over a Hubble time as a probe of the high energy limit of the theory $E \gg H$, which explains why we encounter the EFT cutoff scale Λ .

If the breakdown is indeed due to strong coupling within the EFT, we would expect that a large correction to the onset of eternal inflation would coincide with violations of perturbative unitarity at energies $E = f_\pi$. Since $f_\pi \gg H$, we can approximate the subhorizon region as flat space and can calculate the partial wave amplitudes for two-to-two scattering of ζ . These

amplitudes are provided in Sec. 5.A.3 along with their associated perturbative unitarity bounds. If we take $c_s = 1$, then s -wave scattering in the center of mass frame with incoming energies of $E = f_\pi$ is consistent with perturbativity when

$$-1.85 \leq c_3 \leq 0.85 . \quad (5.64)$$

For comparison, we saw that the non-Gaussian corrections naively imply an infinite reheating volume when $c_3 < 24$ (again for $c_s = 1$). In this sense, the breakdown of our intuition regarding eternal inflation is indeed tied to the breakdown of perturbative unitarity at $E = f_\pi$.

Ultimately, the question of whether or not a given model of inflation is eternally inflating should be calculable. However, clearly the method of calculating the correlation functions to determine equations of Stochastic Inflation is insufficient. Furthermore, nothing about the calculation of the individual correlation functions will change if we work in the UV completion (rather than the EFT). This is particularly clear when Stochastic Inflation is expressed in terms of ζ , so that all the coefficients are constants and can be calculated from the perturbative correlation functions.

5.5.1 Breakdown in DBI

For concreteness, DBI inflation [179] provides a useful analogy from which we can try to understand the breakdown of our calculation [136]. In DBI, the action is given by

$$\mathcal{L} = \Lambda^4 \sqrt{1 + \frac{\partial_\mu \phi \partial^\mu \phi}{\Lambda^4}} - V(\phi) . \quad (5.65)$$

The potential $V(\phi)$ generates a rolling field, $\phi = \dot{\phi}(t + \pi)$. Expanding the square root, we find

$$\Lambda^4 \sqrt{1 - \frac{\dot{\phi}^2(1 + 2\dot{\pi} - \partial_\mu \pi \partial^\mu \pi)}{\Lambda^4}} \rightarrow \sum_n \frac{1}{n!} M_n^4 (2\dot{\pi} - \partial_\mu \pi \partial^\mu \pi)^n , \quad (5.66)$$

where

$$M_n^4 = \Lambda^4 (-1)^n \left(\frac{\dot{\phi}^2}{\Lambda^4} \right)^n \frac{\partial^n}{\partial X^n} \sqrt{1-X} \Big|_{X=\dot{\phi}^2/\Lambda^4}, \quad (5.67)$$

and

$$\frac{c_s^2}{1-c_s^2} = 1 - \frac{\dot{\phi}^2}{\Lambda^4}, \quad (5.68)$$

so that $c_s \ll 1$ requires $\dot{\phi}^2 \simeq \Lambda^4$. Clearly in that limit, any process that involves a transition $\dot{\phi} \simeq H\Delta\phi > \Lambda^2$ will require the full DBI action. In fact, we see the Taylor expansion of Eq. (5.66) will break down when sooner, when

$$\frac{\dot{\phi}^2}{\Lambda^4} \left(2 \frac{\dot{\pi}_c}{f_\pi^2} - \frac{\partial_\mu \pi_c \partial^\mu \pi_c}{f_\pi^4} \right) \ll 1 - \frac{\dot{\phi}^2}{\Lambda^4} = c_s^2 \quad \xrightarrow{c_s \ll 1} \quad \frac{\dot{\pi}_c}{f_\pi^2} \ll \frac{c_s^2}{2}, \quad (5.69)$$

where $\pi_c = f_\pi^2 \pi$ is the canonically normalized field in the EFT of Inflation (see Appendix 5.A for review). Since π_c scales like the energy of the mode E , $\dot{\pi}_c \simeq E^2$ and, therefore, Eq. (5.69) tells us that our Taylor expansion is only valid for energies $E^2 \ll c_s^2 f_\pi^2 / 2 = \Lambda^2 / 2$. The cutoff scale we identified in the EFT is the scale where we can no longer Taylor expand the DBI action.

The DBI example naturally suggests the how to resolve this breakdown: we need to calculate the full transition amplitudes using the UV completion.⁵ In the case of DBI, we expect that modeling large field transitions requires knowing the complete non-perturbative form of the DBI action. In contrast, for smaller transitions, we can Taylor expand the DBI action to reproduce the same results as we would find using the EFT of Inflation. In practice, DBI may not be the simplest model in which to directly calculate the full transition amplitude, as more weakly coupled UV completions of small c_s may offer some advantages; it is possible UV complete this regime of EFT of Inflation parameter space by integrating out a weakly coupled massive field [155, 153, 154, 136]. In that case, we would expect that calculating the transition amplitude requires “integrating in” the high energy field. We leave the exploration of this interesting

⁵The contributions to Stochastic Inflation in DBI were previously discussed in [180, 181]. The contributions for higher derivatives did not appear in those works and thus they did not find the need for a non-perturbative calculation.

direction to future work.

5.6 Conclusions

In this paper, we extended the framework of Stochastic Inflation in single field inflation to include the impact of (equilateral) primordial non-Gaussianity. We showed that the single field consistency conditions demand that these corrections can only include higher derivative terms with constant coefficients. We then calculated a two-loop anomalous dimension in SdSET and used it to determine the cubic derivative correction to Stochastic Inflation.

Using these evolution equations, we set out to calculate the onset of eternal inflation in the presence of non-Gaussian fluctuations. We found that this transition cannot be calculated within the framework of Stochastic Inflation when the EFT of Inflation is not weakly coupled at the scale of the time evolution of the background, $f_\pi = 59H$, which is well above the scale of horizon crossing H . For a wide variety of models producing observable non-Gaussianity, the onset of eternal inflation is incalculable and requires appealing to a UV completion of the Stochastic framework and the EFT of Inflation.

We interpret the breakdown of Stochastic Inflation as a sign that the tail of the probability distribution for the scalar fluctuations is a probe of sub-horizon physics during inflation. This conclusion is relevant to other probes of non-Gaussianity from rare fluctuations [182, 183, 184, 185, 186], most notably as applied to the formation of primordial black holes (PBHs) [187, 188, 189, 190]. Like the onset of eternal inflation, the rate of PBH formation in canonical slow-roll inflation is calculable using Stochastic Inflation, both in the single and multi-field regime (see *e.g.* [168, 167, 169] for discussions of the connection between PBHs and Stochastic Inflation). Nevertheless, generic non-Gaussianity was known to impact these rates of rare fluctuations in ways that might not be calculable in perturbation theory [166]. Our results suggest it is the EFT of Inflation that is breaking down, which implies that one cannot resolve this effect within the EFT itself, *e.g.* by resumming EFT Feynman diagrams.

This work makes a sharp connection between a number of important topics in theoretical and observational cosmology: the regime of validity of cosmological EFTs, primordial non-Gaussianity, probes of the tail of the distribution of scalar fluctuations, eternal inflation, and the de Sitter entropy. A natural next step is to explore the connection between these results in models that are UV completed beyond the cutoff of the EFT of Inflation. Given a concrete model, *e.g.* DBI inflation [179], one could compute the tail of the distribution or the onset of eternal inflation. More generally, de Sitter holography (quantum gravity) also connects many of these topics and offers a parallel and unique perspective on the de Sitter entropy [159, 123, 160, 161], non-Gaussianity [7, 191] and (potentially) eternal inflation [192, 193]. Naturally, one would like to understand the breakdown of Stochastic Inflation from a holographic perspective. Our results imply the need for a deeper non-perturbative definition of eternal inflation, which may provide a concrete opportunity to link these (often) distinct approaches to cosmology.

Acknowledgements

We are grateful to Daniel Baumann, Tom Hartman, Yiwen Huang, Mehrdad Mirbabayi, Gui Pimentel, Rafael Porto, Chia-Hsien Shen, and Eva Silverstein for helpful discussions. D.G. also thanks the participants of *State of the Quantum Universe* for valuable insights. T. C. is supported by the US Department of Energy, under grant no. DE-SC0011640. D. G. and A. P. are supported by the US Department of Energy under grants DE-SC0019035 and DE-SC0009919.

This chapter, in full, has been submitted for publication of the material as it may appear in Timothy Cohen, Daniel Green, Akhil Premkumar, *Journal of High Energy Physics* (2022). The dissertation author was one of the primary investigators and authors of this paper.

Appendices

5.A Calculations for Single Field Inflation

In this appendix, we review the basics of the EFT of Inflation, and review results for the power spectrum and bispectrum that are used for the calculations in the main text. Then in

Sec. 5.A.2, we provide some technical details for how to regulate the key integral that appears in the calculation above using a dimensional regularization like approach that explicitly preserves the symmetries of the problem. We then review the perturbative unitarity constraint derived using flat space amplitudes in Sec. 5.A.3.

5.A.1 EFT of Inflation: Power Spectrum and Bispectrum

The EFT of inflation, in the decoupling limit, is described in terms of a Goldstone boson π that non-linearly realizes time translations that are broken by the evolving background. Since π shifts by a constant under time translations, the variable $U = t + \pi(t, \vec{x})$ transforms linearly under time translations. We can then express the action in terms of U :

$$S = \int dt d^3x \sqrt{-g} \sum_{n=0}^{\infty} \frac{1}{n!} M_n^4(U) (\partial_\mu U \partial^\mu U + 1)^n, \quad (5.70)$$

such that the n^{th} term is $\mathcal{O}(M_n^4 \pi^n)$ (note we are using the $(-+++)$ signature for the metric). The coefficients M_0^4 and M_1^4 are fixed by Einstein's equations (or equivalently by eliminating the tadpole). The resulting quadratic and cubic contributions to the Lagrangian are given by

$$\mathcal{L}_2 = M_{\text{pl}}^2 |\dot{H}| \left(\dot{\pi}^2 - (\vec{\nabla} \pi)^2 \right) + 2M_2^4 \dot{\pi}^2 = \frac{M_{\text{pl}}^2 |\dot{H}|}{c_s^2} \left(\dot{\pi}^2 - c_s^2 (\vec{\nabla} \pi)^2 \right), \quad (5.71)$$

and

$$\mathcal{L}_3 = \left(2M_2^4 - \frac{4}{3} M_3^4 \right) \dot{\pi}^3 - 2M_2^4 \dot{\pi} (\vec{\nabla} \pi)^2, \quad (5.72)$$

where $M_2^4 = M_{\text{pl}}^2 |\dot{H}| (1 - c_s^2) / (2c_s^2)$.

Using $\zeta = -H\pi + \mathcal{O}(\varepsilon \pi^2)$, where $\varepsilon = -\dot{H}/H^2$ is the slow roll parameter, and defining the pion decay constant as $f_\pi^4 \equiv 2M_{\text{pl}}^2 |\dot{H}| c_s$, one finds the power spectrum at zeroth order in slow-roll is

$$\langle \zeta(\vec{k}) \zeta(\vec{k}') \rangle' = \frac{H^4}{2f_\pi^4 k^3} (2\pi)^3 \delta(\vec{k} + \vec{k}') \equiv \frac{\Delta_\zeta}{k^3} (2\pi)^3 \delta(\vec{k} + \vec{k}'), \quad (5.73)$$

and the bispectra are [176]

$$B_{\zeta(\partial_i \zeta)^2}(k_1, k_2, k_3) = -\frac{1}{4} \left(1 - \frac{1}{c_s^2}\right) \cdot \Delta_\zeta^2 \times \frac{(24K_3^6 - 8K_2^2 K_3^3 K_1 - 8K_2^4 K_1^2 + 22K_3^3 K_1^3 - 6K_2^2 K_1^4 + 2K_1^6)}{K_3^9 K_1^3}, \quad (5.74)$$

and

$$B_{\zeta^3}(k_1, k_2, k_3) = 4 \left(1 - \frac{1}{c_s^2}\right) \left(\tilde{c}_3 + \frac{3}{2} c_s^2\right) \cdot \Delta_\zeta^2 \cdot \frac{1}{K_3^3 K_1^3}. \quad (5.75)$$

The coefficient \tilde{c}_3 is defined in [194] such that it is related to our c_3 by

$$\tilde{c}_3 M_2^4 \equiv M_3^4 \equiv c_3 \frac{f_\pi^4}{c_s^5} \rightarrow \tilde{c}_3 = \frac{2c_3}{(1 - c_s^2)c_s^2}, \quad (5.76)$$

so that

$$B_{\zeta^3}(k_1, k_2, k_3) = \left[6(c_s^2 - 1) + 8\frac{c_3}{c_s^2}\right] \cdot \Delta_\zeta^2 \cdot \frac{1}{K_3^3 K_1^3}. \quad (5.77)$$

We have also defined K_i the set of symmetry functions of the magnitudes of the momenta k_{1-3} ,

$$K_1 \equiv k_1 + k_2 + k_3, \quad K_2 \equiv (k_1 k_2 + k_2 k_3 + k_3 k_1)^{1/2}, \quad K_3 \equiv (k_1 k_2 k_3)^{1/3}. \quad (5.78)$$

Since the bispectra are necessarily symmetric under permutations of \vec{k}_i , it is natural to write the correlators in terms of these symmetric functions. The appearance of poles in K_3 is particularly noteworthy, as these are the cosmological avatars of energy conservation (also known as the total energy pole).

5.A.2 Dynamical Dimensional Regularization

When working with scalar fields in fixed dS, we were able to regulate divergent integrals in a symmetry preserving way by introducing a mass for the scalars, a procedure we called dynamical dimensional regularization (dyn dim reg) [65]. Our interest here is in regulating divergent integrals involving the adiabatic mode ζ . However, ζ transforms non-trivially under

the non-linearly realized symmetries defined in Eq. (5.3) above. (This explains why correlation functions of the adiabatic mode ζ are time-independent outside the horizon.) As a result, we cannot regulate divergences by introducing a mass for ζ , without breaking these symmetries. Fortunately, by definition, the background itself breaks time-translations, which will provide us with a way to regulate divergent integrals while respecting the symmetries. Having such a symmetry preserving regulator is important for justifying the consistency of the EFT approach.

To see how dyn dim reg works in this setting, we will recompute the leading quantum-noise term in Stochastic Inflation from correlators of ζ when $c_s = 1$. For comparison, we performed this calculation using a hard cutoff above, see Eq. (5.11). We start with the quadratic action

$$S = \int dt d^3x a^3(t) \frac{M_{\text{pl}}^2 \dot{H}(t)}{H^2(t)} \partial_\mu \zeta \partial^\mu \zeta . \quad (5.79)$$

Here we are making the time dependence of $H(t)$ manifest, since we will use this property to regulate divergences. For a general inflation model, $H(t)$ is some arbitrary function of t . If we define some reference time t_\star , we can therefore expand $H(t)$ as a power series near $t = t_\star$

$$S = \int dt d^3x \frac{M_{\text{pl}}^2 \dot{H}(t_\star)}{H^2(t_\star)} \left(\frac{\tau}{\tau_\star} \right)^{2+2\varepsilon+\eta} (\zeta'^2 - \partial_i \zeta \partial^i \zeta) , \quad (5.80)$$

where

$$\varepsilon \equiv -\frac{\dot{H}}{H^2} , \quad \text{and} \quad \eta = \frac{\dot{\varepsilon}}{H\varepsilon} , \quad (5.81)$$

$\tau \simeq -1/(aH)$ is the conformal time, and we used

$$\tau \frac{d}{d\tau} \log \left(\frac{H^4(t)}{M_{\text{pl}}^2 |\dot{H}(t)|} \right) = \tau \frac{d}{d\tau} \log \left(\frac{H^2(t)}{M_{\text{pl}}^2 \varepsilon(t)} \right) = -2\varepsilon - \eta . \quad (5.82)$$

The resulting power spectrum is

$$\langle \zeta(\vec{k}) \zeta(\vec{k}') \rangle' = \frac{H^4(t_\star)}{4M_{\text{pl}}^2 |\dot{H}(t_\star)|} \frac{1}{k^3} \left(\frac{k_\star}{k} \right)^{2\varepsilon+\eta} \quad (5.83)$$

where $k_* \tau_* = -1$. We can use this to repeat the one-loop calculation we performed in Eq. (5.11) using a hard cutoff:

$$\begin{aligned} \zeta^n &\rightarrow \zeta^{n-2} \frac{n(n-1)}{2} \int \frac{d^3k}{(2\pi)^3} \frac{H^4(t_*)}{4M_{\text{pl}}^2 |\dot{H}(t_*)|} \frac{1}{k^3} \left(\frac{k}{k_*} \right)^{-2\varepsilon-\eta} \\ &= \zeta^{n-2} \frac{n(n-1)}{4\pi^2} \frac{H(t_*)^4}{M_{\text{pl}}^2 |\dot{H}(t_*)|} \left(-\frac{1}{2\varepsilon+\eta} + \log K \tau_* \right), \end{aligned} \quad (5.84)$$

where K is an IR regulator⁶. To regulate the divergence, we introduce the normalized operator and the counterterm $Z - 1$ in the minimal subtraction scheme:

$$\zeta_R^{n-2} = Z \zeta^{n-2} \quad \text{with} \quad Z = 1 + \frac{1}{2\varepsilon+\eta} \frac{n(n-1)}{4\pi^2} \frac{H(t_*)^4}{M_{\text{pl}}^2 |\dot{H}(t_*)|}. \quad (5.85)$$

From here we can determine the dynamical RG by enforcing that our predictions are independent of $aH(t_*)$, which yields

$$\frac{d \log Z}{d \log aH(t_*)} = -\frac{n(n-1)}{4\pi^2} \frac{H(t_*)^4}{M_{\text{pl}}^2 |\dot{H}(t_*)|}. \quad (5.86)$$

For comparison, we can repeat the calculation using a hard UV cutoff aH with $\varepsilon, \eta \rightarrow 0$:

$$\zeta^n \rightarrow \zeta^{n-2} \times \frac{n(n-1)}{4\pi^2} \frac{H^4}{4M_{\text{pl}}^2 |\dot{H}|} \log aH/K. \quad (5.87)$$

This yields a counterterm

$$Z = 1 - \frac{n(n-1)}{4\pi^2} \frac{H^4}{4M_{\text{pl}}^2 |\dot{H}|} \log aH(t_*)/K, \quad (5.88)$$

⁶This result is similar to a $1/(n_s - 1)$ pole found in the one-loop power spectrum in [195]. The appearance of these inverse powers of slow-roll parameters in loop calculations is, a priori, not necessarily problematic as they signal the need for dynamical RG in the sense we describe here.

from which we can recover

$$\frac{d \log Z}{d \log aH(t_*)} = -\frac{n(n-1)}{4\pi^2} \frac{H^4}{M_{\text{pl}}^2 |\dot{H}|}. \quad (5.89)$$

In this sense, using the hard cutoff at one-loop will reproduce the results of a more careful treatment with dynamical dim reg and minimal subtraction. Precisely the same approach can be applied to regulate the two loop integral in the main text as well.

5.A.3 Perturbative Unitarity from Scattering

To understand the results of this paper, it is helpful to understand the energy scales where various processes become important. With the introduction of a non-trivial speed of sound, understanding the physical scales in the problem becomes more challenging, as the distinction between a momentum and energy scale is important. To simplify the problem, we can rescale the spatial coordinates to put time and space on the same footing

$$\tilde{x}^i = x^i/c_s, \quad \tilde{L} = c_s^3 \mathcal{L}, \quad \pi = f_\pi^2 \pi_c, \quad M_n^4 \equiv c_n \frac{f_\pi^4}{c_s^{2n-1}}, \quad \Lambda = f_\pi c_s, \quad (5.90)$$

so that $c_2 \equiv \frac{1}{4}(1 - c_s^2)$. After rescaling, it is convenient to organize the action in terms of the artificially Lorentz invariant derivatives $\tilde{\partial}_\mu$ and time derivatives, so that the action takes the form

$$\tilde{\mathcal{L}} = -\frac{1}{2} (\tilde{\partial} \pi_c)^2 + \frac{1}{\Lambda^2} \left[\alpha_1 \dot{\pi}_c^3 - \alpha_2 \dot{\pi}_c (\tilde{\partial} \pi_c)^2 \right] + \frac{1}{\Lambda^4} \left[\beta_1 \dot{\pi}_c^4 - \beta_2 \dot{\pi}_c^2 (\tilde{\partial} \pi_c)^2 + \beta_3 (\tilde{\partial} \pi_c)^4 \right], \quad (5.91)$$

where

$$\begin{aligned} \alpha_1 &\equiv -2c_2(1 - c_s^2) - \frac{4}{3}c_3, & \alpha_2 &\equiv 2c_2, \\ \beta_1 &\equiv \frac{1}{2}c_2(1 - c_s^2)^2 + 2c_3(1 - c_s^2) + \frac{2}{3}c_4, & \beta_2 &\equiv -c_2(1 - c_s^2) - 2c_3, & \beta_3 &\equiv \frac{1}{2}c_2. \end{aligned} \quad (5.92)$$

Crucially, we notice that the quadratic action is Lorentz invariant in terms of the \tilde{x} variables. The scattering amplitude for $2 \rightarrow 2$ scattering in the center of mass frame is [144]

$$M(s, \theta) = \left(-\frac{9}{4}\alpha_1^2 - 4\alpha_2^2 - 6\alpha_1\alpha_2 + \frac{3}{2}\beta_1 + 2\beta_2 + (3 + \cos^2 \theta)\beta_3 \right) \frac{s^2}{\Lambda^4}. \quad (5.93)$$

Now if we define the partial wave expansion of the amplitude as

$$M(s, \theta) \equiv 16\pi \sum_{\ell} (2\ell + 1) a_{\ell}(s) P_{\ell}(\cos \theta), \quad (5.94)$$

then $|a_{\ell}| \leq 1/2$ in order for the partial waves to be consistent with the optical theorem in perturbation theory, *i.e.*, the theory satisfies the constraint of perturbative unitarity. Integrating the amplitude over $\cos \theta$ we find

$$a_0(s) = \frac{1}{192\pi} \left(-3(3\alpha_1 + 4\alpha_2)^2 + 18\beta_1 + 24\beta_2 + 40\beta_3 \right) \frac{s^2}{\Lambda^4}, \quad (5.95a)$$

$$a_2(s) = \frac{\beta_3}{120\pi} \frac{s^2}{\Lambda^4}. \quad (5.95b)$$

For a_0 , perturbative unitarity places a bound on a complicated linear combination of c_s , c_3 and c_4 . This degeneracy can be broken by considering scattering in boosted frame. In contrast, if we demand $|a_2| < 1/2$ when the external energies are both f_{π} so that $s = 4f_{\pi}^2$, then we find that $c_s > 0.31$ if perturbative unitarity holds [144].

These bounds can be strengthened by considering scattering beyond the center of mass frame. This analysis was performed in [1], leading to the exclusion in terms of c_s and $\bar{\alpha}_1$:

$$\bar{\alpha}_1 = -\frac{4c_3}{3c_s^2} - \frac{1(1-c_s^2)^2}{2c_s^2} = \frac{\alpha_1}{c_s^2}. \quad (5.96)$$

This is the bound shown in Fig. 5.2.

Consistency with the de Sitter Entropy

With some extrapolation, we can also apply these results to the consistency of the de Sitter entropy discussed in Sec. 5.4. Concretely, we could observe more than a de Sitter entropy's worth of modes if we could satisfy the inequalities

$$\frac{\pi^2}{3} - \frac{\pi^2}{72} \left(\left(1 - \frac{1}{c_s^2} \right) (9 + 3c_s^2) + \frac{c_3}{c_s^2} \right) > \Delta_\zeta > \frac{4\pi^2}{3c_s}. \quad (5.97)$$

This appears to be possible when $c_s < 0.095$, but we interpreted as a breakdown of EFT of inflation as the cutoff dropped below the Hubble scale, $\Lambda < H$. We check this interpretation by comparing it to the perturbative unitarity on c_s of the d -wave amplitude, $|a_2(E)| < 1/2$, which implies [144]

$$\frac{E^4}{f_\pi^4} < 30\pi \frac{c_s^4}{1 - c_s^2}. \quad (5.98)$$

Although taking $E = H$ is not well-defined, since we are far from flat space (where the unitarity calculations are performed) in that limit, we can still use this bound as a check on our interpretation of the apparent violation of de Sitter entropy bound. Throwing caution to the wind, we combine this inequalities using $E = H$ to find

$$\frac{8\pi^2}{3c_s} < \frac{H^4}{f_\pi^4} < 30\pi \frac{c_s^4}{1 - c_s^2}. \quad (5.99)$$

The only viable solutions to these inequalities occurs when

$$c_s > 0.68. \quad (5.100)$$

We see that $c_s < 0.095$ clearly falls outside this region, so that it lies in the strongly coupled regime derived using this naive interpretation of the partial wave unitarity bound. The bound on c_s from the de Sitter entropy is a clearly a weaker constraint, but has the advantage that it applies in the de Sitter background directly.

For $c_3 \neq 0$, the flat space perturbative unitarity bounds become more complicated, as the s -wave amplitude depends on c_s , c_3 and c_4 (see Eq. (5.95a)). A proper comparison of the de Sitter entropy and scattering based bounds would require the next (4th) order in the derivative expansion in the Fokker-Planck equation which is beyond the scope of this work.

5.B Solving the Fokker-Planck with Steepest Descents

In this appendix, we will present an alternate solution to the Fokker-Planck equation

$$\frac{\partial}{\partial \mathfrak{t}} P(\zeta; \mathfrak{t}) = \frac{\sigma^2}{2} \frac{\partial^2}{\partial \zeta^2} P(\zeta; \mathfrak{t}) - \frac{\gamma_3}{3!} \frac{\partial^3}{\partial \zeta^3} P(\zeta; \mathfrak{t}) . \quad (5.101)$$

The basic idea is to use the Fourier transform to simplify the derivatives with respect to ζ . Specifically, if we define

$$P(\zeta; \mathfrak{t}) = \int_{-\infty}^{\infty} dk e^{-i\zeta k} P(k; \mathfrak{t}) \quad (5.102)$$

then the Fokker-Planck equation becomes

$$\frac{\partial}{\partial \mathfrak{t}} P(k; \mathfrak{t}) = \left(-k^2 \frac{\sigma^2}{2} - ik^3 \frac{\gamma_3}{3!} \right) P(k; \mathfrak{t}) . \quad (5.103)$$

This can be integrated to obtain

$$P(k; \mathfrak{t}) = C \exp \left(-\frac{k^2 \sigma^2 \mathfrak{t}}{2} - ik^3 \frac{\gamma_3}{3!} \mathfrak{t} \right) . \quad (5.104)$$

To determine the probability distribution of ζ , we take the inverse Fourier transform

$$P(\zeta; \mathfrak{t}) = C \int_{-\infty}^{\infty} dk \exp \left(-i\zeta k - k^2 \frac{\Delta_\zeta}{4\pi^2} \mathfrak{t} - ik^3 \frac{\gamma_3}{3!} \mathfrak{t} \right) . \quad (5.105)$$

For large \mathfrak{t} , we might suspect we can calculate this integral using the method of steepest descents. Specifically, we can deform the k contour in the complex plane so that it goes through a point k_*

such that

$$\frac{d}{dk} \left(-i\zeta k - k^2 \frac{\sigma^2}{2} t - ik^3 \frac{\gamma_3}{3!} t \right) \Big|_{k=k_*} = 0, \quad (5.106)$$

which occurs when

$$k_* = i \frac{\sigma^2}{\gamma_3} \left(1 \pm \sqrt{1 + \frac{2\gamma_3 \zeta}{\sigma^4 t}} \right). \quad (5.107)$$

Noting $\gamma_3 \ll \Delta_\zeta$, we should take the $-$ solution, since it lies closer to the real axis. We will assume $8\pi^4 \gamma_3 \zeta / t \ll 1$ so that

$$k_* \simeq -i \frac{\zeta}{\sigma^2 t} + i \gamma_3 \frac{\zeta^2}{2\sigma^6 t^2}. \quad (5.108)$$

The resulting probability distribution can be determined approximately by using $k = k_* + \bar{k}$

$$\begin{aligned} P(\zeta; t) &\simeq C \exp \left(-\frac{\zeta^2}{2\sigma^2 t} + \frac{\gamma_3}{3!} \frac{\zeta^3}{\sigma^6 t^2} \right) \int_{-\infty}^{\infty} d\bar{k} e^{-t\Delta_\zeta \bar{k}^2 / (2\pi^2)} \\ &\simeq \frac{\tilde{C}}{\sqrt{\Delta_\zeta t}} \exp \left(-\frac{\zeta^2}{2\sigma^2 t} + \frac{\gamma_3}{3!} \frac{\zeta^3}{\sigma^6 t^2} \right), \end{aligned} \quad (5.109)$$

where C and \tilde{C} are constants. Here we used the fact the integrand is analytic in the region enclosed by contours $k \in (-\infty, \infty)$ and $\bar{k} \in (-\infty, \infty)$ to obtain our final result.

This reproduces Eq. (5.34), which we derived from our exact solution. However, we also see that the method of steepest descents will become problematic when we take $2\gamma_3 \zeta / (\sigma^4 t) \geq 1$. This corresponds to the same condition as above for the failure of the Stochastic framework to reliably calculate the tail of the distribution.

Bibliography

- [1] T. Grall and S. Melville, “Inflation in motion: unitarity constraints in effective field theories with (spontaneously) broken Lorentz symmetry,” *JCAP* **09** (2020) 017, arXiv:2005.02366 [gr-qc].
- [2] **Planck** Collaboration, Y. Akrami *et al.*, “Planck 2018 results. IX. Constraints on primordial non-Gaussianity,” *Astron. Astrophys.* **641** (2020) A9, arXiv:1905.05697 [astro-ph.CO].
- [3] R. Bousso, “Holography in general space-times,” *JHEP* **06** (1999) 028, arXiv:hep-th/9906022 [hep-th].
- [4] A. Strominger, “The dS / CFT correspondence,” *JHEP* **10** (2001) 034, arXiv:hep-th/0106113 [hep-th].
- [5] E. Witten, “Quantum gravity in de Sitter space,” in *Strings 2001: International Conference Mumbai, India, January 5-10, 2001*. 2001. arXiv:hep-th/0106109 [hep-th].
- [6] P. O. Mazur and E. Mottola, “Weyl cohomology and the effective action for conformal anomalies,” *Phys. Rev.* **D64** (2001) 104022, arXiv:hep-th/0106151 [hep-th].
- [7] J. M. Maldacena, “Non-Gaussian features of primordial fluctuations in single field inflationary models,” *JHEP* **05** (2003) 013, arXiv:astro-ph/0210603 [astro-ph].
- [8] M. Alishahiha, A. Karch, E. Silverstein, and D. Tong, “The dS/dS correspondence,” *AIP Conf. Proc.* **743** no. 1, (2004) 393–409, arXiv:hep-th/0407125 [hep-th].
- [9] L. H. Ford, “Quantum Instability of De Sitter Space-time,” *Phys. Rev.* **D31** (1985) 710.
- [10] I. Antoniadis, J. Iliopoulos, and T. N. Tomaras, “Quantum Instability of De Sitter Space,” *Phys. Rev. Lett.* **56** (1986) 1319.
- [11] A. A. Starobinsky, “STOCHASTIC DE SITTER (INFLATIONARY) STAGE IN THE EARLY UNIVERSE,” *Lect. Notes Phys.* **246** (1986) 107–126.
- [12] N. C. Tsamis and R. P. Woodard, “Strong infrared effects in quantum gravity,” *Annals Phys.* **238** (1995) 1–82.
- [13] N. C. Tsamis and R. P. Woodard, “The Quantum gravitational back reaction on inflation,” *Annals Phys.* **253** (1997) 1–54, arXiv:hep-ph/9602316 [hep-ph].

- [14] N. C. Tsamis and R. P. Woodard, “Matter contributions to the expansion rate of the universe,” *Phys. Lett.* **B426** (1998) 21–28, arXiv:hep-ph/9710466 [hep-ph].
- [15] S. Weinberg, “Quantum contributions to cosmological correlations,” *Phys. Rev.* **D72** (2005) 043514, arXiv:hep-th/0506236 [hep-th].
- [16] S. Weinberg, “Quantum contributions to cosmological correlations. II. Can these corrections become large?,” *Phys. Rev.* **D74** (2006) 023508, arXiv:hep-th/0605244 [hep-th].
- [17] L. Senatore and M. Zaldarriaga, “On Loops in Inflation,” *JHEP* **12** (2010) 008, arXiv:0912.2734 [hep-th].
- [18] A. M. Polyakov, “Infrared instability of the de Sitter space,” arXiv:1209.4135 [hep-th].
- [19] L. Senatore and M. Zaldarriaga, “The constancy of ζ in single-clock Inflation at all loops,” *JHEP* **09** (2013) 148, arXiv:1210.6048 [hep-th].
- [20] V. Assassi, D. Baumann, and D. Green, “Symmetries and Loops in Inflation,” *JHEP* **02** (2013) 151, arXiv:1210.7792 [hep-th].
- [21] S. Weinberg, “Adiabatic modes in cosmology,” *Phys. Rev.* **D67** (2003) 123504, arXiv:astro-ph/0302326 [astro-ph].
- [22] K. Hinterbichler, L. Hui, and J. Khoury, “Conformal Symmetries of Adiabatic Modes in Cosmology,” *JCAP* **1208** (2012) 017, arXiv:1203.6351 [hep-th].
- [23] D. S. Salopek and J. R. Bond, “Nonlinear evolution of long wavelength metric fluctuations in inflationary models,” *Phys. Rev.* **D42** (1990) 3936–3962.
- [24] P. Creminelli and M. Zaldarriaga, “Single field consistency relation for the 3-point function,” *JCAP* **0410** (2004) 006, arXiv:astro-ph/0407059 [astro-ph].
- [25] C. P. Burgess, R. Holman, L. Leblond, and S. Shandera, “Breakdown of Semiclassical Methods in de Sitter Space,” *JCAP* **1010** (2010) 017, arXiv:1005.3551 [hep-th].
- [26] D. Marolf and I. A. Morrison, “The IR stability of de Sitter: Loop corrections to scalar propagators,” *Phys. Rev.* **D82** (2010) 105032, arXiv:1006.0035 [gr-qc].
- [27] D. Marolf and I. A. Morrison, “The IR stability of de Sitter QFT: Physical initial conditions,” *Gen. Rel. Grav.* **43** (2011) 3497–3530, arXiv:1104.4343 [gr-qc].
- [28] D. Marolf, I. A. Morrison, and M. Srednicki, “Perturbative S-matrix for massive scalar fields in global de Sitter space,” *Class. Quant. Grav.* **30** (2013) 155023, arXiv:1209.6039 [hep-th].
- [29] D. Anninos, T. Anous, D. Z. Freedman, and G. Konstantinidis, “Late-time Structure of the Bunch-Davies De Sitter Wavefunction,” *JCAP* **1511** no. 11, (2015) 048, arXiv:1406.5490 [hep-th].

- [30] C. P. Burgess, R. Holman, and G. Tasinato, “Open EFTs, IR effects & late-time resummations: systematic corrections in stochastic inflation,” *JHEP* **01** (2016) 153, arXiv:1512.00169 [gr-qc].
- [31] V. Gorbenko and L. Senatore, “ $\lambda\phi^4$ in dS,” arXiv:1911.00022 [hep-th].
- [32] M. Baumgart and R. Sundrum, “De Sitter Diagrammar and the Resummation of Time,” arXiv:1912.09502 [hep-th].
- [33] N. C. Tsamis and R. P. Woodard, “Stochastic quantum gravitational inflation,” *Nucl. Phys.* **B724** (2005) 295–328, arXiv:gr-qc/0505115 [gr-qc].
- [34] A. Riotto and M. S. Sloth, “On Resumming Inflationary Perturbations beyond One-loop,” *JCAP* **0804** (2008) 030, arXiv:0801.1845 [hep-ph].
- [35] D. Seery, “A parton picture of de Sitter space during slow-roll inflation,” *JCAP* **0905** (2009) 021, arXiv:0903.2788 [astro-ph.CO].
- [36] J. Serreau and R. Parentani, “Nonperturbative resummation of de Sitter infrared logarithms in the large-N limit,” *Phys. Rev.* **D87** (2013) 085012, arXiv:1302.3262 [hep-th].
- [37] D. Lopez Nacir, F. D. Mazzitelli, and L. G. Trombetta, “ $O(N)$ model in Euclidean de Sitter space: beyond the leading infrared approximation,” *JHEP* **09** (2016) 117, arXiv:1606.03481 [hep-th].
- [38] F. Tanaka, “Coherent Representation of Dynamical Renormalization Group in Bose Systems,” *Prog. Theor. Phys.* **54** (1975) 289–290.
- [39] D. Boyanovsky, H. J. de Vega, R. Holman, and M. Simionato, “Dynamical renormalization group resummation of finite temperature infrared divergences,” *Phys. Rev.* **D60** (1999) 065003, arXiv:hep-ph/9809346 [hep-ph].
- [40] D. Boyanovsky and H. J. de Vega, “Dynamical renormalization group approach to relaxation in quantum field theory,” *Annals Phys.* **307** (2003) 335–371, arXiv:hep-ph/0302055 [hep-ph].
- [41] D. Boyanovsky and H. J. de Vega, “Particle decay in inflationary cosmology,” *Phys. Rev.* **D70** (2004) 063508, arXiv:astro-ph/0406287 [astro-ph].
- [42] P. McDonald, “Dark matter clustering: a simple renormalization group approach,” *Phys. Rev.* **D75** (2007) 043514, arXiv:astro-ph/0606028 [astro-ph].
- [43] D. I. Podolsky, “Dynamical renormalization group methods in theory of eternal inflation,” *Grav. Cosmol.* **15** (2009) 69–74, arXiv:0809.2453 [gr-qc].
- [44] C. P. Burgess, L. Leblond, R. Holman, and S. Shandera, “Super-Hubble de Sitter Fluctuations and the Dynamical RG,” *JCAP* **1003** (2010) 033, arXiv:0912.1608 [hep-th].

- [45] J. M. Maldacena and G. L. Pimentel, “On graviton non-Gaussianities during inflation,” *JHEP* **09** (2011) 045, arXiv:1104.2846 [hep-th].
- [46] S. Raju, “New Recursion Relations and a Flat Space Limit for AdS/CFT Correlators,” *Phys. Rev.* **D85** (2012) 126009, arXiv:1201.6449 [hep-th].
- [47] N. Arkani-Hamed and J. Maldacena, “Cosmological Collider Physics,” arXiv:1503.08043 [hep-th].
- [48] N. Arkani-Hamed, D. Baumann, H. Lee, and G. L. Pimentel, “The Cosmological Bootstrap: Inflationary Correlators from Symmetries and Singularities,” arXiv:1811.00024 [hep-th].
- [49] N. Arkani-Hamed and P. Benincasa, “On the Emergence of Lorentz Invariance and Unitarity from the Scattering Facet of Cosmological Polytopes,” arXiv:1811.01125 [hep-th].
- [50] P. Benincasa, “From the flat-space S-matrix to the Wavefunction of the Universe,” arXiv:1811.02515 [hep-th].
- [51] K. Farnsworth, M. A. Luty, and V. Prilepina, “Weyl versus Conformal Invariance in Quantum Field Theory,” *JHEP* **10** (2017) 170, arXiv:1702.07079 [hep-th].
- [52] J. Polchinski, “Renormalization and Effective Lagrangians,” *Nucl. Phys.* **B231** (1984) 269–295.
- [53] D. Green, M. Lewandowski, L. Senatore, E. Silverstein, and M. Zaldarriaga, “Anomalous Dimensions and Non-Gaussianity,” *JHEP* **10** (2013) 171, arXiv:1301.2630 [hep-th].
- [54] S. R. Behbahani and D. Green, “Collective Symmetry Breaking and Resonant Non-Gaussianity,” *JCAP* **1211** (2012) 056, arXiv:1207.2779 [hep-th].
- [55] A. H. Guth, “The Inflationary Universe: A Possible Solution to the Horizon and Flatness Problems,” *Phys. Rev. D* **23** (1981) 347–356.
- [56] A. D. Linde, “A New Inflationary Universe Scenario: A Possible Solution of the Horizon, Flatness, Homogeneity, Isotropy and Primordial Monopole Problems,” *Phys. Lett. B* **108** (1982) 389–393.
- [57] A. A. Starobinsky, “A New Type of Isotropic Cosmological Models Without Singularity,” *Phys. Lett. B* **91** (1980) 99–102.
- [58] P. D. Meerburg *et al.*, “Primordial Non-Gaussianity,” arXiv:1903.04409 [astro-ph.CO].
- [59] M. Beneke and P. Moch, “On “dynamical mass” generation in Euclidean de Sitter space,” *Phys. Rev. D* **87** (2013) 064018, arXiv:1212.3058 [hep-th].
- [60] E. T. Akhmedov, “Lecture notes on interacting quantum fields in de Sitter space,” *Int. J. Mod. Phys. D* **23** (2014) 1430001, arXiv:1309.2557 [hep-th].

- [61] E. T. Akhmedov, U. Moschella, K. E. Pavlenko, and F. K. Popov, “Infrared dynamics of massive scalars from the complementary series in de Sitter space,” *Phys. Rev.* **D96** no. 2, (2017) 025002, arXiv:1701.07226 [hep-th].
- [62] B.-L. Hu, “Infrared Behavior of Quantum Fields in Inflationary Cosmology – Issues and Approaches: an overview,” arXiv:1812.11851 [gr-qc].
- [63] E. T. Akhmedov, U. Moschella, and F. K. Popov, “Characters of different secular effects in various patches of de Sitter space,” *Phys. Rev.* **D99** no. 8, (2019) 086009, arXiv:1901.07293 [hep-th].
- [64] D. Green and A. Premkumar, “Dynamical RG and Critical Phenomena in de Sitter Space,” *JHEP* **04** (2020) 064, arXiv:2001.05974 [hep-th].
- [65] T. Cohen and D. Green, “Soft de Sitter Effective Theory,” *JHEP* **12** (2020) 041, arXiv:2007.03693 [hep-th].
- [66] T. Cohen, D. Green, A. Premkumar, and A. Ridgway, “Stochastic Inflation at NNLO,” arXiv:2106.09728 [hep-th].
- [67] C. Sleight, “A Mellin Space Approach to Cosmological Correlators,” *JHEP* **01** (2020) 090, arXiv:1906.12302 [hep-th].
- [68] C. Sleight and M. Taronna, “Bootstrapping Inflationary Correlators in Mellin Space,” *JHEP* **02** (2020) 098, arXiv:1907.01143 [hep-th].
- [69] C. Sleight and M. Taronna, “From dS to AdS and back,” arXiv:2109.02725 [hep-th].
- [70] C. G. Bollini and J. J. Giambiagi, “Dimensional Renormalization: The Number of Dimensions as a Regularizing Parameter,” *Nuovo Cim. B* **12** (1972) 20–26.
- [71] G. ’t Hooft, “Dimensional regularization and the renormalization group,” *Nucl. Phys. B* **61** (1973) 455–468.
- [72] E. E. Boos and A. I. Davydychev, “A Method of evaluating massive Feynman integrals,” *Theor. Math. Phys.* **89** (1991) 1052–1063.
- [73] A. V. Smirnov and V. A. Smirnov, “On the Resolution of Singularities of Multiple Mellin-Barnes Integrals,” *Eur. Phys. J. C* **62** (2009) 445–449, arXiv:0901.0386 [hep-ph].
- [74] J. B. Tausk, “Nonplanar massless two loop Feynman diagrams with four on-shell legs,” *Phys. Lett. B* **469** (1999) 225–234, arXiv:hep-ph/9909506.
- [75] C. Anastasiou and A. Daleo, “Numerical evaluation of loop integrals,” *JHEP* **10** (2006) 031, arXiv:hep-ph/0511176.
- [76] M. Czakon, “Automatized analytic continuation of Mellin-Barnes integrals,” *Comput. Phys. Commun.* **175** (2006) 559–571, arXiv:hep-ph/0511200.

- [77] C. Burgess, L. Leblond, R. Holman, and S. Shandera, “Super-hubble de sitter fluctuations and the dynamical rg,” *Journal of Cosmology and Astroparticle Physics* **2010** no. 03, (Mar, 2010) 033033. <http://dx.doi.org/10.1088/1475-7516/2010/03/033>.
- [78] L.-Y. Chen, N. Goldenfeld, and Y. Oono, “The Renormalization group and singular perturbations: Multiple scales, boundary layers and reductive perturbation theory,” *Phys. Rev. E* **54** (1996) 376–394, arXiv:hep-th/9506161.
- [79] Y. Nambu and M. Sasaki, “Stochastic Stage of an Inflationary Universe Model,” *Phys. Lett. B* **205** (1988) 441–446.
- [80] A. A. Starobinsky and J. Yokoyama, “Equilibrium state of a self-interacting scalar field in the De Sitter background,” *Phys. Rev. D* **50** (1994) 6357–6368, arXiv:astro-ph/9407016.
- [81] M. Mirbabayi, “Infrared dynamics of a light scalar field in de Sitter,” *JCAP* **12** (2020) 006, arXiv:1911.00564 [hep-th].
- [82] G. Watson, *A Treatise on the Theory of Bessel Functions*. Cambridge Mathematical Library. Cambridge University Press, 1995.
- [83] V. A. Smirnov, “Evaluating Feynman integrals,” *Springer Tracts Mod. Phys.* **211** (2004) 1–244.
- [84] A. Rajaraman, “On the proper treatment of massless fields in Euclidean de Sitter space,” *Phys. Rev. D* **82** (2010) 123522, arXiv:1008.1271 [hep-th].
- [85] S. Friot and D. Greynat, “On convergent series representations of Mellin-Barnes integrals,” *J. Math. Phys.* **53** (2012) 023508, arXiv:1107.0328 [math-ph].
- [86] O. N. Zhdanov and A. K. Tsikh, “Studying the multiple Mellin-Barnes integrals by means of multidimensional residues,” *Siberian Mathematical Journal* **39** no. 2, (Apr, 1998) 245–260. <https://doi.org/10.1007/BF02677509>.
- [87] B. Ananthanarayan, S. Banik, S. Friot, and S. Ghosh, “Multiple Series Representations of N -fold Mellin-Barnes Integrals,” arXiv:2012.15108 [hep-th].
- [88] K. Enqvist, S. Nurmi, D. Podolsky, and G. I. Rigopoulos, “On the divergences of inflationary superhorizon perturbations,” *JCAP* **04** (2008) 025, arXiv:0802.0395 [astro-ph].
- [89] F. Finelli, G. Marozzi, A. A. Starobinsky, G. P. Vacca, and G. Venturi, “Generation of fluctuations during inflation: Comparison of stochastic and field-theoretic approaches,” *Phys. Rev. D* **79** (2009) 044007, arXiv:0808.1786 [hep-th].
- [90] D. Seery, “Infrared effects in inflationary correlation functions,” *Class. Quant. Grav.* **27** (2010) 124005, arXiv:1005.1649 [astro-ph.CO].
- [91] B. Garbrecht, F. Gautier, G. Rigopoulos, and Y. Zhu, “Feynman Diagrams for Stochastic Inflation and Quantum Field Theory in de Sitter Space,” *Phys. Rev. D* **91** (2015) 063520, arXiv:1412.4893 [hep-th].

- [92] M. Mirbabayi, “Markovian Dynamics in de Sitter,” arXiv:2010.06604 [hep-th].
- [93] M. Baumgart and R. Sundrum, “Manifestly Causal In-In Perturbation Theory about the Interacting Vacuum,” *JHEP* **03** (2021) 080, arXiv:2010.10785 [hep-th].
- [94] A. D. Linde, “Eternally Existing Selfreproducing Chaotic Inflationary Universe,” *Phys. Lett. B* **175** (1986) 395–400.
- [95] A. S. Goncharov, A. D. Linde, and V. F. Mukhanov, “The Global Structure of the Inflationary Universe,” *Int. J. Mod. Phys. A* **2** (1987) 561–591.
- [96] B. Freivogel, “Making predictions in the multiverse,” *Class. Quant. Grav.* **28** (2011) 204007, arXiv:1105.0244 [hep-th].
- [97] P. Creminelli, S. Dubovsky, A. Nicolis, L. Senatore, and M. Zaldarriaga, “The Phase Transition to Slow-roll Eternal Inflation,” *JHEP* **09** (2008) 036, arXiv:0802.1067 [hep-th].
- [98] N. Arkani-Hamed, S. Dubovsky, A. Nicolis, E. Trincherini, and G. Villadoro, “A Measure of de Sitter entropy and eternal inflation,” *JHEP* **05** (2007) 055, arXiv:0704.1814 [hep-th].
- [99] S. Dubovsky, L. Senatore, and G. Villadoro, “The Volume of the Universe after Inflation and de Sitter Entropy,” *JHEP* **04** (2009) 118, arXiv:0812.2246 [hep-th].
- [100] M. Lewandowski and A. Perko, “Leading slow roll corrections to the volume of the universe and the entropy bound,” *JHEP* **12** (2014) 060, arXiv:1309.6705 [hep-th].
- [101] C. W. Gardiner, *Handbook of stochastic methods for physics, chemistry and the natural sciences*, vol. 13 of *Springer Series in Synergetics*. Springer-Verlag, Berlin, third ed., 2004.
- [102] D. Baumann, “Primordial Cosmology,” *PoS TASI2017* (2018) 009, arXiv:1807.03098 [hep-th].
- [103] D. Baumann, A. Nicolis, L. Senatore, and M. Zaldarriaga, “Cosmological Non-Linearities as an Effective Fluid,” *JCAP* **07** (2012) 051, arXiv:1004.2488 [astro-ph.CO].
- [104] H. Georgi, “Effective field theory,” *Ann. Rev. Nucl. Part. Sci.* **43** (1993) 209–252.
- [105] P. Creminelli, “Conformal invariance of scalar perturbations in inflation,” *Phys. Rev. D* **85** (2012) 041302, arXiv:1108.0874 [hep-th].
- [106] A. Premkumar, “Regulating Loops in dS,” arXiv:2110.12504 [hep-th].
- [107] M. Beneke and V. A. Smirnov, “Asymptotic expansion of Feynman integrals near threshold,” *Nucl. Phys. B* **522** (1998) 321–344, arXiv:hep-ph/9711391.
- [108] V. A. Smirnov, “Applied asymptotic expansions in momenta and masses,” *Springer Tracts Mod. Phys.* **177** (2002) 1–262.

- [109] H. Kitamoto, “Infrared resummation for derivative interactions in de Sitter space,” *Phys. Rev. D* **100** no. 2, (2019) 025020, arXiv:1811.01830 [hep-th].
- [110] L. Pinol, S. Renaux-Petel, and Y. Tada, “A manifestly covariant theory of multifield stochastic inflation in phase space,” *JCAP* **04** (2021) 048, arXiv:2008.07497 [astro-ph.CO].
- [111] T. Markkanen, A. Rajantie, S. Stopyra, and T. Tenkanen, “Scalar correlation functions in de Sitter space from the stochastic spectral expansion,” *JCAP* **08** (2019) 001, arXiv:1904.11917 [gr-qc].
- [112] D. Wands, K. A. Malik, D. H. Lyth, and A. R. Liddle, “A New approach to the evolution of cosmological perturbations on large scales,” *Phys. Rev. D* **62** (2000) 043527, arXiv:astro-ph/0003278.
- [113] D. Seery and J. E. Lidsey, “Primordial non-Gaussianities from multiple-field inflation,” *JCAP* **09** (2005) 011, arXiv:astro-ph/0506056.
- [114] D. Wands, “Local non-Gaussianity from inflation,” *Class. Quant. Grav.* **27** (2010) 124002, arXiv:1004.0818 [astro-ph.CO].
- [115] Y. Tada and V. Vennin, “Squeezed bispectrum in the δN formalism: local observer effect in field space,” *JCAP* **02** (2017) 021, arXiv:1609.08876 [astro-ph.CO].
- [116] A. Achúcarro, V. Atal, C. Germani, and G. A. Palma, “Cumulative effects in inflation with ultra-light entropy modes,” *JCAP* **02** (2017) 013, arXiv:1607.08609 [astro-ph.CO].
- [117] X. Chen and Y. Wang, “Quasi-Single Field Inflation and Non-Gaussianities,” *JCAP* **04** (2010) 027, arXiv:0911.3380 [hep-th].
- [118] P. W. Graham, D. E. Kaplan, and S. Rajendran, “Cosmological Relaxation of the Electroweak Scale,” *Phys. Rev. Lett.* **115** no. 22, (2015) 221801, arXiv:1504.07551 [hep-ph].
- [119] M. Geller, Y. Hochberg, and E. Kuflik, “Inflating to the Weak Scale,” *Phys. Rev. Lett.* **122** no. 19, (2019) 191802, arXiv:1809.07338 [hep-ph].
- [120] G. Kartvelishvili, J. Khoury, and A. Sharma, “The Self-Organized Critical Multiverse,” *JCAP* **02** (2021) 028, arXiv:2003.12594 [hep-th].
- [121] G. F. Giudice, M. McCullough, and T. You, “Self-Organised Localisation,” arXiv:2105.08617 [hep-ph].
- [122] N. Arkani-Hamed, S. Dubovsky, A. Nicolis, E. Trincherini, and G. Villadoro, “A Measure of de Sitter entropy and eternal inflation,” *JHEP* **05** (2007) 055, arXiv:0704.1814 [hep-th].
- [123] L. Susskind, “Three Impossible Theories,” arXiv:2107.11688 [hep-th].
- [124] R. Bousso, “Cosmology and the S-matrix,” *Phys. Rev. D* **71** (2005) 064024, arXiv:hep-th/0412197.

- [125] W. Hu, D. N. Spergel, and M. J. White, “Distinguishing causal seeds from inflation,” *Phys. Rev. D* **55** (1997) 3288–3302, arXiv:astro-ph/9605193.
- [126] D. N. Spergel and M. Zaldarriaga, “CMB polarization as a direct test of inflation,” *Phys. Rev. Lett.* **79** (1997) 2180–2183, arXiv:astro-ph/9705182.
- [127] S. Dodelson, “Coherent phase argument for inflation,” *AIP Conf. Proc.* **689** no. 1, (2003) 184–196, arXiv:hep-ph/0309057.
- [128] P. Creminelli, M. A. Luty, A. Nicolis, and L. Senatore, “Starting the Universe: Stable Violation of the Null Energy Condition and Non-standard Cosmologies,” *JHEP* **12** (2006) 080, arXiv:hep-th/0606090.
- [129] C. Cheung, P. Creminelli, A. Fitzpatrick, J. Kaplan, and L. Senatore, “The Effective Field Theory of Inflation,” *JHEP* **03** (2008) 014, arXiv:0709.0293 [hep-th].
- [130] D. Baumann, “Inflation,” in *Theoretical Advanced Study Institute in Elementary Particle Physics: Physics of the Large and the Small*, pp. 523–686. 2011. arXiv:0907.5424 [hep-th].
- [131] D. Green and R. A. Porto, “Signals of a Quantum Universe,” arXiv:2001.09149 [hep-th].
- [132] E. Pajer, “Building a Boostless Bootstrap for the Bispectrum,” *JCAP* **01** (2021) 023, arXiv:2010.12818 [hep-th].
- [133] D. Meltzer, “The Inflationary Wavefunction from Analyticity and Factorization,” arXiv:2107.10266 [hep-th].
- [134] M. Hogervorst, J. a. Penedones, and K. S. Vaziri, “Towards the non-perturbative cosmological bootstrap,” arXiv:2107.13871 [hep-th].
- [135] L. Di Pietro, V. Gorbenko, and S. Komatsu, “Analyticity and Unitarity for Cosmological Correlators,” arXiv:2108.01695 [hep-th].
- [136] D. Baumann and D. Green, “Equilateral Non-Gaussianity and New Physics on the Horizon,” *JCAP* **09** (2011) 014, arXiv:1102.5343 [hep-th].
- [137] X. Chen, M.-x. Huang, S. Kachru, and G. Shiu, “Observational signatures and non-Gaussianities of general single field inflation,” *JCAP* **01** (2007) 002, arXiv:hep-th/0605045.
- [138] D. Seery, “One-loop corrections to a scalar field during inflation,” *JCAP* **11** (2007) 025, arXiv:0707.3377 [astro-ph].
- [139] L. Leblond and S. Shandera, “Simple Bounds from the Perturbative Regime of Inflation,” *JCAP* **08** (2008) 007, arXiv:0802.2290 [hep-th].
- [140] S. Shandera, “The structure of correlation functions in single field inflation,” *Phys. Rev. D* **79** (2009) 123518, arXiv:0812.0818 [astro-ph].

- [141] D. Baumann and D. Green, “A Field Range Bound for General Single-Field Inflation,” *JCAP* **05** (2012) 017, arXiv:1111.3040 [hep-th].
- [142] R. Flauger, D. Green, and R. A. Porto, “On squeezed limits in single-field inflation. Part I,” *JCAP* **08** (2013) 032, arXiv:1303.1430 [hep-th].
- [143] D. Baumann, D. Green, and R. A. Porto, “B-modes and the Nature of Inflation,” *JCAP* **01** (2015) 016, arXiv:1407.2621 [hep-th].
- [144] D. Baumann, D. Green, H. Lee, and R. A. Porto, “Signs of Analyticity in Single-Field Inflation,” *Phys. Rev. D* **93** no. 2, (2016) 023523, arXiv:1502.07304 [hep-th].
- [145] P. Adshead, C. P. Burgess, R. Holman, and S. Shandera, “Power-counting during single-field slow-roll inflation,” *JCAP* **02** (2018) 016, arXiv:1708.07443 [hep-th].
- [146] I. Babic, C. P. Burgess, and G. Geshnizjani, “Keeping an eye on DBI: power-counting for small- c_s cosmology,” *JCAP* **05** (2020) 023, arXiv:1910.05277 [gr-qc].
- [147] **Planck** Collaboration, N. Aghanim *et al.*, “Planck 2018 results. VI. Cosmological parameters,” *Astron. Astrophys.* **641** (2020) A6, arXiv:1807.06209 [astro-ph.CO]. [Erratum: *Astron. Astrophys.* 652, C4 (2021)].
- [148] X. Chen, R. Easther, and E. A. Lim, “Large Non-Gaussianities in Single Field Inflation,” *JCAP* **06** (2007) 023, arXiv:astro-ph/0611645.
- [149] R. Flauger and E. Pajer, “Resonant Non-Gaussianity,” *JCAP* **01** (2011) 017, arXiv:1002.0833 [hep-th].
- [150] R. Flauger, L. McAllister, E. Pajer, A. Westphal, and G. Xu, “Oscillations in the CMB from Axion Monodromy Inflation,” *JCAP* **06** (2010) 009, arXiv:0907.2916 [hep-th].
- [151] R. Flauger, L. McAllister, E. Silverstein, and A. Westphal, “Drifting Oscillations in Axion Monodromy,” *JCAP* **10** (2017) 055, arXiv:1412.1814 [hep-th].
- [152] P. Creminelli, “On non-Gaussianities in single-field inflation,” *JCAP* **10** (2003) 003, arXiv:astro-ph/0306122.
- [153] S. Cremonini, Z. Lalak, and K. Turzynski, “Strongly Coupled Perturbations in Two-Field Inflationary Models,” *JCAP* **03** (2011) 016, arXiv:1010.3021 [hep-th].
- [154] A. Achucarro, J.-O. Gong, S. Hardeman, G. A. Palma, and S. P. Patil, “Features of heavy physics in the CMB power spectrum,” *JCAP* **01** (2011) 030, arXiv:1010.3693 [hep-ph].
- [155] A. J. Tolley and M. Wyman, “The Gelaton Scenario: Equilateral non-Gaussianity from multi-field dynamics,” *Phys. Rev. D* **81** (2010) 043502, arXiv:0910.1853 [hep-th].
- [156] H. E. Kandrup, “STOCHASTIC INFLATION AS A TIME DEPENDENT RANDOM WALK,” *Phys. Rev. D* **39** (1989) 2245.

- [157] F. Finelli, G. Marozzi, A. A. Starobinsky, G. P. Vacca, and G. Venturi, “Stochastic growth of quantum fluctuations during slow-roll inflation,” *Phys. Rev. D* **82** (2010) 064020, arXiv:1003.1327 [hep-th].
- [158] G. W. Gibbons and S. W. Hawking, “Cosmological Event Horizons, Thermodynamics, and Particle Creation,” *Phys. Rev. D* **15** (1977) 2738–2751.
- [159] X. Dong, B. Horn, E. Silverstein, and G. Torroba, “Micromanaging de Sitter holography,” *Class. Quant. Grav.* **27** (2010) 245020, arXiv:1005.5403 [hep-th].
- [160] E. Shaghoulian, “The central dogma and cosmological horizons,” arXiv:2110.13210 [hep-th].
- [161] E. Coleman, E. A. Mazenc, V. Shyam, E. Silverstein, R. M. Soni, G. Torroba, and S. Yang, “de Sitter Microstates from $T\bar{T} + \Lambda_2$ and the Hawking-Page Transition,” arXiv:2110.14670 [hep-th].
- [162] R. Bousso, B. Freivogel, and I.-S. Yang, “Eternal Inflation: The Inside Story,” *Phys. Rev. D* **74** (2006) 103516, arXiv:hep-th/0606114.
- [163] H. Matsui and F. Takahashi, “Eternal Inflation and Swampland Conjectures,” *Phys. Rev. D* **99** no. 2, (2019) 023533, arXiv:1807.11938 [hep-th].
- [164] W. H. Kinney, “Eternal Inflation and the Refined Swampland Conjecture,” *Phys. Rev. Lett.* **122** no. 8, (2019) 081302, arXiv:1811.11698 [astro-ph.CO].
- [165] S. Brahma and S. Shandera, “Stochastic eternal inflation is in the swampland,” *JHEP* **11** (2019) 016, arXiv:1904.10979 [hep-th].
- [166] M. Celería, P. Creminelli, G. Tambalo, and V. Yingcharoenrat, “Beyond perturbation theory in inflation,” *JCAP* **06** (2021) 051, arXiv:2103.09244 [hep-th].
- [167] V. Vennin, “Stochastic inflation and primordial black holes,” other thesis, 9, 2020.
- [168] G. Panagopoulos and E. Silverstein, “Primordial Black Holes from non-Gaussian tails,” arXiv:1906.02827 [hep-th].
- [169] A. Achúcarro, S. Cespedes, A.-C. Davis, and G. A. Palma, “The hand-made tail: Non-perturbative tails from multifield inflation,” arXiv:2112.14712 [hep-th].
- [170] T. Cohen, “As Scales Become Separated: Lectures on Effective Field Theory,” in *TASI 2018*. 2019. arXiv:1903.03622 [hep-ph].
- [171] P. Creminelli, J. Noreña, and M. Simonović, “Conformal consistency relations for single-field inflation,” *JCAP* **07** (2012) 052, arXiv:1203.4595 [hep-th].
- [172] V. Assassi, D. Baumann, and D. Green, “On Soft Limits of Inflationary Correlation Functions,” *JCAP* **11** (2012) 047, arXiv:1204.4207 [hep-th].

- [173] K. Hinterbichler, L. Hui, and J. Khoury, “An Infinite Set of Ward Identities for Adiabatic Modes in Cosmology,” *JCAP* **01** (2014) 039, arXiv:1304.5527 [hep-th].
- [174] D. Green and E. Pajer, “On the Symmetries of Cosmological Perturbations,” *JCAP* **09** (2020) 032, arXiv:2004.09587 [hep-th].
- [175] **Planck** Collaboration, P. A. R. Ade *et al.*, “Planck 2013 results. XXII. Constraints on inflation,” *Astron. Astrophys.* **571** (2014) A22, arXiv:1303.5082 [astro-ph.CO].
- [176] L. Senatore, K. M. Smith, and M. Zaldarriaga, “Non-Gaussianities in Single Field Inflation and their Optimal Limits from the WMAP 5-year Data,” *JCAP* **01** (2010) 028, arXiv:0905.3746 [astro-ph.CO].
- [177] D. Baumann, D. Green, and T. Hartman, “Dynamical Constraints on RG Flows and Cosmology,” *JHEP* **12** (2019) 134, arXiv:1906.10226 [hep-th].
- [178] T. Grall and S. Melville, “Positivity Bounds without Boosts,” arXiv:2102.05683 [hep-th].
- [179] M. Alishahiha, E. Silverstein, and D. Tong, “DBI in the sky,” *Phys. Rev. D* **70** (2004) 123505, arXiv:hep-th/0404084.
- [180] A. J. Tolley and M. Wyman, “Stochastic Inflation Revisited: Non-Slow Roll Statistics and DBI Inflation,” *JCAP* **04** (2008) 028, arXiv:0801.1854 [hep-th].
- [181] L. Lorenz, J. Martin, and J. Yokoyama, “Geometrically Consistent Approach to Stochastic DBI Inflation,” *Phys. Rev. D* **82** (2010) 023515, arXiv:1004.3734 [hep-th].
- [182] J. R. Bond, A. V. Frolov, Z. Huang, and L. Kofman, “Non-Gaussian Spikes from Chaotic Billiards in Inflation Preheating,” *Phys. Rev. Lett.* **103** (2009) 071301, arXiv:0903.3407 [astro-ph.CO].
- [183] R. Flauger, M. Mirbabayi, L. Senatore, and E. Silverstein, “Productive Interactions: heavy particles and non-Gaussianity,” *JCAP* **10** (2017) 058, arXiv:1606.00513 [hep-th].
- [184] X. Chen, G. A. Palma, W. Riquelme, B. Scheihing Hitschfeld, and S. Sypsas, “Landscape tomography through primordial non-Gaussianity,” *Phys. Rev. D* **98** no. 8, (2018) 083528, arXiv:1804.07315 [hep-th].
- [185] M. Münchmeyer and K. M. Smith, “Higher N-point function data analysis techniques for heavy particle production and WMAP results,” *Phys. Rev. D* **100** no. 12, (2019) 123511, arXiv:1910.00596 [astro-ph.CO].
- [186] G. Panagopoulos and E. Silverstein, “Multipoint correlators in multifield cosmology,” arXiv:2003.05883 [hep-th].
- [187] G. Franciolini, A. Kehagias, S. Matarrese, and A. Riotto, “Primordial Black Holes from Inflation and non-Gaussianity,” *JCAP* **03** (2018) 016, arXiv:1801.09415 [astro-ph.CO].

- [188] V. Atal and C. Germani, “The role of non-gaussianities in Primordial Black Hole formation,” *Phys. Dark Univ.* **24** (2019) 100275, arXiv:1811.07857 [astro-ph.CO].
- [189] J. M. Ezquiaga, J. García-Bellido, and V. Vennin, “The exponential tail of inflationary fluctuations: consequences for primordial black holes,” *JCAP* **03** (2020) 029, arXiv:1912.05399 [astro-ph.CO].
- [190] I. Musco, V. De Luca, G. Franciolini, and A. Riotto, “Threshold for primordial black holes. II. A simple analytic prescription,” *Phys. Rev. D* **103** no. 6, (2021) 063538, arXiv:2011.03014 [astro-ph.CO].
- [191] P. McFadden and K. Skenderis, “Holographic Non-Gaussianity,” *JCAP* **05** (2011) 013, arXiv:1011.0452 [hep-th].
- [192] B. Freivogel, Y. Sekino, L. Susskind, and C.-P. Yeh, “A Holographic framework for eternal inflation,” *Phys. Rev. D* **74** (2006) 086003, arXiv:hep-th/0606204.
- [193] Y. Sekino and L. Susskind, “Census Taking in the Hat: FRW/CFT Duality,” *Phys. Rev. D* **80** (2009) 083531, arXiv:0908.3844 [hep-th].
- [194] C. Cheung, A. L. Fitzpatrick, J. Kaplan, and L. Senatore, “On the consistency relation of the 3-point function in single field inflation,” *JCAP* **02** (2008) 021, arXiv:0709.0295 [hep-th].
- [195] J. Kristiano and J. Yokoyama, “Why primordial non-Gaussianity must be very small?,” arXiv:2104.01953 [hep-th].